

UC San Diego

UC San Diego Electronic Theses and Dissertations

Title

Micropatterned co-cultures of hepatocytes and nonparenchymal cells : mechanisms of differentiation, dynamics and applications

Permalink

<https://escholarship.org/uc/item/9q06w180>

Author

Khetani, Salman R.

Publication Date

2006

Peer reviewed|Thesis/dissertation

UNIVERSITY OF CALIFORNIA, SAN DIEGO

**MICROPATTERNED CO-CULTURES OF
HEPATOCTES
AND NONPARENCHYMAL CELLS:
MECHANISMS OF DIFFERENTIATION,
DYNAMICS AND APPLICATIONS**

A dissertation submitted in partial satisfaction of the
requirements for the degree Doctor of Philosophy

in

Bioengineering

by

Salman R. Khetani

Committee in charge:

Professor Sangeeta N. Bhatia, Chair
Professor Shu Chien
Professor Sanjay K. Nigam
Professor Robert L. Sah
Professor Robert H. Tukey

2006

Copyright

Salman R. Khetani, 2006

All rights reserved.

The dissertation of Salman R. Khetani is approved, and it is acceptable in quality and form for publication on microfilm:

Chair

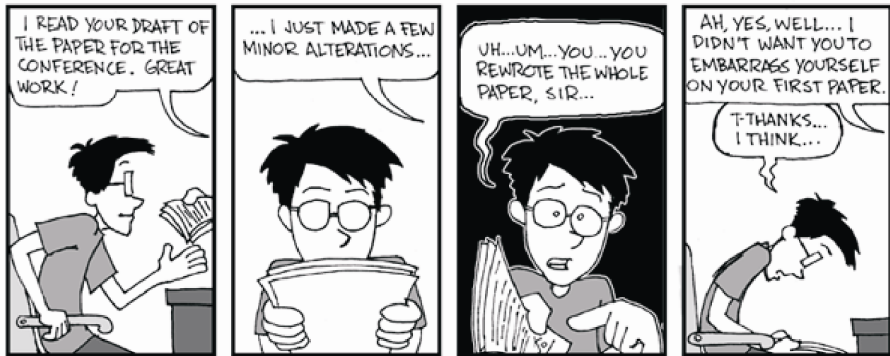
University of California, San Diego

2006

To Mary, Mom and Dad, and Faisal

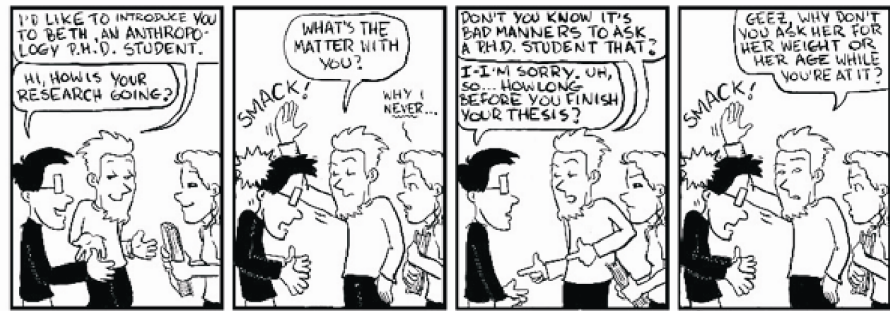


www.phdcomics.com



JORGE CHAM ©THE STANFORD DAILY

phd.stanford.edu/comics



JORGE CHAM ©THE STANFORD DAILY

THANKS TO MIGUEL...

TABLE OF CONTENTS

SIGNATURE PAGE	iii
DEDICATION.....	iv
EPIGRAPH	v
TABLE OF CONTENTS	vi
LIST OF FIGURES.....	xiv
LIST OF TABLES.....	xviii
ACKNOWLEDGEMENTS	xix
VITA	xxiii
ABSTRACT OF THE DISSERTATION.....	xxvi
CHAPTER 1: INTRODUCTION	1
1.1. Cell-Based Therapies for Liver Disease	1
1.1.1. Clinical Significance.....	1
1.1.2. Approaches.....	2
1.1.3. Cell Sourcing	5
1.2. The Liver	8
1.2.1. Structure.....	8

1.2.2. Functions	9
1.3. Cadherins	13
1.3.1. Structure and Mechanisms of Signaling	13
1.3.2. Role in Differentiation.....	14
1.3.3. Role in the Liver	16
1.3.4. T-cadherin.....	16
1.4. Co-Cultivation of Hepatocytes with Nonparenchymal Cells.....	17
1.4.1. Mechanisms Underlying the Co-Culture Effect.....	21
1.5. MEMS (Micro-Electro-Mechanical Systems) as an Enabling Technology....	23
1.5.1. Soft-Lithography.....	24
1.5.2. Electroactive Substrates.....	24
1.6. Drug Development	25
1.6.1. Development Pipeline.....	25
1.6.2. Drug-Induced Liver Disease.....	27
1.7. In Vitro Liver Models for Drug Development.....	30
1.7.1. Primary Hepatocyte Culture Models	30
1.7.2. Utility in Drug Development.....	34
1.8. Scope of this Dissertation	36

**CHAPTER 2: EXPLORING INTERACTIONS BETWEEN
HEPATOCYTES AND NONPARENCHYMAL CELLS USING
GENE EXPRESSION PROFILING.....39**

2.1. Abstract.....	39
2.2. Introduction	40
2.3. Materials and Methods	43
2.3.1. Rat Hepatocyte Isolation.....	43

2.3.2. Fibroblast Culture.....	43
2.3.3. Hepatocyte-Fibroblast Co-Culture.....	44
2.3.4. Analytical Assays.....	45
2.3.5. Microscopy	45
2.3.6. Fibroblast RNA Isolation and Microarray Hybridization	45
2.3.7. Selection of Differentially Expressed Genes.....	46
2.3.8. Microarray Data Analysis	47
2.3.9. Western Blotting and Immunofluorescence.....	47
2.3.10. Statistical Analysis.....	48
2.4. Results	48
2.4.1. Differential Induction of Liver-Specific Functions.....	48
2.4.2. Gene Expression Profiling of Fibroblasts	52
2.4.3. Cell Surface Proteins	56
2.4.4. Extracellular Matrix Proteins	57
2.4.5. Secreted Factors.....	58
2.5. Discussion	63
Acknowledgements.....	67

CHAPTER 3: T-CADHERIN MODULATES HEPATOCYTE FUNCTIONS IN VITRO	68
3.1. Abstract.....	68
3.2. Introduction	69
3.3. Materials and Methods	72
3.3.1. Rat Hepatocyte Isolation and Culture	72
3.3.2. Nonparenchymal Cell Culture	72

3.3.3. T-cadherin Fusion Protein Generation	73
3.3.4. Hepatocyte-Nonparenchymal Co-Cultures	73
3.3.5. Hepatocellular Function Assays	74
3.3.6. Microscopy	75
3.3.7. RNAi Mediated Knockdown of T-Cadherin	75
3.3.8. Western Blotting and Immunofluorescence.....	75
3.3.9. Cell Viability Assessment.....	76
3.4. Results	76
3.4.1. Induction of Hepatocyte Functions by T-cadherin-Transfected CHOs	76
3.4.2. RNAi-Mediated Knockdown of T-cadherin in CHO Cells	78
3.4.3. Upregulation of Functions in Pure Hepatocyte Monolayers on T-cadherin Protein.....	83
3.4.4. Upregulation of Functions in Co-Cultures on T-cadherin Protein.....	84
3.5. Discussion	90
Acknowledgements.....	95

CHAPTER 4: DYNAMIC MODULATION OF HETEROTYPIC CELL-CELL INTERACTIONS VIA ELECTROACTIVE SUBSTRATES.....96

4.1. Abstract.....	96
4.2. Introduction	97
4.3. Materials and Methods	104
4.3.1. Preparation of Gold-Coated Substrates	104
4.3.2. Electroactive Chemistry.....	104
4.3.3. Electrochemical Release of Cells.....	105
4.3.4. Microcontact Printing to Generate Patterned SAMs	105

4.3.5. Stencil-based Process to Generate Patterned SAMs	106
4.3.6. Generation of Micropatterned Hepatocyte-Nonparenchymal Co-Cultures.....	106
4.3.7. Morphological and Functional Analysis of Hepatocyte Cultures	107
4.3.8. Staining of Cellular Necrosis.....	107
4.4. Results	111
4.4.1. Dose-dependent Attachment of Hepatocytes on RGD- Functionalized SAMs	111
4.4.2. Compatibility of the ‘Co-culture Effect’ with Electroactive SAMs	111
4.4.3. Optimization of Electrochemical Release Parameters	112
4.4.4. Characterization of Hepatocyte Morphology and Function Following Fibroblast Release from Co-Culture	112
4.5. Discussion	120
Acknowledgements.....	128

CHAPTER 5: MICROSCALE HUMAN LIVER TISSUE FOR DRUG DEVELOPMENT	129
5.1. Abstract.....	129
5.2. Introduction	130
5.3. Materials and Methods	132
5.3.1. Soft-lithographic Micropatterning of Collagen	132
5.3.2. Photolithographic Micropatterning	133
5.3.3. Hepatocyte Isolation and Culture	133
5.3.4. Fibroblast Culture.....	134
5.3.5. Hepatocyte-Nonparenchymal Co-Cultures	134
5.3.6. Biochemical Assays	135

5.3.7. Microscopy	135
5.3.8. Gene Expression Profiling.....	136
5.3.9. Cytochrome-P450 Induction	137
5.3.10. Phase I & II Enzyme Activity Assays.....	137
5.3.11. Cell Viability Assessment (MTT Assay)	138
5.3.12. Statistical Data Analysis	138
5.4. Results	139
5.4.1. Functional Optimization of Hepatocyte Cultures and Co- Cultures via Microtechnology	139
5.4.2. Fabrication of Miniaturized Microscale Liver Tissues in a Multiwell Format	147
5.4.3. Characterization of Microscale Human Liver Tissues	150
5.4.4. Utility of Microscale Human Liver Tissues in Drug Development.....	154
5.5. Discussion	165
5.5.1. Comparison between Micropatterned Rat and Human Hepatocyte Co-Cultures	166
5.5.2. Miniaturization of Micropatterned Co-Cultures Using Stencils ...	166
5.5.3. Modularity and Cost Benefits of Microscale Liver Tissues.....	167
5.5.4. Comparison of Microscale Liver Tissues with Other Platforms..	168
5.5.5. Evaluation of Hepatotoxicity in Microscale Liver Tissues.....	171
5.5.6. Detection of Clinically Relevant Drug-Drug Interactions in Microscale Liver Tissues.....	173
5.5.7. Conclusions	175
Acknowledgements.....	176

CHAPTER 6: A LONG-TERM MODEL OF THE RAT LIVER FOR EVALUATING DRUG DISPOSITION	177
6.1. Abstract.....	177
6.2. Introduction	178
6.3. Materials and Methods	181
6.3.1. Nonparenchymal Cell Culture	181
6.3.2. Hepatocyte-Nonparenchymal Co-Cultures	182
6.3.3. Hepatocellular Function Assays	183
6.3.4. Staining of Functional Bile Canaliculi.....	184
6.3.5. Acute and Chronic Toxicity Studies	184
6.3.6. Drug-Drug Interaction Studies.....	184
6.4. Results	185
6.4.1. Long-term Morphological and Functional Stability of Co- Cultures	185
6.4.2. Activity of Phase I and Phase II Enzymes	187
6.4.3. Functional Bile Canaliculi.....	188
6.4.4. Drug-Drug Interactions.....	194
6.4.5. Chronic Toxicity of Model Hepatotoxins.....	199
6.4.6. Comparison of Drug Toxicity in Pure Hepatocyte Monolayers and Hepatocyte-Fibroblast Co-Cultures	205
6.4.7. Species-Specific Phase I and II Substrate Metabolism.....	208
6.4.8. Co-Cultivation of Rat Hepatocytes with Liver-derived Nonparenchymal Cells.....	208
6.5. Discussion	212
6.5.1. Functional Comparison Between Random and Micropatterned Co-Cultures.....	213
6.5.2. Considerations in Development of the Long-term Liver Model .	215

6.5.3. Functional Stability of Co-Cultures	217
6.5.4. Altered Substrate Metabolism and Toxicity Due to Drug-Drug Interactions.....	220
6.5.5. Toxicity in Co-Cultures Due to Repeated Exposures with Model Hepatotoxins.....	223
6.5.6. Comparison of Drug Toxicity in Pure Hepatocyte Monolayers and Co-Cultures	225
6.5.7. Differences in Phase I and II Substrate Metabolism between Rat and Human Micropatterned Co-Cultures	227
6.5.8. Future Studies	229
6.5.9. Conclusions	230
Acknowledgements.....	231
CHAPTER 7: SUMMARY AND FUTURE DIRECTIONS	232
7.1. Overall Objectives.....	232
7.2. Microenvironmental Cues for Engineering a Functional Hepatic Tissue....	233
7.3. Dynamic Substrates for Studies of Heterotypic Cell-Cell Signaling	235
7.4. Improved Tissue Models for Drug Development	237
7.5. Conclusions.....	240
REFERENCES	242

LIST OF FIGURES

Figure 1.1: Cell-based therapies for liver disease.	3
Figure 1.2: Liver structure.	11
Figure 1.3: Cell-cell interactions in the liver.	12
Figure 1.4: Structure of classical cadherins.	15
Figure 1.5: The co-culture effect.	20
Figure 1.6: The drug development pipeline.	29
Figure 2.1: Differential induction of liver-specific functions in rat hepatocytes upon co-cultivation with murine fibroblasts.	50
Figure 2.2: Effect of poorly inductive mouse embryonic fibroblasts (MEFs) on hepatic functions in highly inductive 3T3-J2 co-cultures.	51
Figure 2.3: Gene expression profiling of fibroblasts.	53
Figure 2.4: Analysis of the cadherin pathway suggests negative correlation with hepatocyte function.	59
Figure 2.5: Validation of extracellular matrix, decorin, as a potential mediator of cell-cell interaction.	60
Figure 2.6: Hepatocyte culture on paraformaldehyde-fixed fibroblast feeder layers.	61
Figure 2.7: Co-cultivation of murine embryonic 3T3 fibroblasts with primary murine or human hepatocytes.	62
Figure 3.1: Co-cultivation of hepatocytes with T-cadherin-transfected CHO cells.	79
Figure 3.2: Urea synthesis in CHO/hepatocyte co-cultures.	80
Figure 3.3: Activity of CYP1A enzyme in CHO/hepatocyte co-cultures.	81
Figure 3.4: RNAi-mediated knockdown of T-cadherin in CHO cells.	82
Figure 3.5: Upregulation of hepatocyte functions on T-cadherin-coated substrates in a dose-dependent manner.	85

Figure 3.6: Relative hepatocyte attachment and spreading on T-cadherin-coated substrates.	86
Figure 3.7: Long-term induction of functions in hepatocytes on T-cadherin-coated substrates.	87
Figure 3.8: Co-cultures of wild-type CHO cells and hepatocytes on T-cadherin.	88
Figure 3.9: Long-term upregulation of liver-specific functions in MEF-hepatocyte co-cultures on T-Cadherin.	89
Figure 4.1: Electroactive substrate to evaluate dynamics of heterotypic cell-cell interactions	103
Figure 4.2: Electroactive surface chemistry	108
Figure 4.3: Microcontact printing to create electroactive co-cultures	109
Figure 4.4: Stencil-based approach to create electroactive co-cultures	110
Figure 4.5: Hepatocyte attachment to RGD-functionalized SAMs	114
Figure 4.6: The co-culture effect on electroactive substrates.....	115
Figure 4.7: Release of 3T3 fibroblasts from electroactive substrates	116
Figure 4.8: Release of 3T3 fibroblasts from co-cultures on electroactive substrates	117
Figure 4.9: Hepatocyte morphology following release of fibroblasts from co-cultures on electroactive substrates.....	118
Figure 4.10: Hepatocyte function following release of fibroblasts from co-cultures on electroactive substrates.....	119
Figure 5.1: Photolithographic process to create micropatterned co-cultures.....	142
Figure 5.2: Functional optimization of <i>rat</i> hepatocyte co-cultures via micropatterning.....	143
Figure 5.3: Randomly distributed human hepatocyte cultures and co-cultures.	144
Figure 5.4: Micropatterned cultures of pure human hepatocytes.....	145
Figure 5.5: Functional optimization of <i>human</i> hepatocyte co-cultures via micropatterning.....	146
Figure 5.6: Soft lithographic process to fabricate miniaturized microscale liver tissues.	148

Figure 5.7: Microscale liver tissues in a multi-well format.	149
Figure 5.8: Liver-specific functions in microscale human liver tissues.	151
Figure 5.9: Transcriptional profiling of microscale human liver tissues.	152
Figure 5.10: Gene expression level comparison between microscale human liver tissues and pure monolayers.	153
Figure 5.11: Phase I & II enzyme activity in microscale human liver tissues.	156
Figure 5.12: Relative toxicity of compounds in microscale human liver tissues.	157
Figure 5.13: Toxicity profiles generated using microscale human liver tissues.	158
Figure 5.14: Chronic APAP toxicity in microscale human liver tissues.	159
Figure 5.15: Drug-drug interactions in microscale human liver tissues.	160
Figure 5.16: Species-specific induction of CYP1A isoforms in microscale liver tissues.	161
Figure 5.17: Albumin secretion in microscale tissues generated using non- parenchymal liver fraction.	162
Figure 5.18: Liver-specific functions in microscale tissues generated using cryopreserved human hepatocytes.	163
Figure 6.1: Maintenance of hepatocyte morphology in long-term micropatterned co-cultures.	189
Figure 6.2: Long-term induction of hepatocellular functions in micropatterned co- cultures.	190
Figure 6.3: Long-term activity of CYP450 enzymes in micropatterned co-cultures.	191
Figure 6.4: Metabolism of prototypic substrates via Phase I and Phase II pathways.	192
Figure 6.5: Staining of functional bile canaliculi in co-cultures.	193
Figure 6.6: Modulation of CYP450 activity.	196
Figure 6.7: Dexamethasone-mediated enhancement of acetaminophen toxicity.	197
Figure 6.8: Caffeine-mediated enhancement of APAP toxicity in co-cultures treated with CYP3A inducers.	198
Figure 6.9: Dose- and time-dependent toxicity of acetaminophen.	201

Figure 6.10: Dose- and time-dependent toxicity of methapyrilene.....	202
Figure 6.11: Dose- and time-dependent toxicity of pyriline.....	203
Figure 6.12: Changes in cellular morphology in co-cultures following repeated exposures with troglitazone.	204
Figure 6.13: Methapyrilene and pyriline toxicity in pure hepatocyte monolayers and co-cultures.....	206
Figure 6.14: Acetaminophen and troglitazone toxicity in pure hepatocyte monolayers and co-cultures.	207
Figure 6.15: Comparison of Phase I- and Phase II-mediated substrate metabolism in human and rat co-cultures.	210
Figure 6.16: Co-cultivation of rat hepatocytes with nonparenchymal fraction of the liver.	211

LIST OF TABLES

Table 1.1: Nonparenchymal cell types known to stabilize liver-specific functions in primary hepatocytes.	19
Table 2.1: Criteria used in Bullfrog software to detect differentially expressed genes between fibroblasts.....	47
Table 2.2: Fibroblast candidate genes whose expression profiles correlate positively with the hepatocyte functional profile.....	54
Table 2.3: Fibroblast candidate genes whose expression profiles correlate negatively with the hepatocyte functional profile.....	55
Table 5.1: Liver donor information.	164

ACKNOWLEDGMENTS

I have been incredibly fortunate to work with Sangeeta and the brilliant group of people she has recruited over the years. The lab has moved two times, once across the country from UCSD to MIT. However, in all such changes, Sangeeta's dedication to her students has remained constant. She has always been supportive of my research and career goals, and provided me freedom to delineate the conceptual and experimental details of the projects of my choosing. She has treated me like a colleague instead of an employee, even though when I was first starting out, I knew nothing about liver tissue engineering. As a result of Sangeeta's mentorship, I have grown into an independent thinker, a careful experimentalist, and a dedicated scientist. Over the past 5+ years, I have told many incoming students that "Sangeeta is the best advisor in the world", and as I write these words, I hold steadfast in my assertion. I sincerely thank Sangeeta for all she has and continues to do for my professional development.

My experience as a graduate student was made much more meaningful by the amazing members of Sangeeta's laboratory. It is a pleasure to work with people who are not only brilliant and hard-working, but are so generous and kind. Jen Felix, our former lab manager, taught me most of the cell culture I know. Though she had the important and time-consuming task of running the lab efficiently, Jen never hesitated to assist me in learning the art of biological experimentation. Jared Allen, Valerie Liu, Vicki Chin, Dirk Albrecht, Tom Pisanic, Jen Koh and Chris Flaim were the students in the lab when I first joined. These extraordinary individuals accepted me into their circle and provided any advice they could on the process of getting a doctorate. Of course, their technical expertise enabled me to move forward. I especially want to thank Dirk Albrecht (now a

post-doctoral fellow) for always providing helpful advice (technical and personal), and being so generous with his document ‘templates’, which eased the burden on me as I went through the process of writing and defending my dissertation. Austin Derfus, Geoffrey Von Maltzahn, Todd Harris, Alice Chen and Sukant Mittal joined the group as students within 1 to 4 years after my start, and have kept the tradition of generosity, brilliance and hard work alive. Our post-doctoral fellows over the years have allowed me to benefit from their wealth of experience. Soonjo Kwon worked with me one-on-one to jumpstart my research, while Warren Chan provided much needed advice on how to go through graduate school without getting ‘jaded’. Greg Underhill continues to patiently answer my million annoying questions and has taught me key biological techniques, for which I am very grateful. Elliot Hui and Dave Eddington have helped me refine my ideas and have shared their diverse skill sets without hesitation. Dal-Hee Min has recently joined our group from University of Chicago as a post-doctoral fellow. My few encounters with her have been quite positive, and I am sure she will make an important contribution to the culture and research of our lab. I consider each and every one of these individuals as my life-long friend and colleague. Without them, my graduate school experience would have been ordinary at best.

I have had the good fortune to work with several talented undergraduate students throughout my graduate tenure. Brandon Fanelli, Ian Gaudet, Craig Sharp, Ihui Wu and Julia Kiberd assisted with various aspects of my research. I am very grateful to them for their hard work and enthusiasm.

I would also like to thank my dissertation committee, whose timely suggestions have enabled me to finish my thesis. These professors have challenged me to think broadly about my research, and have provided the necessary encouragement throughout the graduate school process.

Next, I would like to thank my parents, Ramzan and Amina, who have always been emotionally and financially supportive of my academic endeavors. They tutored me religiously during the formative years of my early schooling, and continue to provide the parental advice which allows me to make sound decisions to progress personally and professionally. Almost 14 years ago, my parents left a good life in the United Arab Emirates behind and immigrated to the US for only one reason: to provide their children with better educational opportunities than what was available in the Middle East at that time. I will always be grateful to them for their sacrifice and love for their children. My younger brother, Faisal, has been a source of creative insights and thought-provoking conversations about all imaginable topics. I am truly blessed to have him in my life.

My wife, Mary, has supported me with all her heart throughout my journey as a graduate student. In fact, had I the documentation to prove it, UCSD would probably award her a PhD in Bioengineering as well since she has gone through all my experiences (good and bad) with me 😊. From making me home-cooked meals to listening to my ramblings about what my data meant to just hugging me when I was down, Mary has been the catalyst in all dimensions of my life. Furthermore, she has provided valuable suggestions which have undoubtedly improved the quality of this work. Mary's love and dedication to our marriage are aspects which I cherish the most. Her brilliance and love for helping people in whichever way possible are inspirations for me. I can't imagine going through any meaningful journey in my life without her.

I would also like to acknowledge my funding sources. A Jacobs fellowship and a National Institutes of Health training grant from UCSD provided tuition and stipend support for 2 years, while a graduate fellowship from the National Science Foundation provided support for an additional three years. Additional research funding came from

NSF CAREER, NIH NIDDK, Deshpande Center (MIT), and the David and Lucile Packard Foundation.

The text of Chapter 2, in part, is a reprint of the material as it appears in *Hepatology* (Khetani, S.R., Szulgit, G., Del Rio, J.A., Barlow, C., and Bhatia, S.N., “Exploring Interactions between Rat Hepatocytes and Nonparenchymal Cells Using Gene Expression Profiling.” *Hepatology* 2004, volume 40, issue 3, pages 545-554). This material was reprinted with permission of John Wiley & Sons, Inc. The text of Chapter 5, in part, has been submitted for publication (Khetani, S.R. and Bhatia, S.N., “Microscale Human Liver Tissue for Drug Development”). The dissertation author was the primary researcher and author and conducted the research that forms both of these chapters.

VITA

- 2006 Ph.D., Bioengineering
University of California at San Diego, La Jolla, California
- 2002 M.S., Bioengineering
University of California at San Diego, La Jolla, California
- 2000 B.S., Electrical Engineering (computer option)
B.S., Biomedical Engineering (electronics option)
Summa cum laude
Marquette University, Milwaukee, Wisconsin

Awards and Honors

National Science Foundation Graduate Research Fellowship, 2001-2004
Jacobs Fellowship, University of California at San Diego, 2000-2001
Top Scholar in Biomedical Engineering Award, Marquette University, 1999
Tau Beta Pi National Engineering Honor Society, 1997 – present
Ignatius Scholarship, Marquette University, 1995-1999

Teaching Experience at the University of California – San Diego

Head/Senior Teaching Assistant, Department of Bioengineering, 2003-2005
Biotechnology Laboratory (BE162), 2003
Foundations of Tissue Engineering Science (BE241A – Graduate Level), 2002, 2003
Cell and Tissue Engineering (BE166A), 2002
Bioengineering Physiology (BE140A), 2001

Patents Pending

UCSD Reference number: SD2005-016-1PCT - “Molecules with Effects on Hepatocytes and Liver Function,” Khetani, S.R. and Bhatia, S.N.

UCSD Reference number: SD2005-247-1 - “Microscale Engineered in Vitro Human Liver Tissue for Drug Development,” Khetani, S.R. and Bhatia, S.N (provisional patent).

Journal Articles

Khetani, S.R., Ranscht, B., and Bhatia, S.N., “T-cadherin modulates hepatocyte functions in vitro” (In preparation, 2006).

Khetani, S.R., Yeo, W.S., Mrksich, M., and Bhatia, S.N., “Dynamic modulation of heterotypic cell-cell interactions via electroactive substrates” (In preparation, 2006).

Khetani, S.R., and Bhatia, S.N., “Long-term model of the rat liver for studying drug disposition in vitro” (In preparation, 2006).

Allen, J.W., **Khetani, S.R.**, Johnson, R.S., and Bhatia, S.N., “In Vitro Liver Tissue Model Established From Transgenic Mice: Role of HIF-1alpha on Hypoxic Gene Expression” (Submitted January 2006).

Khetani, S.R., and Bhatia, S.N., “Microscale Human Liver Tissue for Drug Development” (Submitted December 2005).

Chen, A.A*, Derfus, A.M*, **Khetani, S.R.**, and Bhatia, S.N., “Quantum Dots to Monitor siRNA Delivery and Improve Gene Silencing.” *Nucleic Acids Research* 33(22):190 (2005) (* These authors contributed equally).

Khetani, S.R., Szulgit, G., Del Rio, J.A., Barlow, C., and Bhatia, S.N., “Exploring Interactions between Rat Hepatocytes and Nonparenchymal Cells Using Gene Expression Profiling.” *Hepatology* 40(3): 545-554 (2004).

Allen, J.W., **Khetani, S.R.**, and Bhatia, S.N., “In Vitro Zonation and Toxicity in a Hepatocyte Bioreactor.” *Toxicological Sciences* 84: 110-119 (2004).

Book Chapters

Underhill, G.H., Felix, J., Allen, J.W., Tsang, V.L., **Khetani, S.R.**, and Bhatia, S.N., “Tissue Engineering of the Liver.” In: Culture of Cells for Tissue Engineering, Freshney (ed.), Academic Press (2005 - in press).

Selected Abstracts and Presentations

†**Khetani, S.R.**, and Bhatia, S.N., “Microscale Engineered Human Liver Tissue for Drug Development.” Annual Meeting of the Biomedical Engineering Society (BMES), Baltimore, MD (September 2005).

Khetani, S.R., Ranscht, B., and Bhatia, S.N., “T-cadherin Modulates Hepatocyte Functions In Vitro.” Gordon Research Conference on Cell Contact and Adhesion, Andover, NH (June 2005).

†**Khetani, S.R.**, and Bhatia, S.N., “Microscale Engineered Liver Tissue for Toxicant Testing.” Annual Meeting of the Biomedical Engineering Society (BMES), Philadelphia, PA (October 2004).

Khetani, S.R., Yeo, W-S., Szulgit, G., Del Rio, J.A., Mrksich, M., Barlow, C., and Bhatia, S.N., “Exploring Cell-Cell Interactions Using Gene Expression Profiling and Dynamic Substrates.” Federation of American Societies for Experimental Biology (FASEB) Meeting on Mechanisms of Liver Growth, Development and Disease, Snowmass, CO (August 2004).

†**Khetani, S.R.**, Yeo, W-S., Szulgit, G., Del Rio, J.A., Mrksich, M., Barlow, C., and Bhatia, S.N., “Exploring Mechanisms of Cell-Cell Interaction in Hepatic Co-Cultures Using Gene Expression Profiling and Dynamic Substrates.” Annual Meeting of the Biomedical Engineering Society (BMES), Nashville, TN (October 2003).

Khetani, S.R., Yeo, W-S., Szulgit, G., Del Rio, J.A., Mrksich, M., Barlow, C., and Bhatia, S.N., “Exploring Cell-Cell Interactions Using Gene Expression Profiling and Dynamic Substrates.” California Tissue Engineering Meeting, La Jolla, CA (September 2003).

Khetani, S.R., Szulgit, G., Del Rio, J.A., Barlow, C., and Bhatia, S.N., “Exploring Mechanisms of Cell-Cell Interaction in Hepatic Co-cultures Using Gene Expression Profiling.” Annual Meeting of the Biomedical Engineering Society (BMES), Houston, TX (October 2002).

Khetani, S.R., Szulgit, G., Del Rio, J.A., Barlow, C., and Bhatia, S.N., “Exploring Mechanisms of Cell-Cell Interaction in Hepatic Co-cultures Using Gene Expression Profiling.” Southern California Tissue Engineering Symposium, Los Angeles, CA (September 2002).

Khetani, S.R., Szulgit, G., Del Rio, J.A., Barlow, C., and Bhatia, S.N., “Exploring Mechanisms of Cell-Cell Interaction in Hepatic Co-cultures Using Gene Expression Profiling.” American Association for the Study of Liver Diseases (AASLD) Meeting on Human Liver Cells in Biomedical Research, Warrenton, VA (June 2002).

†Podium presentation

ABSTRACT OF THE DISSERTATION

MICROPATTERNED CO-CULTURES OF HEPATOCYTES
AND NONPARENCHYMAL CELLS:
MECHANISMS OF DIFFERENTIATION,
DYNAMICS AND APPLICATIONS

by

Salman R. Khetani

Doctor of Philosophy in Bioengineering
University of California, San Diego, 2006
Professor Sangeeta N. Bhatia, Chair

Engineered liver tissue has the potential to support patients with hepatic dysfunction as well as provide an *in vitro* model of the liver for pharmaceutical drug development. Such applications mandate the use of primary hepatocytes- the parenchymal cell of the liver; however, hepatocytes rapidly lose viability and phenotypic functions *in vitro*. Co-cultivation of hepatocytes with nonparenchymal cells (NPC) has been reported to prevent this deterioration. Several aspects of this so-called ‘co-culture effect’ remain incompletely understood: the molecular mechanisms by which NPC stabilize liver-specific functions, dynamics of interaction (i.e. whether continuous NPC support is

required to maintain hepatic functions), and whether this model system can provide a useful tool for drug development. In this dissertation, gene expression profiling, electroactive surface chemistry, and microfabrication tools are used to answer these questions. First, a functional genomic approach utilizing gene expression profiling was developed to identify and validate molecular mediators that modulate liver-specific functions in co-cultures. Second, the role of one candidate, T-cadherin, was characterized in detail. T-cadherin was found to upregulate hepatocyte functions in vitro upon presentation in both cellular (CHO cells) and acellular (immobilized protein) contexts. Third, micropatterned electroactive substrates were used to selectively release fibroblasts at various time points from co-culture to probe the dynamics of cell-cell interaction. Results indicated that continuous fibroblast stimulation was required to maintain hepatic functions. Finally, soft lithography tools were utilized to develop miniaturized, multi-well co-culture models of the human and rat liver that were stable for several weeks. Utility of microscale tissues for evaluating species-specific drug metabolism, drug-drug interactions, and susceptibility to a panel of hepatotoxins was demonstrated. These studies will have an impact on developing functional models of liver tissue for use in fundamental hepatology, cell-based therapies for liver disease and pharmaceutical drug development. Furthermore, the methods developed here can be generalized to other tissues where cell-cell interactions modulate cellular fates.

CHAPTER 1

INTRODUCTION

1.1. Cell-Based Therapies for Liver Disease

1.1.1. Clinical Significance

Liver failure causes over 30,000 deaths every year in the United States alone, with over 2 million deaths estimated worldwide. When this process occurs in a healthy individual, it is termed acute liver failure (ALF) or fulminant hepatic failure (FHF). On the other hand, when loss of liver function complicates an existing chronic liver disease, the term ‘acute-on-chronic liver failure’ is commonly utilized [1]. Loss of liver function leads to deficiencies in synthesis of proteins, including clotting factors, albumin, and anti-proteases. Accumulation of ammonia and other toxic byproducts (i.e. bilirubin) normally metabolized by the liver is typically associated with multiple organ failure, jaundice, coagulopathy, encephalopathy, hepatic coma and brain death [2].

Until recently, ALF/FHF had a mortality rate in excess of 80% [3]; however, with better understanding and recognition of the condition, intensive care monitoring, and the advent and evolution of orthotopic liver transplantation (OLT), survival rates have improved considerably [4]. The most common indications for OLT are chronic hepatitis (inflammation), alcoholic liver disease and cirrhosis (scarring). Despite resourceful use of donor livers through split liver transplantation and living related donors, organs remain in scarce supply, and such shortage is getting worse over time due to the spread of hepatitis

C [5]. For instance, in 1999, of the 14,707 individuals on the U.S. wait list, only 4498 received liver transplants and 1709 died while waiting (United Network for Organ Sharing, UNOS, Annual Report, www.unos.org, 1999). As of January 2006, the wait list for liver transplants is at 17,863 individuals, second only to 68,428 individuals waiting for kidney transplants. Furthermore, patients receiving transplants are subjected to the risk of surgical complications, and the cost and complications associated with a lifetime of immunosuppressive therapy. Transplantation of genetically modified xenografts (baboon, pig livers) has been explored to alleviate the shortage in organ supply [6] [7]; however, problems with immune rejection and the risk of transmitting animal viruses to humans have hindered their clinical success [8, 9]. Therefore, even though liver transplantation continues to evolve as an effective treatment for liver disease, there is clearly a need for the development of alternative strategies.

1.1.2. Approaches

Cell-based therapies have been proposed as an alternative to whole organ transplantation, as a temporary bridge to transplantation, and/or an adjunct to traditional therapies during liver regeneration [1]. The three main approaches that have been proposed include: transplantation of isolated hepatocytes [10-12], implantation of tissue-engineered constructs [13, 14], and perfusion of blood through an extracorporeal (outside the body) bioartificial device containing parenchymal liver cells called hepatocytes [15-17] (Figure 1.1). Despite significant investigations into each of these areas, progress has been slow due to the propensity for isolated hepatocytes to rapidly lose viability and key liver-specific functions *in vitro* [18, 19].

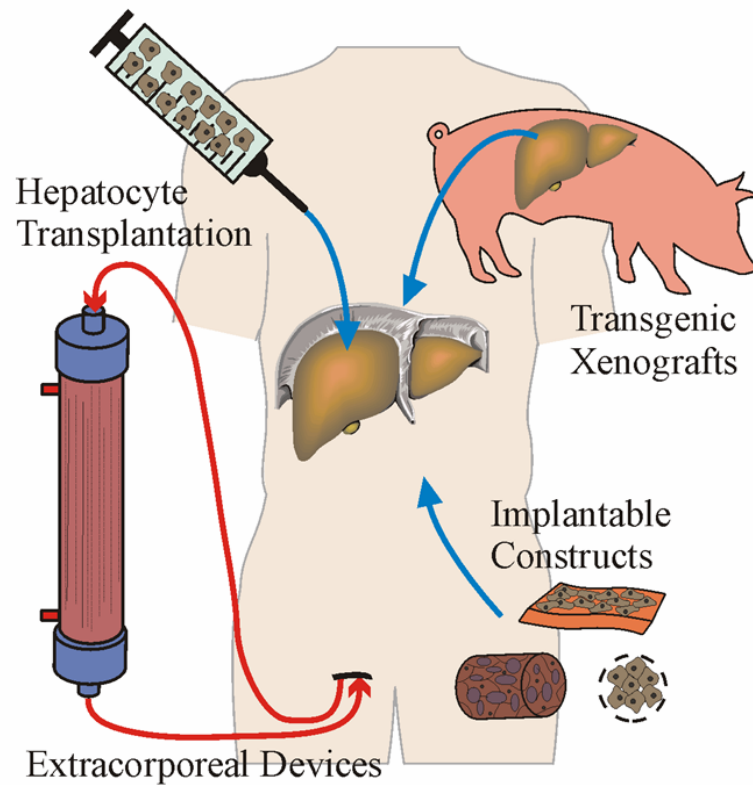


Figure 1.1: Cell-based therapies for liver disease. Extracorporeal liver devices perfuse patient's blood or plasma through bioreactors containing liver cells (typically primary hepatocytes). Hepatocytes are transplanted directly in suspension or implanted on scaffolds (natural or synthetic). Transgenic animals are being raised to harvest humanized livers for transplantation purposes in order to alleviate the shortage of human donor organs. From [1].

Hepatocyte transplantation coupled with gene therapy has been explored as a treatment to congenital metabolic defects [20]. Delivery of isolated hepatocytes in suspension is typically performed by intravenous or peritoneal administration. This mode of cellular therapy aims to take advantage of hepatocyte ability to regenerate and reconstitute liver functions upon engraftment into the spleen or liver. Critical elements in effective regeneration are a proper *in vivo* 'hepato-trophic' microenvironment and available sites for cell growth. Though progress has been made in identifying such elements in animals, studies in humans remain to be done. Inefficient cell engraftment (~10%), limited cell survival and an inadequate supply of human hepatocytes remain major limitations of isolated cell transplantation [9]. Although transplantation studies in animals are ongoing, only a few reports have explored utility in human-specific acute liver failure.

Tissue engineering of implantable cellular constructs is another emerging cell-based therapy for liver disease; however, significant limitations have to be overcome before this approach can become a clinical reality. Being anchorage-dependent cells, hepatocytes are immobilized on natural and synthetic scaffolds, encapsulated in aggregates, or cultured *ex vivo* to form liver 'organoids' and surgically transplanted [21-26]. Despite advances in culture techniques for hepatocytes and an improved understanding of tissue morphogenesis *in vitro*, tissue engineering of the liver shares many limitations with the cell transplantation arena: inadequate hepatocyte supply, immune rejection, and lack of long-term viability [9]. Furthermore, implantable constructs face additional challenges such as transport limitations due to lack of a vasculature, decline of phenotypic functions in hepatocytes upon isolation from the liver's *in vivo* microenvironment, and the ability of tissues to reorganize over time [27]. To our knowledge, no attempts have been made to use tissue-engineered constructs to treat liver disease in humans. In the

future, engineered implantable constructs may be able to precisely regulate several aspects of the hepatocyte phenotype in a spatio-temporal manner once investigators have obtained a more fundamental understanding of the determinants of liver-specific gene expression in hepatocytes.

Extracorporeal flow circuits have also been used to provide temporary liver support to patients while they wait either for a whole organ transplant or for their liver to regenerate itself (for review see [28] and [1]). Non-biological approaches utilizing hemoperfusion or hemodialysis over charcoal have shown limited success, presumably because they lack the essential metabolic and synthetic capability of the liver [29]. It is now widely recognized that incorporation of liver cells (i.e. hepatocytes) into extracorporeal devices is important for clinical efficacy [9]. Though device designs including hollow fiber devices, flat plate systems, perfusion beds, and suspension reactors have shown encouraging results, their implementation into a clinical setting has been difficult [30-36]. Several hollow fiber based BALs have undergone clinical trials recently [37-40]; however, only moderate benefit was reported [9]. Furthermore, a conclusive measure of efficacy was confounded by factors like disease etiology and stage of encephalopathy. A successful bioartificial liver (BAL) design must include effective bidirectional transport, a stable cellular microenvironment and simple scale-up for clinical efficacy.

1.1.3. Cell Sourcing

The full complement of liver-specific functions required in cell-based therapies to positively affect clinical outcomes remains unknown. Functionality of devices is typically determined using surrogate markers of each class of liver-specific functions (i.e. detoxification, synthetic). The implicit assumption is that liver cells deemed 'stable' via

measurements of surrogate markers will be capable of performing other unmeasured or unknown functions that are essential in liver physiology.

Primary hepatocytes are the most widely utilized cells in engineered therapies [9]. Though human hepatocytes from non-transplantable livers are the preferred source for cell-based therapies, they are in limited supply. Despite liver's tremendous regenerative capacity *in vivo*, investigators have not been able to grow human hepatocytes *in vitro* with any considerable success. Thus, most devices that have undergone clinical trials use readily available porcine hepatocytes; however, aside from the fear of transmitting animal viruses to humans, there are considerable differences between animal and human hepatocytes in pathways of xenobiotic metabolism (i.e. cytochrome-P450 enzyme activity) [41]. The development of a highly functional liver cell line is an obvious strategy to overcome growth limitations of human hepatocytes *in vitro*. Several cell lines have been derived via immortalization of primary hepatocytes or from hepatocellular carcinomas. However, the risk of transferring oncogenic factors to patients (especially with implanted cells), along with abnormal levels and repertoire of liver-specific functions has limited the use of cell lines for cell-based therapies [42-44].

In light of cell sourcing problems, stem cells from within and outside the liver have been explored as expandable sources of liver cells (hepatocytes, biliary epithelial cells) [45-48]. Stem cells are self-renewing (replication into a daughter cell with equivalent developmental potential) and can differentiate into specialized cell types with proper microenvironmental stimuli. Potential stem cells sources for cell-based therapies are embryonic stem (ES) cells, liver progenitors and transdifferentiated non-hepatic cells [49-52]. Though ES cells may ultimately provide an unlimited source of hepatocytes, their differentiation down the human hepatic lineage has not been demonstrated with any considerable success. Oval cells are bipotential, committed progenitors that can

repopulate the liver in injury models where proliferation of mature liver cells is impaired (i.e. primary biliary cirrhosis) [53]. Even though oval cells can propagate in culture, some transplantation studies demonstrate that their capacity to repopulate the liver is less than mature hepatocytes [54]. There is also evidence that hematopoietic stem cells (HSC) from bone-marrow can differentiate into hepatocytes in vitro without fusion (i.e. merging of two cells into one) [55]. However, in vivo work by several groups has shown that bone marrow transplantation by itself cannot generate sufficient numbers of hepatocytes for clinical efficacy [51]. In addition to ES cells, oval cells and HSC, multi-potent adult progenitor cells (MAPC) and monocytes have also been shown to give rise to hepatocyte-like cells in vitro [48, 56]. In spite of tremendous promise, the field of liver stem cells remains highly contentious and many challenges (biological and regulatory) have to be overcome before any type of stem cell (including ES cells) will become a source of large populations of terminally differentiated hepatocytes.

Regardless of the cell source, maintenance of long-term liver-specific functions in mature hepatocytes in vitro will be crucial to the clinical success of cell-based therapies for liver disease. Primary hepatocytes are notoriously difficult to maintain in culture as they rapidly lose viability and phenotypic functions [57, 58]. It is therefore imperative to gain a fundamental understanding of the cues that modulate liver-specific functions in an attempt to engineer the appropriate microenvironment for hepatocytes. Such an insight could improve the efficacy, life-time and cost-effectiveness of therapies utilizing engineered liver tissues.

1.2. The Liver

1.2.1. Structure

The liver is an organ of the digestive tract and is located in the abdominal cavity. It is the second largest organ of the body (skin being the largest), weighs ~1200-1600 grams in an adult human, and receives ~25% of the cardiac output [59]. Anatomically, it is separated into a large right and a small left lobe (Figure 1.2A). The blood supply to the liver comes from two major blood vessels on its right lobe: the hepatic artery (one-third of the blood) and the portal vein (two-thirds). The portal vein brings nutrient- and hormone-rich venous blood from the spleen, pancreas, and small intestines to the liver for processing before entry into the systemic circulation. The hepatic veins drain directly into the inferior vena cava posterior to the liver. The liver possesses a remarkable capacity to regenerate itself after injury. Within a few weeks after partial hepatectomy (surgical removal of two-thirds of the liver), liver mass can return to pre-surgery levels [60].

In order to engineer a microenvironment for liver cells that maintains their key phenotypic functions, one can look at the precisely defined architecture of the liver in vivo where hepatocytes interact with extracellular matrix, nonparenchymal cells and soluble factors (i.e. hormones). In the repeating functional unit of the liver called the lobule, hepatocytes are arranged in unicellular plates along the sinusoid where they experience homotypic cell interactions (Figure 1.2B). Lobules are polyhedrons (typically pentagonal or hexagonal) that are centered on a draining central vein. Portal triads at each corner of a lobule contain portal venules, arterioles and bile ductules. Sinusoids are small capillaries coursing through the space of Disse which lacks a basement membrane and is lined by a fenestrated endothelium. Hepatocytes constitute ~70% of the liver mass. Several types of junctions (i.e. gap junctions, cadherins, and tight junctions) and

bile canaliculi at the interface of hepatocytes facilitate the coordinated excretion of bile to the bile duct and subsequently to the gall bladder. Several types of nonparenchymal cells including stellate cells, cholangiocytes (biliary ductal cells), fenestrated sinusoidal endothelial cells, and Kupffer cells (macrophages) interact with hepatocytes to modulate their functions (Figure 1.3). Furthermore, hepatocytes are sandwiched between layers of extracellular matrix in the space of Disse, the composition of which varies along the length of the sinusoid [61]. Finally, physiochemical gradients (i.e. oxygen, hormones) provide hepatocytes in various parts of the sinusoid with different functions. Therefore, a precisely defined micro-architecture, coupled with specific cell-cell and cell-matrix interactions allows the liver to carry out its many diverse functions.

1.2.2. Functions

The liver can be simply described as the chemical factory of the body with over 500 functions. Some of these functions include protein synthesis (albumin, clotting factors), cholesterol metabolism, bile production, glucose and fatty acid metabolism, and detoxification of endogenous (bilirubin, ammonia) and exogenous (drugs and environmental compounds) substances. Subset of liver-specific functions (i.e. detoxification) has to be retained in an engineered hepatic tissue for it to be effective in cell-based therapies for liver disease.

The liver is the major organ for the biotransformation of xenobiotics, which can enter the body either intentionally (drugs) or unintentionally (environmental toxins). Xenobiotics undergo three phases of metabolism in hepatocytes. Phase I is the first-pass metabolism of lipophilic compounds into water-soluble metabolites for the purpose of removal from the body. Phase I reactions are mainly mediated by the cytochrome P450 enzyme family (CYP450) which specializes in oxidation and reduction reactions. The key

CYP450 isoforms in human liver include 1A2, 2A6, 2C9, 2C19, 2D6, 2E1 and 3A4. Of these enzymes, CYP3A4 is present in the highest quantity and participates in the biotransformation of over 50% of current xenobiotics. Phase II enzymes conjugate highly polar molecules such as glucose, sulfate or glutathione to xenobiotics and/or their metabolites. The highly polar products of phase II are transported out of hepatocytes via the bile canaliculi into the bile, or they are released back into the blood for excretion via the kidneys (sometimes referred to as Phase III). Metabolites can be de-conjugated by gut bacteria and reabsorbed, which leads to a repeat of phase I-III metabolism in the liver (sometimes called enterohepatic recirculation). Though the aforementioned sequence of events in the liver is typically referred to as ‘metabolic detoxification’, many xenobiotics can be metabolized into pharmacologically active or highly toxic compounds [41].

Within the liver lobule, hepatocytes are partitioned into three zones based on morphological and functional variations along the length of the sinusoid from the portal triad to the central vein [62]. Zonal differences have been observed in many hepatocytes functions, including oxidative energy metabolism, carbohydrate metabolism, lipid metabolism, nitrogen metabolism, bile conjugation, and xenobiotic metabolism [63]. Such compartmentalization of gene expression is thought to underlie the liver’s ability to operate as a ‘glucostat’. Zonal differences in expression of CYP450 enzymes has also been implicated in the zonal hepatotoxicity observed with some xenobiotics [64]. Possible modulators of zonation include blood-borne hormones, oxygen tension, pH levels, extracellular matrix composition, and innervation.

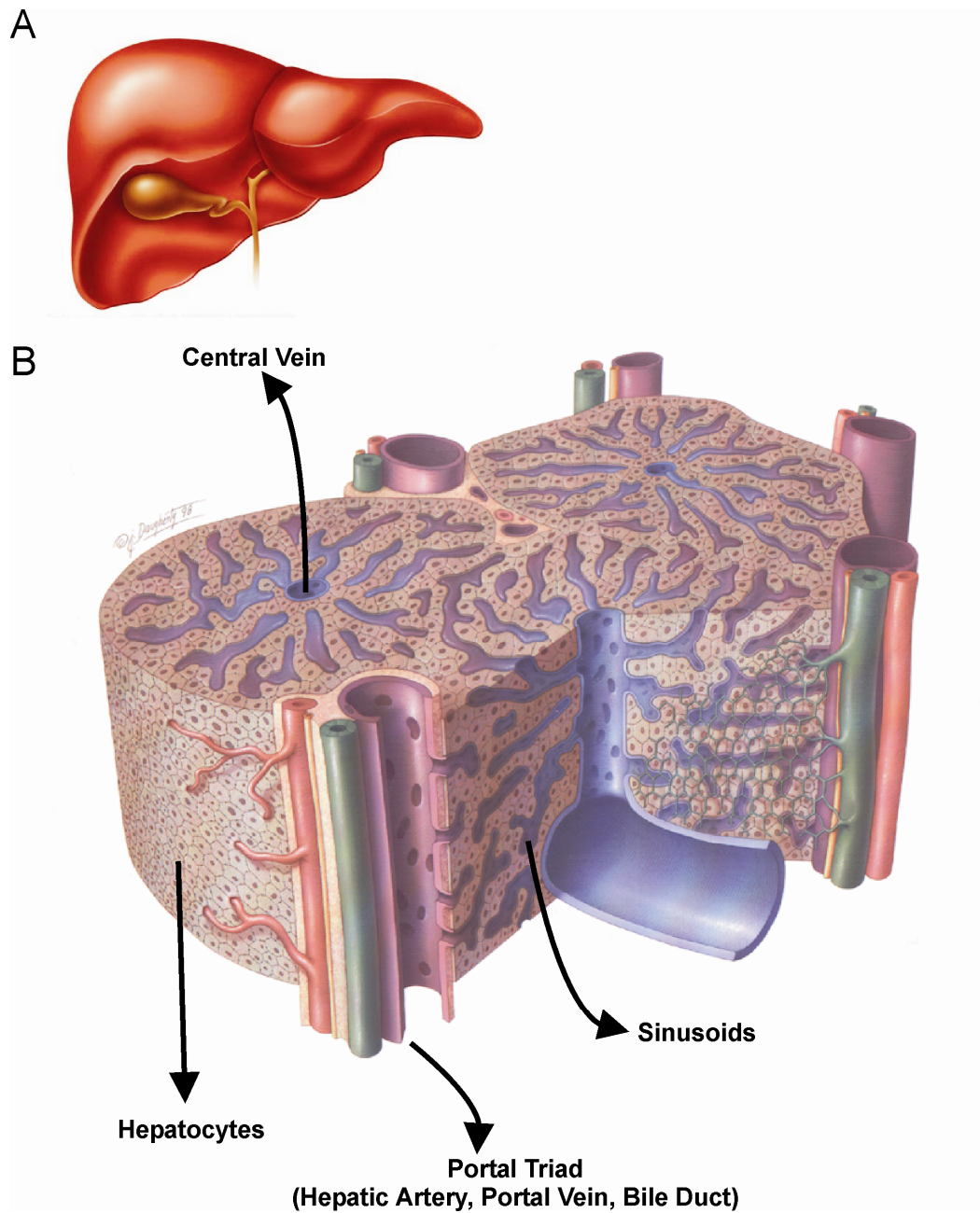


Figure 1.2: Liver structure. **A)** Schematic of the liver with its large right and small left lobes. **B)** Schematic showing the structure of the repeating unit of the liver, the lobule. Hepatocytes are arranged in cords along the length of the sinusoid. Nutrient and oxygen rich blood flows into the sinusoid from the intestine via the portal vein. About $\frac{1}{4}$ of the liver blood supply comes from the hepatic artery. After being processed by the hepatocytes, the blood enters the central vein.

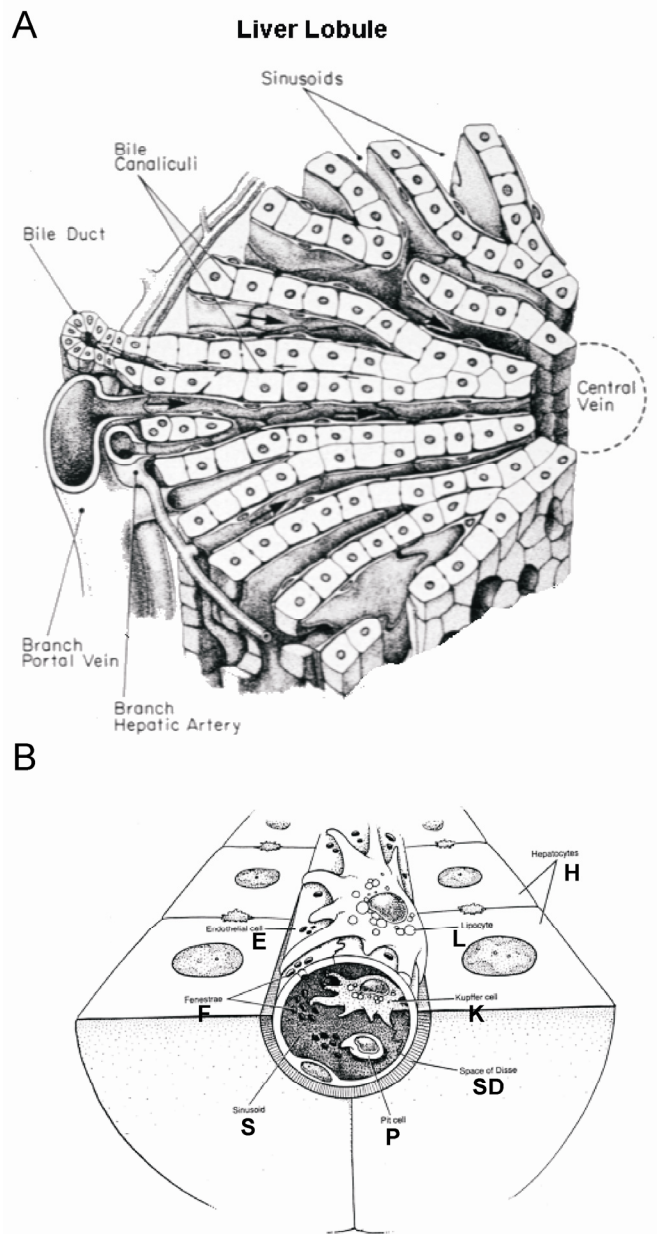


Figure 1.3: Cell-cell interactions in the liver. **A)** Liver lobule with hepatocytes arranged in cords. Bile canaliculi at the interface of hepatocytes facilitate the coordinated excretion of bile to the bile duct and subsequently to the gall bladder. **B)** The adult consists of differentiated hepatocytes (H) separated from a fenestrated endothelium (E) by the Space of Disse (SD). Lipocytes (stellate or Ito cells) are elaborate, extensive processes that encircle the sinusoid (L). Biliary ductal cells or cholangiocytes contact hepatocytes toward the end of the hepatic sinusoid (not depicted); Kupffer macrophages (K), and Pit cells (P, a type of natural killer cell) are free to roam through the blood and tissue compartment. Thus, the adult liver provides a scaffold for many complex cell–cell interactions that allow for effective, coordinated organ function. Adapted from [65].

1.3. Cadherins

1.3.1. Structure and Mechanism of Signaling

Cadherins are a diverse superfamily of molecules that mediate calcium dependent cell-cell adhesion in all solid tissues of an organism. Members of this superfamily include classical cadherins, desmosomal cadherins, proto-cadherins, 7TM cadherin, T-cadherin, and some other cadherin-related molecules, such as the FAT protein of *Drosophila*. The majority of cadherins are single pass transmembrane glycoproteins whose N terminus is located outside the cell while the C-terminus is situated intracellularly. Classical cadherins have five repeating extracellular units along with a highly conserved cytoplasmic domain that is linked to the cell actin cytoskeleton via linker catenin molecules (Figure 1.4) [66]. Cell-cell adhesion occurs predominantly through homophilic interaction between cadherin family members; however, heterophilic interactions have been demonstrated with integrins, growth factor receptors and other cadherins [67]. Cadherin contacts have been observed between different cell types in model systems such as invading melanoma and surrounding endothelia, migration of oligodendrocytes over astrocytes, and between kidney epithelia and fibroblasts [68-70].

Research into the possible roles of cadherins has focused heavily on their adhesive properties during tissue formation. For instance, cell sorting and condensation during embryogenesis are commonly attributed to cadherins. Recently, cadherins have been implicated in regulating cellular fates such as differentiation, growth, and apoptosis [71-73]. By bringing opposing membranes of neighboring cells in close proximity, cadherins may allow secondary membrane-bound proteins to interact and cause signaling events [74]. Furthermore, with their ability to control cell polarization, cadherins could affect signal transduction by restricting spatial mobility of membrane-bound proteins.

Lastly, cadherins may themselves act as receptors or ligands to cause direct signaling events. Even though the cytoplasmic domain of cadherins generally lacks any enzymatic activity, its association with another co-receptor (i.e. transmembrane tyrosine phosphatases) or intracellular signaling molecules (i.e. catenins, adaptor protein SH2) can mediate signal transduction [74-76]. For example, β -catenin can transduce signals to the nucleus by interacting with TCF transcription factors.

1.3.2. Role in Differentiation

Several lines of evidence using function-blocking antibodies, forced expression of exogenous protein, or genetic manipulation indicate that cadherins, in addition to physically linking cells together, play an important role in cellular differentiation [71, 74]. For instance, the loss of functional E-cadherin shifts epiblast cells of mouse embryos from an epithelial to mesenchymal phenotype [73], disrupts thymocyte differentiation [77], and interferes with the maturation of the erythroid lineage [78]. Function-blocking antibodies directed against N-cadherin not only disrupt differentiation of epiblast cells into skeletal muscle [72], but also appear to affect heart morphogenesis and the differentiation of cardiomyocytes [79]. Studies with P-cadherin knockout mice suggest that this cadherin plays a role in negative growth control of the mammary gland, in addition to maintaining the undifferentiated state of this tissue [80]. In vitro studies with E-cadherin negative embryonic cells (ES) that were “rescued” with different cadherins have implicated cadherins in direct formation and differentiation of various tissues. For example, constitutive expression of E-cadherin in these ES cells results in the formation of epithelia exclusively, expression of N-cadherin results in formation of neuroepithelia and cartilage, and expression of R-cadherin results in the formation of striated muscle and epithelia [81, 82].

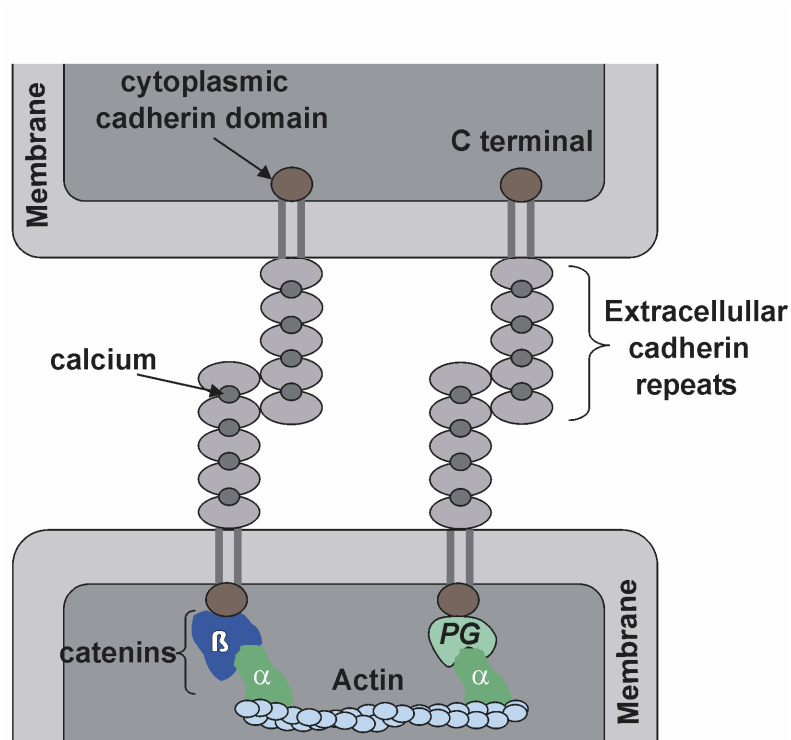


Figure 1.4: Structure of classical cadherins. Cadherins are cell-cell adhesion molecules with five extracellular repeats, a transmembrane domain and a cytoplasmic region that links to cytoskeletal actin with catenin linker molecules. From [58].

1.3.3. Role in the Liver

Cadherins mediate cell-cell interactions in both the developing and adult liver. In the liver, hepatocytes express E-cadherin (epithelial), N-cadherin (neural), and LI-cadherin (liver-intestine) [83]. Sinusoidal endothelial cells express VE-cadherin (vascular-endothelial) and cholangiocytes express E-cadherin [83, 84]. In regeneration and hepatocarcinoma, E-cadherin is dynamically regulated in hepatocytes, suggesting it may play a role in hepatic functions [85, 86]. In vitro, E-cadherin has been postulated to play a role in homotypic hepatocellular interactions [87], formation of intact bile canaliculi [88], receptivity to extracellular matrix signals [89], and morphogenesis of 3-dimensional aggregates [86, 90]. In hepatocyte-nonparenchymal co-cultures, E-cadherin expression in L-929 chaperone cells was recently shown to correlate positively with induced liver-specific functions in primary rat hepatocytes [91].

1.3.4. T-cadherin

T cadherin (truncated cadherin) is unique compared to classical cadherins because it lacks both the transmembrane and cytoplasmic regions [92]. Instead, it is anchored to the membrane via a GPI moiety (glycosylphosphatidylinositol). Even though T-cadherin mediates calcium-dependent adhesion, it is not concentrated at cell-cell junctions of transfected cells in culture. Adhesion by this truncated cadherin is compromised by treatment with enzymes (i.e. phosphatidylinositol-specific phospholipase C, PI-PLC) that remove GPI-anchored proteins. T-cadherin is highly expressed in the human heart, expressed to a lesser extent in the brain, lung, muscle and kidney, and slightly detectable in the pancreas and liver [93]. The amino acid motif of T-cadherin has been well conserved through vertebrate evolution, implying that that it may have a biological significance in higher animals. T-cadherin has been shown to have diverse roles in

physiology and pathophysiology, which include: negative guidance cue for motor axon projections [94], tumor suppressor factor in various types of cancer [95-97], an atypical lipoprotein-binding protein [98]. However, the role of T-cadherin in the liver remains largely unexplored. Recently, T-cadherin was shown to bind to high molecular forms of the hormone adiponectin [99], which synergies with insulin in the liver to increase glycogen stores and inhibit gluconeogenesis. Lack of a cytoplasmic domain, coupled with the presence of T-cadherin in membrane domains enriched in other GPI-anchored proteins as well as signaling molecules such as SRC family kinases, suggests that this molecule may be involved more in intercellular signaling instead of adhesion, possibly as a sensor of the local microenvironment [66, 100, 101].

1.4. Co-Cultivation of Hepatocytes with Nonparenchymal Cells

Heterotypic interactions between parenchymal cells (i.e. hepatocytes) and their nonparenchymal neighbors are known to be important in the liver *in vivo*. The formation of liver from the endodermal foregut and mesenchymal vascular structures during development is believed to be mediated by heterotypic interactions [102, 103]. In the adult liver, hepatocytes interact with a variety of nonparenchymal cell types including sinusoidal endothelial cells, biliary ductal cells, Kupffer macrophages and fat-storing Ito cells (also called stellate cells). These nonparenchymal cells modulate cell fate processes of hepatocytes under both physiologic and pathophysiologic conditions [104, 105].

In vitro, hepatocyte viability and a variety of liver-specific functions (i.e. albumin secretion, urea synthesis, and cytochrome-P450 activity) can be stabilized for several weeks upon co-cultivation with a plethora of nonparenchymal cell types (the ‘co-culture effect’, see Figure 1.5) [65]. Hepatocytes in co-cultures maintain the polygonal morphology, distinct nuclei and nucleoli, well-demarcated cell-cell borders, and a visible

bile canaliculi network for many weeks as typically seen in freshly isolated cells and in vivo. On the other hand, hepatocytes in pure monolayers rapidly (hours) lose viability, while surviving cells spread out to adopt a fibroblastic morphology [57]. Hepatocyte-nonparenchymal co-cultures have been utilized to investigate various physiologic and pathophysiologic processes including host response to sepsis [106, 107], mutagenesis [108, 109], xenobiotic toxicity [110, 111], response to oxidative stress [112], lipid metabolism [113, 114], and induction of the acute phase response [115, 116]. Co-cultures have also gained particular interest due to their relevance to both hepatic tissue engineering and development of in vitro models for pharmaceutical drug screening [32, 117].

Hepatocytes from multiple species (i.e. chick embryo, rat, mouse, porcine, human) have been shown to be stabilized in co-culture [58, 110, 118-122]. Additionally, a variety of both liver- and non-liver-derived nonparenchymal cell types have been reported to induce hepatic function in co-culture to various extents (Table 1.1) [108, 117, 120, 122-127]. In particular, murine 3T3 fibroblasts have been shown to induce the highest levels of albumin secretion in primary rat hepatocytes, followed by rat liver endothelial cells, rat dermal fibroblasts, rat liver epithelial cells and bovine aortic endothelial cells [65]. Induction has been reported by nonparenchyma (both primary and immortalized) derived from a different species than the primary hepatocytes, suggesting possible conservation of underlying mechanisms [65, 120, 128, 129]. Lastly, negligible hepatocyte growth occurs in co-cultures containing non-liver-derived nonparenchymal cells, which suggests that growth-arrest of these cells prior to seeding onto hepatocyte cultures may allow maintenance of constant cell numbers towards precise study of both sub-populations [65].

Table 1.1: Nonparenchymal cell types known to stabilize liver-specific functions in primary hepatocytes. Primary hepatocytes are stabilized to various degrees by liver- and non-liver-derived nonparenchyma. Liver-derived cells include those found in the adult liver [stellate cells, rat liver epithelial cells of presumed biliary origin (RLECs) and sinusoidal endothelial cells]. Non-liver-derived nonparenchymal cell types include murine 3T3 fibroblasts, lung and kidney epithelia, and bovine aortic endothelia. From [65].

Liver derived	Non-liver derived
RLECs	Bovine aortic endothelia
Stellate cells	Canine kidney epithelia
Sinusoidal endothelial cells	Chinese hamster epithelia
Kupffer macrophages	Embryonic murine fibroblasts (3T3)
Nonparenchymal liver portion	Human fibroblast
	Human lung epithelia
	Human venous endothelia
	Monkey kidney epithelia
	Rat dermal fibroblast

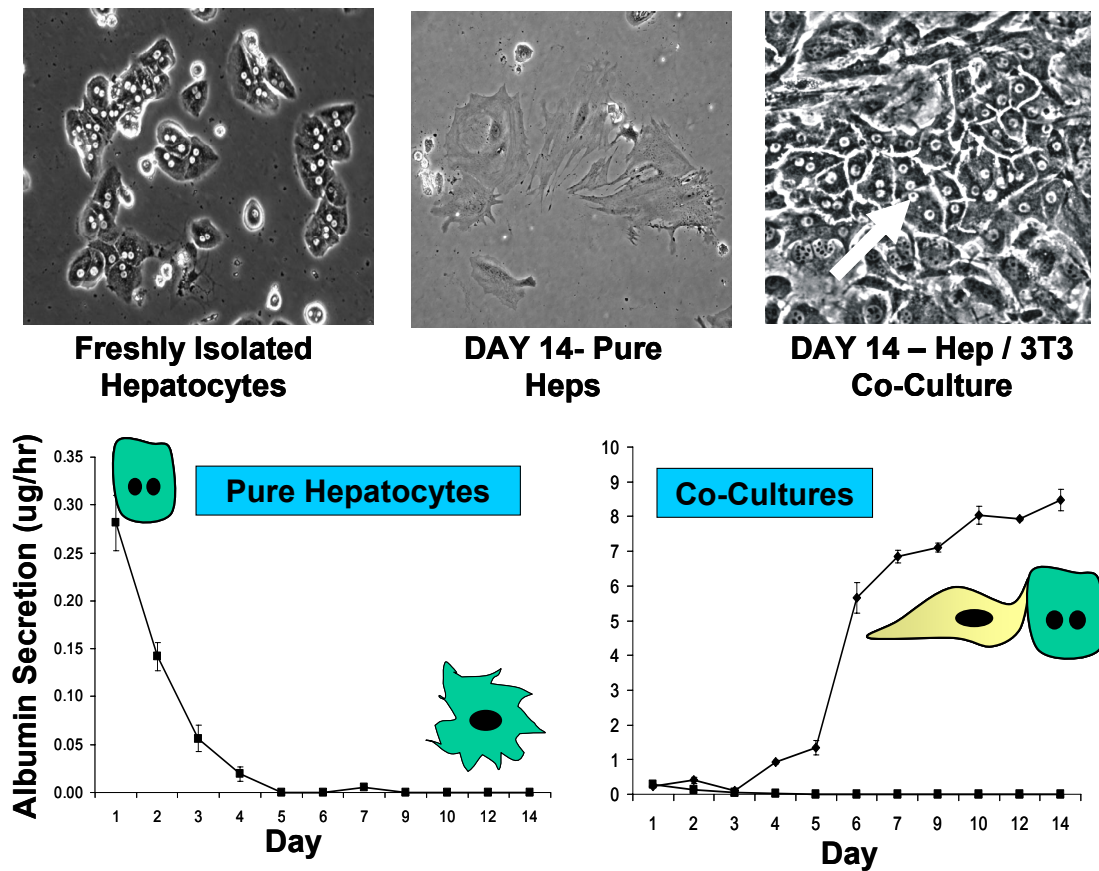


Figure 1.5: The co-culture effect. Primary hepatocytes from a variety of species (human, rat, mouse, porcine) lose viability and liver-specific functions in culture upon isolation from the microenvironment of the liver. Co-cultivation with nonparenchymal cells from within and outside the liver has been shown to stabilize a variety of hepatic functions. Shown here is loss of albumin secretion (marker of liver's synthetic ability) in primary rat hepatocytes cultured on collagen. However, an upregulation of albumin secretion is seen when these hepatocytes are co-cultivated with 3T3 murine embryonic fibroblasts. Furthermore, hepatocytes in co-cultures maintain the polygonal morphology (see arrow), visible bile canaliculi and distinct nuclei and nucleoli as seen in freshly isolated cells and in vivo. On the other hand, hepatocytes in pure culture adopt a fibroblastic morphology. Error bars represent standard error of the mean ($n=3$).

1.4.1. Mechanisms Underlying the Co-Culture Effect

In spite of significant investigation over the last two decades, the precise molecular mechanisms underlying the ‘co-culture effect’ have not been clearly elucidated. The potential molecular mediators of cell-cell communication include: soluble factors (i.e., cytokines), insoluble extracellular matrix molecules (i.e. collagen) and cell-cell contact molecules (i.e. membrane-bound cadherins). Studies attempting to assess the contribution of soluble factors in co-culture models have produced contradictory results, while nonparenchymal-conditioned culture medium has been shown to be universally ineffective in stabilizing hepatocyte functions [65, 124, 130, 131]. Studies on extracellular matrix-mediated effects on liver-specific gene expression in co-cultures have been inconclusive. Extracellular matrix components such as reticulin fibers, collagen I, IV, fibronectin, laminin, and entactin have all been observed in co-cultures [126, 132, 133]. Though matrix deposition patterns specific to co-cultures have been demonstrated, a causative relationship has not been shown [125, 133, 134].

Until recently, the role of heterotypic cell-cell contact in induction of liver-specific functions in hepatocyte-nonparenchymal co-cultures has remained unclear. Mesnil et al [135] demonstrated that hepatocytes in close proximity to epithelial cells in sparse cultures maintained viability and differentiated functions as compared to hepatocytes lacking heterotypic contact. Rigorous evidence supporting the role of cell-cell contact as a potential mediator of the co-culture effect was reported in 1991 by Corlu et al [136]. These authors identified a novel cell surface protein, LRP (liver-regulating protein), that played a role in maintenance of hepatocyte functions in co-culture with liver epithelial cells. Albumin secretion, cytoskeletal organization, and ECM deposition were modulated by addition of a monoclonal antibody against LRP; however, such modulation occurred only when the antibody was added early in culture. Finally, of the different hepatocyte-

stabilizing nonparenchymal cell types tested, only specific ones immunostained positive for LRP (sinusoidal cells and Ito cells were positive, vascular endothelia and biliary ductal cells were negative), suggesting that LRP is not the only molecular mediator of the co-culture effect [137].

Besides LRP, heterotypic cell-cell contact via gap junctions and cadherins has also been implicated in modulating hepatocyte functions in co-cultures. For instance, in one study, levels of connexin-43 protein (subunits that assemble to form gap junctions) in stellate cell sub-clones correlated with albumin messenger RNA levels in co-cultivated hepatocytes. Furthermore, functional heterotypic gap junctions between the two cell types were observed as demonstrated by microinjection of Lucifer Yellow [138]. The presence of gap junctional communication between hepatocytes and stellate cells *in vitro* may be similar to *in vivo* communication between these cell types [139]. However, heterotypic gap junctions have not been seen between hepatocytes and 3T3 murine fibroblasts in co-culture (our unpublished observations). In a study by Moghe and coworkers, levels of E-cadherin expressed by mouse 'chaperone' L-929 cells positively correlated with albumin and urea secretion by primary rat hepatocytes in co-culture [91]. In particular, L-929 cells expressing E-cadherin induced a 55 to 65% increase in hepatocyte functions upon co-culture as compared to E-cadherin deficient controls. Blocking antibodies against E-cadherin (specific to murine L-929) diminished such functional increases. Both heterotypic and homotypic E-cadherin junctions were seen via immunofluorescent staining. Notably, substantial differentiated function was observed in hepatocytes co-cultured with the E-cadherin null L-929 mutants. In addition, hepatocytes formed homotypic cadherins junctions via E-cadherin (hepatocyte-hepatocyte); yet high density hepatocyte cultures do not retain differentiated functions to

the extent seen in co-culture (our unpublished observations). For these two reasons, it is unlikely that E-cadherin acts alone to mediate the complete 'co-culture' effect.

In summary, several types of molecules have been implicated (receptors, gap junctions, E-cadherin, extracellular matrix molecules) in induction of hepatocyte functions by nonparenchymal cells. However, a complete molecular definition of the 'co-culture effect' remains undetermined. In the future, identification of critical molecules that modulate hepatocyte differentiation may have implications in hepatic tissue engineering, stem cell biology, and pathophysiology of liver disease. New approaches may be required to gain insight in this area.

1.5. MEMS (Micro-Electro-Mechanical Systems) as an Enabling Technology

Micro-Electro-Mechanical Systems (MEMS) are devices that combine electrical and mechanical components at the micron scale. Recently, microfluidics has augmented the functionality of such devices [140]. Since many biological species are on the length scale of MEMS devices, the interface between biology and microtechnology encompasses many diverse areas and levels of biological complexity. These include: DNA arrays (genes), immunoassays (proteins), miniaturized lab-on-a-chips (genes, proteins, and sensors), and finally the integration of live cells (bacterial and mammalian) with semiconductor materials and components [141-147]. Furthermore, microfabrication techniques have been utilized in biomedical research to exert control over cell adhesion at the 1-100 μm length scale. Such 'micropatterned' cultures have been used to study diverse phenomena such as: effects of cell spreading on cell fate [148], cell-cell interaction on differentiation [121], and surface topology on cell migration [149-151]. Microfabrication tools thus provide investigators with the ability to define the biochemical and cellular composition of a substrate on the micron scale [152].

1.5.1. Soft-Lithography

Microfabrication based strategies are routinely being extended to the area of “soft lithography”, which is based on printing and molding using polymeric stamps with the patterns of interest in bas-relief [153]. This particular technique extends the capability afforded by photolithography by allowing patterning of complex biologically-relevant molecules, fabrication of microfluidic devices, and patterning of live cells [154-156]. Polymeric devices such as stamps, channels, stencils on the 50 μm scale (biologically useful) can be created rapidly and inexpensively, and they can be reused for many applications.

PDMS (Polydimethylsiloxane) based stencils allow patterning of cells on homogenous or heterogeneous substrates [157]. Cells are seeded while the stencil is sealed to the substrate. Subsequent removal of the stencil allows the underlying unpatterned areas to be used for various purposes, including seeding of a secondary cell type or assessing cell migration. Stencils can be reused several times for many applications. Their production typically involves microfabrication of a master template via photolithography, which can be reused several hundred times.

1.5.2. Electroactive Substrates

Tools to spatially and systematically control different cell populations are crucial for mechanistic studies of heterotypic cell-cell signaling for applications such as reconstruction of functional tissue constructs *in vitro*. One particular tool utilizes a strategy that can release individual ligands (i.e. adhesive peptides) selectively from a self-assembled monolayer (SAM) of alkanethiolates on gold, which currently are the best class of substrates to control the structure, density and pattern of immobilized ligands [158-162]. The structure of ligands can vary depending on the application at hand. Ligands are attached to the SAM through a redox-active group that can undergo electrochemical

oxidation (using gold as working electrode) and subsequent cleavage to release the ligand into solution. Since SAMs are stable to the electrical potentials typically applied, they can be used to present multiple types of ligands, but release only a fraction. These dynamic substrates allow real-time control over cell-substrate and cell-cell interactions in order to mimic *in vivo*-like processes.

1.6. Drug Development

1.6.1. Development Pipeline

The drug development pipeline contains several phases, which include: therapeutic target identification and validation, lead compound identification, lead optimization, preclinical testing using *in vitro* tissue models and whole animal studies, and clinical trials in humans. Following demonstration of safety and efficacy in clinical trials, a new drug application (NDA) application is filed with the Food and Drug Administration (FDA). The drug is launched into the market once FDA approval is secured [163]. Recent estimates indicate that it takes nearly \$800 million dollars and 10-15 years of development time to bring a new drug to market [164].

New chemical entities enter the drug discovery process through combinatorial synthesis and rational drug design incorporating information about the target of action. High-throughput screening utilizing biochemical assays is used to identify leads which produce the required effect (i.e. binding to target protein) at high concentrations. Physicochemical properties such as solubility, lipophilicity, and stability are used as criteria for a secondary round of screening. Next, selected leads undergo ADME/Tox (absorption, distribution, metabolism, elimination and toxicity) characterization via *in vitro* tissue models in the optimization phase of drug development. *In vitro* systems

include caco-2 cell line for evaluation of intestinal absorption, and hepatocytes, microsomes or liver slices for evaluation of liver-specific metabolism and toxicity (see section 1.7 for details on liver models). Most drug candidates fail at this stage and only a few show sufficient safety and efficacy to merit further development. In vitro and in vivo studies with whole animals are carried out on the most promising candidates. Pharmacokinetic and metabolism data from these studies is then used to design clinical trials in humans [163] (Figure 1.6). Ultimately, a successful drug has several key characteristics, which include: adequate bioactivity, appropriate physiochemical properties to enable formulation development, an ability to cross crucial membranes, appropriate metabolic stability, and safety and efficacy in humans [165].

Compounds identified as ‘favorable’ in a screening campaign can provide the core structure around which hundreds of thousands of analogues are synthesized. An iterative process of screening and resynthesis identifies compounds with the proper balance of therapeutic activity and ADME/Tox properties. Typically, the amount of materials required and the cost associated with development increases substantially as chemicals progress through the phases of the drug development pipeline. Overall, the pharmaceutical industry spends ~\$0.2 billion on in vitro toxicology, \$1.3 billion on in vivo toxicology, and \$1.5 on ADME screening [165].

Progress in molecular biology coupled with the ready availability of genomic data has spurred remarkable advances in the identification of novel therapeutic targets. Furthermore, impressive technological developments have been made in the automation of combinatorial synthesis and high-throughput biochemical screening of lead compounds. As a result of these advances, a bottleneck has been created downstream in drug development. While whole animal models provide valuable in vivo data in later stages of drug development, they are too slow for real-time feedback in a drug discovery

campaign. Additionally, significant animal-to-animal variability typically necessitates five to ten animals per compound per dose, sometimes in both genders [166]. Therefore, incorporation of in vitro, high-throughput ADME/Tox screening into drug development provides several advantages: earlier elimination of potentially toxic drugs, reduction in variability by allowing hundreds of experiments per animal, and human liver models without patient exposure.

Almost 90% of lead candidates identified by current in vitro screens do not become successful drugs [167, 168]. Of the lead compounds that enter Phase I clinical trials, 50% fail to become drugs due to unforeseen liver toxicity and bioavailability issues [165, 167]. Therefore, much progress needs to be made in developing in vitro tissue platforms that not only enable high-throughput ADME/Tox screening, but are also highly predictive of human-specific clinical outcomes. It is widely believed that the identification of problems early in drug screening represents the single largest cost-saving opportunity for the pharmaceutical industry [169].

1.6.2. Drug-Induced Liver Disease

Due to its major role in xenobiotic metabolism, the liver is a target for many chemical toxicants. Thus, drug-induced liver disease (DILD) represents a serious challenge for clinicians, the pharmaceutical industry and regulatory agencies worldwide [170]. Liver toxicity due to drugs or toxicants can be either due to accumulation of the parent compound or due to toxic metabolites that damage proteins and/or nucleic acids in liver cells. Exogenous compounds can produce all forms of acute and chronic hepatobiliary disease which includes hepatitis, cholestasis, steatohepatitis, cirrhosis, and hepatocellular carcinoma [171]. DILD can be predictable (high incidence and dose-related) or unpredictable (low incidence and may or may not be dose related).

Unpredictable reactions can be viewed as either immune-mediated hypersensitivity or idiosyncratic and may be difficult to detect even in clinical trials due to the latency (weeks to months) and low incidence (1 in 500 to 1 in 50,000) [170].

DILD is the leading cause of acute liver failure (ALF) in the United States alone (50% of the cases) [4]. Acetaminophen (analgesic found in many over-the-counter medications such as Tylenol) accounts for the bulk of such cases. About 10% of DILD-induced ALFs are due to idiosyncratic toxicity, which occurs in a small proportion of individuals exposed to a drug, probably due to unique environmental and genetic factors [170]. Drug-induced hepatotoxicity is also the leading cause of drug failures in clinical trials [172]. Lastly, post-market occurrence of drug hepatotoxicity is the leading cause of market withdrawals, modifications of use and label warnings [173].

Occurrence of drug hepatotoxicity in clinical and post-market settings has been largely attributed to the inadequacy of animal models to predict human-specific liver responses [174]. Several reasons for such inadequacy have been proposed, including: species-specific differences in drug metabolism pathways, lack of human-relevant environmental and genetic factors in well-controlled laboratory settings, and inability of healthy animals to model humans with specific diseases [175]. The pharmaceutical industry has responded by incorporating a variety of *in vitro human* liver models in the ADME/Tox screening phase (see next section for details). However, several limitations of existing human liver models necessitate the building of better models that can help eliminate problematic compounds earlier in drug discovery to reduce development costs, increase likelihood of clinical success, and reduce the risk for patient exposure to unsafe drugs [165].

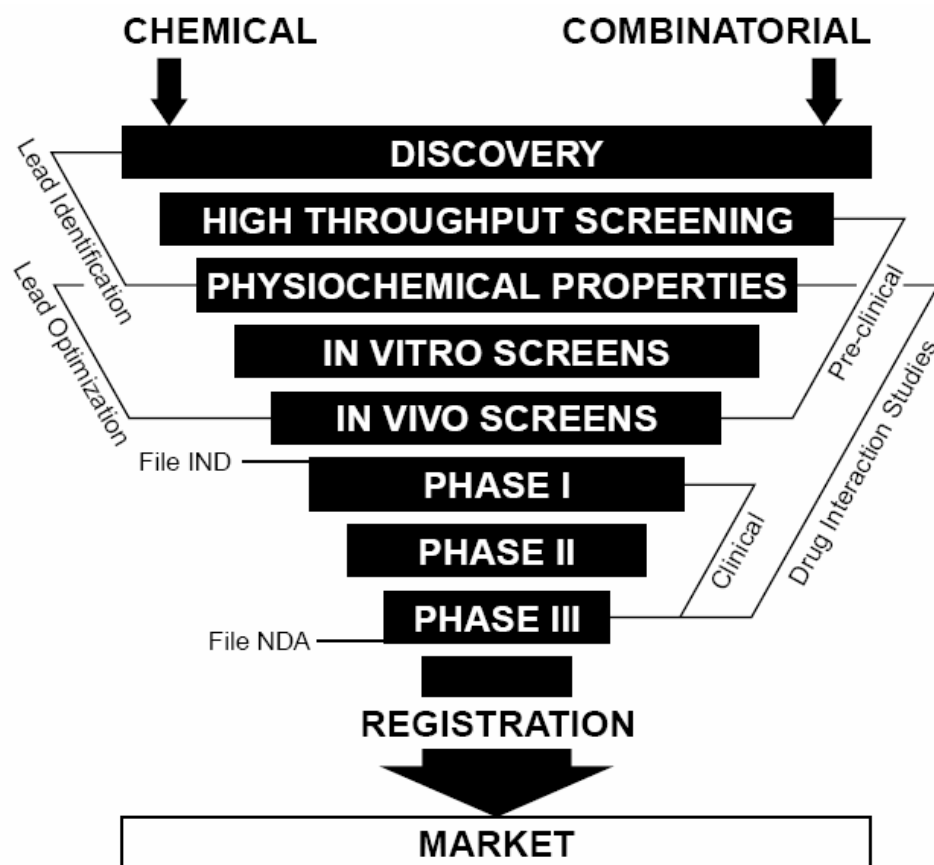


Figure 1.6: The drug development pipeline. Lead compounds are identified via high-throughput screening for activity against a chosen therapeutic target (typically biochemical assays). Then, a panel of screens with in vitro tissue models and in vivo studies in live animals are used to optimize leads for physicochemical as well as ADME/Tox (absorption, distribution, metabolism, elimination, toxicity) properties. In order to conduct clinical trials with humans (phases I-III), an IND (investigational new drug) application is filed for a particular drug with the appropriate balance of therapeutic activity and ADME/Tox properties. A new drug application (NDA) is filed with regulatory agencies (i.e. Food and Drug Administration) following clinical trials. Upon approval, the drug is launched into the market. From [163].

1.7. In Vitro Liver Models for Drug Development

Several in vitro liver models have been used for short-term (hours) investigation of xenobiotic metabolism and toxicity [165, 176]. Perfused whole organs, liver slices and wedge biopsies maintain many aspects of liver's in vivo microenvironment and architecture; however, they suffer from limited drug availability to inner cell layers, and are not suitable for enzyme induction studies due to limited viability (<24 hours) [41, 177-179]. Furthermore, whole organs do not reduce the number of animals required and are difficult to use in high throughput applications. Purified liver fractions (i.e. microsomes containing CYP450 enzymes) and single enzyme systems (i.e. lymphoblastoid cell line expressing cDNAs for few drug metabolism enzymes), on the other hand, are used in high-throughput systems to identify enzymes involved in the metabolism of a particular drug [180, 181]; however, they lack the complete spectrum of gene expression and cellular machinery required for liver-specific metabolism and toxicity. Lastly, cell lines derived from hepatoblastomas (HepG2) or from immortalization of primary hepatocytes (HepLiu, SV40 immortalized) are finding limited use as reproducible, inexpensive models of hepatic tissue [42-44]. However, no cell line has been developed that maintains liver-specific functions at physiologic levels. Usually such cell lines are plagued by abnormal levels and repertoire of hepatic functions [165].

1.7.1. Primary Hepatocyte Culture Models

Due to the inadequacy of the aforementioned in vitro liver models, research has increasingly turned towards isolated hepatocytes for use in evaluation of xenobiotic metabolism and toxicity [176, 182-184]. Unlike microsomes, freshly isolated hepatocytes contain complete, undisrupted enzymes and cofactors. However, scarce availability and significant sample-to-sample variability of human donor livers have limited use of intact

hepatocytes in drug discovery and development. Since many companies routinely isolate 5 to 20 billion viable hepatocytes per human liver sample, there is a push in the liver community towards optimizing cryopreservation protocols which can be used to store hepatocytes for months. Cryopreserved human hepatocytes, besides enhancing convenience and ease of experimentation, can be used from the same batch for multiple experiments at different times and across laboratories, thereby reducing the variability associated with procured livers. The limited data available on cryopreserved human hepatocytes suggests that their post-thaw functions are similar to that of fresh hepatocytes [185, 186]. Additionally, protocols now exist which allow thawed hepatocytes in suspension to attach and spread on collagen-coated substrates, which may enhance their long-term utility.

Drug metabolism studies are routinely carried out with primary hepatocytes in suspension immediately (hours) following collagenase-mediated isolation from the liver. Studies have shown that the expression levels of key enzymes in suspended hepatocytes are close to *in vivo* levels [187, 188]. However, since hepatocytes are anchorage-dependent cells, suspension cultures can only be used for short-term studies. In order to assess the long-term (days to weeks) effects of xenobiotics on liver-specific metabolism and toxicity, adherent cultures of hepatocytes are required. In spite of their recognized advantages, primary hepatocytes are notoriously difficult to maintain in culture as they rapidly lose viability and phenotypic functions (i.e. CYP450 activities) upon isolation from their *in vivo* microenvironment [57, 58, 65]. Such 'de-differentiated' hepatocytes are typically unresponsive to enzyme inducers, which severely limits their use [189].

Over the last couple of decades, investigators have been able to stabilize several hepatocyte functions using soluble factor supplementation, extracellular matrix manipulation, and co-culture with various liver and non-liver derived nonparenchymal

cell types. Addition of low concentrations of hormones, corticosteroids, cytokines, vitamins, or amino acids has been shown to stabilize a few liver-specific functions in hepatocytes [190-192]. Additionally, some complex serum-free hormonally defined culture media (serum-free HDM) have been proposed for culturing hepatocytes [193]; however, such formulations do not allow for the satisfactory maintenance of liver-specific gene expression and differentiated functions in hepatocytes beyond a short period [176]. In rat hepatocyte cultures treated with serum-free HDM, only transitory improvements in plasma protein production rates and drug metabolism enzyme levels have been previously reported [194, 195].

Presentation of extracellular matrices of different compositions and topologies can also induce phenotypic functions in hepatocytes [196-199]. For instance, hepatocytes from a variety of species (human, mouse, rat) secrete albumin when sandwiched between two layers of rat tail collagen-I (double-gel) (our unpublished data and [197]). However, a recent study by Sivaraman et al has shown that CYP450 activities in rat hepatocytes decline over time in the double-gel model [165]. Furthermore, the presence of an overlaid layer of collagen presents transport barriers for drug candidates [1]. Culture of hepatocytes on a substratum coated with Matrigel (laminin-rich basement membrane extract derived from a mouse sarcoma) induces formation of adherent 3-dimensional heterogeneous (in size) spheroids and leads to retention of key hepatocyte functions including CYP450 activity [200]. Additionally, confluent hepatocyte monolayers on collagen subsequently coated with a thin layer of Matrigel (i.e. Matrigel overlay) have shown utility in evaluating xenobiotic-mediated CYP450 induction *in vitro* [182]. While Matrigel can induce limited functions in rodent hepatocytes, it appears to have fewer effects on human hepatocytes [41]. Furthermore, the significance of effects due to Matrigel is difficult to interpret since contamination with proteins, hormones, and

growth-factors has been previously reported [176, 201]. Lastly, Matrigel substratum and overlay modifications allow rat hepatocytes to survive and function for a few more days than in conventional monolayers on collagen; however, an imbalance of phase I/II detoxification processes has been reported to occur in such Matrigel-based platforms (i.e. decline in CYP450 activities) [202].

Cell-cell interactions, both homotypic (hepatocyte-hepatocyte) and heterotypic (hepatocyte-nonparenchymal) have also been shown to improve viability and differentiated functions of hepatocytes. Culture of hepatocytes in multi-layer spheroidal aggregates (3-dimensional) suspended in incubation medium has been shown to induce few hepatic functions [203-205]. However, spheroidal-based models suffer from major limitations, which have limited their utility in drug development applications. Such limitations include: fusion of small heterogeneous spheroids into large aggregates; cell death in aggregate center due to insufficient transport of nutrients and oxygen; difficulty in precise estimation of cell number per aggregate; and, limited survival of hepatocytes (days at most) [176, 205-207]. Co-cultivation of primary hepatocytes from multiple species with a plethora of nonparenchymal cell types (fibroblast, endothelia) from within and outside the liver has been shown to support various liver-specific functions [65, 176, 208] – see section 1.4 for details. Studies have shown that specific proteins involved in the phases of drug metabolism (I-III) remain functional in certain co-culture models[209]. Co-cultures thus serve as simple, monolayer platforms which can stabilize key hepatic functions.

Several multilayer or spheroid-based ‘3D’ hepatocellular tissues with continuous perfusion in bioreactors have also been reported in the literature [1, 127, 206, 210-212]. However, such systems have not been utilized to any considerable degree in the drug development pipeline, possibly due to several key disadvantages, which include: complex

design and construction of bioreactors; non-uniform transport of nutrients, oxygen and drug candidates in multilayer heterogeneous tissues; and, restricted *in situ* observation of cells. As the liver itself is composed of flat, anastomosing 'plates' that are typically one cell thick, two dimensional (monolayer) platforms of the liver may suffice for many ADME/Tox applications. Furthermore, since monolayer systems (confluent monolayers, collagen sandwich or Matrigel overlay) are still the most commonly utilized platforms in industry [176, 182], improved models of the liver in monolayer format can be mapped easily to existing laboratory protocols including robotic fluid handling, *in situ* microscopy, and colorimetric/fluorescent plate-reader assays.

1.7.2. Utility in Drug Development

Applications of isolated hepatocytes in drug discovery and development include screening for metabolic stability, drug-drug interactions, and liver-specific toxicity. Metabolic stability is a key criterion for selection of lead drug candidates that proceed to preclinical trials. Due to species-specific differences in drug metabolism, human hepatocyte cultures can identify the metabolite profiles of drug candidates. Subsequently, structure information may be used to deduce the mechanism by which the metabolites are generated, with the ultimate goal of focusing clinical studies. Though there are quantitative differences, there is good *in vivo* to *in vitro* correlation in drug biotransformation activity when isolated hepatocytes are used [213]. Metabolite profiles obtained via human hepatocyte *in vitro* models can also be used to choose the appropriate animal species to act as the human surrogate for preclinical pharmacokinetic, pharmacodynamic and toxicological studies. Studies have shown that interspecies variations are retained *in vitro* and are different depending on the drug being tested [189, 214, 215].

Multiple drug therapy can lead to drug-drug interactions, resulting in serious pharmacological and/or toxicological consequences [216-219]. Such interactions have created significant problems for the pharmaceutical industry and regulatory agencies, resulting in termination of clinical development, refusal of approval, severe prescribing restrictions and withdrawal from the market. Drug-drug interactions typically involve a drug's ability to interfere with the metabolism of a co-administered drug via induction or inhibition of metabolism enzymes (i.e. CYP450). While drug-drug interaction via enzyme inhibition is a safety concern due to toxic compound buildup, therapeutic failure is the major concern for enzyme induction. In certain cases, enzyme induction allows a xenobiotic to accelerate its own biotransformation (referred to as 'auto-induction'). The results of induction and inhibition studies *in vitro* help determine whether specific clinical trials are needed to address drug-drug interactions and enable doctors to avoid potentially dangerous drug combinations. Though microsomes are used frequently to study xenobiotic inhibition of CYP450 enzymes, isolated hepatocytes are the only proven preclinical system which responds to known clinical inducers such as Rifampin and Phenobarbital [182]. When hepatocyte morphology and liver-specific functions are retained in culture, CYP450 enzymes are inducible with a similar specificity and magnitude as that seen *in vivo* [189, 214].

The *in vitro* toxicology community is aiming towards the replacement and reduction of whole animals, along with refinement of toxicity assays. Since hepatocytes contain most of the drug metabolizing enzymes in the liver, they represent an attractive system to study xenobiotic toxicity. Additionally, use of primary hepatocytes allows toxicity and metabolism to be studied simultaneously, which is an important advantage, since in many cases these parameters interact *in vivo*. However, due to rapid de-differentiation *in vitro*, isolated hepatocytes are currently used only for high-dose acute

toxicity studies (hours). Thus, chronic, long-term toxicity cannot be evaluated with any considerable success. Even though hepatocytes experience the first major insult of liver toxins, nonparenchymal cells of the liver are important in the progression of liver disease [220]. For instance, liver inflammation is caused via cytokines released by endothelial and Kupffer cells. Hence, lack of nonparenchymal cells in current hepatocyte models is a disadvantage for certain studies of hepato-toxicity. Development of an in vitro liver model which not only maintains long-term stability of liver-specific functions in hepatocytes, but also incorporates nonparenchymal cells (i.e. co-cultures) is desirable.

1.8. Scope of this Dissertation

Primary hepatocytes are notoriously difficult to maintain in vitro as they rapidly lose viability and liver-specific functions. Over two decades ago, Guillouzo and colleagues discovered that phenotypic functions in primary rat hepatocytes can be stabilized to a limited extent upon co-cultivation with another liver epithelial cell type (the ‘co-culture effect’) [125]. Since then, a plethora of different co-culture systems have been described utilizing hepatocytes from multiple species and nonparenchymal cells from within and outside the liver [65]. In spite of significant investigation, several aspects of hepatic co-cultures remain undetermined. In particular, there is paucity of data on the molecular mediators of the co-culture effect. Furthermore, it is not clear whether continuous signaling from non-parenchymal cells is required to maintain hepatic functions (i.e. dynamics of cell-cell interaction). Lastly, an important application for robust in vitro liver models is the screening of pharmaceutical drug candidates for liver-specific metabolism and toxicity. A handful of studies have demonstrated activity of few drug metabolism enzymes in specific co-culture models [209]; however, the integration of

hepatic co-cultures into an optimized and miniaturized platform, designed and validated specifically for drug development, remains an unexplored research interface.

In light of unanswered questions about co-cultures, the overall objectives of this dissertation were to: a) Develop and experimentally validate a functional genomic approach to identify molecular mediators of the ‘co-culture effect’, b) Develop a method utilizing electroactive self-assembled monolayers to release nonparenchymal cells from co-cultures, and subsequently characterize liver-specific functions in hepatocytes, c) Develop miniaturized, multiwell co-culture models of human and rat liver tissue with optimized microscale architecture for pharmaceutical drug development.

Chapter 2 describes the development and validation of a functional genomic approach utilizing gene expression profiling to isolate molecular mediators potentially involved in epithelial-nonparenchymal interactions *in vitro*. This approach is applied to a hepatocyte-fibroblast co-culture model in order to produce the first global molecular definition of a hepatocyte-stabilizing microenvironment. Microarray data analysis is subsequently used to identify a handful of candidate genes that may modulate liver-specific functions. Two candidates are experimentally shown to play a role in hepatocyte-nonparenchymal interactions *in vitro*.

Chapter 3 characterizes the role of one candidate, T-cadherin, in induction of liver-specific functions in hepatocytes. Both cellular (membrane-bound on a nonparenchymal cell) and a-cellular (immobilized purified recombinant protein) presentation of T-cadherin are shown to upregulate hepatocyte functions *in vitro*.

Chapter 4 presents the development of a method that utilizes electroactive self-assembled monolayers (SAMs) to selectively release fibroblasts at various time points from co-culture to probe the dynamics of cell-cell interaction. The utility and compatibility of SAMs for constructing hepatic co-cultures is first explored. Then,

conditions for the release of murine fibroblasts are established. Lastly, characterization of hepatocyte morphology and liver-specific functions following fibroblast release is presented.

Chapter 5 describes the development of a framework that combines tissue engineering and microtechnology to develop robust *in vitro* models of tissues. This framework is used to create a miniaturized, multi-well, co-culture model of the human liver with optimized microscale architecture. Extensive characterization using several independent criteria (i.e. transcriptional profiling, biochemical assays) is carried out to demonstrate that the microscale tissues are functionally stable for several weeks. Lastly, the utility of this multiwell platform for studying drug metabolism, drug-drug interactions, and susceptibility to a panel of hepatotoxins is demonstrated using assays commonly employed in the pharmaceutical industry.

Chapter 6 describes the development of a long-term co-culture model of the rat liver for evaluating drug disposition *in vitro*. The impact of microscale architecture on long-term stability of different liver-specific functions in co-cultures is explored. Next, altered metabolism and hepato-toxicity of model liver toxins due to drug-drug interactions is demonstrated in co-cultures. The dose- and time-dependent toxicity of model Hepatotoxins in co-cultures is also investigated, followed by differences in substrate metabolism across rat and human liver tissues developed in this dissertation.

Chapter 7 summarizes the work presented in this dissertation, suggests future directions, and describes the potential contributions of this work to various fields, such as cell-based therapies for liver disease and *in vitro* liver models for drug development.

CHAPTER 2

EXPLORING INTERACTIONS BETWEEN HEPATOCYTES AND NONPARENCHYMAL CELLS USING GENE EXPRESSION PROFILING

2.1. Abstract

Co-cultivation of primary hepatocytes with a plethora of nonparenchymal cells (from within and outside the liver) has been shown to support hepatic functions in vitro. Despite significant investigation into this phenomenon, the molecular mechanism underlying epithelial-nonparenchymal interactions in hepatocyte co-cultures remains poorly understood. In this study, we present a functional genomic approach utilizing gene expression profiling to isolate molecular mediators potentially involved in induction of liver-specific functions by nonparenchymal cells. Specifically, primary rat hepatocytes were co-cultivated with closely related murine fibroblast cell types (3T3-J2, NIH-3T3, Mouse Embryonic Fibroblasts) to allow their classification as 'high', 'medium', or 'low' inducers of hepatic functions. These functional responses were correlated with fibroblast gene expression profiles obtained using Affymetrix GeneChips™. Microarray data analysis provided us with 17 functionally characterized candidate genes in the cell communication category (cell surface, extracellular matrix, secreted factors) that may be involved in induction of hepatic functions. Further analysis using various databases (i.e. PubMed, GenBank) facilitated prioritization of the candidates for functional

characterization. We experimentally validated the potential role of two candidates in our co-culture model. The cell surface protein, N-cadherin, was localized to hepatocyte-fibroblast borders, while adsorbed decorin upregulated hepatic functions in pure cultures as well as in co-cultures with low-inducing fibroblasts. In the future, identifying mediators of hepatocyte differentiation may have implications for both fundamental hepatology and cell-based therapies (e.g. bioartificial liver devices). More generally, the functional genomic approach presented here may be utilized to investigate mechanisms of cell-cell interaction in a variety of tissues and disease states.

2.2. Introduction

The development and function of tissues depend on interactions between nonparenchymal and epithelial cells to modulate differentiation, proliferation, and migration. Specifically, epithelial-nonparenchymal interactions are important in physiology [221], pathophysiology [222], cancer [223], development [224], and in attempts to replace tissue function through ‘tissue engineering’ [225]. While the functional importance of such cell-cell interactions is well established, in many cases, the underlying molecular mechanisms remain elusive. Investigation of these phenomena is further confounded by the diversity of supportive cell types found in organs. For example, fibroblasts are often classified together based on their morphology, mesenchymal markers, and adherence to tissue culture plastic; however, even fibroblasts in a single organ can vary significantly in their transcriptional profiles [226]. Even though such dramatic transcriptional variations in nonparenchymal cells would be expected to impact their interaction with surrounding epithelia, a correlation of nonparenchymal gene expression with epithelial function has not been systematically explored. Such correlative data should offer insight into the underlying mechanisms of cell-cell interaction in a given

tissue. In this study, a robust hepatic model of epithelial-nonparenchymal interactions was so examined.

In vivo, liver development requires interaction of the endodermal hepatic bud with the surrounding mesenchyme, with soluble signals FGF-2 and BMP-4 being essential for early specification [227]. However, cell-cell contact through unknown mediators is also required for further liver development [228]. In vitro, co-cultivation of primary hepatocytes with a plethora of distinct nonparenchymal cell types from different species and organs has been shown to support differentiated hepatocyte function in a manner reminiscent of hepatic organogenesis [65, 208]. These hepatocyte-nonparenchymal co-cultures have been used to study various aspects of liver physiology and pathophysiology such as lipid metabolism [114], and induction of the acute-phase response [116]. This area of investigation has gained particular interest due to its relevance to both hepatic tissue engineering [32] and development of in vitro models for pharmaceutical drug screening [128].

Despite significant investigation, a complete picture of the molecular mediators of epithelial-nonparenchymal interaction in hepatocyte co-cultures is unavailable. To date, the data suggest that both matrix deposition [125, 126] and direct cell-cell contact [65, 91, 136] play a role in the 'co-culture effect', whereas soluble factors have proven to be largely ineffective [124, 128, 131]. Two promising candidate cell surface proteins are E-cadherin [91] and liver regulating protein (LRP) [208]; however, nonparenchymal cells lacking E-cadherin and LRP retain the ability to support hepatic functions, suggesting that neither is the sole mediator of the 'co-culture effect' [137]. Indeed, it is likely that several distinct mechanisms cooperate to modulate hepatocyte function in co-cultures. Nevertheless, at least some of these multifactorial mechanisms appear to be highly conserved in mammals as primary hepatocytes from a variety of species (i.e. human, rat,

mouse, porcine) are stabilized to different extents by nonparenchymal cells from different species, tissues or embryological origin (epithelial or mesenchymal) [65, 114, 120, 129]. Thus, identification of a set of nonparenchymal-derived signals that support hepatocyte differentiation would have broad fundamental and technological implications.

Conventional approaches to investigate mechanisms of cell-cell interaction have included conditioned media and transwell culture. In hepatocyte co-cultures, these techniques have recently been supplemented with microfabrication-based patterning tools that provide additional insight into mechanisms of cell-cell communication [65]. Despite the progress in available technology to study epithelial-nonparenchymal interactions, examination of potential molecular mediators in hepatocyte co-cultures has generally progressed through serial investigation of individual candidates. In the era of functional genomics, the opportunity now exists to correlate global patterns of gene expression with functional responses resulting from cell-cell interaction. As has been widely demonstrated, DNA microarrays coupled with bioinformatic tools offer the ability to perform quantitative, parallel measurements of gene expression [226, 229].

In this study, we present a gene expression profiling approach to identify nonparenchymal genes that may modulate hepatocyte function *in vitro*. First, a 'functional profile' of cell-cell interaction was established by measurement of liver-specific functions in hepatocytes upon co-cultivation with several closely related murine fibroblasts, which were subsequently scored as high, medium, or low inducers of hepatic function. Finally, fibroblast gene expression profiles obtained via Affymetrix GeneChips™ were correlated with the hepatocyte functional profile. Using microarray data analysis, we reduced the list of ~12,000 fibroblast genes and expressed sequence tags (ESTs) to a handful of candidate genes that may modulate hepatocyte function in co-cultures. Of the candidates we identified, two were subsequently shown to play a role in

epithelial-nonparenchymal interaction in our model system, thereby validating our approach. Ultimately, the functional genomic approach presented here may serve as a general tool to facilitate mechanistic study of cell-cell interactions in diverse fields such as tissue engineering, stem cell biology, and cancer.

2.3. Materials and Methods

2.3.1. Hepatocyte Isolation

Primary rat hepatocytes were isolated from 2- to 3-month-old adult female Lewis rats (Charles River Laboratories, Wilmington, MA) weighing 180-200g, by a modified procedure of Seglen [230]. Detailed procedures for hepatocyte isolation and purification were previously described [197]. Routinely, 200-300 million cells were isolated with 85%-95% viability, as judged by trypan-blue exclusion. Nonparenchymal cells, as judged by their size (<10 μm diameter) and morphology (non-polygonal), were less than 1%. For specific experiments, primary human hepatocytes were purchased from vendors and cultured as described in 'Chapter 5' of this dissertation. Similar protocols were followed for hepatocytes of rat, mouse or human origin. Hepatocyte culture medium consisted of Dulbecco's Modified Eagle's medium (DMEM from Invitrogen, Carlsbad, CA) with high glucose, 10% (v/v) fetal bovine serum, 0.5 U/mL insulin, 7 ng/mL glucagon, 7.5 $\mu\text{g}/\text{mL}$ hydrocortisone, and 1% (v/v) penicillin-streptomycin.

2.3.2. Fibroblast Culture

3T3-J2 fibroblasts were the gift of Howard Green (Harvard Medical School) [231]. Mouse Embryonic Fibroblasts (MEFs) were the gift of James Thomson (University of Wisconsin-Madison), and NIH-3T3 cells were purchased from the

American Type Culture Collection. 3T3 fibroblast culture medium consisted of DMEM with high glucose, 10% bovine calf serum and 1% penicillin-streptomycin. MEF culture medium consisted of 10% fetal bovine serum instead of calf serum and was supplemented with 1% (v/v) nonessential amino acids.

2.3.3. Hepatocyte-Fibroblast Co-Culture

Tissue culture-treated six-well plates were coated by adsorption of 0.13 mg/mL collagen (type-I) in water for 1 hour at 37° C. Purification of collagen from rat tail tendons was previously described [197]. Briefly, rat tail tendons were denatured in acetic acid, salt-precipitated, dialyzed against HCl, and sterilized with chloroform. Pure hepatocyte cultures and hepatocyte/fibroblast co-cultures on decorin utilized co-adsorption of 0.13 mg/mL collagen-I and different concentrations of bovine decorin (Sigma, St. Louis, MO). Protein-coated culture dishes were seeded with 125,000 hepatocytes in 1 mL of hepatocyte culture medium. After 24 hours, 125,000 fibroblasts were added in 1 mL of fibroblast culture medium. For co-culture experiments involving three different cell types, fibroblasts were growth-arrested by incubation in mitomycin-C (Sigma) supplemented culture medium (10µg/mL) for 2 hours at 37°C. Each of the fibroblast types was then added to hepatocyte cultures at 350,000 cells per mL of its respective culture medium. For all co-cultures, the culture medium was replaced to hepatocyte culture medium 24 hours after fibroblast seeding and subsequently replaced daily.

For experiments with fibroblast 'feeder layers', 3T3-J2 cells grown to confluency on collagen in hepatocyte culture medium were 'fixed' via incubation in 4% paraformaldehyde (Electron Microscopy Sciences, Hatfield, PA) for 10 min, followed by three rinses with phosphate buffered saline (1X PBS). Hepatocytes were seeded directly

onto fixed fibroblasts. For conditioned media studies, hepatocyte culture medium was first incubated on proliferating fibroblasts (pure cultures) cultured on tissue culture plastic for 24 hours. Then, such conditioned media was first filtered with a 0.2 μm syringe filter to remove any live cells or cellular debris, and then transferred to wells with cultured rat hepatocytes on collagen.

2.3.4. Analytical Assays

Spent media was stored at -20°C . Urea concentration was assayed using a colorimetric endpoint assay utilizing diacetylmonoxime with acid and heat (Stanbio Labs, Boerne, TX). Albumin content was measured using enzyme linked immunosorbent assays (MP Biomedicals, Irvine, CA) with horseradish peroxidase detection and o-phenylenediamine or 3,3',5,5"-tetramethylbenzidine (TMB, Fitzgerald Industries, Concord, MA) (Sigma) as substrates [197].

2.3.5. Microscopy

Specimens were observed and recorded using a Nikon Diaphot microscope equipped with a SPOT digital camera (SPOT Diagnostic Equipment, Sterling Heights, MI), and MetaMorph Image Analysis System (Universal Imaging, Westchester, PA) for digital image acquisition.

2.3.6. Fibroblast RNA Isolation and Microarray Hybridization

Pure fibroblast cultures were grown in duplicate on collagen-coated polystyrene in their respective media for 24 hours, after which the media was replaced to hepatocyte culture media to mimic co-culture conditions to the extent possible. After an additional 24 hours, fibroblast RNA was extracted at $\sim 80\%$ confluency using TRIzol-LS

(Invitrogen). Each one of the duplicate fibroblast RNA samples was labeled, hybridized to an Affymetrix (Santa Clara, CA) MG-U74Av2 microarray, and scanned as described previously [232]. Briefly, double-strand cDNA was synthesized using a T7- (dt)24 primer (Oligo) and reverse transcription (Invitrogen) cDNA was then purified with phenol/chloroform/isoamyl alcohol in Phase Lock Gels, extracted with ammonium acetate and precipitated using ethanol. Biotin-labeled cRNA was synthesized using the BioArray™ HighYield™ RNA Transcript Labeling Kit, purified over RNeasy columns (Qiagen, Valencia, CA), eluted and then fragmented. The quality of expression data was assessed using the manufacturer's instructions which included criteria such as low background values and 3'/5' actin and GAPDH (Glyceraldehyde-3-phosphate dehydrogenase) ratios below 2. The gene expression data is available at http://lmrt.mit.edu/gene_expression/fibroblasts as a community resource.

2.3.7. Selection of Differentially Expressed Genes

All expression data was scaled to a target intensity of 200 (Affymetrix MAS 4.0 software), which corresponds to ~3-5 transcripts per cell [232]. Six microarray experiments were performed, which included 3 fibroblast cell lines prepared and hybridized in duplicate. These data were used to generate pair-wise comparison files for every cell type combination (i.e. 3T3-J2 replicate-1 versus NIH-3T3 replicate-1, 12 files total). These comparison files were then filtered using BullFrog filtering software [233] to detect genes that were consistently differentially expressed. Criteria used for filtering were selected (Table 2.1) based on their ability to yield false-positive rates of less than 1% (# of genes differentially expressed in replicates / total genes). These criteria [234] had to be consistent in at least ten of twelve comparisons.

Table 2.1: Criteria used in Bullfrog software to detect differentially expressed genes between fibroblasts. Abbreviations: I (increase), MI (marginal increase), D (decrease), MD (marginal decrease), and P (present). Note: Directional stringency implies that the sign of a change is same in all comparisons.

Difference call of	I, MI, D, MD
Fold change \geq	1.8
Average difference change \geq	50
Absolute call	P
Directional stringency?	Yes

2.3.8. Microarray Data Analysis

Filtered data was exported to GeneSpring software (Agilent Technologies, Palo Alto, CA) and hierarchical clustering was employed with vector-angle distance metric to generate clusters of specific expression profiles. Other unsupervised (statistically driven) analysis methods (self-organizing maps and k-means clustering) yielded similar results to those obtained using hierarchical clustering. Clusters whose average expression profiles correlated with hepatocyte functional profiles (i.e. high-medium-low albumin and urea secretion) were selected as candidate genes for further analysis, which included functional annotation via the NetAffx analysis portal (Affymetrix). NetAffx integrates information from various public databases such as GenBank and Swissprot.

2.3.9. Western Blotting and Immunofluorescence

Fibroblasts grown on collagen-coated surfaces in hepatocyte culture medium were lysed in RIPA buffer (Upstate Biotech, Charlottesville, VA) with protease inhibitor cocktail (Roche, Indianapolis, IN). Lysates were separated by polyacrylamide gel electrophoresis and transferred onto a PVDF membrane, blocked, incubated with

primary antibody (Santa Cruz Biotechnology, Santa Cruz, CA) and horseradish peroxidase-conjugated secondary antibody (Sigma), and visualized by chemiluminescence (Pierce SuperSignal, Pierce Biotechnology, Rockford, IL). For indirect immunofluorescence, samples were fixed with 4% paraformaldehyde, permeabilized with Triton-X100, stained with primary and fluorescein isothiocyanate (FITC) conjugated secondary antibodies (Santa Cruz Biotech), and counterstained with Hoechst.

2.3.10. Statistical Analysis

Experiments were repeated 2-3 times with duplicate or triplicate samples for each condition. For functional assays, one representative outcome is presented where the same trends were observed in multiple trials. Statistical significance was determined using one-way ANOVA (analysis of variance) or Student's t-test and Tukey's post-hoc test on Prism (GraphPad Software, San Diego, CA). All error bars represent standard error of the mean (SEM).

2.4. Results

2.4.1. Differential Induction of Liver-specific Functions

In order to categorize nonparenchymal cells by their ability to induce hepatic functions, we co-cultured primary rat hepatocytes with three closely related murine fibroblasts: 3T3-J2 and NIH-3T3 cell lines and primary mouse embryonic fibroblasts (MEFs). Induction of hepatic functions was scored by measurements of urea and albumin synthesis as markers of liver's metabolic and synthetic functions, respectively. Figure 2.1A compares functions of hepatocytes in the three co-cultures to hepatocytes in pure culture. Hepatic functions were highest in the 3T3-J2 co-culture, followed by the

NIH-3T3 co-culture, the MEF co-culture, and undetectable in hepatocytes cultivated alone. Furthermore, hepatocyte morphology deteriorated in pure cultures, whereas all co-cultures were populated with polygonal hepatocytes with distinct nuclei and bright intercellular borders (Figure 2.1B). Thus, 3T3-J2 cells were scored as ‘high inducers’, NIH-3T3 cells as ‘medium inducers’, and MEFs as ‘low inducers’ of hepatic functions.

In order to explore whether the poorly inductive fibroblasts (MEF) could inhibit hepatocyte function, we co-cultivated hepatocytes with a 1:1 mixture of highly inductive (3T3-J2) and poorly inductive fibroblasts (MEFs). Fibroblasts were growth-arrested with mitomycin-C to prevent confounding effects of proliferation of both fibroblast populations. Our results indicated that poorly inductive fibroblasts did not significantly diminish the function of hepatocytes in highly inductive cultures (Figure 2.2).

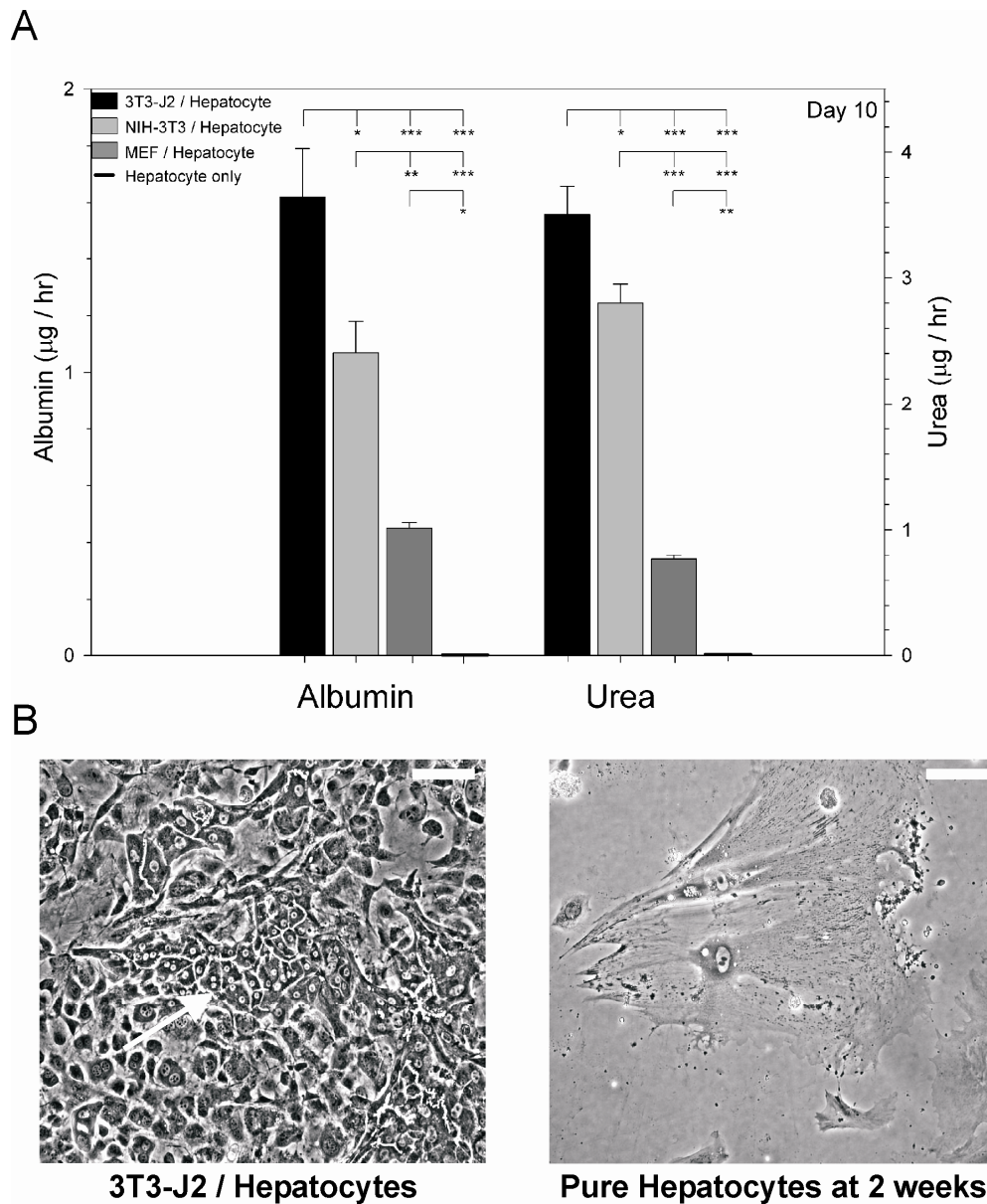


Figure 2.1: Differential induction of liver-specific functions in rat hepatocytes upon co-cultivation with murine fibroblasts. A) Rate of albumin and urea production by hepatocytes on day 10 of co-culture with three different murine fibroblasts. These trends were observed over many days. Inductive capacity of fibroblasts was therefore scored as follows: 3T3-J2 > NIH-3T3 > Mouse Embryonic Fibroblasts. **B)** In all co-cultures, hepatocytes exhibited polygonal morphology (arrow), distinct nuclei, and visible bile canaliculi, whereas hepatocyte morphology deteriorated in pure cultures. * $p < 0.05$, ** $p < 0.01$, *** $p < 0.001$ (one-way ANOVA and Tukey's post-hoc test). Error bars represent SEM ($n = 4$). Scale bars represent 200 μm .

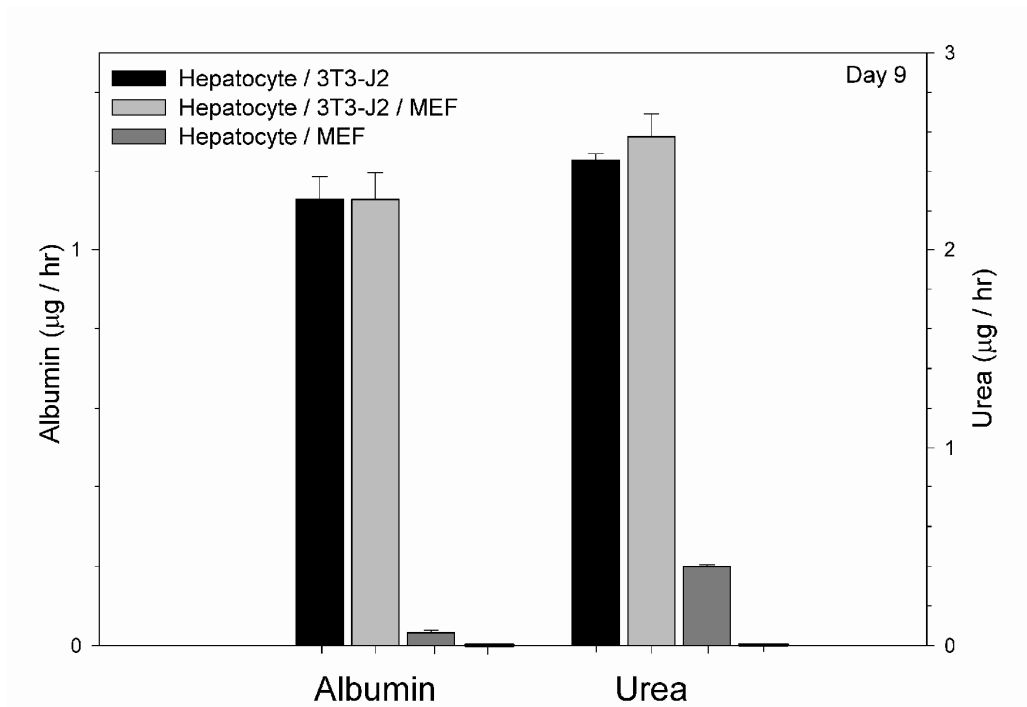


Figure 2.2: Effect of poorly inductive mouse embryonic fibroblasts (MEFs) on hepatic functions in highly inductive 3T3-J2 co-cultures. These experiments were conducted to explore the potential for MEFs to actively inhibit highly functional co-cultures. Shown here is rate of albumin and urea production by hepatocytes on day 9 of co-culture with a mixture of mouse embryonic and 3T3-J2 fibroblasts. These trends were observed over many days. Error bars represent SEM (n=3).

2.4.2. Gene Expression Profiling of Fibroblasts

In order to investigate the potential mediators of epithelial-nonparenchymal interactions in hepatocyte co-cultures, we utilized gene expression profiling. As part of this process (Figure 2.3A), Affymetrix GeneChips™ were used to first quantify messenger RNA levels in pure fibroblast cultures grown on type-I collagen in hepatocyte culture medium to mimic co-culture conditions to the extent possible (Figure 2.3B). The data was then filtered to detect genes that were consistently differentially expressed across the different fibroblast cell lines. Subsequently, we employed hierarchical clustering (Figure 2.3C) to obtain candidate genes whose expression profiles correlated positively (high-medium-low, Table 2.2) and negatively (low-medium-high, Table 2.3) with the pattern of hepatocyte induction observed (see Figure 2.1). Finally, all candidate genes were functionally annotated using the NetAffx analysis portal (Affymetrix). In conducting further analysis, we focused on proteins found on or around fibroblasts that may be involved with cell-cell communication including cell surface proteins, extracellular matrix molecules, and secreted factors. Below, we highlight key candidates of interest that may be worthy of further investigation and present experimental data suggesting two candidates may play a role in hepatocyte co-cultures.

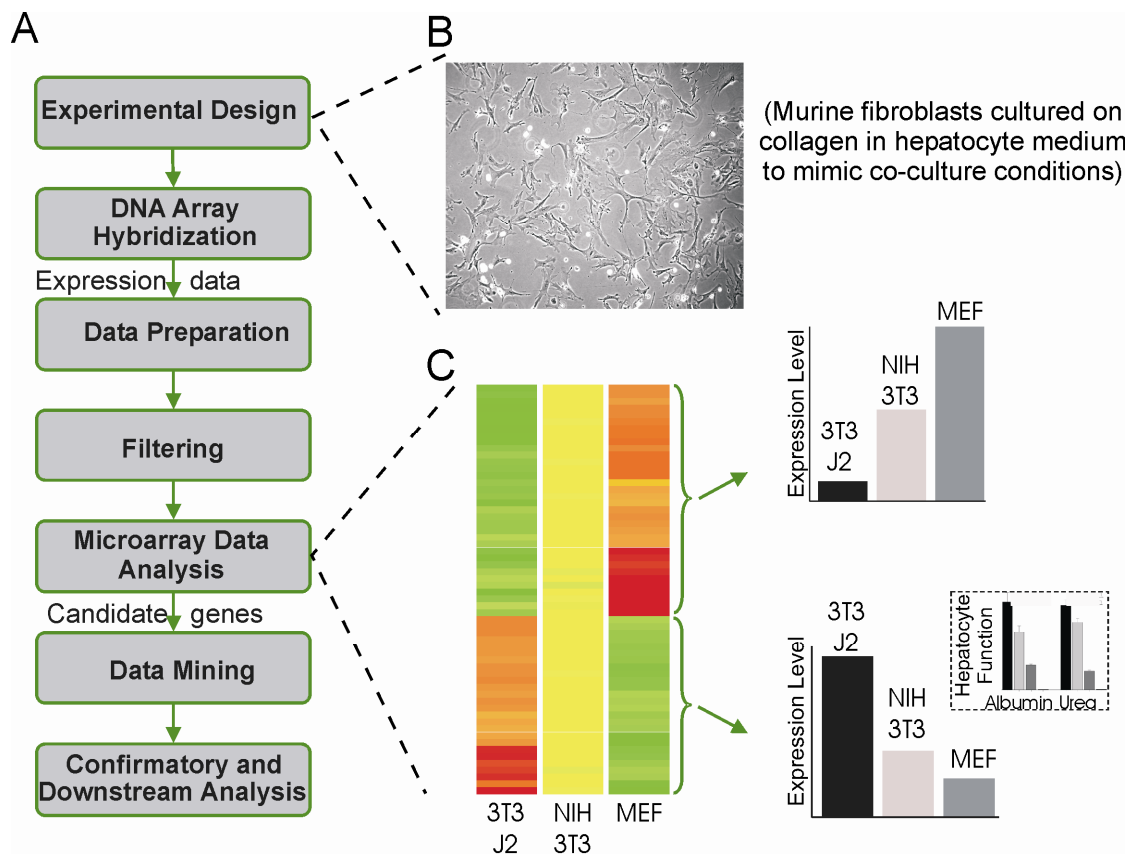


Figure 2.3: Gene expression profiling of fibroblasts. **A)** Flowchart depicting the use of DNA microarrays to obtain candidate genes involved with cell-cell interaction. Total RNA of fibroblasts (3T3-J2, NIH-3T3, Mouse Embryonic Fibroblasts) was harvested, labeled, and hybridized to Affymetrix GeneChips™. Expression data was normalized, filtered, analyzed and functionally annotated to obtain candidate genes. See Methods for additional details. **B)** Phase contrast micrograph depicting fibroblast morphology (mouse embryonic fibroblasts) on collagen-coated polystyrene in hepatocyte culture medium. **C)** Clusterogram produced using hierarchical clustering with vector-angle distance metric is shown where rows are gene expression values and columns represent different fibroblast cell types. In this clusterogram, genes with similar expression profiles across conditions are clustered together. High expression level is indicated by red, low expression by green and medium expression by yellow. Average expression profiles of specific clusters that correlate positively and negatively with inductive profiles (shown as an inset) are shown to the right of the clusterogram.

Table 2.2: Fibroblast candidate genes whose expression profiles correlate positively with the hepatocyte functional profile. See Figure 2.1A for the functional profile.

ACCESSION #	DESCRIPTION
CELL SURFACE PROTEINS	
Z12171	Delta-like 1 homolog (Drosophila)
SECRETED FACTORS	
X99572	C-fos induced growth factor (VEGF-D)
U49513	Small inducible cytokine A9
U49430	Ceruloplasmin
EXTRACELLULAR MATRIX OR MATRIX REMODELING	
X53929	Decorin
TRANSCRIPTION FACTORS	
M21065	Interferon regulatory factor 1
M31419	204 interferon-activatable protein
OTHER	
X53824	Splicing factor, arginine/serine-rich 3
AB017020	Heterogeneous nuclear ribonucleoprotein D-like protein JKTBP
L00993	Autoantigen La (SS-B)
U00431	High mobility group box 1
Z72486	DNA polymerase delta small subunit (pold2)
M86377	Esk kinase
J00388	Mouse dihydrofolate reductase gene: 3' end
X07967	Pm1 protein
AW122347 (EST)	Rac GTPase-activating protein 1
AA655369 (EST)	Translocase of inner mitochondrial membrane 8 homolog a, yeast
Unknown function EST Accession #: AI037577, AI846197, AI841894, AI606951, AA940036, AI746846, AI551087, AA222883, AI848479	

Table 2.3: Fibroblast candidate genes whose expression profiles correlate negatively with the hepatocyte functional profile. See Figure 2.1A for the functional profile.

ACCESSION #	DESCRIPTION
CELL SURFACE PROTEINS	
L03529, AW046032 (EST)	Thrombin receptor (PAR-1)
X66084	Hyaluronic acid receptor (CD44)
M90365	Junction plakoglobin (cadherin associated)
SECRETED FACTORS	
AJ243964	Dickkopf homolog 3 (<i>Xenopus laevis</i>)
X69619	Inhibin beta-A
M70642	FISP-12 protein
U77630	Adrenomedullin
EXTRACELLULAR MATRIX OR MATRIX REMODELING	
X66976	Procollagen, type VIII, alpha 1
X62622	Tissue inhibitor of metalloproteinase 2
CYTOSKELETAL ASSOCIATED	
M12347	Actin, alpha 1, skeletal muscle
U58513	Rho-associated coiled-coil forming kinase 2
U73199	Rho interacting protein 2
CELL CYCLE	
U09507	Cyclin-dependent kinase inhibitor 1A (P21)
TRANSCRIPTION FACTORS	
D76440	Necdin
AJ002366	General transcription factor IIIH, polypeptide 1
INTRACELLULAR SIGNALING	
U15784	Src homology 2 domain-containing transforming prot. C1
AF053367	PDZ and LIM domain 1 (elfin)
U58883	SH3 domain protein 5
U58882	LIM and SH3 protein 1
OTHER	
X87817	Dihydropyrimidinase-like 3
Y13832	Maternally expressed gene 3
U41739, AI839950 (EST)	Four and a half LIM domains 1
AW125478 (EST)	Protease, serine, 11 (Igf binding)
AI183109 (EST)	Translin-associated factor X
AJ007376	DEAD box polypeptide, Y chromosome
D12713	SEC23A (<i>S. cerevisiae</i>)
M31775, AW046124 (EST)	Cytochrome b-245, alpha polypeptide
Unknown function EST Accession #: AI848471, AI183109, AI648831	

2.4.3. Cell Surface Proteins

Several studies have implicated cell surface proteins in epithelial-nonparenchymal interactions in hepatocyte co-cultures [91, 136]. Our gene expression profiling yielded Dlk-1 (Delta-like homolog), whose expression profile correlated positively (i.e. high-medium-low) with ability of fibroblasts to induce functions in hepatocytes. Dlk-1 belongs to the EGF-like homeotic protein family that includes proteins such as the Notch receptor and its homologues (Table 2.2) [235]. Dlk-1 is strongly expressed in the mouse fetal liver in hepatoblasts and has been implicated in differentiation of several non-hepatic cell types, suggesting that it may play a functional role in hepatocyte co-cultures [235, 236].

Further analysis of plakoglobin (γ -catenin) revealed that many of its interaction partners from the cadherin superfamily of cell adhesion molecules also had negative expression profiles (Figure 2.4A). Classical cadherins, which are transmembrane proteins linked to the actin cytoskeleton via regulatory molecules such as catenins (Figure 2.4B), may play roles in differentiation and heterotypic cell-cell interactions [70, 71]. In the liver, cadherins are expressed in both hepatocytes and surrounding nonparenchyma under both physiologic and pathophysiologic conditions [83, 85]. In co-cultures of hepatocytes with L-929 chaperone cells, E-cadherin expression correlated positively with induced hepatocyte functions [91]; however, over-expression of E-cadherin in the developing liver prevents normal liver development [237]. In our co-cultures, we verified protein expression and localization of N-cadherin and γ -catenin at homotypic and heterotypic junctions using immunofluorescence (Figure 2.4C). Thus, the negative correlation of cadherin-related molecules with hepatocyte function merits further investigation.

2.4.4. Extracellular Matrix Proteins

Matrix deposition and remodeling have been implicated as key features of hepatocyte co-cultures [125, 126]. In our data, the gene expression of collagen-VIII correlated negatively with inductive ability of fibroblasts. This non-fibrillar short-chain matrix protein is present in the arterioles and venules of normal liver [238] and may play an instructional role in differentiation of other cell types [239]. Even though the effect of collagen-VIII on hepatic functions has not been studied, other collagens (collagen-I) are responsible for dramatic changes in hepatocellular phenotype [197]. Matrix remodeling via metalloproteinases and their inhibitors (tissue inhibitor of metalloproteinase; TIMP) may be an important feature of hepatocyte co-cultures [208]. In our system, the expression of TIMP-2 correlated negatively with inductive ability of fibroblasts, suggesting that an imbalance in matrix remodeling may also underlie the hepatic dysfunction found in MEF co-cultures (low functioning).

The only matrix protein whose expression profile correlated positively with fibroblast inductive ability was decorin, which is a chondroitin sulfate-dermatan sulfate proteoglycan that binds to collagen [240]. Decorin is a major liver proteoglycan that shows early and strong upregulation during liver regeneration following partial hepatectomy, even though its role in this process is unclear [241]. To validate our functional genomic approach, we conducted preliminary studies to investigate decorin's effect on hepatocellular functions *in vitro*. Due to the collagen-binding activity of decorin, hepatocyte function on collagen was compared to surfaces with co-adsorbed collagen and decorin. In pure hepatocyte cultures, albumin production was upregulated by 122% and urea secretion by 36% on decorin (Figure 2.5A). In co-cultures of hepatocytes and MEFs ('low inducers'), hepatic functions were upregulated in a dose-dependent manner on adsorbed decorin as compared to collagen alone, resulting in up to 40% of albumin secretion rate seen in co-culture with 'high inducers' (Figure 2.5B).

2.4.5. Secreted Factors

Studies assessing the role of soluble factors in hepatocyte co-culture models have yielded variable results. For example, treatment of hepatocytes with media ‘conditioned’ by nonparenchymal cells is typically ineffective [128, 131]. Nonetheless, secreted factors that are labile or are locally sequestered in matrix may play a role in cell-cell interaction. In our analysis, gene expression profile of vascular endothelial growth factor D (VEGF-D) correlated positively with induction of liver-specific functions. In addition to their role in angiogenesis, VEGFs play protective roles in liver regeneration (VEGF-A) and show dynamic pattern of expression in the developing liver (VEGF-D) [242, 243]. Besides VEGF-D, Dickkopf homolog 3 exhibited a negative expression profile. Found primarily in mesenchymal lineages, Dickkopfs (dkk) are secreted proteins that have been implicated in modulating inductive epithelial-mesenchymal interactions [244].

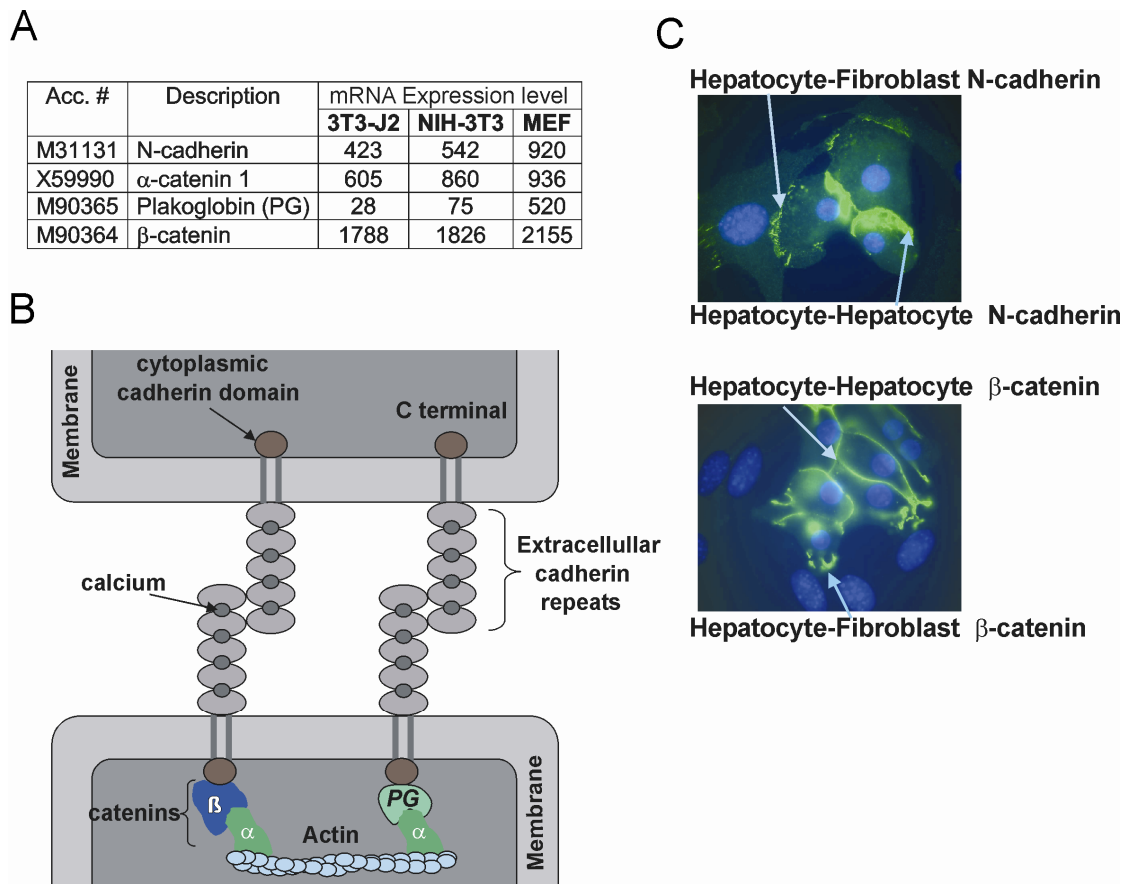


Figure 2.4: Analysis of the cadherin pathway suggests negative correlation with hepatocyte function. **A)** Since the expression profile of plakoglobin (PG), which interacts with cadherins, correlated negatively with inductive ability of fibroblasts in unsupervised analysis, we checked expression profiles of other constituents of the cadherin pathway and found them to be similar to that of PG. Values indicate average of duplicate samples, scaled to an intensity of 200. **B)** Classical cadherins are transmembrane proteins whose cytoplasmic domains anchor to the actin cytoskeleton by interacting with various signaling molecules such as β -catenin, plakoglobin (γ -catenin), and α -catenin. **C)** Immunofluorescent staining of N-cadherin (top) and β -catenin (bottom) demonstrate protein expression and localization at both homotypic (hepatocyte-hepatocyte) and heterotypic (hepatocyte-fibroblast) cell-cell junctions in hepatocyte co-cultures. Nuclei are counterstained with Hoechst. Representative staining is shown for 3T3 (medium inducers) co-cultures, but protein localization was seen in all co-cultures.

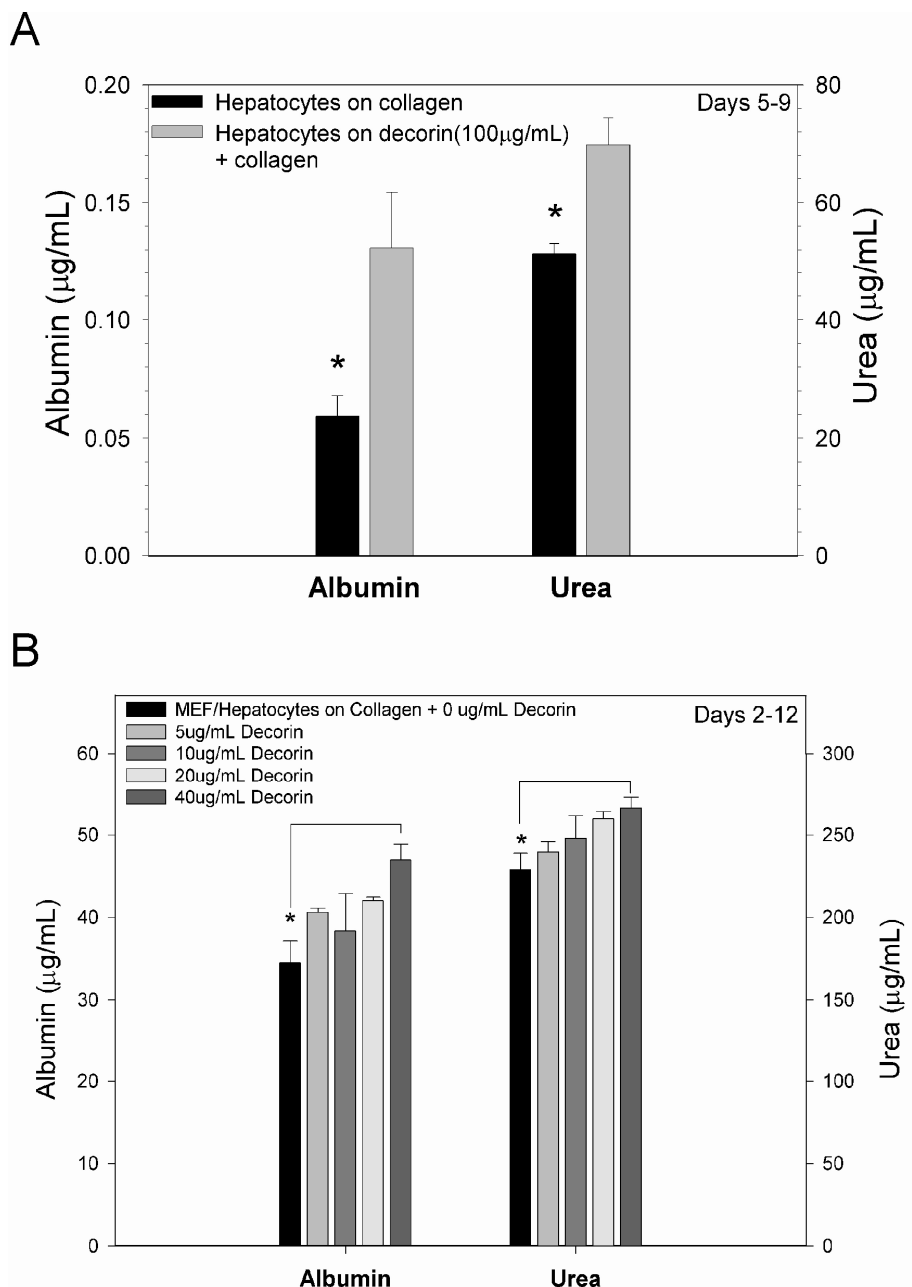


Figure 2.5: Validation of extracellular matrix, decorin, as a potential mediator of cell-cell interaction. **A)** Upregulation of total urea and albumin production in hepatocytes plated alone on adsorbed decorin (summation over days 5-9). **B)** Dose-dependent upregulation of total hepatic functions in co-cultures of hepatocytes and low function-inducing mouse embryonic fibroblasts (summation over days 2-12) on adsorbed decorin. * $p < 0.05$ (two-tailed Student's t-test). Error bars are SEM ($n=3$).

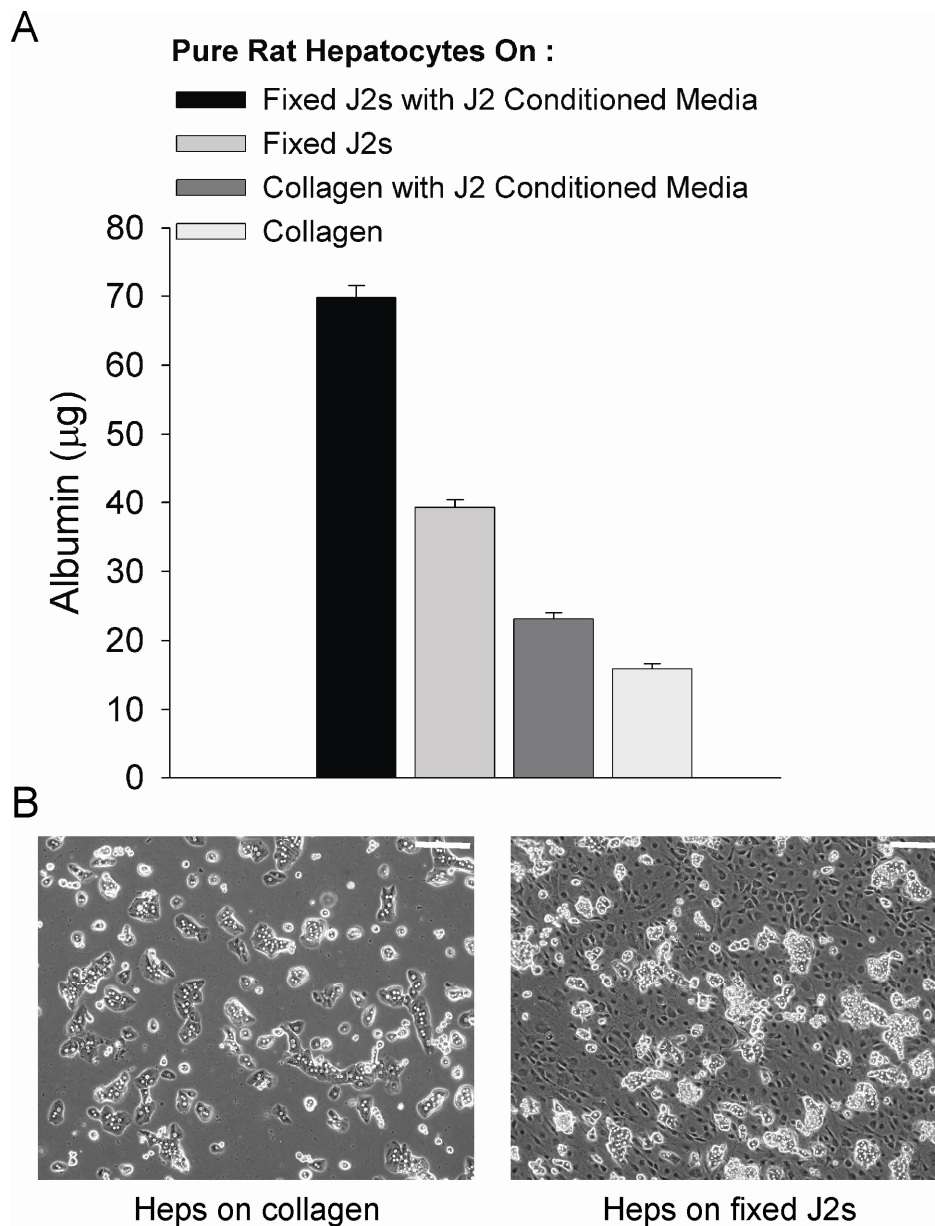


Figure 2.6: Hepatocyte culture on paraformaldehyde-fixed fibroblast feeder layers. **A)** Shown here is albumin secretion (cumulative over 2 weeks) by rat hepatocytes cultured on different types of substratum with or without 3T3-J2 conditioned culture media. Substrata included adsorbed collagen (type I) or a paraformaldehyde-fixed 3T3-J2 feeder layer. For conditioned media studies, hepatocyte culture medium incubated for 24 hours with proliferating 3T3-J2s was transferred to cultured rat hepatocytes in separate wells. Error bars are SEM (n=3). One-way ANOVA with Tukey's post-hoc test showed that all conditions were significantly different from each other (pairwise comparisons, $p < 0.05$). **B)** Phase contrast micrographs of hepatocytes on adsorbed collagen or on a fixed fibroblast layer (day 1 shown, scale bars are 200 μm).

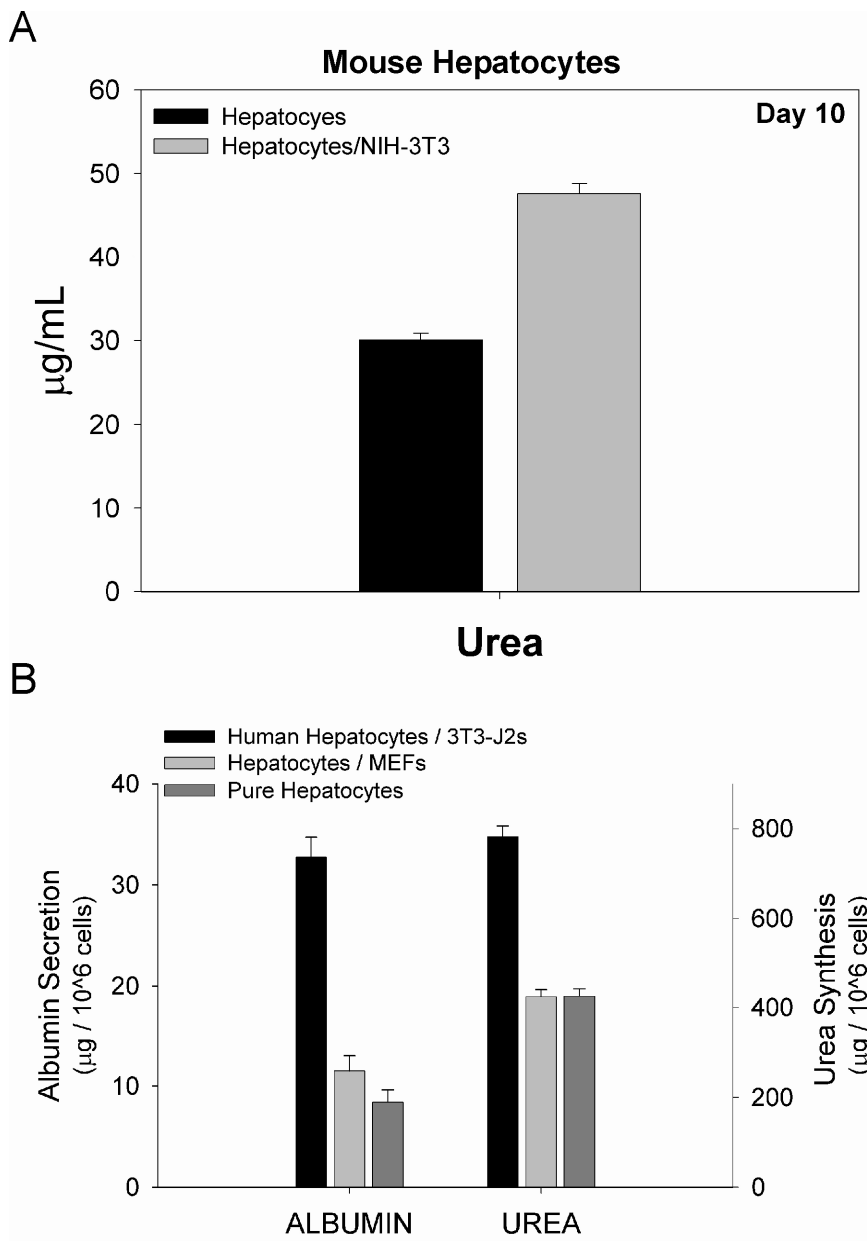


Figure 2.7: Co-cultivation of murine embryonic 3T3 fibroblasts with primary murine or human hepatocytes. A) Upregulation of urea secretion was seen in co-cultures of primary murine hepatocytes and NIH-3T3 fibroblasts as compared to pure hepatocyte controls. Representative day 10 of co-culture is shown, but trends were seen for multiple days. **B)** Liver-specific functions (cumulative over 2 weeks) in pure cultures of primary human hepatocytes on collagen are compared to functions in hepatocyte/fibroblast co-cultures. ‘MEFs’ represents mouse embryonic fibroblasts. All error bars are SEM (n=3).

2.5. Discussion

In the era of genomic medicine, biomedical phenomena may be investigated via global analyses rather than through the study of individual molecular species. This systems-level approach has been used to stratify clinical trials and predict metastatic potential of tumors [245]. In this study, we present a functional genomic approach to explore the mechanisms of cell communication in epithelial-nonparenchymal interactions in a hepatic model system. Functional outcomes were scored and correlated with patterns of gene expression in a manner that can be generalized to the study of a variety of biological phenomena. Specifically, primary hepatocytes were co-cultivated with various nonparenchymal cell lines (NPCs) to produce variable induction of liver-specific functions. Nonparenchymal genes whose expression correlated positively (i.e. stimulatory) and negatively (i.e. inhibitory) with the hepatic functional profile were catalogued for further experimental study. Using this approach, we identified 17 functionally characterized candidates in the relevant cell communication categories (cell surface, extracellular matrix, secreted factors), and produced the first global molecular definition of a hepatocyte-stabilizing nonparenchymal microenvironment. Finally, we experimentally validated the role of two candidates (decorin, N-cadherin) in hepatocyte-fibroblast interactions in our model system. These data provide a limited set of candidates that may be investigated for their role in induction of liver-specific functions, some of which may have technological implications (i.e. stabilizing hepatocellular function in cell-based therapies).

In developing our gene expression profiling approach to study cell-cell interactions, we considered several experimental variables. First, we considered the possibility that nonparenchymal cells receive reciprocal signals from surrounding epithelia. Therefore, the ideal source of nonparenchymal cells for gene expression profiling would have been those that have undergone co-cultivation with hepatocytes.

However, due to the experimental difficulty of rapidly purifying nonparenchymal RNA from hepatocyte co-cultures, we profiled pure fibroblast cultures as a first step towards identifying candidate genes involved with induction of liver functions. Previous experimental evidence as well as our own studies (see Figure 2.6) suggest that nonviable feeder layers (irradiated, desiccated, fixed, mitomycin-C treated) induce liver-specific functions in hepatocytes, lending support to the idea that at least some nonparenchymal-derived signals do not require reciprocal signaling [65, 130]. To the extent possible, we mimicked other aspects of the co-culture environment (media formulation and extracellular matrix coating) in pure fibroblast cultures to obtain a set of candidates that are involved with the functional outcomes we measured. Next, to address the possibility that hepatic function varied between co-cultures due to variations in cell shape, average hepatocyte projected surface area was measured in each condition and found to be similar (data not shown) [148]. Additionally, we noted that DNA microarrays report on messenger RNA levels rather than protein expression. We therefore verified select candidates at the protein level using western blotting (data not shown) and immunofluorescence. Thus, our gene expression profiling approach is merely a necessary first step in dissecting the mechanisms of cell-cell interaction.

The choice of nonparenchymal cells (NPCs) used in this study was another key parameter in the experimental design. A variety of both liver and non-liver derived NPCs have been reported to induce hepatic function in co-culture [65, 125, 126]. Furthermore, induction has been reported by NPCs (both primary and immortalized) derived from a different species than the primary hepatocytes, suggesting possible conservation of underlying mechanisms [114, 120, 128, 129, 131]. The ready availability and ease of culture of immortalized murine embryonic fibroblasts has led to a resurgence of interest in their influence on hepatocyte functions for applications in bioartificial liver devices [32,

65, 124]. In order to broaden our findings in rat hepatocytes, we also demonstrated coculture-mediated stabilization of hepatocytes from the same species (murine) and another species (human) as the fibroblasts (see Figure 2.7). Finally, since 3T3 and primary murine embryonic fibroblasts are commonly used as supporting feeder layers in other organ systems [231, 246], the gene expression data acquired in this study may be useful in a number of other applications. In the future, we aim to study the role of candidate genes elucidated in murine fibroblast cell lines in nonparenchymal cells of the liver specifically (e.g. sinusoidal endothelial cells).

The categorization of candidate genes into two groups (positive or negative correlations with induction profiles) was based on the premise that ‘low inducer’ fibroblasts could, in fact, be actively inhibiting hepatocyte function. In order to test this hypothesis, we co-cultivated hepatocytes with a mixture of MEFs (low inducers) and 3T3-J2s (high inducers). Both fibroblast cell types were growth arrested to prevent confounding effects of differential proliferation. Our results indicated no significant decrease in function due to the addition of MEFs as compared to control co-cultures (hepatocyte/3T3-J2), suggesting that either MEFs lack active inhibitory signals or that hepatic induction by 3T3-J2s dominates over any inhibition by MEFs. Nonetheless, these preliminary experiments cannot conclusively rule out the existence of inhibitory molecules. Indeed, one of our candidates, N-cadherin, was recently reported to inhibit chondrogenic differentiation of limb mesenchymal cells upon over-expression in vitro [247].

Of the 17 functionally characterized candidates in the cell communication category obtained in our analysis, two candidates were experimentally validated. Unsupervised analysis of the data showed that gene expression of decorin, an extracellular matrix proteoglycan, correlated positively with inductive activity. Experimentally, we

confirmed that decorin did indeed induce liver functions in both pure hepatocyte cultures and in co-cultures of hepatocytes with fibroblasts that had 'low' inductive activity (Figure 2.5). Despite decorin's inductive ability, neither culture achieved maximal production rates of hepatic markers (as with 3T3-J2s) due to the addition of decorin alone. These data serve to validate the gene expression profiling approach and confirm the hypothesis that cell-cell interaction is likely to be multifactorial. Analysis of the cadherin pathway emerged from the identification of plakoglobin (γ -catenin) as a candidate. N-cadherin, γ -catenin, and β -catenin expression profiles also correlated negatively with inductive activity. We confirmed the localization of N-cadherin and β -catenin at heterotypic (fibroblast/hepatocyte) junctions using immunofluorescence (Figure 2.4), providing the first evidence, in our hands, of functional communication between the cell types. In contrast, other groups have shown a positive inductive role for E-cadherin [91]. Interaction between N- and E-cadherin pathways has also been reported [248]; therefore, the interplay between various cadherins merits further investigation in hepatocyte co-cultures.

In summary, we have developed a gene expression profiling approach to facilitate the study of cell-cell interactions. The nonparenchymal gene expression data provided online (http://lmrt.mit.edu/gene_expression/fibroblasts) can also be utilized to identify candidate genes by other investigators in diverse areas such as the self-renewal of embryonic stem cells on nonparenchymal feeder layers [246] and differentiation of keratinocytes on fibroblasts [231]. In the future, we plan to evaluate the functional role of promising candidates in our co-cultures using function-blocking antibodies, RNA interference (RNAi), and overexpression of candidate genes. Identification of a set of critical proteins that mediate hepatocyte differentiation will have implications in both hepatocellular therapies and liver development. In addition, continued application of

functional genomics and gene expression profiling to epithelial-nonparenchymal systems may provide fundamental insights into global and tissue-specific regulatory gene networks that control tissue development and function.

Acknowledgements

We are grateful to Jennifer Felix for hepatocyte isolation, Shankar Subramaniam for helpful informatics advice, James Thomson for providing Mouse Embryonic Fibroblasts, Howard Green for providing 3T3-J2 fibroblasts, and Ian Gaudet and Craig Sharp for assistance with cell culture and biochemical assays.

The text of Chapter 2, in part, is a reprint of the material as it appears in *Hepatology* (Khetani, S.R., Szulgit, G., Del Rio, J.A., Barlow, C., and Bhatia, S.N., “Exploring Interactions between Rat Hepatocytes and Nonparenchymal Cells Using Gene Expression Profiling.” *Hepatology* 2004, volume 40, issue 3, pages 545-554). This material was reprinted with permission of John Wiley & Sons., Inc. The dissertation author was the primary researcher and author and conducted the research that forms this chapter.

CHAPTER 3

T-CADHERIN MODULATES HEPATOCYTE FUNCTIONS IN VITRO

3.1. Abstract

Co-cultivation of hepatocytes with nonparenchymal cells from within and outside the liver has been shown to support hepatic functions in vitro. Despite significant investigation into this phenomenon, the molecular mechanisms underlying epithelial-nonparenchymal interactions in hepatocyte co-cultures remain largely undetermined. In contrast to classical cadherins such as E- and N-cadherin, truncated-cadherin (T-cadherin) lacks an intracellular domain and is anchored to the cell membrane through a glycosylphosphatidyl inositol (GPI) moiety. This unique cadherin has been implicated as a signaling molecule in diverse fields such as oncology and cardiovascular physiology; however, its role in modulation of liver-specific functions both in vitro and in vivo remains undiscovered. In this study, we demonstrate that cellular (membrane-bound on a nonparenchymal cell) and a-cellular (i.e. recombinant purified protein) presentation of T-cadherin to rat hepatocytes induces in them a diverse set of phenotypic functions in vitro. Specifically, Chinese hamster ovary cells (CHOs) transfected with mouse T-cadherin upregulated hepatocyte functions (albumin secretion, urea synthesis, cytochrome-P450 activity) in co-cultures over wild-type controls. Furthermore, adherent culture of hepatocytes on a substratum containing purified T-cadherin protein enhanced functions in a dose-dependent manner in both pure cultures and co-cultures negative for T-

cadherin expression. In the future, continued elucidation of molecular mediators of hepatic differentiation will be important towards building highly functional *in vitro* models of liver tissue for use in fundamental investigations in hepatology, cell-based therapies for liver disease and pharmaceutical drug screening.

3.2. Introduction

Primary hepatocytes from a variety of species (rodent, human, mouse, porcine) are notoriously difficult to maintain in culture as they rapidly (hours) lose viability and phenotypic functions upon isolation from the *in vivo* microenvironment of the liver [57, 58, 249]. Over the last few decades, investigators have used various methods to stabilize hepatocyte functions *in vitro* including: extracellular matrix manipulation [197, 198, 214], media additives [190-192], and co-cultivation with a plethora of liver and non-liver-derived non-parenchymal cell types (co-cultures) [65, 208]. Hepatocyte-nonparenchymal co-cultures, in particular, have been shown to stabilize several liver-specific functions *in vitro* [65]. Furthermore, such co-cultures have been used to study various aspects of liver physiology and pathophysiology such as lipid metabolism [114], and induction of the acute-phase response [116]. This area of investigation has gained particular interest due to its relevance to both hepatic tissue engineering [32] and development of *in vitro* models for pharmaceutical drug screening [128, 176].

In spite of over two decades of investigation, the molecular mediators underlying the induction of liver-specific functions in hepatocyte-nonparenchymal co-cultures remain largely undetermined. To date, the data suggest that both matrix deposition [125, 126] and direct cell-cell contact [65, 91, 136] play a role in the ‘co-culture effect’, whereas soluble factors have proven to be largely ineffective [128, 131]. Two promising candidate cell surface proteins are E-cadherin [91] and liver regulating protein (LRP) [208];

however, nonparenchymal cells lacking E-cadherin and LRP retain the ability to support hepatic functions, suggesting that neither is the sole mediator of the ‘co-culture effect’ [137]. Indeed, it is likely that several distinct mechanisms cooperate to modulate hepatocyte function in co-cultures. Nevertheless, at least some of these multifactorial mechanisms appear to be highly conserved in mammals as primary hepatocytes from a variety of species (i.e. human, rat, mouse, porcine) are stabilized to different extents by nonparenchymal cells from different species, tissues or embryological origin (epithelial or mesenchymal) [65, 114, 120]. Thus, identification of a set of nonparenchymal-derived signals that support hepatocyte differentiation would have broad fundamental and technological implications.

In our previous work exploring interactions between hepatocytes and nonparenchymal cells using gene expression profiling, we identified cadherins as potential mediators of liver-specific functions [58]. Cadherins are a diverse superfamily of molecules that mediate calcium dependent cell-cell adhesion in all solid tissues of an organism. Besides their well established roles as cell-cell adhesion molecules in tissue segregation and morphogenesis, cadherins can influence cell fate processes such as differentiation, growth, and apoptosis in a multitude of cell types [67, 71, 250]. In the liver, cadherins are expressed in both hepatocytes and surrounding nonparenchyma under both physiologic and pathophysiologic conditions [83, 85, 86]. In vitro, E-cadherin has been postulated to play a role in homotypic hepatocellular interactions [87], formation of intact bile canaliculi [88], receptivity to extracellular matrix signals [89], and morphogenesis of 3-dimensional aggregates [86, 90]. In hepatocyte-nonparenchymal co-cultures, E-cadherin expression in L-929 chaperone cells was recently shown to correlate positively with induced liver-specific functions in co-cultures [91].

In contrast to classical cadherins, which are transmembrane proteins linked to the actin cytoskeleton via catenins, T-cadherin (also referred to as CDH13 or H-cadherin) lacks transmembrane and cytoplasmic domains, and is anchored to the cell membrane through a glycosylphosphatidylinositol (GPI) moiety [92]. Several studies have suggested that T-cadherin plays an important role in signal transduction apart from mediating homophilic cell-cell adhesion [101, 251, 252]. The amino acid motif of T-cadherin has been well conserved through vertebrate evolution, which implies that it may have a biological significance in higher animals [93]. T-cadherin has been shown to have diverse roles in physiology and pathophysiology, which include: negative guidance cue for motor axon projections [94], tumor suppressor factor in various types of cancer [95-97], and an atypical lipoprotein-binding protein [98]. However, the role of T-cadherin in the liver remains largely unexplored.

In this study, we demonstrate that both cellular and a-cellular presentation of T-cadherin can induce diverse liver-specific functions in primary rat hepatocytes *in vitro*. Specifically, Chinese hamster ovary cells (CHOs) were first transfected with mouse T-cadherin and then co-cultivated with primary rat hepatocytes. We show here that T-cadherin positive CHOs upregulated hepatocyte functions over wild-type controls. Subsequent knockdown of T-cadherin in transfected CHOs using RNA interference (RNAi) prior to initiation of coculture caused liver-specific functions to be down-regulated for several weeks. Furthermore, culture of hepatocytes on a substratum of purified T-cadherin protein induced phenotypic functions in a dose-dependent manner in both pure cultures and co-cultures where the nonparenchymal cells lacked endogenous T-cadherin expression. We anticipate that incorporation of molecules such as T-cadherin within natural and synthetic biomaterials will be necessary for engineering an optimal microenvironment or 'niche' for hepatocytes.

3.3. Materials and Methods

3.3.1. Rat Hepatocyte Isolation and Culture

Primary rat hepatocytes were isolated from 2- to 3-month-old adult female Lewis rats (Charles River Laboratories, Wilmington, MA) weighing 180-200 g, by a modified procedure of Seglen [230]. Detailed procedures for hepatocyte isolation and purification were previously described [197]. Routinely, 200-300 million cells were isolated with 85%-95% viability, as judged by trypan-blue exclusion. Nonparenchymal cells, as judged by their size (<10 μm diameter) and morphology (non-polygonal), were less than 1%. Hepatocyte culture medium consisted of Dulbecco's Modified Eagle's medium (DMEM from Invitrogen, Carlsbad, CA) with high glucose, 10% (v/v) fetal bovine serum (FBS), 0.5 U/mL insulin, 7 ng/mL glucagon, 7.5 $\mu\text{g}/\text{mL}$ hydrocortisone, and 1% (v/v) penicillin-streptomycin (pen/strep).

3.3.2. Nonparenchymal Cell Culture

Chinese Hamster Ovary (CHO) cells were the gift of Barbara Ranscht (Burnham Institute, La Jolla, CA). CHOs were transfected by calcium phosphate coprecipitation with pcD-Tcad (plasmid containing the coding region of T-cadherin) and pSV2neo (plasmid carrying neomycin resistance, American Type Culture Collection, Rockville, MD) as described previously [253]. CHOs were cultured at 37°C with 5% CO₂ in Minimal Essential Medium (MEM Alpha GlutaMAX™ 1X with ribonucleosides and deoxyribonucleosides, Invitrogen) supplemented with 10% FBS, 0.1 mM sodium hypoxanthine, 0.016 mM thymidine (1X hypoxanthine-thymidine or HT supplement), 1 mM sodium pyruvate, 0.1 mM non-essential amino acids and 1% (v/v) pen/strep. Mouse Embryonic Fibroblasts (MEFs) were the gift of James Thomson (University of

Wisconsin at Madison). MEF culture medium consisted of DMEM with 10% fetal bovine serum, 0.1mM non-essential amino acids and 1% (v/v) pen/strep.

3.3.3. T-cadherin Fusion Protein Generation

Histidine-tagged T-cadherin fusion protein was provided by B. Ranscht. Briefly, mouse T-cadherin cDNA was amplified by PCR (using mTcad in PBS as a template) with a forward primer set at the initiator codon and a FLAG-His6-tagged reverse primer set at 100bp upstream from a unique Hind III site. The obtained PCR product was ligated into the pCEP4 mammalian vector (Invitrogen) and transfected into 293 cells with the Polyfect transfectant reagent according to the manufacturer's procedure (Qiagen, Valencia, CA). T-cadherin fusion protein expressing cells were selected and expanded in media containing 300 µg/ml hygromycin. Serum free media supernatant was concentrated with an Amicon concentrator, cell debris removed by ultracentrifugation, fusion protein purified over a nickel column according to the manufacturer's protocol (Qiagen) and its purity checked by electrophoresis and silver staining (Daiichi Pure Chemicals Co).

3.3.4. Hepatocyte-Nonparenchymal Co-Cultures

Tissue culture-treated plates were coated by adsorption of 0.1 mg/mL collagen (type-I) in water for 1 hour at 37° C. Purification of collagen from rat-tail tendons was previously described [197]. Briefly, rat-tail tendons were denatured in acetic acid, salt-precipitated, dialyzed against HCl, and sterilized with chloroform. For experiments utilizing purified, histidine-tagged T-cadherin fusion protein, culture plates were first treated with T-cadherin dissolved in calcium supplemented (1 mM) phosphate buffered saline solution (Ca²⁺ PBS) for 3 hours at 37°C. Excess T-cad solution was aspirated and substrates were further coated with type-I collagen (1 µg/mL in Ca²⁺ PBS for 1 hour at

37°C) to promote hepatocyte attachment. Protein-coated culture dishes were seeded with hepatocytes (0.3×10^6 cells per 10 cm^2) in hepatocyte culture medium (1 mL per 10 cm^2). For co-culture experiments, CHOs (~1 million cells per 10 cm^2) or MEFs (~0.6 million cells per 10 cm^2) were seeded in their respective medium 12-24 hours after initiation of adherent hepatocyte cultures. The culture medium was replaced to hepatocyte culture medium 24 hours later and subsequently replaced daily.

3.3.5. Hepatocellular Function Assays

Spent media was stored at -20°C . Urea concentration was assayed using a colorimetric endpoint assay utilizing diacetylmonoxime with acid and heat (Stanbio Labs, Boerne, TX). Albumin content was measured using enzyme linked immunosorbent assays (MP Biomedicals, Irvine, CA) with horseradish peroxidase detection and 3,3',5,5'-tetramethylbenzidine (TMB, Fitzgerald Industries, Concord, MA) as substrate [197]. For some experiments, cultures were treated with $3 \mu\text{M}$ 3-Methylcholanthrene (Sigma St. Louis, MO) dissolved in hepatocyte culture medium for 2 consecutive days to induce cytochrome-P450 1A (CYP1A) enzyme levels. Control cultures were treated with solvent alone (Dimethylsulfoxide, DMSO) to measure baseline enzyme activity. CYP1A activity was assessed via dealkylation of ethoxy-resorufin (ER, Sigma) into fluorescent resorufin. Briefly, cultures were incubated with $5 \mu\text{M}$ ER dissolved in DMEM without phenol red for 30-60 min. Resorufin fluorescence (excitation/emission: 530/590 nm) in collected supernatants was quantified by means of a fluorescence micro-plate reader (Molecular Devices, Sunnyvale, CA).

3.3.6. Microscopy

Specimens were observed and recorded using a Nikon Diaphot microscope equipped with a SPOT digital camera (SPOT Diagnostic Equipment, Sterling Heights, MI), and MetaMorph Image Analysis System (Universal Imaging, Westchester, PA) for digital image acquisition.

3.3.7. RNAi Mediated Knockdown of T-Cadherin

T-cadherin-transfected CHO cells were treated with 50 nM siRNA (siGENOME SMARTpool reagent M-049465, Dharmacon) targeted against the T-cadherin (also known as CDH13) mRNA sequence (accession number NM_019707). siRNA was delivered via cationic liposome transfection reagent (Lipofectamine 2000, Invitrogen) according to manufacturer's protocol. Briefly, 100 pmol liposome reagent was diluted to 250 μ l with 1X-DMEM and incubated at room temperature for 15 min. 50 nM siRNA, also diluted to 250 μ l with 1X DMEM, was then mixed with liposome dilution and incubated an additional 15 min. Cells were incubated with the liposome-siRNA complexes in 1 mL total serum-free media. Six hours after transfection, serum-free media was replaced with serum-supplemented CHO culture media. After 2-3 hours, CHO cells treated with siRNA were trypsinized and plated onto adherent hepatocyte cultures on collagen to create co-cultures.

3.3.8. Western Blotting and Immunofluorescence

Cultures were lysed in RIPA buffer (Upstate Biotech, Charlottesville, VA) with protease inhibitor cocktail (Roche, Indianapolis, IN). Lysates were separated by polyacrylamide gel electrophoresis and transferred onto a PVDF membrane, blocked, incubated with primary T-cadherin antibody (gift of B. Ranscht) and horseradish peroxidase conjugated secondary antibody (Sigma), and visualized by chemiluminescence

(Pierce SuperSignal, Pierce Biotechnology, Rockford, IL). For indirect immunofluorescence, samples were fixed with 4% paraformaldehyde and stained with primary T-cadherin antibody (1:150 dilution) and fluorescein isothiocyanate (FITC) conjugated secondary antibodies (Santa Cruz Biotech).

3.3.9. Cell Viability Assessment

Cell viability was measured via the MTT (3-(4,5-dimethylthiazol-2-yl)-2,5-diphenyl tetrazolium bromide; Sigma) assay, which involves cleavage of the tetrazolium ring by mitochondrial dehydrogenase enzymes to form a purple precipitate. MTT was added to cells in DMEM without phenol red at a concentration of 0.5 mg/mL. After an incubation time of 1 hour, the purple precipitate was dissolved in a 1:1 solution of DMSO and Isopropanol. The absorbance of the solution was measured at 570 nm (SpectraMax spectrophotometer, Molecular Devices, Sunnyvale, CA)

3.4. Results

3.4.1. Induction of Hepatocyte Functions by T-cadherin-Transfected CHOs

In order to determine if cellular presentation of T-cadherin (T-cad) via heterotypic cell-cell interactions could induce liver-specific functions in primary rat hepatocytes, we co-cultivated these cells with either Chinese hamster ovary (CHO) cells that were positive for T-cadherin protein (T-cad-CHO/hep) or null wild-type CHOs (WT-CHO/hep). Expression of T-cad protein in CHOs post-transfection was verified via Western blotting and Immunofluorescence (data not shown). Figure 3.1A compares the time-course of albumin secretion (surrogate marker for synthesis of liver-specific proteins) in pure hepatocyte monolayers, T-cad-CHO/hep co-cultures and WT-

CHO/hepatocyte co-cultures. Pure hepatocyte monolayers showed a rapid decline in albumin secretion, with undetectable levels by day 5 of culture. WT-CHO/hep co-cultures, on the other hand, displayed relative stability in albumin secretion after an initial period of decline. We observed on average a 1.4 fold upregulation in albumin secretion in the T-cad-CHO/hep model over null wild-type controls for the first week of co-culture, and such upregulation increased to 4.2 fold as the co-cultures aged. Hepatocyte morphology improved over time in all co-cultures and became similar to the polygonal morphology of freshly isolated cells with distinct nuclei/nucleoli and appearance of bile canaliculi (Figure 3.1B). Hepatocytes in pure monolayers, on the other hand, spread out to adopt a 'fibroblastic' morphology as typically seen in such cultures (data not shown).

We next followed synthesis of urea (marker of nitrogen metabolism) in pure hepatocyte monolayers and CHO/hep co-cultures over a 2-week period (Figure 3.2). Consistent with the albumin secretion data, urea synthesis in pure hepatocyte monolayers declined to undetectable levels after one week in culture. In CHO/hep co-cultures, on the other hand, we observed several quantitative differences between urea and albumin secretion. First, by day 4 of co-culture, urea synthesis had increased to 354% of day 2 values, and then it declined over the next 14 days to 23%. Next, the difference in urea synthesis between WT-CHO/hep and T-cad-CHO/hep models was negligible for the first week of co-culture; however, by day 8, there was a 1.4 fold upregulation in the T-cad positive model, by day 14 the upregulation had increase to 5 fold, and by day 18, urea could not be detected in the WT-CHO/hep model, whereas hepatocytes were secreting urea at a rate of 20 $\mu\text{g}/\text{day}/\text{million}$ in the T-cad-CHO/hep co-cultures.

Figure 3.3 compares activity of CYP1A enzyme (marker of xenobiotic detoxification) in CHO-hep co-cultures at baseline (panel A) and upon induction for 2 consecutive days with a prototypic inducer, 3-Methylcholanthrene - 3MC (panel B). As

with albumin and urea secretion, we observed upregulation of baseline CYP1A activity in T-cad-CHO/hep co-cultures over their wild-type counterparts (1.2 fold upregulation by 1 week and 2 fold at end of 2 weeks). However, quantitative differences in CYP1A activity between these two co-culture models were negligible upon treatment with 3MC, possibly due to maximal induction of CYP1A levels following 2 days of induction.

3.4.2. RNAi-Mediated Knockdown of T-cadherin in CHO Cells

In order to demonstrate that upregulation of liver-specific functions in the T-cad-CHO/hep model as compared to the WT-CHO/hep model (see Figures 3.1-3.3) was specifically due to T-cadherin protein, we transfected T-cad positive CHOs with siRNA (specific to T-cad mRNA) prior to initiation of co-cultures. Our results indicated that T-cadherin protein in CHOs was knocked down to negligible levels for at least 3 days post transfection (Figure 3.4A). Furthermore, liver-specific functions in co-cultures of siRNA-treated CHOs and hepatocytes were down-regulated by 50% as compared to untreated controls (Figure 3.4B), and such down-regulation was observed for up to 2 weeks (time-course kinetics not shown).

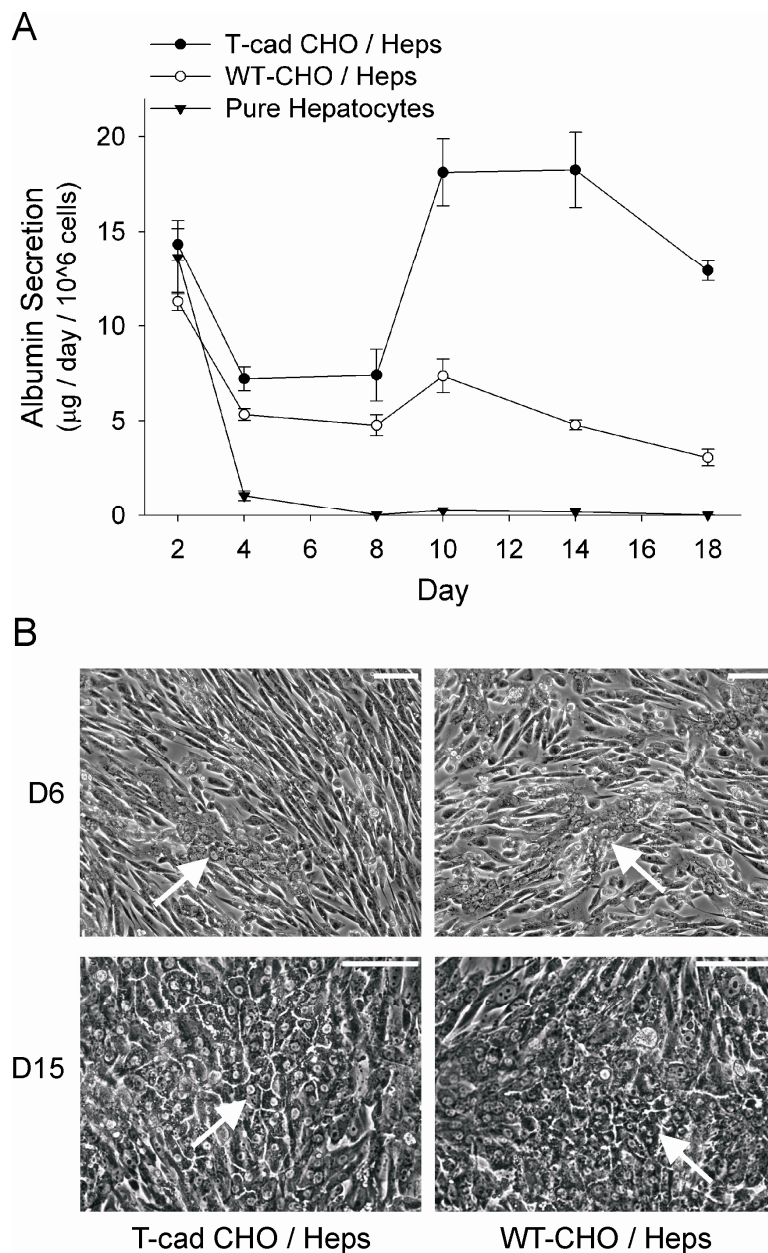


Figure 3.1: Co-cultivation of hepatocytes with T-cadherin-transfected CHO cells. **A)** Chinese Hamster Ovary (CHO) cells expressing mouse T-cadherin (T-cad) protein after transfection with corresponding gene upregulated albumin secretion in primary rat hepatocytes as compared to wild-type (WT) CHOs, which are null for T-cadherin. Pure hepatocyte cultures showed a monotonic decline in function. Error bars are standard error of the mean ($n=3$). **B)** Hepatocyte morphology improved over time in co-cultures (see arrows in Day 6 and 15 phase contrast micrographs), with appearance of polygonal shape, distinct nuclei and nucleoli, and bile canaliculi. Scale bars are 100 μm .

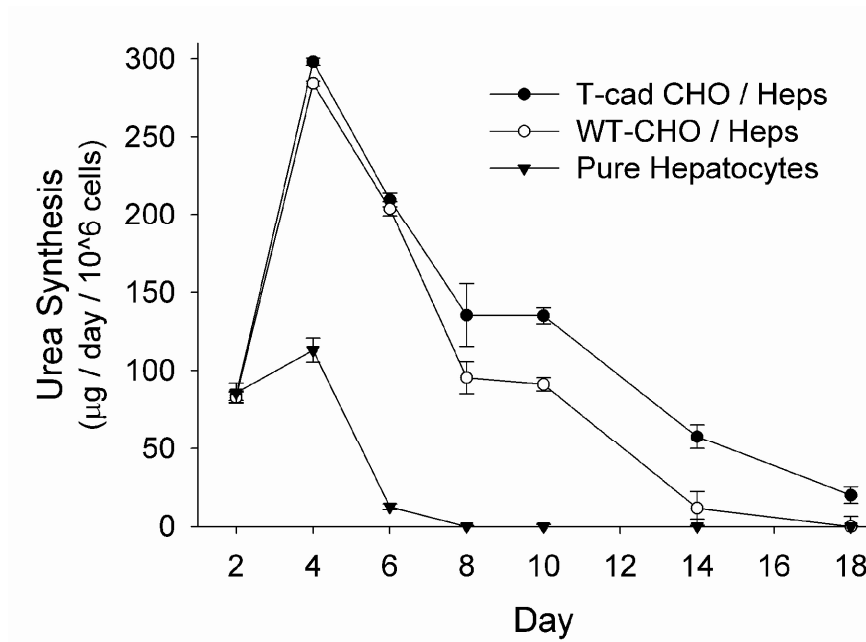


Figure 3.2: Urea synthesis in CHO/hepatocyte co-cultures. ‘WT-CHO / Heps’ refer to co-cultures of wild-type CHO cells (negative for T-cadherin protein expression) and primary rat hepatocytes. ‘T-cad CHO / Heps’ refers to co-cultivation of T-cadherin-transfected CHO cells with hepatocytes.

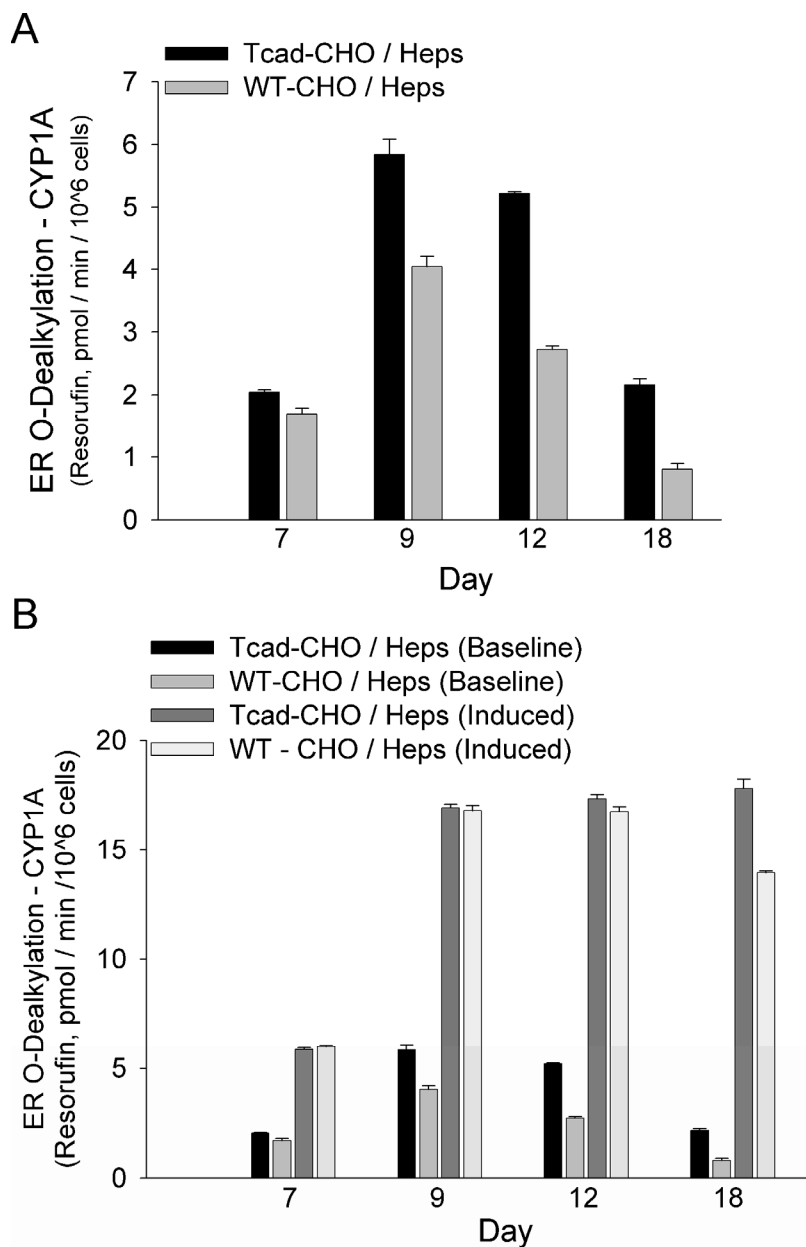


Figure 3.3: Activity of CYP1A enzyme in CHO/hepatocyte co-cultures. **A)** Upregulation of CYP1A enzyme activity in primary rat hepatocytes upon co-cultivation with T-cadherin positive CHOs as compared to wild-type CHOs, which are negative for T-cad. Enzyme activity is expressed as picomoles of resorufin formed in 1 million hepatocytes per minute of incubation with substrate, ethoxy-resorufin. **B)** Induction of CYP1A enzyme levels in co-cultures after incubation with prototypic inducer 3MC (3-Methylcholanthrene) for 2 consecutive days. Baseline activity represents incubation with solvent alone (dimethylsulfoxide). Error bars represent SEM (n=3).

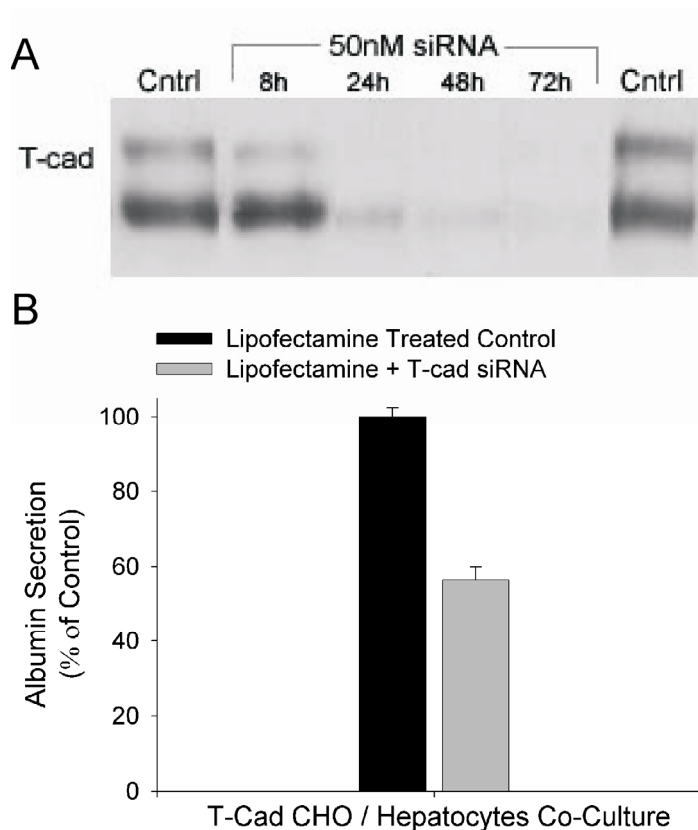


Figure 3.4: RNAi-mediated knockdown of T-cadherin in CHO cells. **A)** T-cadherin positive CHO cells were transfected with either lipofectamine (control) or lipofectamine complexed with siRNA specific for mouse T-cadherin messenger RNA. T-cadherin protein levels post-transfection were visualized via Western blotting at various time points (see Methods). Equal amounts of protein were loaded into each lane. T-cadherin proteins of 95 and 100 kD are expressed by transfected CHO cells (the two bands seen). The 95 kD protein is mature T-cad, while the 100 kD protein is a pre-peptide. **B)** Down-regulation of albumin secretion in rat hepatocytes co-cultivated with siRNA-treated CHO cells as compared to controls. Data represents average of days 4-14 of co-culture. Error bars correspond to standard error of the mean (n=3). Note: Data for this figure was collected with the help of Alice A. Chen of our laboratory.

3.4.3. Upregulation of Functions in Pure Hepatocyte Monolayers on T-cadherin Protein

After demonstrating that cellular presentation of T-cadherin (i.e. transfected CHO) can induce liver-specific functions in hepatocytes, we wanted to determine if similar responses could be obtained upon utilization of purified mouse T-cadherin. Our preliminary studies indicated that hepatocytes do not attach to adsorbed T-cad protein (data not shown). Therefore, we adsorbed type-I collagen after T-cad coating to promote hepatocyte attachment. In Figure 3.5, we show that hepatocytes functions were induced in a dose-dependent manner on T-cad. Albumin secretion increased by 43% over collagen-only (i.e. no t-cad) control at the lowest T-cad protein concentration utilized (1 $\mu\text{g}/\text{mL}$). Such secretion showed an optimum (64% increase) at 10 $\mu\text{g}/\text{mL}$ and declined with increasing T-cad coating densities. In contrast, urea synthesis in hepatocytes increased monotonically with T-cad coating densities greater than 1 $\mu\text{g}/\text{mL}$. CYP1A activity also showed monotonic increases as T-cad concentrations increased from 1 $\mu\text{g}/\text{mL}$ to 40 $\mu\text{g}/\text{mL}$. Of the three liver-specific functions assessed, CYP1A activity was upregulated to the greatest degree (113% increase at 40 $\mu\text{g}/\text{mL}$ T-cad coating density as compared to collagen-only control), followed by urea synthesis (72%) and then albumin secretion (64%).

To verify that functional increases on varying levels of T-cad were not due to differences in attachment efficiencies, we conducted viability assessment (MTT assay, see methods) 12 hours after hepatocyte attachment and observed no differences across conditions (Figure 3.6A). Next, to address the possibility that hepatic function varied between T-cad coating densities due to variations in cell shape, we qualitatively inspected hepatocyte morphology 24 hours post seeding (Figure 3.6B) and as the cultures aged and found no observable differences.

Though purified T-cadherin induced hepatocyte functions in a dose-dependent manner, it was not able to prevent loss of viability and decline in functions that is characteristic of pure hepatocyte monolayers on collagen (Figure 3.7). Nonetheless, liver-specific functions were detected in cultures on T-cad protein one week after functions in control cultures had reached undetectable levels.

3.4.4. Upregulation of Functions in Co-Cultures on T-cadherin Protein

In order to determine if purified T-cadherin could upregulate hepatocyte functions in 'stable' co-culture models of the liver, we co-cultivated primary rat hepatocytes adherent on T-cad coated substrates with cell types lacking endogenous T-cad protein expression, namely wild-type CHOs and mouse embryonic fibroblasts (MEF). In Figure 3.8, we show that purified T-cad protein induced albumin secretion in WT-CHO/hep co-cultures in a dose-dependent manner. Function in co-cultures of T-cad-transfected CHOs and hepatocytes on collagen-alone is shown for comparison. In Figure 3.9, we show long-term (weeks) upregulation of liver-specific functions (albumin secretion and urea synthesis) in MEF/hepatocyte co-cultures that were seeded on a substratum containing T-cad fusion protein.

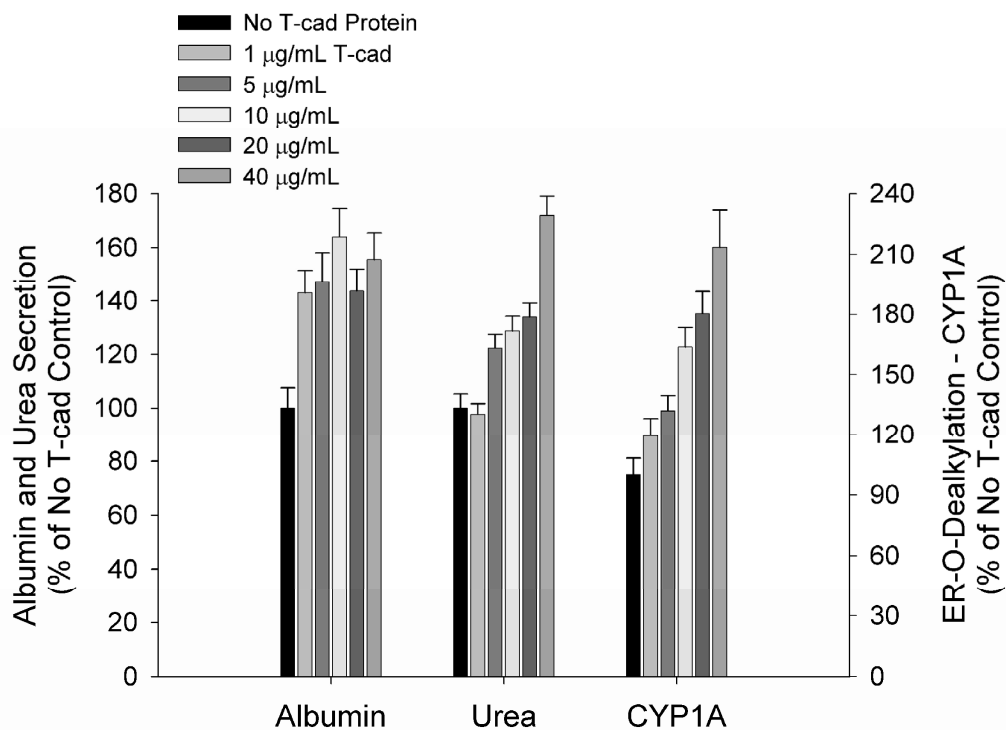


Figure 3.5: Upregulation of hepatocyte functions on T-cadherin-coated substrates in a dose-dependent manner. Tissue culture plates were coated by adsorption of purified histidine-tagged T-cadherin fusion protein at various concentrations (see Methods). Subsequent coating of substrates with collagen allowed hepatocytes to attach and interact with T-cad. Hepatocyte functions (albumin secretion, urea synthesis, and cytochrome P450 1A1 activity) varied in a dose-dependent manner with T-cadherin. CYP1A1 activity was assayed via the de-alkylation of ethoxy-resorufin into fluorescent resorufin. Albumin and urea data represents average values for days 5 to 14 of culture, while CYP1A data is a representative time point on day 10. Error bars represent SEM (n=3).

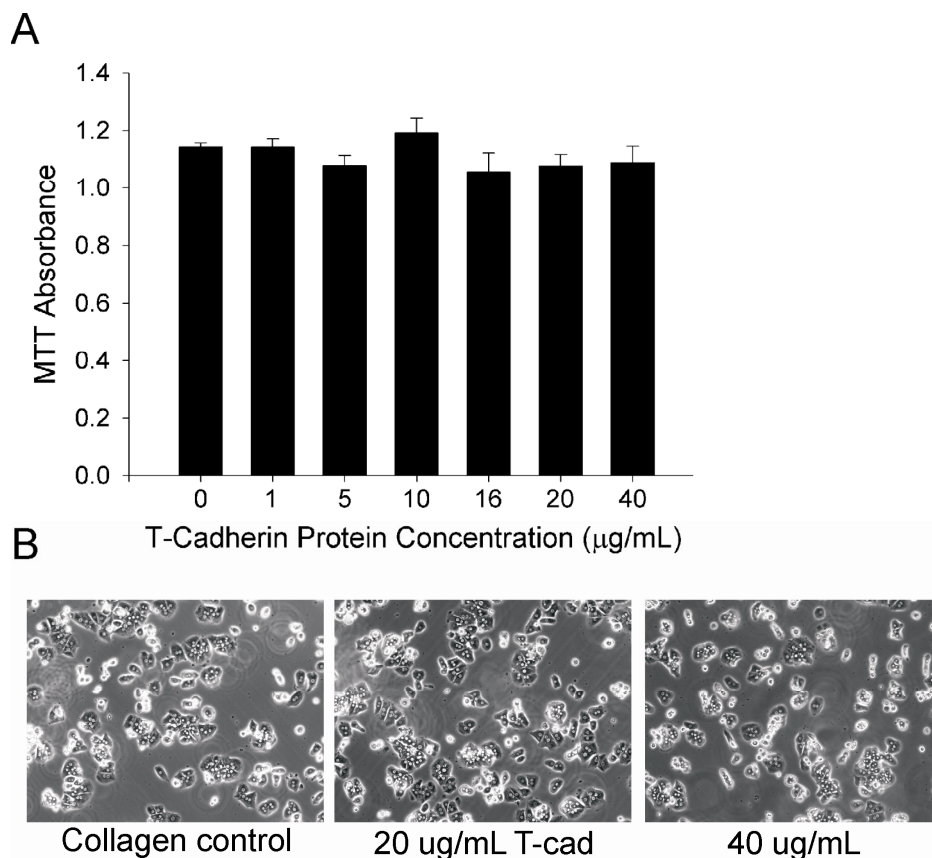


Figure 3.6: Relative hepatocyte attachment and spreading on T-cadherin-coated substrates. Tissue culture plates were coated by adsorption of purified histidine-tagged T-cadherin fusion protein at various concentrations. Subsequent coating of substrates with collagen allowed hepatocytes to attach and interact with T-cad. **A)** Shown here is hepatocyte viability on T-cad coated substrates 12 hours after seeding, as assessed via mitochondrial activity (MTT assay – see methods). The viability values for increasing doses of T-cad were found to be statistically similar (assessed using one-way ANOVA). Error bars represent standard error of the mean (n=3). **B)** Phase contrast micrographs showing hepatocyte morphology on T-cad coated substrates 1 day after seeding. No qualitative differences in hepatic morphology across varying T-cad densities were observed.

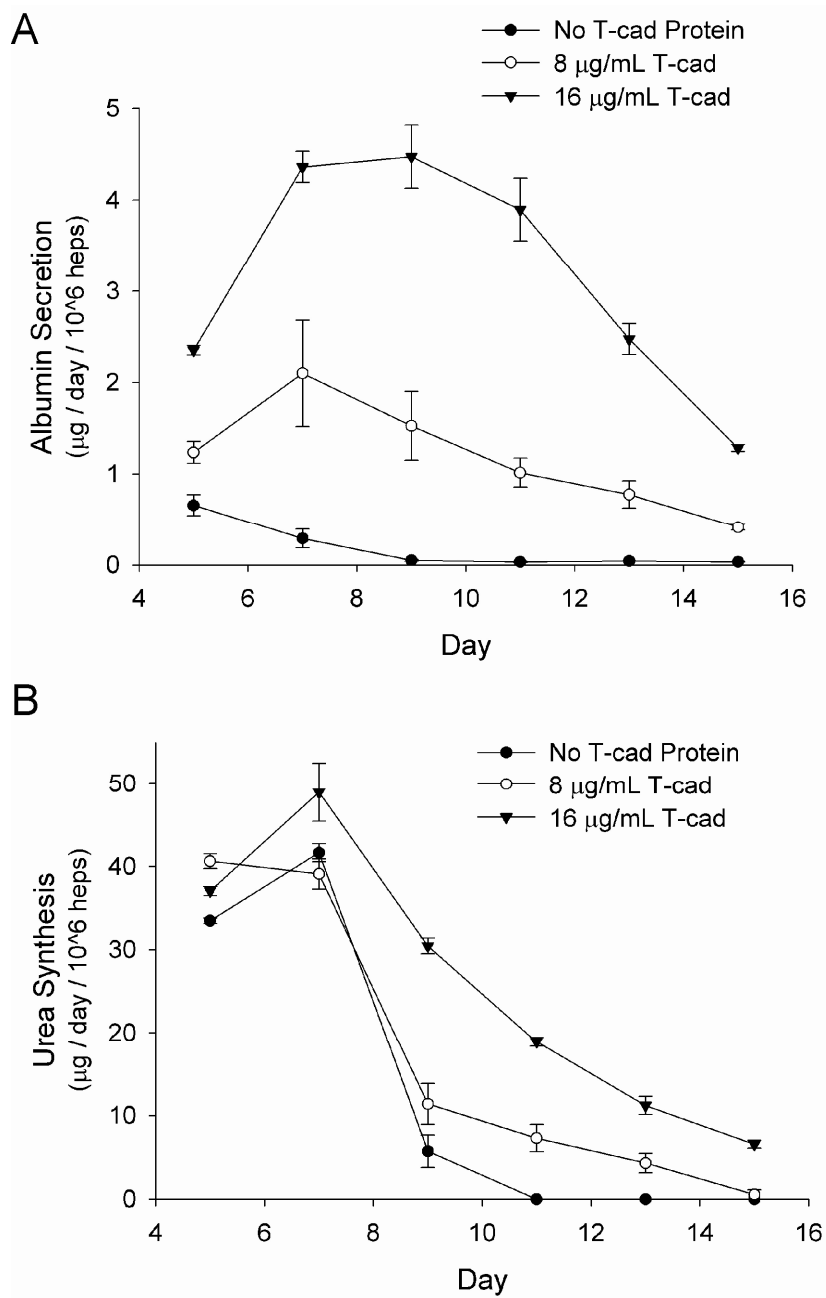


Figure 3.7: Long-term induction of functions in hepatocytes on T-cadherin-coated substrates. **A)** Time course of albumin secretion in pure hepatocytes seeded on collagen (i.e. No Tcad) or collagen with varying levels of purified T-cadherin protein (8 and 16 µg/mL). **B)** Time-course functional data as in 'A' except urea synthesis is shown. Error bars represent standard error of the mean (n=3).

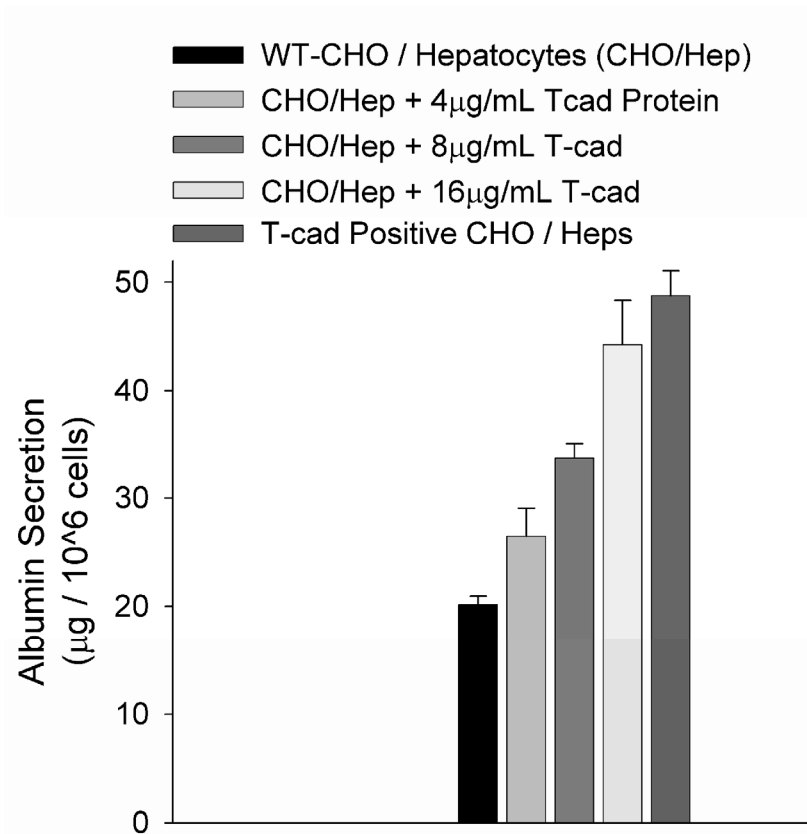


Figure 3.8: Co-cultures of wild-type CHO cells and hepatocytes on T-cadherin. Co-cultures were created by adding wild-type CHO cells lacking endogenous T-cad expression to adherent hepatocyte cultures on T-cad coated substrates. Albumin secretion varied in a dose-dependent manner with T-cadherin in such co-cultures. For comparison, function in co-cultures of T-cad positive CHO and hepatocytes on collagen is shown. Data represents cumulative albumin secretion for days 4-14 of co-culture. Error bars are SEM (n=3).

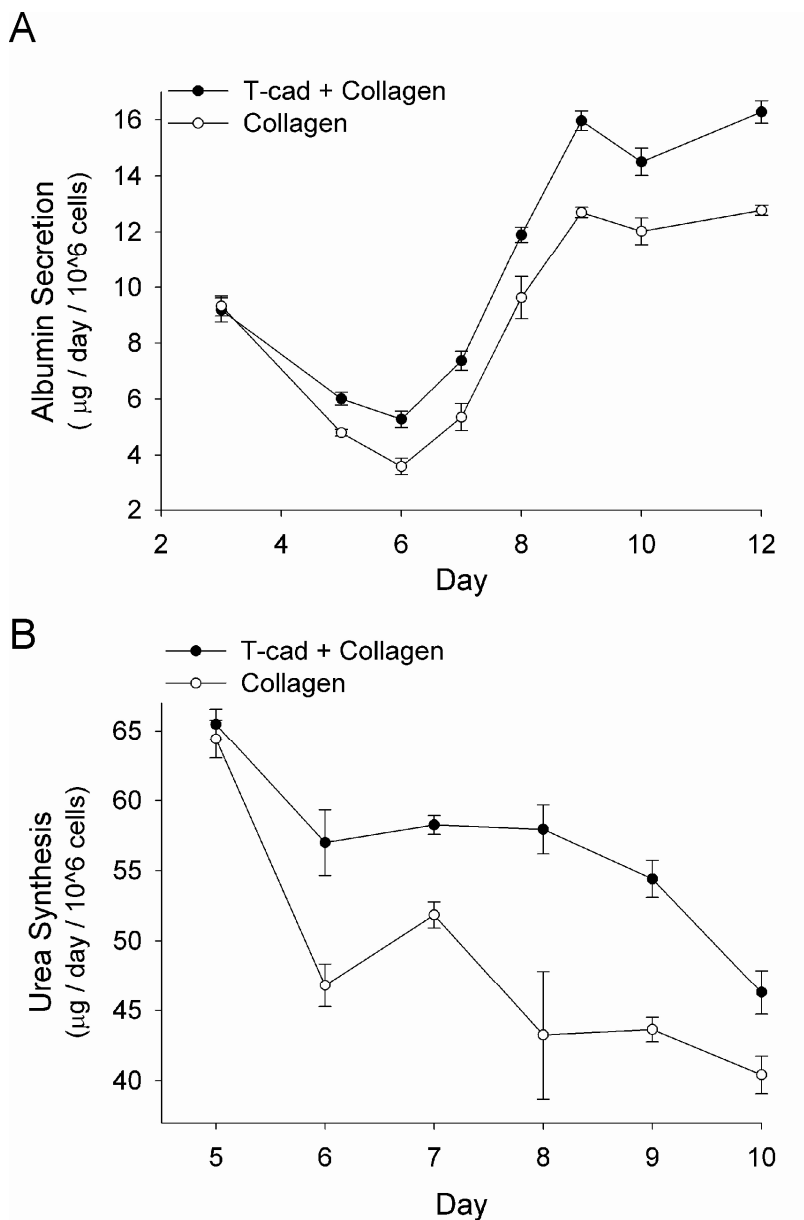


Figure 3.9: Long-term upregulation of liver-specific functions in MEF-hepatocyte co-cultures on T-Cadherin. Tissue culture plates were coated by adsorption of purified histidine-tagged T-cadherin fusion protein (5 µg/mL). Subsequent coating of substrates with collagen (5 µg/mL) allowed hepatocytes to attach and interact with T-cad. After 24 hours of hepatocytes seeding, mouse embryonic fibroblasts (MEFs) that lack endogenous T-cad expression were seeded onto adherent hepatocytes to create co-cultures. Albumin secretion (**A**) and urea synthesis (**B**) were higher in co-cultures plated on T-cadherin as compared to collagen-only controls. Error bars represent SEM (n=3).

3.5. Discussion

It is widely known that primary hepatocytes from several different species lose viability and phenotypic functions within a few days of isolation from the highly complex and intricate microenvironment of the liver [57, 58, 249]. In vitro, co-cultivation of hepatocytes with liver and non-liver derived nonparenchymal cells provides for robust induction of diverse liver-specific functions ('co-culture effect') [65, 208]. However, in spite of its discovery over two decades ago, the co-culture effect remains poorly understood in its underlying molecular mechanisms.

Recently, we developed and validated a functional genomic approach to identify potential molecular mediators of hepatocyte-nonparenchymal cellular interactions [58]. In particular, T-cadherin message levels positively correlated with the ability of murine embryonic fibroblasts to induce hepatocyte functions in co-culture. In this study, we demonstrate that both cellular and a-cellular presentation of T-cadherin to rat hepatocytes induces in them a diverse set of liver-specific functions. Specifically, a co-culture model was first developed in which CHO cells interact with hepatocytes to stabilize their phenotypic functions. Then, these CHO cells were stably transfected with mouse T-cadherin before co-cultivation with hepatocytes. Using this model of heterotypic cellular presentation of T-cadherin, we demonstrated that the synthetic, metabolic and detoxification functions of hepatocytes were upregulated over wild-type null controls. Further RNAi-mediated knockdown of T-cadherin in transfected CHOs prior to initiation of co-culture caused down-regulation of hepatocyte functions for up to 2 weeks. Next, we showed that a substratum of purified T-cadherin was able to induce hepatocyte functions in both pure cultures and co-cultures where the nonparenchymal cells lacked endogenous T-cadherin expression (i.e. mouse embryonic fibroblasts and wild-type CHOs). Taken together, our data demonstrates for the first time that the atypical T-

cadherin, typically thought to be a signaling rather than a homotypic adhesion molecule, is involved in regulation of liver-specific functions in primary hepatocytes.

In order to assess stability of the hepatic phenotype, we measured albumin secretion, urea synthesis and cytochrome P450 1A activity as surrogate markers for liver-specific protein production, nitrogen metabolism and activity of drug metabolism enzymes, respectively. In co-cultures of T-cadherin-transfected CHO cells and primary rat hepatocytes, we observed several quantitative differences between the kinetics of albumin and urea secretion. Albumin levels, in particular, declined to 50% of day 2 values by day 4 and remained so until day 8. Following that initial refractory period, we observed an upregulation and stabilization of albumin secretion to 130% of day 2 values. Urea synthesis, on the other hand, increased to 354% of day 2 values by day 4, and then it declined over the next 18 days to 23%.

The mechanism underlying the aforementioned differences between the kinetics of the two functional markers has not been explicitly investigated in this study. However, we did observe that the CHO cells in co-cultures grew rapidly and depleted the culture medium of nutrients and oxygen faster than the media change schedule. As a result, the pH over the first week of co-culture became fairly acidic as assessed qualitatively by the yellow color of the pH indicator dye (phenol red) in the media. After the first week, the pH returned back to physiologic value (i.e. 7.2 to 7.4, qualitative observation with media color) as the CHO cells possibly adapted to their new microenvironment containing hepatocytes and hepatocyte-specific culture medium. Concomitant with the return of pH in co-cultures to physiologic values, we observed improvement of hepatocyte morphology, which became similar to the polygonal morphology of freshly isolated cells with distinct nuclei/nucleoli and appearance of bile canaliculi. Previously published studies have shown that chronic metabolic acidosis in humans and HepG2 cells

(carcinoma-derived human liver cell line) can cause decreased synthesis of albumin [254, 255]. Additionally, metabolic acidosis leads to increased production of nitrogenous waste in urine samples of human patients (i.e. negative nitrogen balance) [254]. Since urea is the chief nitrogenous compound of urine, the increase in nitrogenous waste most likely correlates with increased production of urea in these patients. In the first week of our co-cultures, when the cells experienced an acidic microenvironment, we speculate that increased synthesis of urea may have been due to high levels of ‘protein-wasting’, which may include degradation of albumin. Though such a hypothesis is consistent with the literature, the molecular pathways connecting low pH to protein degradation and a negative nitrogen balance remain unclear. Gene expression profiling of hepatocytes under conditions of varying pH values may shed some insight into such pathways.

The mode of purified T-cadherin protein presentation (i.e. adsorbed, soluble) was important for modulation of liver-specific functions in hepatocytes. Supplementation of culture medium with varying concentrations of T-cad did not induce hepatocyte functions to any considerable degree (data not shown). On the other hand, adsorbed T-cad enhanced hepatocyte functions in a dose-dependent manner, and functions were detected even a week after they had declined to undetectable levels in control cultures on collagen. However, despite T-cad’s inductive ability in adsorbed format, it was not able to rescue hepatocytes from eventual decline, suggesting that several molecules may coordinate to produce a differentiated hepatocyte phenotype. For future studies, clustering of histidine-tagged T-cadherin onto nickel-coated microbeads for coating of hepatocyte cultures may provide an opportunity to reintroduce fresh protein at a later time point in culture in order to modulate hepatocellular fates. For example, Brieva et al found that co-cultivating hepatocytes with E-cadherin positive chaperone cells induced liver-specific functions and suppressed DNA synthesis, while incubating hepatocytes with

E-cadherin functionalized microbeads caused the reverse response [256]. Thus, similar to E-cadherin, the mode of T-cadherin presentation may allow switching between multiple hepato-cellular fates. We anticipate that an optimal microenvironment for maintaining the hepatic phenotype will need to present multiple molecules via different modes in organized spatio-temporal patterns.

In addition to creating pure cultures of hepatocytes on T-cadherin, we also created co-cultures on T-cad in which the nonparenchymal cells lacked endogenous T-cad expression. We found that T-cad induced a dose-dependent upregulation of liver-specific functions in hepatocytes upon co-cultivation with wild-type CHO cells. Furthermore, co-cultivation of hepatocytes with mouse embryonic fibroblasts on T-cad coated substrates also caused upregulation of hepatic functions. In a recently published study, we showed that RNAi-mediated knockdown of T-cadherin protein in 3T3-J2 fibroblasts diminishes their capacity to induce high levels of functions in rat hepatocytes [257]. Taken together, these data sets show that T-cadherin can upregulate liver-specific functions in multiple co-culture models of the liver.

Results of this study illustrate that T-cadherin modulates different hepatocyte functions *in vitro*. However, the *in vivo* role of T-cad in the liver remains unclear. Preliminary immunofluorescent staining of mouse liver sections by the Ranscht group at the Burnham Institute (unpublished data not shown) suggests that T-cadherin is expressed on the endothelium of center venules and not on hepatocytes. In a recently published study, T-cad was shown to be a receptor for the hormone, adiponectin, which synergizes with insulin to increase glycogen stores and suppress gluconeogenesis in the liver [99]. It is plausible that T-cad on liver endothelia binds adiponectin and causes a cascade of signaling events that ultimately leads to blockade of gluconeogenesis in hepatocytes. Furthermore, T-cad expression in the liver may be dynamically modulated

with changes in levels of insulin and adiponectin (i.e. after meals). Our data suggests that T-cadherin can modulate several different types of liver-specific functions in hepatocytes and thus may have a broad role in liver physiology.

In liver pathophysiology, a recent report by Adachi et al shows that T-cadherin is selectively expressed in intra-tumoral capillary endothelial cells in hepatocellular carcinomas (HCC) [258]. The authors also demonstrate via an in vitro transwell assay that FGF-2 secretion by HepG2 cells (isolated from HCC) induced T-cadherin protein expression in sinusoidal endothelial cells. Though T-cad has been shown to be silenced at the transcriptional level in tumor cells of many different organs and thus thought to be a tumor suppressor gene, Adachi et al hypothesize based on their data that FGF-2 secretion by HCC in vivo induces T-cad expression in endothelia of the tumor capillaries, which then positively mediates tumor angiogenesis via interaction with adiponectin. However, further studies are needed to confirm the diverse roles of T-cadherin in liver physiology and disease.

Consistent with in vivo data, we observed that T-cadherin protein was not expressed either in freshly isolated hepatocytes or in those co-cultivated with CHO cells (western blotting and immunofluorescence data not shown). Thus, the molecular identity of the hepatocyte binding partner of T-cadherin remains currently undetermined. Heterophilic interactions of cadherins have been demonstrated with integrins, growth factor receptors and other types of cadherins [67, 68]. Since hepatocytes express multiple types of cadherins (i.e. N- and E-cadherin) [83], the interplay of these molecules with nonparenchymal-derived T-cadherin merits further investigation. In the future, gene expression profiling of hepatocytes on T-cadherin substrata may shed some insight into the molecular mechanisms underlying induction of liver-specific functions.

In conclusion, this study demonstrates that different types of liver-specific functions are upregulated for several weeks in hepatocytes upon presentation of T-cadherin either bound to the membrane of a nonparenchymal cell or adsorbed to tissue culture plastic. In the future, T-cadherin and other molecular mediators of hepatic differentiation may prove useful towards building highly functional in vitro models of the liver for fundamental hepatology, cell-based therapies for liver disease and drug development.

Acknowledgements

We are grateful to Jennifer Felix for rat hepatocyte isolation, Barbara Ranscht for generously providing T-cadherin-transfected and wild-type CHO cells and recombinant T-cadherin protein, Alice Chen for assistance with RNAi studies, and James Thomson for providing Mouse Embryonic Fibroblasts.

CHAPTER 4

DYNAMIC MODULATION OF HETEROTYPIC CELL-CELL INTERACTIONS VIA ELECTROACTIVE SUBSTRATES

4.1. Abstract

Self-assembled monolayers (SAMs) of alkanethiolates on gold offer unprecedented molecular-level control over the pattern, structure and density of ligands (i.e. cell adhesion peptides) presented to cells. Recently, SAMs have been modified to present ligands that can be released or tethered to the surface in real-time upon application of an electrical stimulus. Though considerable progress has been made in characterizing these so-called electroactive substrates, their application to the study of heterotypic cell signaling (i.e. interactions between multiple cell types) remains largely unexplored. In this study, we have developed novel methodologies utilizing electroactive substrates to study the dynamics of epithelial-nonparenchymal interactions. We have subsequently applied these methodologies to a robust in vitro model of the liver in which primary hepatocytes (liver parenchymal cells) are stabilized upon co-cultivation with murine embryonic 3T3 fibroblasts. Specifically, our objective was to determine whether fibroblast signaling is required continuously in co-culture to maintain liver-specific functions in hepatocytes. We demonstrate that selective and efficient release of fibroblasts from micropatterned co-cultures at various time points (up to 5 days after

initiation of culture) caused necrosis in the hepatocyte population and led to a significant decline in liver-specific function (i.e. albumin secretion) over the course of 1 week. Results of this study suggest that insoluble nonparenchymal products (i.e. cell-cell contact and extracellular matrix molecules) may be necessary to maintain differentiated functions in primary hepatocytes. Such results may have implications for the development of in vitro liver models for applications such as cell-based therapies for liver disease and pharmaceutical drug screening. In the future, continued application of dynamic substrates to diverse model systems in which heterotypic signaling regulates cell fate processes (i.e. keratinocytes and fibroblasts; astrocytes and neural stem cells) may elucidate fundamental mechanisms underlying physiology and disease.

4.2. Introduction

Modulation of cell fate processes (differentiation, migration, proliferation and apoptosis) in embryology, physiology and pathophysiology depends on interactions between multiple cell types [259-261]. Furthermore, such heterotypic cell-cell interactions are regulated dynamically in both space and time to affect tissue form and function. In the case of the liver in vivo, interactions between a variety of nonparenchymal cells (i.e. sinusoidal endothelial cells, kupffer cells, stellate cells) and parenchymal hepatocytes are necessary to maintain the diverse and complex functions of the liver [220]. In vitro, co-cultivation with nonparenchymal cells from both within and outside the liver has been shown to induce a diverse set of phenotypic functions in hepatocytes from multiple species (i.e. porcine, human, rat, and mouse) [65]. Such co-cultures have been utilized as robust models of the liver for fundamental studies of physiology [65] and pathophysiology [116], and have been explored in bioartificial liver devices towards sustaining patients while they wait for a whole organ transplant or for their liver to

regenerate itself [32]. Even though this so-called ‘co-culture effect’ was discovered over two decades ago [125], the dynamics of hepatocyte-nonparenchymal interactions have yet to be elucidated. In particular, it is unclear whether continuous nonparenchymal signaling is required to maintain hepatocyte functions in co-culture. Until recently, cell culture tools did not exist to address such an issue; however, over the last few years, novel techniques have emerged that allow rigorous control over cell-cell and cell-matrix interactions.

In conventional cell culture approaches, substrates (i.e. tissue culture polystyrene, glass) are typically incubated with a solution of extracellular matrix (ECM) protein, which adsorbs to the surface in an essentially irreversible manner. Adsorbed proteins can undergo lateral diffusion on the surface, exchange with other serum proteins in solution and can be denatured, which may render them biologically inactive. Due to such complex mechanisms underlying protein adsorption, the properties of substrates created via standard approaches are difficult to control [158]. Furthermore, dynamic control over protein composition and presentation of active ligands to cells is not possible with such approaches. Release of cells from culture substrates is routinely accomplished via enzymatic treatment (i.e. trypsin); however, spatial control over release of specific cell populations is hindered by a lack of control over protein adsorption.

The aforementioned limitations of conventional approaches have spurred the development of tailored surfaces which offer rigorous control over the structure, density and pattern of immobilized ligands (i.e. cell-adhesion peptides). Self-assembled monolayers of alkanethiolates on gold are currently the best class of substrates for such applications [161]. These monolayers can be functionalized with a variety of ligands (i.e. enzymes, proteins, oligonucleotides) and are compatible with cell culture conditions. Furthermore, substrates containing micropatterns of SAMs with varying functional

groups can be prepared using well-characterized lithographic techniques. Micropatterned SAMs have been extensively utilized to uncover novel mechanisms underlying biological phenomena [148, 153, 262].

Recently, Mrksich and colleagues have extended the functionality of SAMs to prepare substrates in which the activities of discrete ligands can be modulated in real-time [147, 162]. Their strategy uses redox-active groups tethered to SAMs to activate or inactivate immobilized ligands when electrical potentials are applied. In one example, the Mrksich group first created micropatterns of 'electroactive' and 'inactive' SAMs using soft-lithography (i.e. microcontact printing), and subsequently demonstrated release of fibroblasts selectively from the electroactive domains which contained tethered RGD (arginine-glycine-aspartic acid, cell adhesion peptide) prior to electrochemical treatment [162]. In another instance, electrochemical treatment caused attachment of RGD to the underlying SAMs and caused migration of cells that were initially confined to fibronectin-coated inactive domains [263]. Lastly, the Mrksich group has developed a substrate which allows release of one type of ligand and reattachment of a second ligand at a later time point [264]. In spite of considerable progress in the development of the underlying chemistry of electroactive substrates, their application to the study of cell-cell interactions in an important biological system has not been demonstrated.

Langer and colleagues have recently reported the design of a SAM-coated surface which exhibits dynamic changes in surface wetting (i.e. hydrophilicity and hydrophobicity) upon application of an electrical stimulus [265]. A molecule with a negative terminus- (16-mercaptop) hexadecanoic acid (MHA)- is arranged on a gold surface with optimized intermolecular spacing (lower density than standard 'packed' SAMs). With such an optimized spacing, the surface displays its hydrophilic, negatively charged terminus upon application of a negative electric potential to the gold coating. On the other hand,

application of a positive charge induces electrostatic attraction between the gold surface and the negatively charged MHA terminus, causing this molecule to bend and display its hydrophobic regions. These specialized SAMs remain in early experimental stages and have not been applied to studies of cell-cell interaction. Furthermore, it is unclear if the MHA molecules can be functionalized with specific ligands such as surface receptors and cell adhesion peptides to facilitate biological studies. Instead, the authors suggest utility of MHA-coated gold in the development of medical devices and sensors with digitally responsive surfaces.

Besides electroactive SAMs, several other groups have recently explored the use of dynamic stimuli-responsive surface chemistries for cell patterning. For instance, Okano and colleagues have patterned a thermo-responsive polymer called poly(N-isopropyl acrylamide) or pNIPA onto tissue culture substrates [266]. Below its lower critical solution temperature of 31°C, pNIPA is in a hydrophilic, swollen state that is non-fouling (i.e. prevents protein adsorption) and therefore prevents cell attachment. As the temperature increases, this polymer collapses and its hydrophobic character increases, making it conducive to cell culture. Thus, removal of a cell culture from an incubator (typically set at 37°C) results in release of cells selectively from the patterned pNIPA regions, which can then be seeded with a secondary cell type to create co-cultures. Recently, Ratner and colleagues have used a photolithographically fabricated microheater array to spatially control pNIPA transition [267]. The authors use this strategy to create a localized change in surface adhesive behavior which leads to site-specific cell attachment (i.e. patterning). Thermally-responsive polymers have shown to be important for the harvesting of cells and tissues; however, they do not offer the molecular-level control necessary for rigorous studies of cell-cell interactions. Furthermore, the use of thermo-responsive chemistries may pose a challenge in routine cell culture studies since

temperature fluctuations occur frequently in the handling and feeding of *in vitro* cellular constructs.

New generations of synthetic, polymeric materials are being developed by several different groups for use as three-dimensional extracellular microenvironments in therapeutic and basic biological studies [268]. In particular, recent advances include artificial ECM networks formed from protein polymers or peptide-conjugated synthetic polymers that present bioactive ligands to cells and respond to cell-secreted signals to enable proteolytic remodeling. Such ‘smart’ biomaterials have been utilized to demonstrate differentiation of stem cells into neurons, repair of bone, and induction of angiogenesis (*i.e.* sprouting of new blood vessels from pre-existing ones). For instance, Hubbell and colleagues have developed fibrin-based matrices modified with cell adhesion peptides and peptide substrates for cellular processes [269]. Release of proteases by cells resulted in remodeling of the substrate. The complexity of these biomaterials has been augmented to include binding sites for growth factors and other signaling molecules within the synthetic matrix. Development of such ‘bulk’ strategies has increased the complexity of model substrates towards sophisticated cell-biomaterial interactions. However, synthetic biomaterials in their current form are not amenable to dynamic control of cell-cell and cell-matrix interactions.

In this study, our objective was to investigate the dynamics of hepatocyte-nonparenchymal interactions *in vitro*. In particular, we wanted to determine whether continuous heterotypic signaling with nonparenchymal cells is required to maintain liver-specific functions in hepatocytes. To answer this question, we chose electroactive substrates developed by the Mrksich group due to the ability to control in real-time and on a molecular level, the presentation of ligands to cells (see Figure 4.1). We developed soft-lithographic processes to create micropatterned co-cultures in which hepatocytes

were seeded onto collagen-coated, 'inactive' domains, while fibroblasts attached to electroactive domains containing RGD-functionalized SAMs. Following several different optimizations (i.e. 3T3 sub-clone selection, electrochemical parameters), fibroblasts from micropatterned co-cultures were released at various time points, and hepatocyte morphology and function were subsequently monitored. Our results indicated that hepatocytes required continuous fibroblast signaling to maintain their phenotypic functions in co-culture. In particular, release of fibroblasts caused necrosis in hepatocyte islands and accompanying decline of phenotypic function. In the future, our methodology using electroactive substrates may be used to study cell-cell signaling in other model systems where reciprocal interactions between multiple cell types modulate cellular fates.

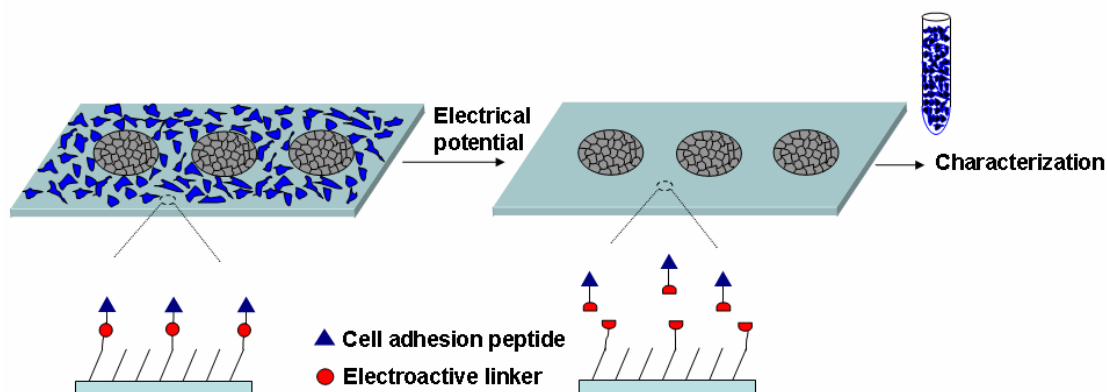


Figure 4.1: Electroactive substrate to evaluate dynamics of heterotypic cell-cell interactions. Shown here is a dynamic substrate that can selectively release immobilized cell adhesion peptides and thus regulate, in real-time, cell attachment to a substrate as well as heterotypic cell-cell interactions. Micropatterned co-cultures are first created and then subjected to electrochemical treatment. The cell type on ‘electroactive domains’ releases from the culture substrate, while the cell type on the non-electroactive islands remains attached to the underlying extracellular matrix scaffold. Characterization such as morphological analysis and global gene expression profiling can be carried out on the cells to evaluate the dynamics of cell-cell interaction. Electroactive substrates contain self-assembled monolayers of functionalized alkanethiolates on gold. Cell adhesion peptides are tethered to the monolayer through an electroactive linker. Upon application of an electrical potential, the linker undergoes cleavage to release the adhesion peptide and the attached cells in the surrounding cell culture medium.

4.3. Materials and Methods

4.3.1. Preparation of Gold-Coated Substrates

Glass coverslips were cleaned in Piranha solution (sulfuric acid: 30% hydrogen peroxide, 70:30) for 30 minutes, washed thoroughly with deionized water and pure ethanol, and dried under a stream of nitrogen. Titanium (5 nm) and then gold (15 nm) were evaporated onto the glass coverslips using an electron beam evaporator (Thermionics VE-100) at a rate of 0.2 ~ 0.4 nm/sec and a pressure of 9×10^{-7} Torr.

4.3.2. Electroactive Chemistry

Mrksich and colleagues have extended the functionality of self-assembled monolayers (SAM) on gold by developing chemistries that can release immobilized ligands from the underlying SAM surface [162]. The specific electroactive chemistry utilized in this study is presented in Figure 4.2. The electroactive quinone ester and the tri-(ethylene glycol)-terminated disulfide were synthesized by the Mrksich group (work of Woon-Seok Yeo) using previously published protocols [162, 264]. These two molecules were first dissolved in pure ethanol and then mixed in various ratios (0.1 – 1% vol/vol electroactive molecule in background of tri-ethylene glycol) prior to incubation with gold-coated substrates (i.e. glass coverslips). Over a period of several hours (8-12 hours), the alkanethiolates formed a SAM on the gold surface. Subsequent incubation of the substrate with cysteine-containing RGD (CGRGDS) caused this cell adhesion peptide to be tethered to the underlying SAM via conjugation to the electroactive quinone ester. Upon application of an electrochemical stimulus (see next sub-section for details), the quinone was reduced to hydroquinone, and then a cyclization reaction gave a lactone with release of the RGD ligand from the underlying SAM.

4.3.3. Electrochemical Release of Cells

Electrochemistry was performed in a custom designed electrochemical cell with the monolayer-coated gold as the working electrode, a platinum wire as the counter electrode and a silver/silver chloride reference electrode (Bioanalytical Systems, West Lafayette, IN). The electrochemical cell consisted of a polydimethylsiloxane (PDMS) chamber sealed to the gold substrate and filled with culture medium. Voltage (-550 to -700 mV) was applied to the cultures for 4-5 minutes using a potentiostat (CV-27 from Bioanalytical Systems). Media with released cells was aspirated and adherent cultures were rinsed 2-3 times to remove loosely attached cells on the electroactive domains.

4.3.4. Microcontact Printing to Generate Patterned SAMs

Microcontact printing (μ CP) provides a convenient method for patterning SAMs of alkanethiolates on gold with features of sizes down to 1 μ m (Figure 4.3). In this method, a photoresist (UV sensitive polymer) pattern was first created on a substrate (glass or silicon) using traditional photolithography, the details of which are presented in Chapter 5. Then, this photoresist 'master' was covered with a solution of PDMS prepolymer and activator (10:1 Sylgard-184 PDMS to activator ratio). Upon heating at 65°C for 2 hours, the PDMS polymerized and was subsequently peeled off the photoresist master to yield a stamp. This PDMS stamp was 'inked' with a solution of hydrophobic hexadecanethiol (HDT) in ethanol using a cotton swab, dried under a stream of nitrogen for 30 seconds and manually brought into contact with a surface of gold (typically gold-plated glass coverslips). The HDT was transferred to the surface only at those regions where the stamp made contact with the surface. Thus, this process created a pattern of hydrophobic SAMs that was defined by the pattern of the stamp. Multiple stamps were cast from a single master and each stamp was used hundreds of times. The HDT-patterned gold substrate was incubated with another solution of alkanethiolates (i.e.

electroactive molecules in tri-ethylene glycol) for 12-18 hours to coat the remaining bare gold areas with SAMs. The patterned substrates were then rinsed with ethanol, dried thoroughly under nitrogen and incubated with a solution of CGRGDS, which reacted with the electroactive linker and became tethered to the surface. Collagen adsorbed selectively to the HDT regions, while the RGD-functionalized tri-ethylene glycol regions resisted non-specific protein adsorption.

4.3.5. Stencil-based Process to Generate Patterned SAMs

A novel soft-lithographic method that we have developed and characterized in this study utilizes elastomeric PDMS stencils (Figure 4.4). Similar to stamps, PDMS stencils are also created using a photoresist master. However, the objective is to yield a thin membrane with through-holes in it instead of ‘posts’ for stamping. The details of creating stencils using a compression-molding process are given elsewhere in detail [157]. A gold-plated substrate is first coated with electroactive SAMs as described in previous sections. Then, the stencil is gently placed onto the substrate and tapped lightly to ensure proper sealing. The stencil/substrate assembly is exposed to oxygen plasma for ~1 minute to remove the SAM from regions not protected by the PDMS posts. Incubation of the assembly with collagen allows this protein to adsorb to bare gold via the through-holes in the stencil. Following drying of the culture well, the stencil is peeled off the substrate, which is then incubated with CGRGDS to tether it to electroactive domains.

4.3.6. Generation of Micropatterned Hepatocyte-Nonparenchymal Co-Cultures

Primary rat hepatocytes and murine 3T3 fibroblasts were cultured using the procedures described in chapter 2. Hepatocytes selectively attached to collagenous domains in micropatterned SAM-coated substrates. Once hepatocytes had spread out to

fill the islands completely (20-24 hours later), nonparenchymal cells were seeded on the RGD-functionalized electroactive domains. Electrochemical treatment of micropatterned co-cultures cleaved the RGD from the surface and thus selectively released the nonparenchymal cells from the co-cultures. Hepatocyte islands, on the other hand, remained attached to the underlying substrate.

4.3.7. Morphological and Functional Analysis of Hepatocyte Cultures

Specimens were observed and recorded using a Nikon Diaphot microscope equipped with a SPOT digital camera (SPOT Diagnostic Equipment, Sterling Heights, MI), and MetaMorph Image Analysis System (Universal Imaging, Westchester, PA) for digital image acquisition. Spent media was stored at -20° C. Albumin content was measured using enzyme linked immunosorbent assays (MP Biomedicals, Irvine, CA) with horseradish peroxidase detection and 3,3',5,5"-tetramethylbenzidine (TMB, Fitzgerald Industries, Concord, MA) as substrate [197].

4.3.8. Staining of Cellular Necrosis

The dye, ethidium homodimer-1 (Invitrogen, Carlsbad, CA), was utilized to identify necrosis in specific cell populations. This dye enters leaky dead or dying cells, binds to DNA and stains the nuclei red (excitation/emission: 528/617 nm). Calcein-AM was utilized to verify live cells in adherent cultures. Calcein gets cleaved by active cytoplasmic esterases into a fluorescent green product (excitation/emission: 494/517 nm). Cultures were first incubated with a mixture of ethidium homodimer-1 (2.5 µg/mL) and calcein-AM (5 µg/mL) for 30 minutes, then washed 3 times with fresh media, and lastly visualized under fluorescence microscopy.

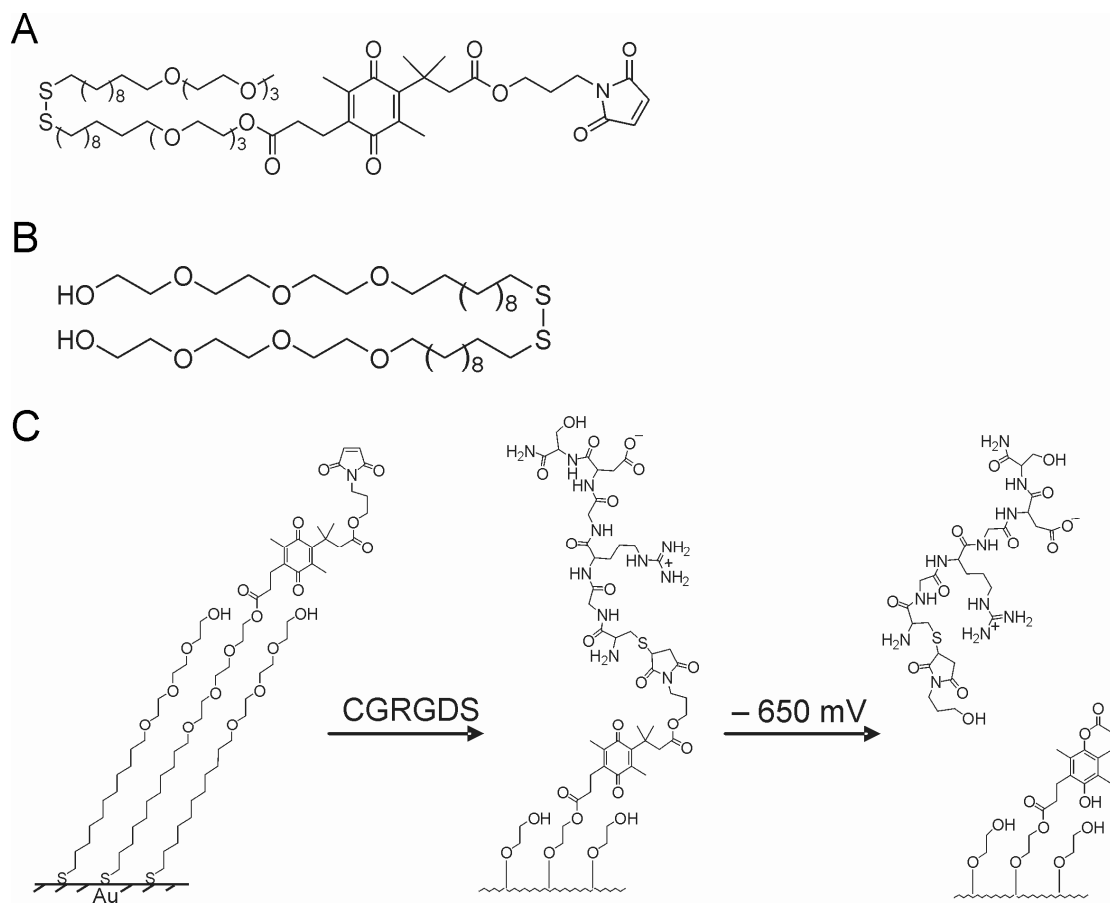


Figure 4.2: Electroactive surface chemistry. **A.** Electroactive quinone ester. **B.** Tri(ethylene glycol)-terminated disulfide. **C.** Structure of functionalized alkanethiolates on gold used to prepare dynamic substrates and strategies for selective immobilization and subsequent release of ligands. A monolayer presenting a maleimide tethered to electroactive quinone ester captures cysteine-containing Arg-Gly-Asp (RGD) peptide. Upon electrochemical reduction of the quinone to the corresponding hydroquinone, a cyclization reaction ensues to give a lactone with release of RGD.

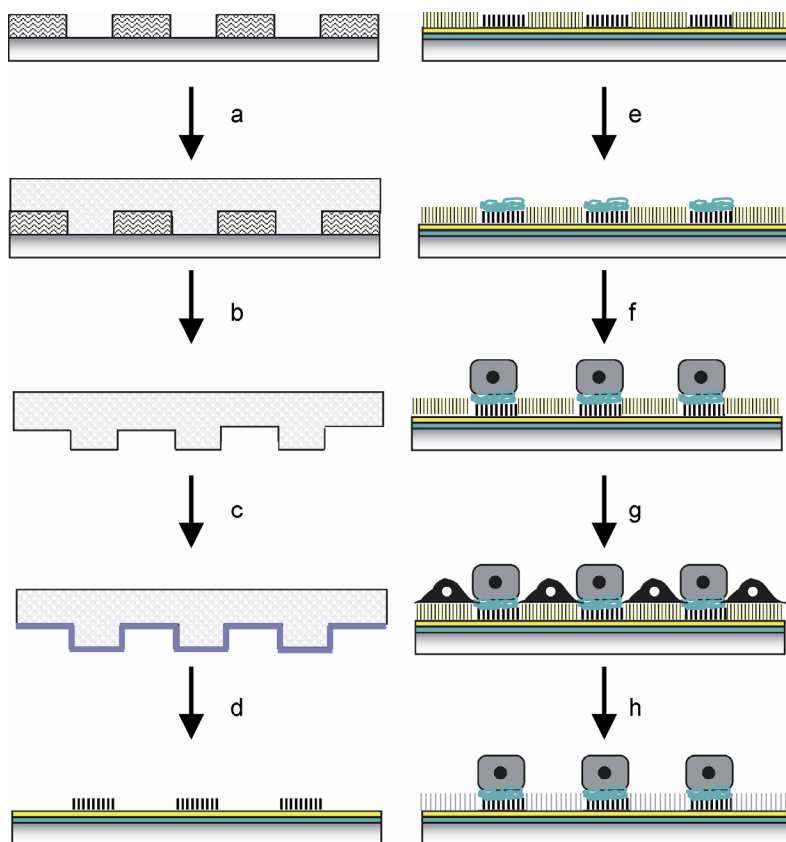


Figure 4.3: Microcontact printing to create electroactive co-cultures. a) Polydimethyl-siloxane (PDMS) pre-polymer solution (10:1 pre-polymer to initiator ratio) is poured onto a photoresist-patterned substrate (i.e. silicon wafer with SU-8 photoresist micropattern) and allowed to cure for 2 hours at 65°C. b) Next, the PDMS polymer is peeled off the substrate to yield a 'stamp'. c) The PDMS stamp is 'inked' with a solution of hexadecanethiol (HDT, non-electroactive). d) Subsequently, the inked stamp is sealed to a gold-plated substrate (i.e. glass coverslip) via gentle pressing for 15-20 seconds in order to create micropatterned self-assembled monolayers (SAMs) of HDT. The stamp is removed and the substrate is incubated with a solution of functionalized alkanethiolates (0.1-0.25% vol/vol electroactive molecules in a tri-ethylene glycol background) for 12-18 hours to form electroactive SAMs in the remaining gold regions. Patterned substrates are subsequently incubated for 30 minutes with a solution of a cell adhesion peptide (i.e. CGRGDS in phosphate buffered saline) that undergoes a covalent attachment to the electroactive alkanethiolates. e) Substrates are further treated with extracellular matrix molecule (i.e. collagen, fibronectin) that adsorbs selectively to the hexadecanethiol domains. f) Hepatocytes then selectively attach to collagenous domains. g) Fibroblasts are seeded in the remaining RGD-functionalized electroactive areas. h) Application of an electrochemical potential to the gold (typically -600 to -700 mV for 4-5 minutes with gold as the working electrode) releases the RGD and fibroblasts from the surface.

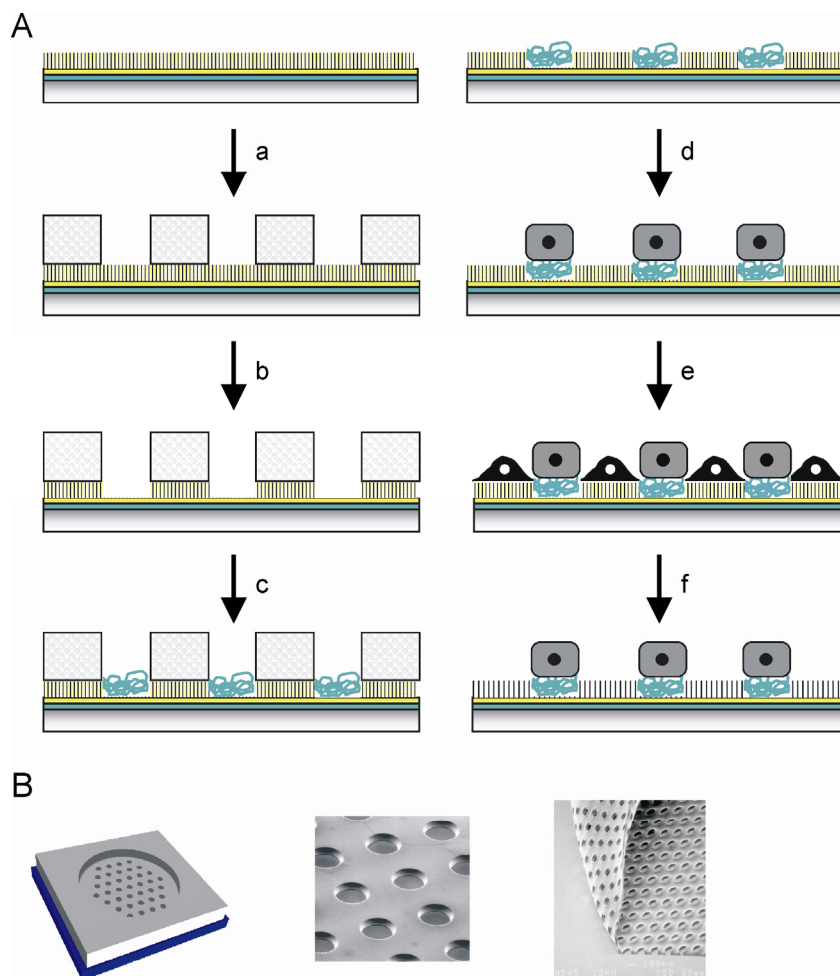


Figure 4.4: Stencil-based approach to create electroactive co-cultures. a) A polydimethylsiloxane (PDMS) stencil (thin membrane with through-holes) is sealed to a gold-plated substrate (i.e. glass coverslip) coated with self-assembled monolayers of functionalized alkanethiolates (0.1-0.25% vol/vol electroactive molecules in a tri-ethylene glycol background). b) The assembly is exposed to oxygen plasma for 30 seconds to 1 minute to remove SAMs from areas not protected by the PDMS. c) The assembly is treated with collagen, which adsorbs to the bare gold via the through-holes in the stencil membrane. Next, the stencil is peeled off to expose the underlying SAMs. Incubation for 30 minutes with a solution of a cell adhesion peptide (i.e. CGRGDS in phosphate buffered saline) causes covalent attachment of the peptide to the electroactive alkanethiolates. d) Hepatocytes then selectively attach to collagenous domains. e) Fibroblasts are seeded in the remaining RGD-functionalized electroactive regions. f) Application of an electrochemical potential to the gold (typically -600 to -700 mV for 4-5 minutes with gold as working electrode) releases the RGD and fibroblasts from the surface. **B)** Shown here are schematics and electron micrographs of a stencil sealed to a substrate.

4.4. Results

4.4.1. Dose-dependent Attachment of Hepatocytes on RGD-Functionalized SAMs

For the soft-lithographic methodologies presented in the ‘Methods’ section to work, it is imperative that hepatocyte attachment to the RGD-functionalized electroactive domains remains minimal, whereas both fibroblast attachment and release are robust. Therefore, we evaluated the dose-dependent attachment of primary rat hepatocytes on substrates coated uniformly with RGD-functionalized electroactive SAMs. Our results (Figure 4.5) indicated that, when compared to uncoated and collagen-coated polystyrene controls, hepatocyte attachment to RGD densities as high as 1% (in a background of triethylene glycol) was minimal. However, hepatocyte attachment did increase in a dose-dependent manner with RGD. Therefore, for subsequent studies, we chose RGD densities less than or equal to 0.25% since hepatocyte attachment was negligible.

4.4.2. Compatibility of the ‘Co-culture Effect’ with Electroactive SAMs

To release fibroblasts from co-culture and assess hepatocyte morphology and functions, we first had to determine if the ‘co-culture effect’ (i.e. stabilization of hepatic phenotype by nonparenchymal cells such as fibroblasts) was induced on electroactive substrates. Micropatterned co-cultures of primary rat hepatocytes and 3T3-J2 fibroblasts were first created using microcontact printing (see Methods), and then hepatocyte morphology and liver-specific functions (albumin and urea secretion) were monitored over the course of 2 weeks. Our results showed that fibroblasts on electroactive RGD were able to induce high levels of functions in rat hepatocytes (seeded on inactive collagen-coated domains), whereas a decline in viability and functions was confirmed in pure hepatocyte monolayers (Figure 4.6).

4.4.3. Optimization of Electrochemical Release Parameters

Various 3T3 sub-clones (J2, NIH, Swiss, and L1) can stabilize liver-specific functions in hepatocytes [58]. However, we anticipated that each sub-clone may have a different dose-dependent attachment profile to electroactive RGD. Furthermore, release of specific sub-clones from micropatterned co-culture may be more efficient than others. In order to test our hypothesis, we created micropatterned SAM-coated substrates using the previously described soft-lithographic processes (see Methods). Then, fibroblasts were seeded on the entire substrate to create pure cultures. Attachment to varying doses of electroactive RGD was assessed qualitatively (data not shown here) and release parameters (time and level of voltage) were also optimized. We found that the swiss-3T3 sub-clone attached well to RGD densities between 0.1 and 0.25% (as determined via hepatocyte attachment studies) and their release was efficient upon application of -650 mV for 4-5 minutes. At these electrochemical parameters, the underlying SAM has been shown previously to remain intact [162, 264]. Other sub-clones, on the other hand, were either too 'sticky' (i.e. NIH cells did not release from substrate at RGD densities as low as 0.1%) or did not attach well to the substrate at the RGD densities of interest (i.e. J2 cells). In Figure 4.7, we demonstrate release of Swiss 3T3 cells from electroactive domains. Immediately upon application of electrical potential to the gold surface, cells on the electroactive domains rounded up and began to detach from the surface. Gentle washing of the monolayer revealed a pattern of fibroblasts only on 'non-cleavable' islands.

4.4.4. Characterization of Hepatocyte Morphology and Function Following Fibroblast Release from Co-culture

Using the parameters determined in previous sections, we created electroactive co-cultures and released fibroblasts either 1 or 5 days after initiation of co-cultures. In Figure 4.8, we show micrographs that demonstrate near complete fibroblast release (day

1) from co-culture. A high magnification examination of hepatocyte islands revealed very minimal fibroblast contamination. Hepatocyte islands following fibroblast release were observed morphologically and spent culture media was collected for biochemical assessment of liver-specific albumin secretion (marker of liver's synthetic ability). Over the course of 1 week, hepatocyte islands displayed high amount of necrosis, which was verified by a fluorescent dye, ethidium homodimer (Figure 4.9). Furthermore, a decline in albumin secretion accompanied the loss of hepatocyte viability (Figure 4.10).

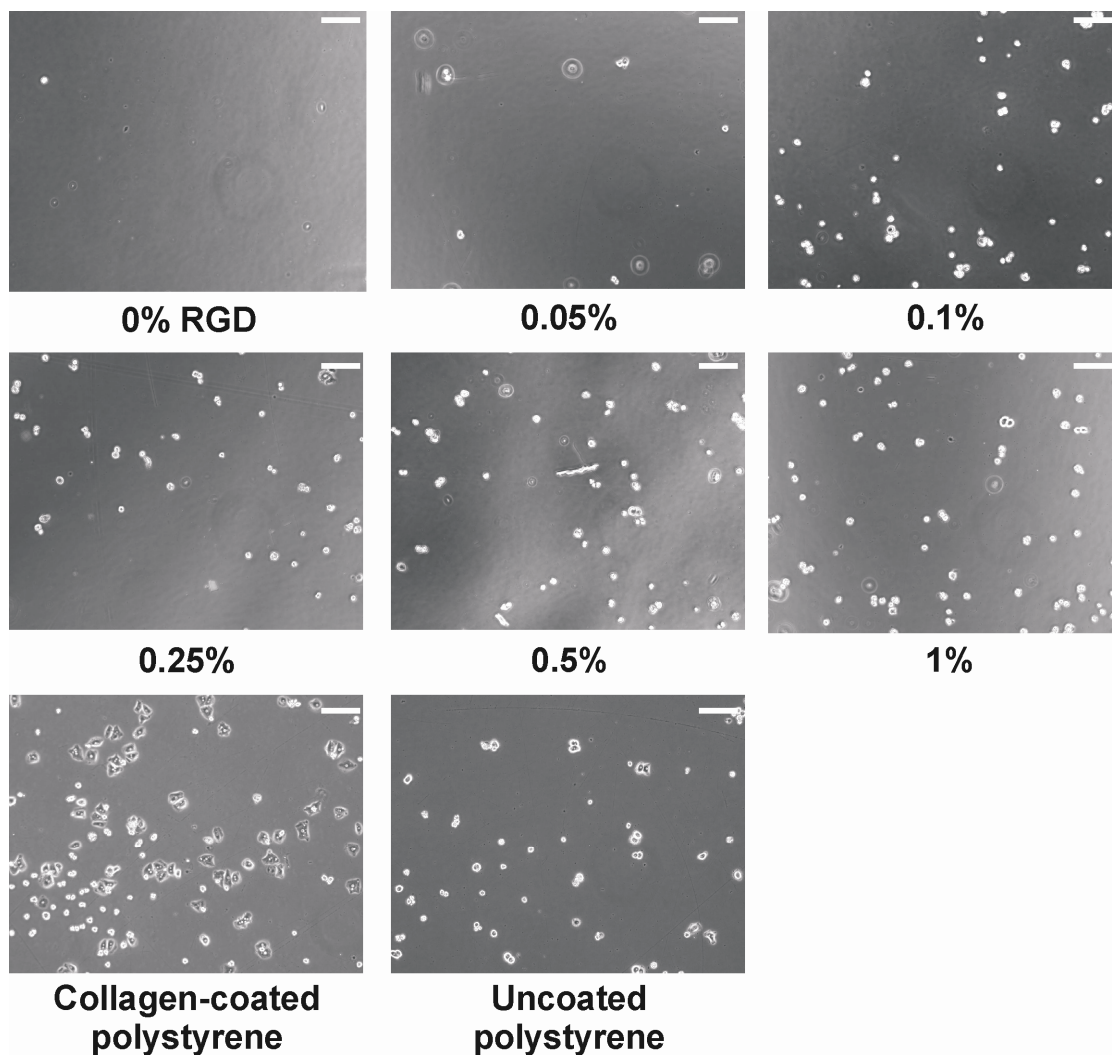


Figure 4.5: Hepatocyte attachment to RGD-functionalized SAMs. Gold-plated glass coverslips were incubated with varying concentrations of RGD-functionalized electroactive alkanethiolates in a background of tri-ethyleneglycol (0 – 1% volume/volume) for 12-18 hours in order to create SAMs. Primary rat hepatocytes were seeded in serum-supplemented culture medium onto the substrates. Twelve hours after seeding, cultures were washed with media and phase contrast micrographs were subsequently recorded. As a positive control, type I collagen-coated tissue culture polystyrene was used for hepatocyte culture, while un-coated polystyrene served as a negative control. Scale bars represent 100 μm .

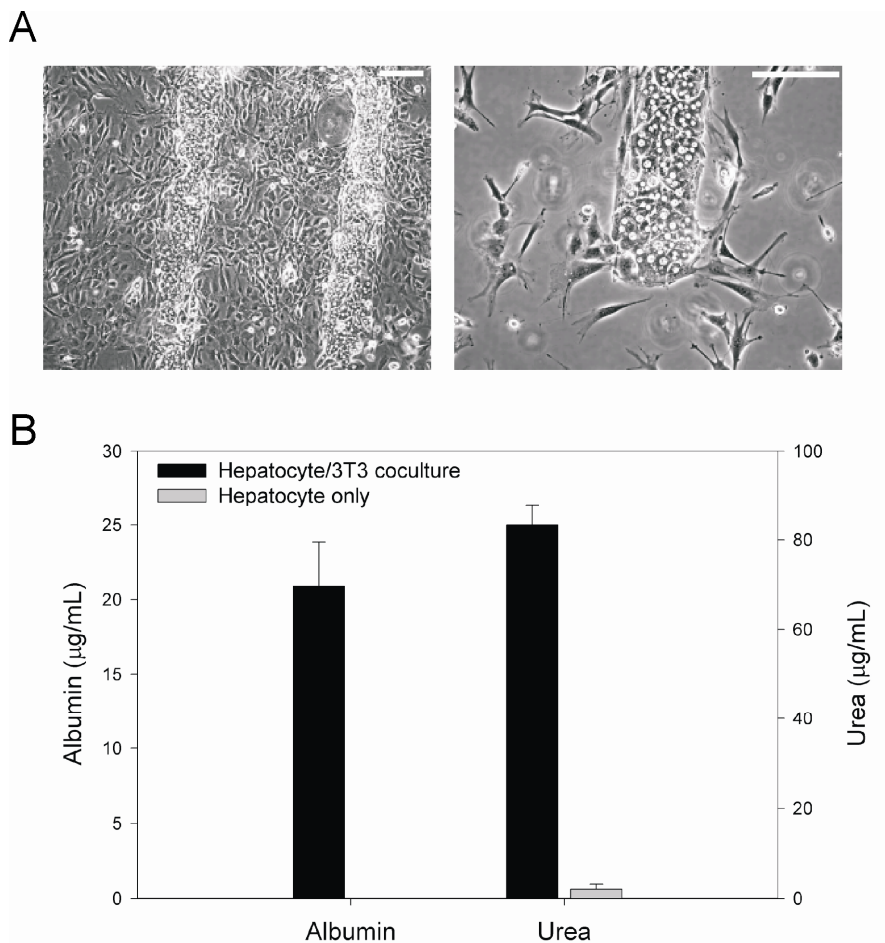


Figure 4.6: The co-culture effect on electroactive substrates. A) Phase contrast micrographs at increasing magnifications showing micropatterned co-cultures of primary rat hepatocytes and murine embryonic 3T3 fibroblasts (J2 sub-clone). Hepatocytes are arranged in 100 μm collagen-coated (on hexadecanethiol self-assembled monolayers) lines, while fibroblasts are attached to RGD-functionalized electroactive SAMs. Scale bars represent 100 μm . **B)** Upregulation of hepatocyte functions (albumin and urea secretion) is seen in micropatterned hepatocyte-fibroblast co-cultures, while pure hepatocytes decline in viability (not shown here) as well as functions. Shown here are cumulative functions over a period of 2 weeks. Error bars represent standard error of the mean ($n=3$).

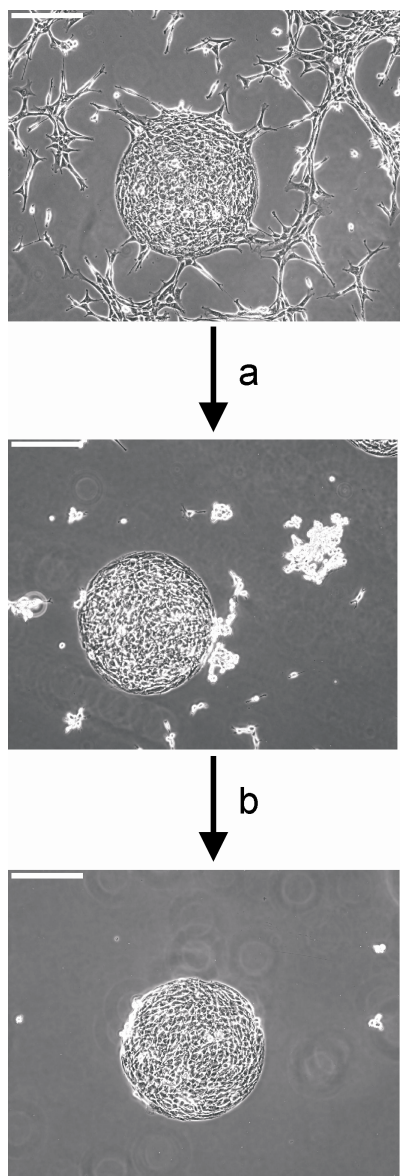


Figure 4.7: Release of 3T3 fibroblasts from electroactive substrates. Substrates with micropatterned circular (500 μm diameter) domains of hexadecanethiol (HDT) SAMs surrounded by electroactive SAMs were created using the strategy outlined in Figure 4.3. Swiss 3T3 fibroblasts were then seeded onto the substrate. Next, the cultures were subjected to electrochemical treatment (-650 mV for 4 minutes) – step ‘a’. A few seconds later, fibroblasts on the electroactive domains rounded up and started to detach from the underlying substrate. Upon washing with culture medium (step ‘b’), cells on electroactive domains came off completely and circular colonies of fibroblasts remained attached to HDT domains. Scale bars represent 250 μm .

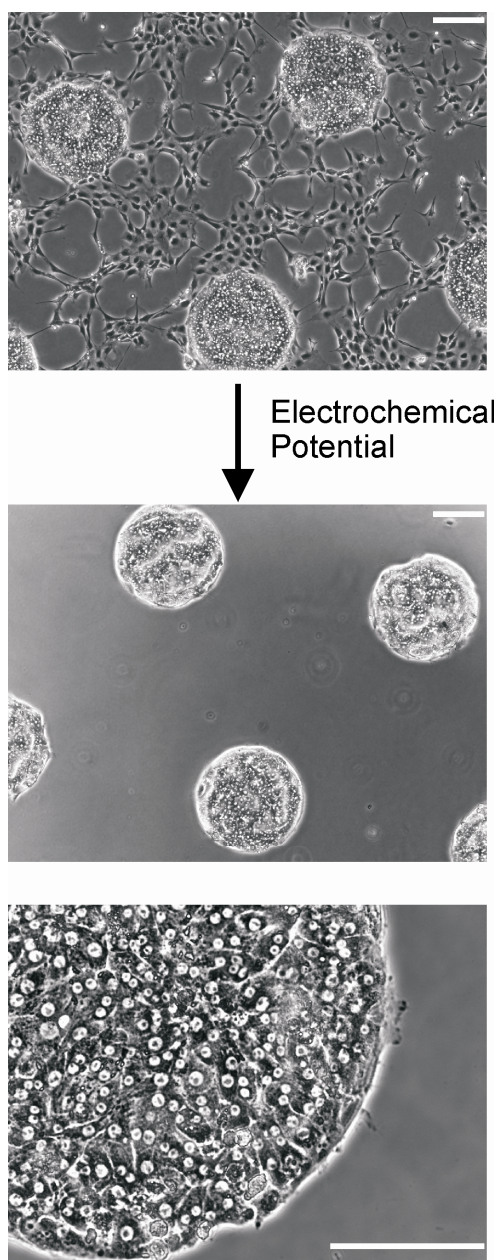


Figure 4.8: Release of 3T3 fibroblasts from co-cultures on electroactive substrates. Micropatterned co-cultures of primary rat hepatocytes and Swiss 3T3 fibroblasts were created using the strategy outlined in figure 4.4. Next, the co-cultures (day 2) were subjected to electrochemical treatment (-650 mV for 4 minutes) and subsequently washed with culture medium to remove fibroblasts. Micrographs at increasing magnifications show the near complete release of fibroblasts from co-cultures. Scale bars are 250 μm .

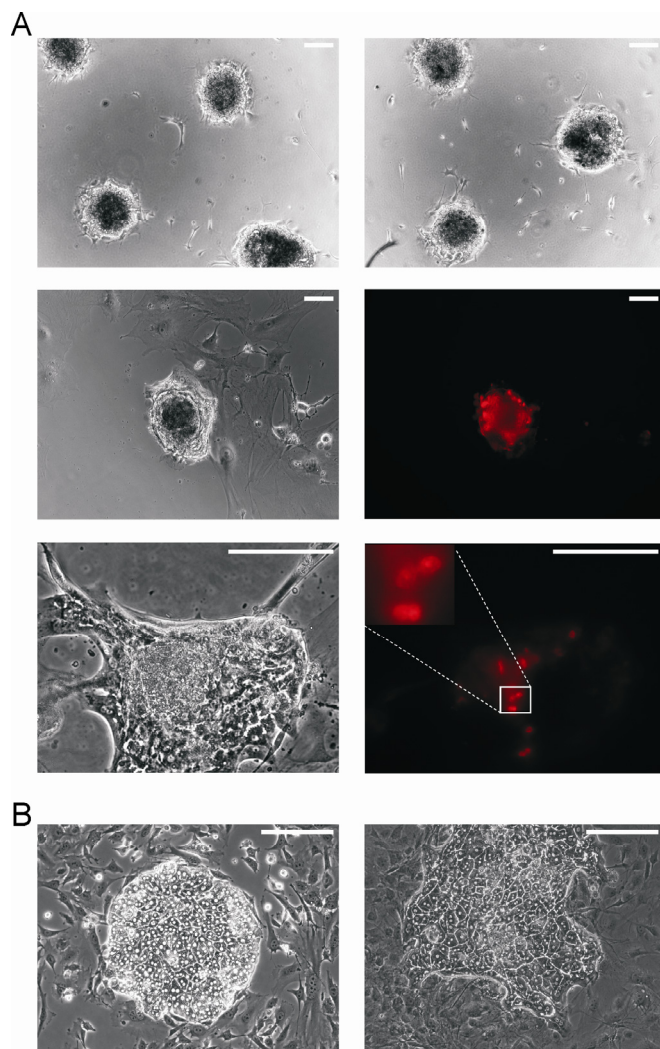


Figure 4.9: Hepatocyte morphology following release of fibroblasts from co-cultures on electroactive substrates. Micropatterned co-cultures of primary rat hepatocytes and Swiss 3T3 fibroblasts were created using the methodology outlined in figure 4.4. Next, the co-cultures (5 days later) were subjected to electrochemical treatment (-650 mV for 4 minutes) and subsequently washed with culture medium to remove fibroblasts. Hepatocyte morphology was assessed 1 week after fibroblast release. **A)** Phase contrast micrographs at increasing magnifications showing necrosis in center of hepatocyte islands 1 week post fibroblast removal. The necrosis was verified using a fluorescent dye which enters the ‘leaky’ membranes of dead cells and binds to DNA in nuclei (ethidium homodimer) – see fluorescent micrographs. **B)** Hepatocytes retain their stereotypical polygonal morphology in micropatterned co-cultures on ‘non-cleavable’ RGD. These co-cultures were subjected to identical electrochemical treatments as in ‘A’, but no fibroblast release was seen. Scale bars represent 250 μm .

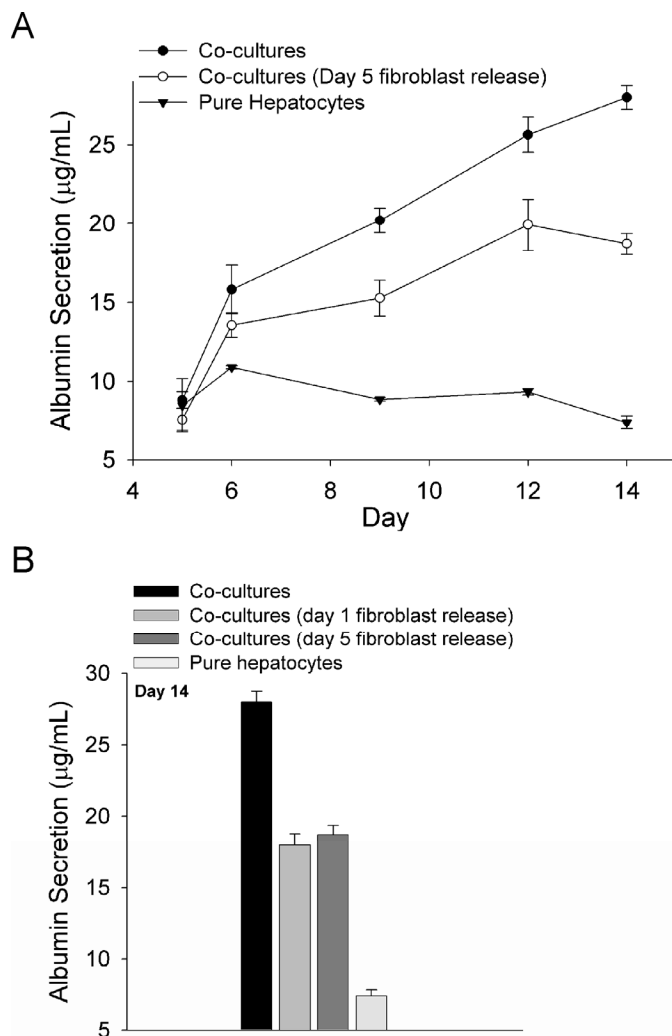


Figure 4.10: Hepatocyte function following release of fibroblasts from co-cultures on electroactive substrates. Micropatterned co-cultures of primary rat hepatocytes and Swiss 3T3 fibroblasts were created using the strategy outlined in figure 4.4. Next, the co-cultures (day 1 or 5) were subjected to electrochemical treatment (-650 mV for 4 minutes) and subsequently washed with culture medium to remove fibroblasts. ‘Non-cleavable’ control co-cultures were created on non-electroactive RGD-functionalized alkanethiolates and subjected to the same protocol as the electroactive co-cultures. Albumin secretion in collected media samples was measured via an enzyme-linked immunosorbent assay (ELISA). **A**) Time-course of albumin secretion in non-cleavable co-cultures, co-cultures from which fibroblasts were released on day 5, and in pure hepatocytes. **B**) Albumin secretion (representative day 14 shown) in ‘non-cleavable’ co-cultures, co-cultures from which fibroblasts were either released on day 1 or day 5, and in pure hepatocytes. Error bars represent standard error of the mean ($n = 3$).

4.5. Discussion

Interactions between parenchymal cells and their nonparenchymal neighbors can influence cellular fates in physiological and pathophysiological processes. Such interactions have also been shown to play important roles in models of tissues in vitro [123, 270, 271]. For instance, liver-specific functions in primary hepatocytes can be stabilized upon co-cultivation with a variety of nonparenchymal cells types [65]. This so-called ‘co-culture effect’ has been demonstrated across multiple species over the last two decades; however, the dynamics of heterotypic cell-cell interactions in such systems remain unclear. Conventional cell culture strategies rely on complex adsorption of proteins to a surface and thus are not amenable to dynamic control over cell-cell and cell-matrix interactions. The recent development of electroactive self-assembled monolayers on gold now presents the opportunity to rigorously explore the dynamics of heterotypic cell-cell signaling.

In this study, we have utilized electroactive self-assembled monolayers (SAMs) on gold to evaluate the dynamics of heterotypic cell-cell interactions in hepatocyte-nonparenchymal co-cultures. First, we developed and optimized soft-lithographic processes to create micropatterned co-cultures in which hepatocytes were seeded on collagen-coated, ‘inactive’ SAMs and subsequently surrounded by 3T3 fibroblasts attached on RGD-functionalized, electroactive alkanethiolates. Second, we optimized the RGD concentration which produced a) minimal hepatocyte attachment, but robust fibroblast attachment and spreading; and, b) efficient release of fibroblasts under electrochemical conditions that maintained SAM fidelity. Third, we optimized the electrochemical conditions for fibroblast release specifically from co-cultures. Such an optimization involved a) determination of 3T3 sub-clone (i.e. 3T3-J2, 3T3-NIH, and 3T3-J2) suitable for release from co-culture, and b) voltage level and time of electrochemical treatment. Fourth, fibroblasts were released from micropatterned co-cultures (500 μm

hepatocyte islands with 1200 μm center-to-center spacing) at various time points (1 and 5 days after initiation of co-culture) by application of electrical potential (-650 mV for 4-5 minutes). Lastly, morphology and liver-specific function of adherent hepatocytes were monitored over the course of 1 week following fibroblast release. Our results showed that necrosis developed in hepatocyte islands over time only in 'released' co-cultures. Consistent with necrosis in hepatocyte islands, we observed a decline in albumin secretion (surrogate marker of liver-specific protein production). Furthermore, no statistically significant differences were observed in the kinetics of hepatocyte function when fibroblasts were released on day 1 or day 5 of co-culture.

In order to selectively release fibroblasts from co-culture, it was necessary to seed hepatocytes on 'inactive', collagen-coated domains, ones that are unresponsive to electrochemical treatment. Such electroactive co-cultures were created by first creating micropatterns of SAMs on a gold-plated substrate. Subsequent adsorption of collagen was localized to hydrophobic (inactive) SAMs, while the remaining tri-(ethylene glycol) areas resisted protein adsorption and therefore, hepatocyte attachment. Soft lithography, a set of techniques for fabricating microstructures for biological applications, overcomes many shortcomings of photolithography with its use of elastomeric polymeric devices that can be synthesized conveniently, rapidly and inexpensively [153]. This set of techniques has been widely used in the literature to pattern SAMs. In this study, we developed two distinct soft-lithographic methods to create micropatterned co-cultures, one utilizing microcontact printing (Figure 4.3) and other elastomeric stencils (Figure 4.4).

In the microcontact printing strategy to create electroactive co-cultures, a PDMS mold is utilized to first 'stamp' a micropattern of inactive, hexadecanethiol (HDT) SAMs onto a gold-plated substrate (i.e. glass coverslip). The remaining bare gold areas are then coated with electroactive SAMs (0.05-0.25% vol/vol in a background of tri-ethylene

glycol). Further incubation of the substrate with collagen causes this extracellular matrix protein to selectively adsorb to the HDT domains. Next, the cell adhesion peptide, CGRGDS reacts with the electroactive linker and becomes tethered to the underlying SAM. Hepatocytes selectively attach to the collagen-coated HDT regions, while fibroblasts are seeded on the electroactive RGD areas. This microcontact printing method is commonly utilized in the literature to prepare micropatterned substrates of alkanethiol SAMs [160]. Another novel method that we devised here involves coating the gold substrate entirely with electroactive SAMs. Then, a stencil with through-holes is placed onto the substrate and the whole assembly is exposed to oxygen plasma for 30 seconds to 1 minute. The oxygen plasma etches away the SAMs down to the bare gold only in exposed regions, ones not protected by the PDMS. The assembly is subsequently exposed to collagen, which binds to the underlying gold via through-holes in the stencil. Following drying of the assembly under light air flow in a tissue culture biosafety cabinet, the stencil is peeled off and the substrate is subjected to an identical protocol as that used for microcontact printing.

Each of the aforementioned soft-lithographic methods has particular advantages and disadvantages. For instance, in the microcontact printing method, only a reusable PDMS stamp is required, whereas in the other method, a reusable stencil and an oxygen plasma generator is needed, which is typically not available in standard biology laboratories and is often found in clean-room facilities designed for semiconductor manufacturing. However, the stencil protects the electroactive linker regions from exposure to the 'sticky' collagen solution. Though the tri-(ethylene glycol) background is very effective at resisting protein adsorption, in our experience, such resistance can break down if 'high' concentrations of collagen are utilized ($> 500 \mu\text{g}/\text{mL}$ in water or PBS). Improper sealing of the stencil to the substrate can cause oxygen plasma-mediated

degradation of SAMS in unwanted regions. In this study, we typically noticed such effects on the periphery of the culture well, suggesting that sealing of the stencil was inconsistent throughout the gold substrate. Such imperfections only occurred though once the stencil had been reused many times (> 5). The use of a PDMS stamp avoids the sealing problems with stencils; however, in microcontact printing, there is a need for an additional molecule (HDT) to make certain regions amenable to matrix adsorption.

In order to isolate the effect of electrochemical treatment from the release of fibroblasts in electroactive co-cultures, we utilized a control surface in which RGD was tethered to an inactive linker, one which does not cleave upon application of an electrochemical stimulus (non-cleavable). Protocols used to create micropatterned co-cultures and subject them to electrochemistry were identically followed for both non-cleavable and cleavable substrates. Our results indicated that electrochemical treatment in non-cleavable co-cultures did not affect either the induction of liver-specific functions or the morphology of hepatocytes over several weeks (see Figure 4.10). The ability to create a control surface that is identical to the cleavable surface except for the nature of a linker is a distinct advantage of electroactive substrates over conventional methodologies which utilize differential sensitivity of various cell types to specific proteases (i.e. selective trypsinization) in order to obtain selective separation of specific cells from co-culture.

We chose day 1 and day 5 for release of fibroblasts from micropatterned co-cultures. These days were selected to provide early and late time points of release. Our results indicated (not shown here) that near complete release of fibroblasts was not possible after day 5, possibly due to regional degradation of underlying SAMs by cell-specific protease activity. Release of fibroblasts from co-culture at either day 1 or 5 induced necrosis in hepatocyte islands. The presence of such necrosis (as opposed to some other intracellular change such as lipid accumulation) was verified via a DNA-

binding fluorescent dye, ethidium homodimer, which is known to enter 'leaky' dead or dying cells and stain the nuclei red (see Figure 4.9). Only the hepatocytes on the periphery of each micropatterned island (single cell deep layer) appeared to have survived following 1 week after release, possibly due to signaling from a few fibroblasts that had migrated onto the collagen-coated domains prior to electrochemical release. We arrested the growth of fibroblasts using mitomycin C to ensure that after release, the ones remaining on the substrate would not grow onto the hepatocyte islands. Necrosis initiating from the center of the hepatocyte islands along with cell survival at the island periphery suggests that direct contact with fibroblasts can maintain hepatocyte viability. However, homotypic fibroblast-fibroblast interactions were determined to be necessary in maintaining viability in all hepatocytes attached to the collagen-coated domains.

We chose 500 μm hepatocyte islands with 1200 μm center-to-center spacing due to previous results showing high hepatocyte function and retention of pattern fidelity in this micropatterned configuration over the course of 2 weeks in co-culture [123]. However, varying the micropatterned configuration is relatively straight-forward (i.e. change of stamp or stencil) with the soft-lithographic methods presented in this study. In the future, we plan to investigate the effect of homotypic hepatocyte interactions (i.e. islands of varying diameters) on functional and morphological outcomes following fibroblast release. It is possible that island size may be inversely proportional to the longevity and function of hepatocytes following bulk removal of fibroblasts. That is, smaller islands may function better and survive longer as compared to larger ones, possibly due to effective signaling from fibroblasts attached to the island periphery.

In our laboratory, we have recently developed a novel dynamic substrate (unpublished work of Dr. Elliot Hui, post-doctoral fellow) in which two silicon 'combs', each pre-seeded with a different cell type (i.e. hepatocytes and fibroblasts), are brought

into contact to initiate heterotypic cell-cell interactions. Using such a substrate, we have demonstrated that removal of fibroblast contact from co-culture (at 18 hours) causes rapid decline of hepatocyte viability and phenotypic functions (albumin and urea secretion). Therefore, these results serve to corroborate the data presented in this study using electroactive SAMs.

Release of fibroblasts from co-culture at day 1 or day 5 caused decline of hepatocyte albumin secretion over the course of 1 week. However, hepatocyte function did not decline to the levels measured in pure hepatocyte cultures which were devoid of any fibroblast interaction (unstable cultures). Judging from the significant necrosis that developed in hepatocyte islands following removal of bulk fibroblast interactions, we expected a greater functional decline than what was measured. However, as discussed previously, non-specific SAM degradation typically occurs due to stencil lift-off and plasma exposure in unwanted regions, typically on the periphery of the culture well. Serum proteins adsorb to such 'exposed' regions, which leads to generation of randomly distributed co-cultures that are unresponsive to electrochemical treatment. We anticipate that it is due to these random co-cultures that albumin secretion in 'released' co-cultures remained higher than pure hepatocytes. Therefore, assessment of local hepatocyte morphology and function (i.e. immunofluorescent albumin staining) is probably more indicative of experimental outcomes. Regardless of the discrepancy between morphological and functional observations apparent in this study, the conclusions are clear: hepatocyte viability and function are compromised significantly upon removal of bulk heterotypic cell-cell interactions.

In optimizing the conditions for this study, we tried a variety of different 3T3 sub-clones available either through the American Type Culture Collection (ATCC) or through academic laboratories. Our results indicated (not shown here) that each sub-

clone had a distinct dose-dependent attachment and spreading profile on electroactive RGD. Furthermore, some 3T3 clones were easier to release from the surface under electrochemical conditions that did not damage the underlying SAMs (-650 mV for 4-5 minutes). The reasons underlying these differences remain to be elucidated. However, we speculate that differences in the expression level of various integrins in each sub-clone may underlie the varied responses. For the purpose of this study, we chose Swiss 3T3 cells since they showed robust attachment and near complete release from the underlying SAM at relevant concentrations of electroactive RGD (i.e. ones which yielded minimal hepatocyte attachment and spreading).

In this study, we have studied the effect of fibroblast removal on the hepatic phenotype. There is some evidence in the literature that stabilization and responsiveness of nonparenchymal cells can also be modulated by hepatocyte neighbors [272, 273]. In the future, we plan to create adherent cultures of fibroblasts released from co-culture in order to determine effects of signaling with hepatocytes. Analysis of fibroblast shape, spreading and migratory behavior may provide indications of such reciprocal signaling. Global gene expression profiling on both the hepatocyte and fibroblast populations from co-culture may further provide fundamental insights into global and specific regulatory gene networks that are modulated due to heterotypic interactions. Furthermore, in addition to albumin secretion, we plan to assess diverse hepatocyte functions (i.e. cytochrome P450 enzyme activity, urea secretion, Phase II enzyme activity) to supplement the results of this study. Lastly, co-cultivation of freshly isolated hepatocytes with 'co-culture conditioned' fibroblasts (i.e. ones released from micropatterned co-cultures at different time points) may modulate kinetics of the co-culture effect.

In its current design, fibroblasts can be released from electroactive co-cultures at a single time point (up to 5 days). However, in vivo, parenchymal cells such as hepatocytes

can interact with multiple nonparenchymal cell types over the course of a given process. In order to study such phenomena, we need a dynamic substrate that offers the ability to repeatedly release and attach cells. Recently, Mrksich and colleagues have extended the capabilities of their electroactive substrates by developing strategies in which ligands can be tethered to SAMs and released into solution dynamically upon electrochemical treatment [264]. In the future, we plan to utilize such surfaces to release fibroblasts from co-culture at specific time points and then reintroduce them at a later time point in order to determine if unstable hepatocytes can be dynamically ‘rescued’. Furthermore, we plan to study the role of multiple liver-derived nonparenchymal cell (NPCs) types such as sinusoidal endothelial cells and kupffer macrophages in modulating hepatic functions. In such a study, release of one liver-derived NPC type from co-culture, followed by introduction of another NPC type may shed some insight into physiological and pathophysiological mechanisms of cell-cell interactions in the liver.

Taken together, the work presented here advances the field of dynamic substrates from the study of cell-matrix interactions to the study of heterotypic cell-cell interactions. Application of electroactive SAMs to hepatocyte-nonparenchymal co-cultures showed that continuous fibroblast signaling was important for maintaining differentiated functions of primary rat hepatocytes. Thus, insoluble nonparenchymal products such as cell-cell contact and extracellular matrix molecules may be required for long-term phenotypic stability of hepatocytes. Such a finding has implications for engineering an optimal functional liver tissue for cell-based therapies for liver disease, pharmaceutical drug screening and fundamental studies of liver physiology and pathophysiology. We anticipate that continued use of dynamic substrates to evaluate cell-cell interactions in a multitude of tissue models may provide mechanistic insights into *in vivo* processes.

Acknowledgements

We are grateful to Woon-Seok Yeo (Mrksich Lab, University of Chicago) for generously providing reagents as well as hands-on training on the use of electroactive substrates, Milan Mrksich for insightful discussions, Jennifer Felix for rat hepatocyte isolation and Howard Green (Harvard Medical School) for providing 3T3-J2 fibroblasts.

CHAPTER 5

MICROSCALE HUMAN LIVER TISSUE FOR DRUG DEVELOPMENT

5.1. Abstract

The function of living tissues is dependent on hierarchical structural features that extend from the single cell ($\sim 10\ \mu\text{m}$) to functional subunits ($100\ \mu\text{m}$ - $1\ \text{mm}$) that in turn coordinate organ functions (\sim centimeters). Historically, conventional cell culture has dispersed tissues into single cells while higher-order processes have been largely neglected. The convergence of semiconductor-driven microtechnology tools with the biomedical arena now presents the opportunity to fabricate microscale tissue subunits towards improving the phenotypic functions of *in vitro* tissue models. As has been demonstrated in the area of DNA microarrays, microtechnology also offers the potential to revolutionize biological assays simply through the benefits of miniaturization (e.g. scalability, cost). Here, we present a miniaturized, multiwell model of human liver tissue with optimized microscale architecture that exhibits liver-specific functions for several weeks in monolayer culture. The need for improved *in vitro* models of human liver tissue is underscored by the unacceptably high rate of pre-launch and post-market attrition of pharmaceutical drug candidates due to unforeseen human liver toxicity. We demonstrate utility of our microscale human liver by characterizing global gene expression, phase-I and phase-II xenobiotic metabolism, secretion of liver-specific products, and susceptibility to a panel of hepatotoxins. The combination of

microtechnology and tissue engineering has the potential to spur development of other individual models of tissues (e.g. kidney, gut, fat, blood-brain barrier) and their integration into a multi-component, ‘lab-on-a-chip’ platform.

5.2. Introduction

The coordinated functions of living tissues emerge from the interactions of many individual cells. In turn, cellular fates are influenced not only by cell-autonomous programs, but also by their local microenvironment or ‘niche’, which includes: neighboring cells, extracellular matrix, soluble factors, and physical forces. In order to study individual cellular responses to distinct local stimuli, one must utilize tools that allow control over these inputs on the order of single cell dimensions ($\sim 10\ \mu\text{m}$). In the arena of semiconductor microfabrication, precision control over surface properties at these dimensions is trivial as the latest devices include nanometer-scale features. Thus, over the last decade, microtechnology tools have emerged both to probe biomedical phenomena at relevant length scales (e.g. role of cell shape & cell-cell interaction in proliferation) [123, 148, 152, 262, 270, 274, 275] *and* to miniaturize and parallelize biomedical assays (e.g. DNA microarrays, immunoassays, microfluidics) [140, 276]. Accordingly, here we describe the application of microtechnology tools both to study the impact of tissue structure on function and use the findings to fabricate miniature tissues in a multiwell format amenable to pharmaceutical drug development.

Our interest in liver tissue stems from the central role of liver in drug metabolism and toxicity. Drug-induced liver toxicity is the leading cause of acute liver failures and post-market drug withdrawals [170, 173]. Preclinical studies are constrained by species-specific variation between human and animal hepatocellular functions (i.e. cytochrome-P450) [174], necessitating supplementation of *in vivo* animal data with *in vitro* assays

designed to assess human responses [175, 277]. Thus, several imperfect human liver models are utilized: acellular microsomes, immortalized cell lines, liver slices, and primary human hepatocytes in suspension or cultured upon extracellular matrix [176, 278]. Of these, hepatocytes are generally considered to be the ‘gold standard’ for evaluating drug disposition *in vitro* [182]. However, hepatocyte culture models routinely used in the pharmaceutical industry have several key limitations, which include: diffusion barriers and limited scalability of collagen sandwich models (i.e. hepatocytes sandwiched between two layers of collagen gel); batch-to-batch variability and unknown molecular composition of basement membrane gels (i.e. tumor-derived Matrigel) [201]; and most importantly, rapid (hours to a few days) loss of viability and key liver-specific functions [176]. Furthermore, such models rely on inconsistent, randomly distributed confluent monolayers while neglecting the impact of microscale cellular architecture on hepatocyte functions. Accordingly, there is a pressing need for better *in vitro* models of the human liver that can eliminate compounds with undesirable ADME/Tox properties (absorption, distribution, metabolism, excretion and toxicity) earlier in drug development, where chemical choices and modifications are made before commitment of significant development resources [279].

We have previously shown that photolithographic micropatterning can be used to modulate liver-specific functions in rodent hepatocytes upon co-cultivation with non-parenchymal cells (co-cultures) [65, 121, 123, 275, 280, 281]. In this study, we have used such a technique to optimize phenotypic functions of primary *human* hepatocytes in pure monolayer cultures and co-cultures. Furthermore, we describe the development of a novel microtechnology-based process that uses elastomeric stencils to miniaturize human liver tissue in an industry-standard multiwell format for higher-throughput screening. Our model consists of primary human hepatocytes and supportive non-parenchymal cells

arranged in empirically optimized spatial configurations. We demonstrate that our microscale human liver tissues remain functional for several weeks as assessed by transcriptional profiling, biochemical assays of liver-specific protein secretion and nitrogen metabolism, and activity of drug metabolism enzymes. Lastly, we show utility of our platform in drug development by characterizing drug-drug interactions and susceptibility to a panel of hepatotoxins.

5.3. Materials and Methods

5.3.1. Soft-lithographic Micropatterning of Collagen

Elastomeric Polydimethylsiloxane (PDMS) stencil devices [157], consisting of thin membranes ($\sim 300\ \mu\text{m}$) with through-holes ($500\ \mu\text{m}$ with $1200\ \mu\text{m}$ center-to-center spacing) at the bottom of each well of a 24-well mold were provided by Surface Logix, Inc (Brighton, MA). Stencil devices were first sealed (via gentle pressing) to tissue culture-treated polystyrene omnitrays (Nunc, Rochester, NY), then each well was incubated with a solution of type-I collagen in water ($100\ \mu\text{g}/\text{mL}$) for 1 hour at 37°C . Purification of collagen from rat tail tendons was previously described [197]. The excess collagen solution in each well was aspirated, the stencil was removed and a PDMS “blank” (24-well mold without stencil membranes) was applied. Collagen-patterned polystyrene was stored dry at 4°C for up to 2 weeks. In some cases, micropatterned collagen was fluorescently labeled via incubation (1 hour at room temperature) with Alexa Fluor® 488 carboxylic acid, succinimidyl ester (Invitrogen, Carlsbad, CA) dissolved in phosphate buffered saline (PBS) at $20\ \mu\text{g}/\text{mL}$.

5.3.2. Photolithographic Micropatterning

Detailed procedures for microfabrication of substrates and subsequent modifications were previously described [121]. Briefly, 35 mm glass coverslips were spin-coated ($\sim 1.5 \mu\text{m}$) with positive photoresist (S1818, Shipley Corporation). Coverslips were then baked to drive off excess solvents and exposed to UV light in a bottom side mask aligner (Karl Suss, Waterbury Center, VT) through transparency photo-masks printed at 8000 d.p.i (CAD/Art Services). Exposed photoresist was then developed (Microposit 354 Developer, Shipley), rinsed in deionized water and baked to complete curing. To ensure complete removal of UV-exposed photoresist down to the bare glass, coverslips were exposed to oxygen plasma (base vacuum 80 mTorr, oxygen pressure 200 mTorr, 200 Watts for 10 minutes). Coverslips were subsequently rinsed with water and immersed in a $100 \mu\text{g}/\text{mL}$ solution of collagen type-I for 1 hour at 37°C . Substrates were then sonicated (Fisher, Pittsburgh, PA) in acetone for 3 minutes to remove residual photoresist, rinsed several times with water, dried under a stream of air, and stored dry at 4°C for up to 2 weeks prior to use. Uniform collagen-modified substrates to be used for randomly distributed cultures were generated by exposing the entire photoresist-coated coverslip with UV light, and subsequently following the processing procedures outlined above for micropatterned wafers.

5.3.3. Hepatocyte Isolation and Culture

Primary *rat* hepatocytes were isolated and cultured as described in the 'Methods' section of Chapter 2 of this dissertation. Primary human hepatocytes were purchased in suspension from vendors permitted to sell products derived from human organs procured in the United States of America by federally designated Organ Procurement Organizations. Hepatocyte vendors included: In Vitro Technologies (Baltimore, MD), Cambrex Biosciences (Walkersville, MD), BD Gentest (Woburn, MA), ADMET

Technologies (Durham, NC), CellzDirect (Pittsboro, NC) and Tissue Transformation Technologies (Edison NJ). All work was done with the approval of COUHES (Committee on use of human experimental subjects). Upon receipt, human hepatocytes were pelleted via centrifugation at 50 \times g for 5 minutes (4°C). The supernatant was discarded, cells were re-suspended in hepatocyte culture medium, and viability was assessed using trypan blue exclusion (typically 70-90% viable cells). 'Plateable' cryopreserved human hepatocytes were purchased from In Vitro Technologies. Hepatocyte culture medium consisted of Dulbecco's Modified Eagle's medium (DMEM) with high glucose, 10% (v/v) fetal bovine serum, 0.5 U/mL insulin, 7 ng/mL glucagon, 7.5 μ g/mL hydrocortisone, and 1% (v/v) penicillin-streptomycin. In order to quantify the number of cells adhered to each collagen-coated island, phase contrast micrographs were taken 4 hours after hepatocyte seeding, followed by manual cell counting in several islands from multiple experiments to get an average 'cells per island' value.

5.3.4. Fibroblast Culture

3T3-J2 fibroblasts were the gift of Howard Green (Harvard Medical School) [231]. Cells were cultured at 37°C, 5% CO₂ in DMEM with high glucose, 10% (v/v) fetal bovine serum, and 1% (v/v) penicillin-streptomycin. In some cases, fibroblasts were growth-arrested by incubation with 10 μ g/mL Mitomycin-C (Sigma, St. Louis, MO) in culture media for 2 hours at 37°C.

5.3.5. Hepatocyte-Nonparenchymal Co-Cultures

In order to create micropatterned co-cultures, hepatocytes were seeded in serum-free hepatocyte culture medium on collagen-patterned substrates, resulting in a hepatocyte pattern due to selective cell adhesion. The cells were washed with media 2

hours later to remove unattached cells and incubated with serum-supplemented hepatocyte media overnight. 3T3-J2 fibroblasts were seeded in serum-supplemented fibroblast medium 12-24 hours later to create co-cultures. Culture medium was replaced to hepatocyte medium 24 hours after fibroblast seeding and subsequently replaced daily. For randomly distributed cultures, hepatocytes were seeded in serum-supplemented hepatocyte culture medium on substrates (glass or polystyrene) with a uniform coating of collagen. In some cases, the whole nonparenchymal fraction of the human liver (NP-fraction purchased from ADMET Technologies) was seeded in hepatocyte culture medium to create hepatocyte/NP-fraction co-cultures. In some cases, hepatocytes were fluorescently labeled via incubation (1 hour at 37°C) with Calcein-AM (Invitrogen) dissolved in culture media at 5 µg/mL. Fibroblasts were fluorescently labeled with CellTracker (Orange CMTMR, Invitrogen) as per manufacturer's instructions.

5.3.6. Biochemical Assays

Spent media was stored at -20° C. Urea concentration was assayed using a colorimetric endpoint assay utilizing diacetylmonoxime with acid and heat (Stanbio Labs, Boerne, TX). Albumin content was measured using enzyme linked immunosorbent assays (MP Biomedicals, Irvine, CA) with horseradish peroxidase detection and 3,3',5,5"-tetramethylbenzidine (TMB, Fitzgerald Industries, Concord, MA) as a substrate [197].

5.3.7. Microscopy

Specimens were observed and recorded using a Nikon Diaphot microscope equipped with a SPOT digital camera (SPOT Diagnostic Equipment, Sterling Heights, MI), and MetaMorph Image Analysis System (Universal Imaging, Westchester, PA) for digital image acquisition.

5.3.8. Gene Expression Profiling

Micropatterned hepatocyte-fibroblast co-cultures were washed 3 times with phosphate buffered saline (PBS) to remove traces of serum, followed by treatment with 0.05% Trypsin/EDTA (Invitrogen) for 3 minutes at 37°C. We found that fibroblasts were much more sensitive to trypsin-mediated detachment than hepatocytes arranged in clusters (500 μm) via micropatterning. Following incubation with trypsin, plates were shook mildly to remove loosely attached fibroblasts, the supernatant was aspirated and the attached hepatocytes (~95% purity) were washed 3 times with serum-supplemented hepatocyte medium to neutralize and remove traces of trypsin from the cultures. Hepatocyte RNA was extracted via TRIzol (Invitrogen) and purified using the RNeasy kit (Qiagen) as per manufacturers' instructions. The RNA was labeled, hybridized to an Affymetrix Human U133 Plus 2.0 Array, and scanned as described previously [232]. Briefly, double-strand cDNA was synthesized using a T7- (dt)24 primer (Oligo) and reverse transcription (Invitrogen) cDNA was then purified with phenol/chloroform/isoamyl alcohol in Phase Lock Gels, extracted with ammonium acetate and precipitated using ethanol. Biotin-labeled cRNA was synthesized using the BioArray™ HighYield™ RNA Transcript Labeling Kit, purified over RNeasy columns (Qiagen), eluted and then fragmented. The quality of expression data was assessed using the manufacturer's instructions which included criteria such as low background values and 3'/5' actin and GAPDH (Glyceraldehyde-3-phosphate dehydrogenase) ratios below 2. All expression data was imported to GCOS (GeneChip Operating System version 1.2) and scaled to a target intensity of 2500 to enable comparison across conditions. Further analysis was carried out in Microsoft Excel.

5.3.9. Cytochrome-P450 Induction

Stock solutions of prototypic CYP450 inducers (Sigma) were made in Dimethylsulfoxide (DMSO), except for Phenobarbital, which was dissolved in water at 40 mM. Cultures were treated with inducers (Rifampin 25 μ M, β -Naphthoflavone 30 μ M or 50 μ M, Phenobarbital 1 mM, Omeprazole 50 μ M) dissolved in hepatocyte culture medium for 4 days. Control cultures were treated with solvent (DMSO) alone for calculations of fold induction. To enable comparisons across inducers, DMSO levels were kept constant at 0.06% (v/v) for all induction conditions.

5.3.10. Phase I & II Enzyme Activity Assays

Chemicals were purchased from Sigma: Coumarin (CM), 7-Hydroxycoumarin (7-HC), Ethoxyresorufin (ER), Resorufin (RR), Ketoconazole (KC), Sulfaphenazole (SP), Methoxsalen (MS) Salicylamide (SC) or purchased from BD-Gentest: 7-methoxy-4-trifluoromethylcoumarin (MFC), 7-benzyloxy-4-trifluoromethylcoumarin (BFC), 7-hydroxy-4-trifluoromethylcoumarin (7-HFC). Cultures were incubated with substrates (CM, MFC, BFC at 50 μ M, ER at 8 μ M, 7-HC at 100 μ M) dissolved in DMEM without phenol red for 1 hour at 37°C. For inhibition studies, cultures were incubated with substrates in the presence of specific inhibitors (MS at 25 μ M with CM, SP at 50 μ M with MFC, KC at 50 μ M with BFC, SC at 3 mM with 7-HC). The reactions were stopped by collection of the incubation medium. Then, potential metabolite conjugates formed via Phase II metabolic activity were hydrolyzed by incubation of supernatants with β -glucuronidase/arylsulfatase (Roche, Indianapolis, IN) for 2 hours at 37° C. Samples were diluted 1:1 in quenching solution and fluorescent metabolite formation was quantified by means of a fluorescence micro-plate reader (Molecular Devices, Sunnyvale, CA) as described elsewhere in detail [181, 282]. Production of 7-HC from CM is a reaction (CM 7-Hydroxylation) mediated by CYP2A6 in humans, production of 7-HFC from BFC or

MFC (dealkylation) is mediated by several different CYP450s, and production of RR from ER (dealkylation) is mediated by CYP1A2. Conjugation of 7-HC with glucuronic acid and sulfate groups is mediated by Phase II enzymes, UDP-Glucuronyl-transferase and Sulfo-transferase, respectively.

5.3.11. Cell Viability Assessment (MTT assay)

Cultures were incubated with various concentrations of compounds dissolved in culture medium for 24 hours (acute toxicity) or extended time periods (chronic toxicity, 1-4 days). Cell viability was subsequently measured via the MTT (3-(4,5-dimethylthiazol-2-yl)-2,5-diphenyl tetrazolium bromide; Sigma) assay, which involves cleavage of the tetrazolium ring by mitochondrial dehydrogenase enzymes to form a purple precipitate. MTT was added to cells in DMEM without phenol red at a concentration of 0.5 mg/mL. After an incubation time of 1 hour, the purple precipitate was dissolved in a 1:1 solution of DMSO and Isopropanol. The absorbance of the solution was measured at 570 nm (SpectraMax spectrophotometer, Molecular Devices, Sunnyvale, CA). To calculate percent viability, the MTT absorbance values in treated cultures were normalized to the values in un-treated controls.

5.3.12. Statistical Data Analysis

Experiments were repeated 2-3 times with duplicate or triplicate samples for each condition. Data from representative experiments is presented, whereas similar trends were seen in multiple trials. All error bars represent standard error of the mean (SEM).

5.4. Results

5.4.1. Functional Optimization of Hepatocyte Cultures and Co-Cultures via Microtechnology

We have previously developed a photolithographic cell patterning technique which allows study of the relative role of homotypic (hepatocyte-hepatocyte) and heterotypic (hepatocyte-nonparenchymal) cell-cell interactions in stabilization of liver-specific functions in vitro (Figure 5.1) [65]. In previously published studies, we evaluated the role of cell-cell interactions on the phenotypic functions of primary *rat* hepatocytes upon co-cultivation with 3T3-J2 fibroblasts (co-cultures) [65, 123]. We used the experimental design shown in Figure 5.2 (see phase micrographs), which varies the size of the hepatocyte islands from single cell islands (36 μm) to large circular colonies several millimeters in diameter (17.8 mm). Using this design, co-cultures were created in which the heterotypic interface varied over three orders of magnitude as estimated by image analysis; however, the ratio of cell populations, as well as total number of cells seeded on each substrate remained constant. In contrast, in conventional cell culture conditions, cell-cell interactions are typically varied by changing seeding density which, in turn, is coupled to both cell number and ratio of cell populations. We found that liver-specific functions (albumin and urea secretion) were upregulated in co-cultures as compared to pure hepatocyte monolayers. However, the degree of upregulation varied with the micropatterned geometry. Rat co-cultures with a larger initial heterotypic interface (i.e. single cell islands) had highest levels of liver-specific functions, while only a modest upregulation was seen for the two patterns with the largest island sizes (Figure 5.2). Hepatocytes in smaller patterns (<250 μm) intermingled significantly, whereas larger islands assumed a relatively stable conformation for several weeks.

Due to data showing that liver-specific functions of primary rat hepatocytes can be a) stabilized upon co-cultivation with 3T3-J2 fibroblasts and b) optimized using photolithographic micropatterning, we hypothesized that similar outcomes could be achieved with primary *human* hepatocytes towards development of an *in vitro* model of human liver tissue. Thus, we created randomly distributed co-cultures of human hepatocytes and 3T3-J2 fibroblasts and observed robust up-regulation of liver-specific functions (albumin secretion, urea synthesis, CYP1A2 activity) over pure hepatocyte controls, which showed a monotonic decline in such functions (Figure 5.3A). Human hepatocytes in co-cultures maintained their polygonal morphology, distinct nuclei and nucleoli, and bile canaliculi as typically seen *in vivo*, whereas in pure cultures, hepatocytes rapidly lost viability and those surviving spread out to adopt a 'fibroblastic' morphology (Figure 5.3B).

After demonstrating that 3T3-J2 fibroblasts can indeed stabilize primary human hepatocytes *in vitro*, we evaluated the effect of micropatterning on modulation of liver-specific functions in such co-cultures. In order to enable comparisons across species, our human work used pattern geometries similar to those used for previously published rat studies. We varied collagen island diameter over several orders-of-magnitude and observed that human hepatocyte clustering consistently improved liver-specific functions when compared to randomly-distributed (i.e. unorganized) controls. Such a trend was seen for both pure hepatocyte cultures (Figure 5.4) and hepatocyte-3T3 co-cultures (Figure 5.5). Specifically, in pure hepatocyte monolayers, 490 μm and 4800 μm hepatocyte island configurations provided for higher functions than the single cell array (i.e. 36 μm). In co-cultures, on the other hand, 490 μm hepatocyte islands (1230 μm center-to-center spacing) provided for the balance of homotypic and heterotypic interactions which yielded optimal albumin and urea secretion. As with rat co-cultures, the 36 μm human hepatocyte islands reorganized within a day, thereby dissipating the

pattern. The configurations with the two large island sizes (490, 4800 μm), however, maintained pattern fidelity for the duration of the cultures, typically several weeks. Thus, the 'optimal' micropatterned configuration was identified as $\sim 500 \mu\text{m}$ hepatocyte islands with $\sim 1200 \mu\text{m}$ center-to-center spacing.

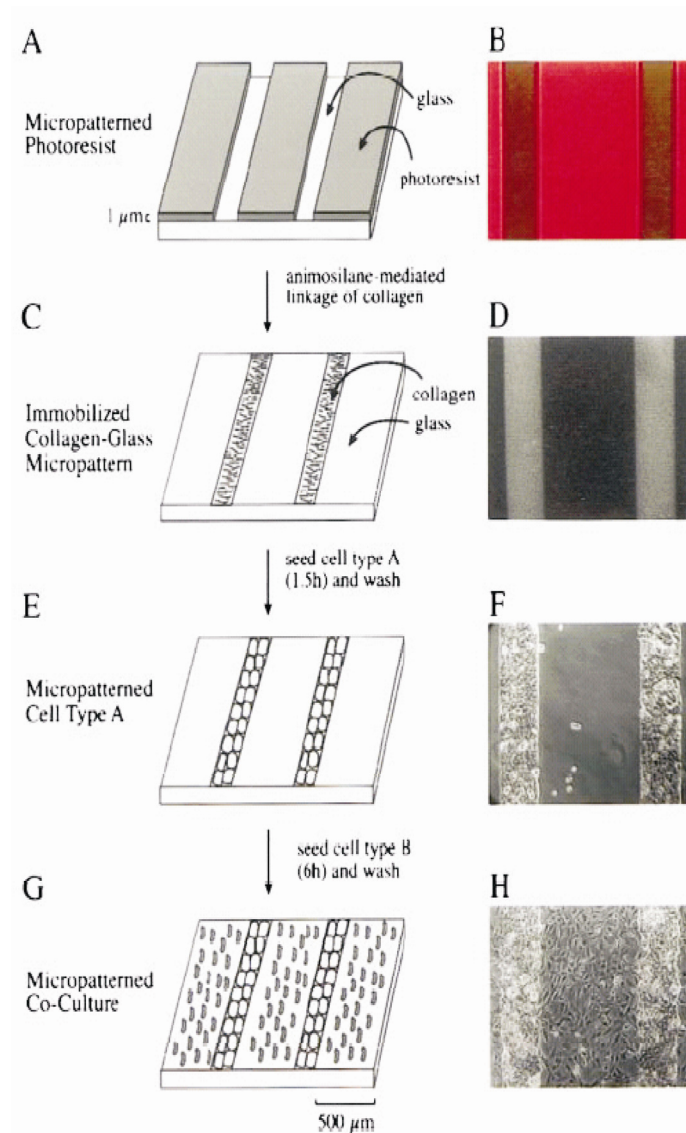


Figure 5.1: Photolithographic process to create micropatterned co-cultures. Glass wafers are spin-coated with photoresist (light-sensitive polymer), exposed to UV light through a photo-mask to generate a photoresist pattern (A), which can be visualized via epifluorescence microscopy (B). Collagen is physisorbed to the substrate; the photoresist is stripped-off using acetone, which leaves a collagen pattern on glass (C). Fluorescently labeled collagen pattern is shown in 'D'. Seeding of hepatocytes in serum-free culture medium yields micropatterned cultures due to selective adhesion of hepatocytes to collagenous domains (E-F). Substrates are rinsed with media a few hours later to remove unattached cells and incubated in serum-supplemented media overnight. Addition of nonparenchymal cells in serum-supplemented culture medium results in micropatterned co-cultures (G-H). Shown here are primary rat hepatocytes surrounded by 3T3-J2 fibroblasts. From [65].

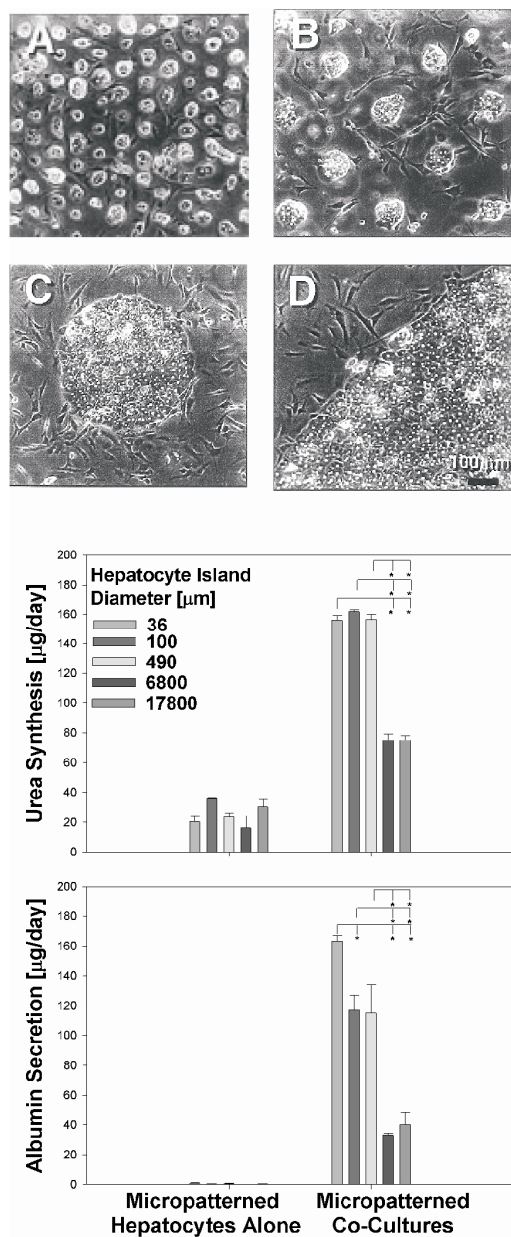


Figure 5.2: Functional optimization of rat hepatocyte co-cultures via micropatterning. Phase contrast micrographs of micropatterned co-cultures of primary rat hepatocytes and 3T3-J2 fibroblasts are shown. Ratio of cell populations and total cell numbers are constant across pattern geometries, which have a broad range of heterotypic interface. A: 36 μm hepatocyte islands with 90 μm center-to-center spacing (36/90); B: 100/250; C: 490/1230; D: 6800/16900. Liver-specific functions (albumin secretion, urea synthesis) were higher in co-cultures as compared to pure hepatocyte cultures. However, degree of upregulation varied with micropatterned geometry (17800 μm represents a single hepatocyte island surrounded by fibroblasts). Adapted from [65].

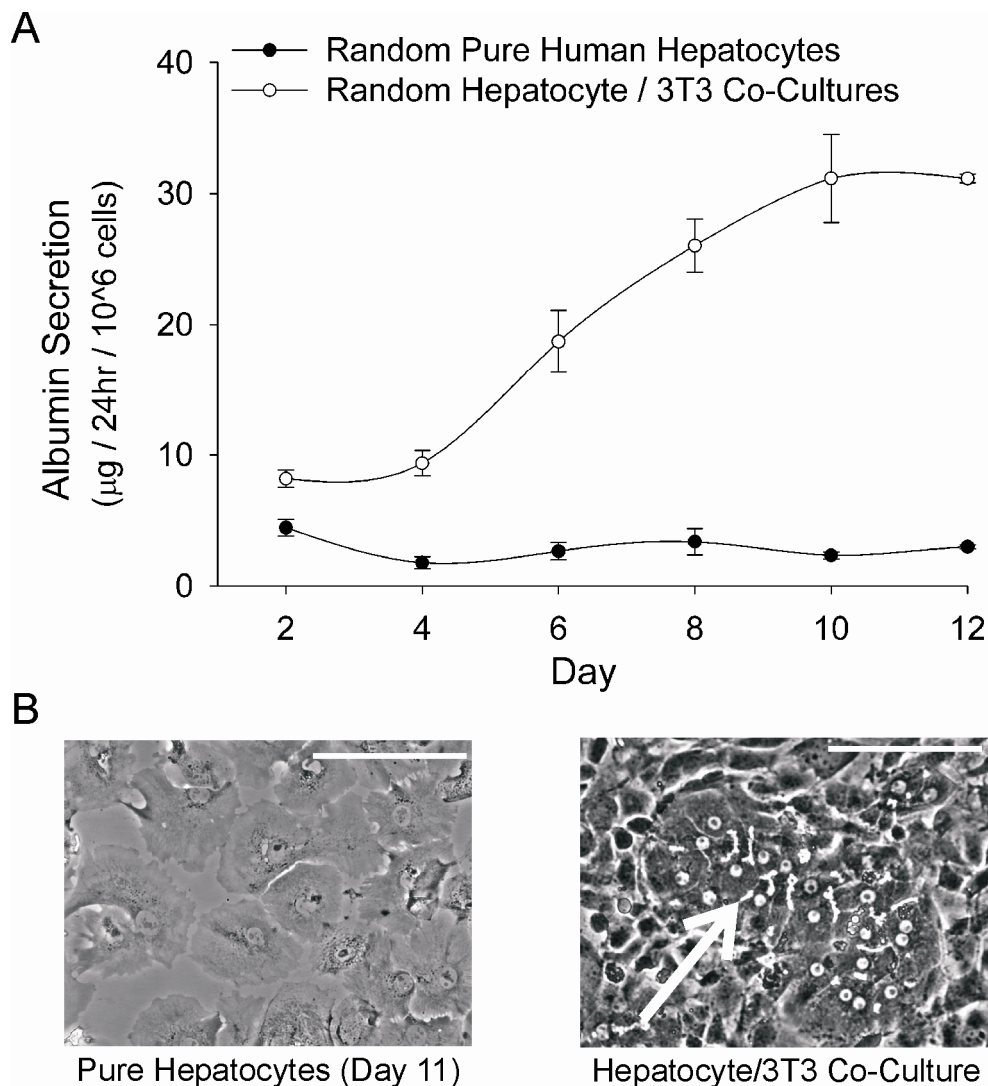


Figure 5.3: Randomly distributed human hepatocyte cultures and co-cultures. **A)** Rate of albumin secretion (a marker for synthesis of liver-specific proteins) by human hepatocytes in pure monolayer cultures and upon co-cultivation with 3T3-J2 murine embryonic fibroblasts randomly distributed on collagen-coated polystyrene. Several other functions were also stabilized in hepatocyte/3T3 co-cultures (i.e. urea secretion, cytochrome-P450 activity) as compared to unstable pure monolayers (data not shown). **B)** In pure cultures, hepatocytes adopt a ‘fibroblastic’ morphology, whereas in co-cultures they maintain their polygonal shape (arrow), distinct nuclei and nucleoli, and visible bile canaliculi as typically seen in vivo (scale bars represent 200 µm).

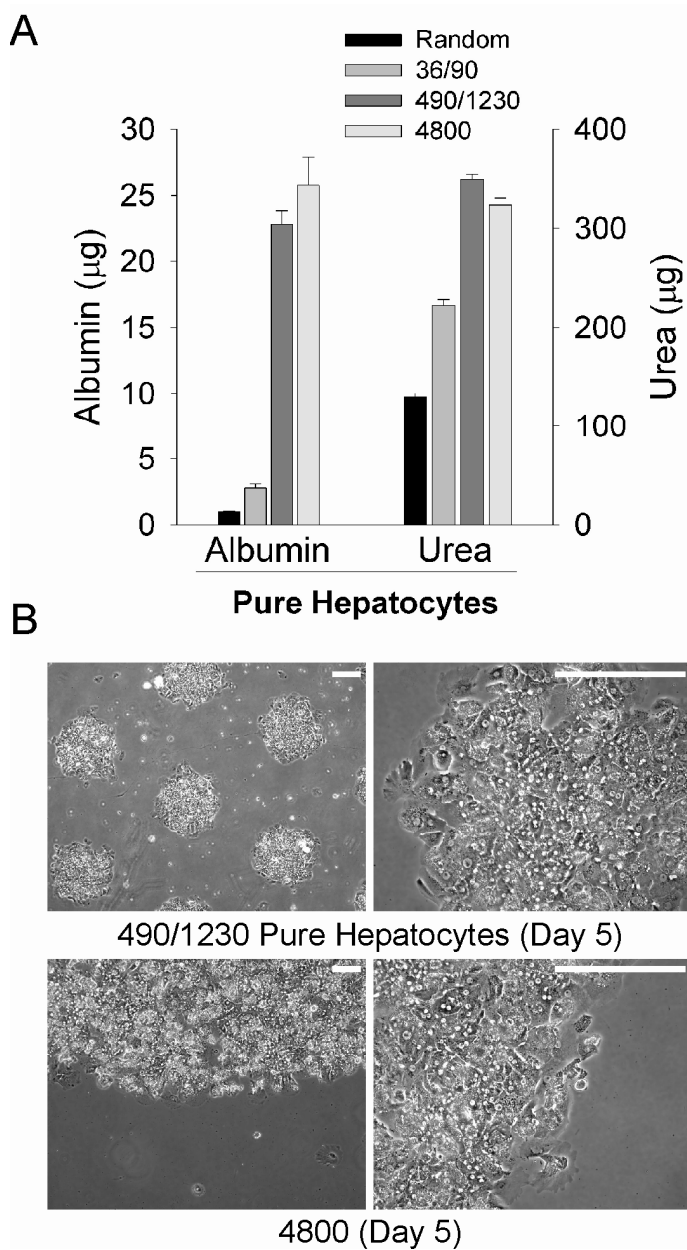


Figure 5.4: Micropatterned cultures of pure human hepatocytes. **A)** Cumulative liver-specific functions (albumin and urea secretion) over 2 weeks are compared for micropatterned cultures. Hepatocytes were organized on collagen-coated islands of prescribed and increasing diameters using photolithography. Island size (36, 490, 4800 μm) and center-to-center spacing (i.e. 90 μm for 36 μm islands) between islands for each configuration were selected to keep total hepatocyte numbers constant. Randomly distributed control cultures (“Random”) on collagen were generated to enable comparisons. **B)** Phase contrast micrographs of pure hepatocyte cultures. Scale bars represent 250 μm . Error bars represent standard error of the mean ($n = 3$).

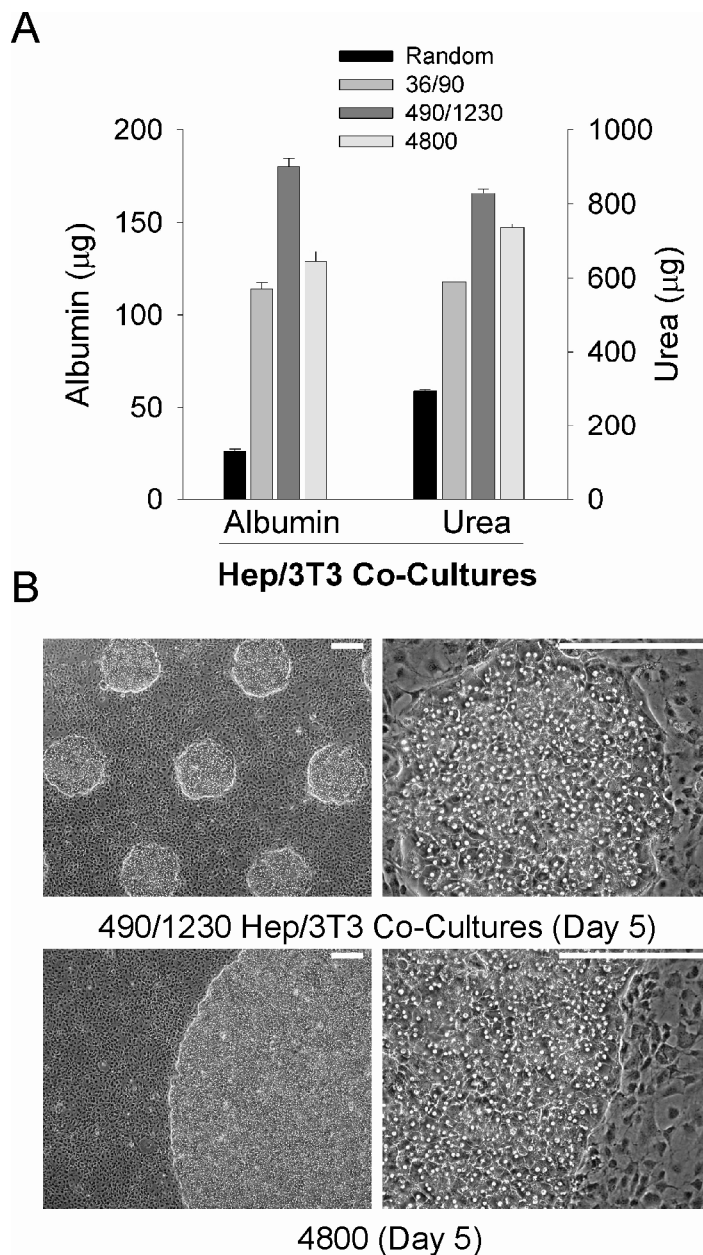


Figure 5.5: Functional optimization of *human* hepatocyte co-cultures via micropatterning. **A)** Cumulative liver-specific functions over 2 weeks are compared for micropatterned co-cultures. Hepatocytes were organized on collagen-coated islands of prescribed dimensions using photolithography, and then surrounded by 3T3-J2 fibroblasts 24 hours after hepatocyte spreading. Island size (36, 490, 4800 μm) and center-to-center spacing (i.e. 90 μm for 36 μm islands) between islands were selected to keep total cell numbers and cell type ratios constant. Randomly distributed control co-cultures ('Random') on collagen were generated to enable comparisons. **B)** Phase contrast micrographs of co-cultures. Scale bars are 250 μm . Error bars are SEM ($n = 3$).

5.4.2. Fabrication of Miniaturized Microscale Liver Tissues in a Multiwell Format

In order to create miniaturized micropatterned co-cultures in a multiwell format, we developed a process using polydimethylsiloxane (PDMS) stencils (gift of Surface Logix, Inc) consisting of 300 μm membranes with through-holes at the bottom of each well in a 24-well mold (Figure 5.5). To micropattern all culture wells simultaneously, the multiwell assembly was sealed against a polystyrene plate (omnitray). Collagen (type I) was physisorbed to exposed polystyrene, the stencil was removed, and a 24-well PDMS 'blank' (without membranes in each well) was applied to the plate in order to maintain the multi-well format of the system. 'Micropatterned' cultures were created by selective adhesion of primary human hepatocytes to collagenous domains. Subsequent seeding of nonparenchymal cells (i.e. 3T3-J2 fibroblasts) in serum-supplemented culture medium created micropatterned co-cultures. The diameter of through-holes in the stencil membrane determined the size of collagenous domains and thereby the balance of homotypic and heterotypic interactions in the microscale tissue. This diameter was determined using the functional optimization studies as detailed in the previous sections, and found to be $\sim 500\mu\text{m}$ hepatocyte islands with $\sim 1200\mu\text{m}$ center-to-center island spacing. Thus, the microscale human liver tissue developed and characterized herein represents 24-well plates with each well containing $\sim 10,000$ hepatocytes organized in 37 colonies of 500 μm diameter, for a total of 888 repeating hepatic microstructures per plate (Figure 5.6A).

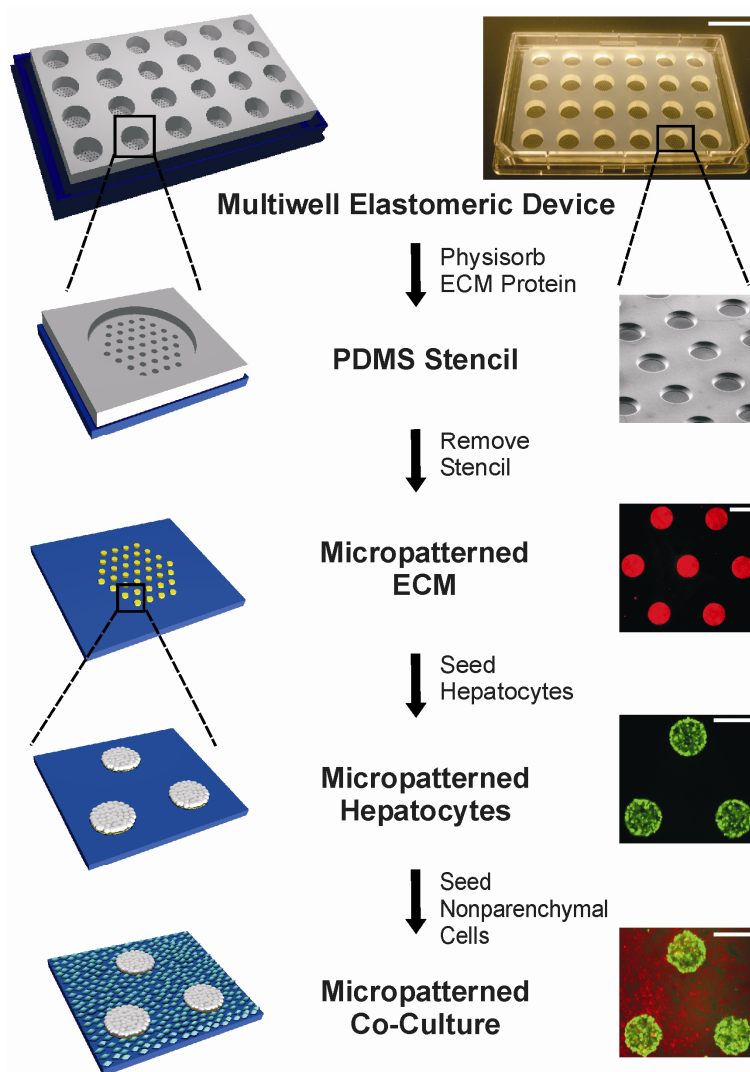


Figure 5.6: Soft lithographic process to fabricate miniaturized microscale liver tissues. Schematic of the process flow aside photomicrographs taken at each step. A reusable PDMS stencil is seen consisting of membranes with through-holes at the bottom of each well in a 24-well mold. To micropattern all wells simultaneously, the device is sealed under dry conditions to a culture substrate. A photograph of a device (scale bar is 2 cm) sealed to a polystyrene omni-tray is seen along with an electron micrograph of a thin stencil membrane. Each well is incubated with a solution of extracellular matrix protein to allow protein to adsorb to the substrate via the through-holes. The stencil is peeled off leaving micropatterned ECM protein on the substrate (fluorescently labeled collagen pattern shown, scale bar is 500 μm). A 24-well PDMS ‘blank’ lacking membranes is then sealed to the plate before cell seeding (not shown here). Primary hepatocytes selectively adhere to matrix-coated domains, allowing supportive non-parenchymal cells to be seeded in serum-supplemented culture media into the remaining bare areas (hepatocytes labeled green and fibroblasts orange, scale bar is 500 μm).

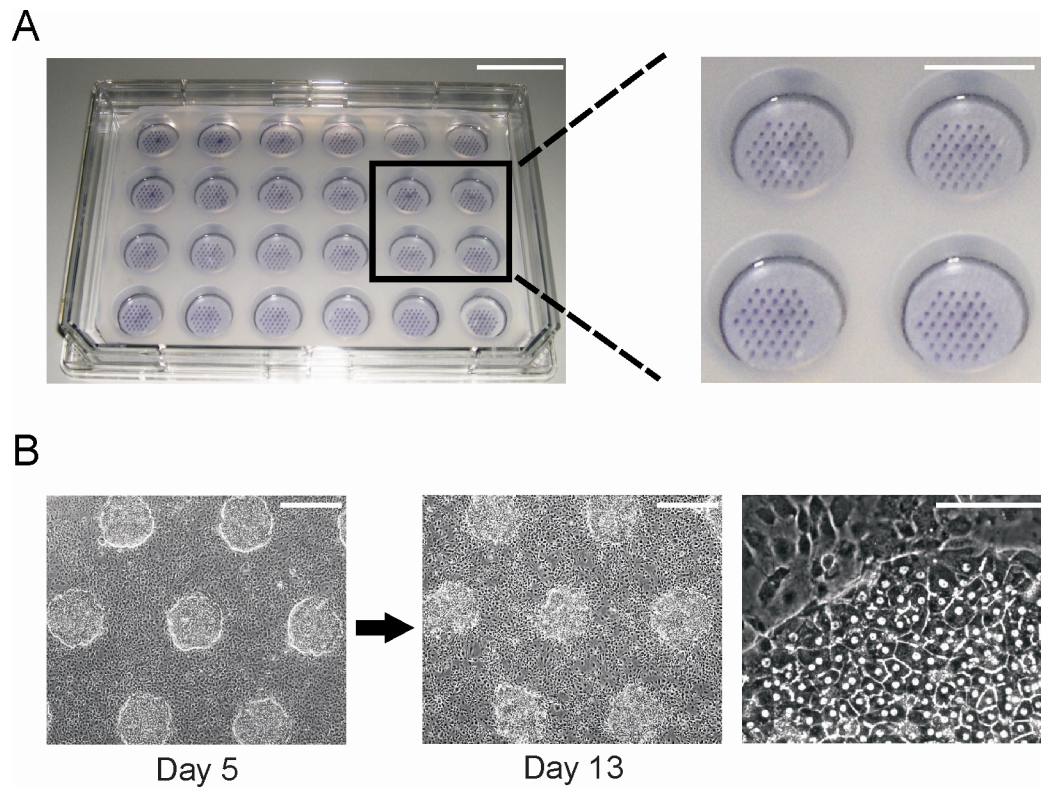


Figure 5.7: Microscale liver tissues in a multi-well format. A) A photograph of a 24-well device is shown with repeating hepatic microstructures (37 colonies of 500 μm diameter with 1200 μm center-to-center spacing between colonies in each well) stained purple for mitochondrial activity via the MTT assay (see Methods, scale bar 2 cm and 1 cm for enlargement). Hepatocyte islands accumulated greater amounts of purple precipitate as compared to surrounding 3T3-J2 fibroblasts primarily due to higher hepatic mitochondrial activity. **B)** Phase contrast micrographs of optimal micropatterned human hepatocyte-fibroblast co-cultures. Images depict pattern fidelity over time and hepatocellular morphologic features include bile canaliculi (scale bars are 500 μm , 500 μm , and 100 μm from left-to-right).

5.4.3. Characterization of Microscale Human Liver Tissues

In order to qualitatively assess the stability of our microscale human liver tissues, hepatocyte morphology and persistence of microscale organization were monitored and found to be maintained for duration of the culture, typically 3-6 weeks (Figure 5.6B). To quantitatively assess the stability of liver-specific functions, we measured albumin and urea secretion and found both markers to be stable for several weeks in our platform (Figure 5.7). To obtain a more global perspective, we gene expression profiled human hepatocytes from 1-week old microscale tissues (day 6) via selective trypsinization to remove fibroblasts (~95% purity, see Methods). For comparison, we characterized gene expression of fresh, unorganized, pure hepatocytes (12 hours after plating, day 1) considered to be the 'gold standard' and unorganized pure hepatocytes on day 6 as their liver-specific functions declined. Global scatter plot comparison revealed that gene expression intensities in hepatocytes from 1-week old microscale tissues were similar to intensities in pure hepatocytes on day 1 as assessed by the slope (0.96) of a least-squares linear fit (Figure 5.8A). Furthermore, phase-II xenobiotic metabolism genes in hepatocytes from microscale tissues were expressed at levels similar to those in pure hepatocytes on day 1 (Figure 5.8B). We noted that expression levels of cytochrome-P450 (CYP450) genes were significantly down-regulated in pure hepatocytes by day 6, whereas hepatocytes in our platform retained expression at high levels (Figure 5.9A). Similar trends were seen for genes from diverse pathways of liver-specific functions such as gluconeogenesis, drug transporters, coagulation factors and cell surface receptors (Figure 5.9B).

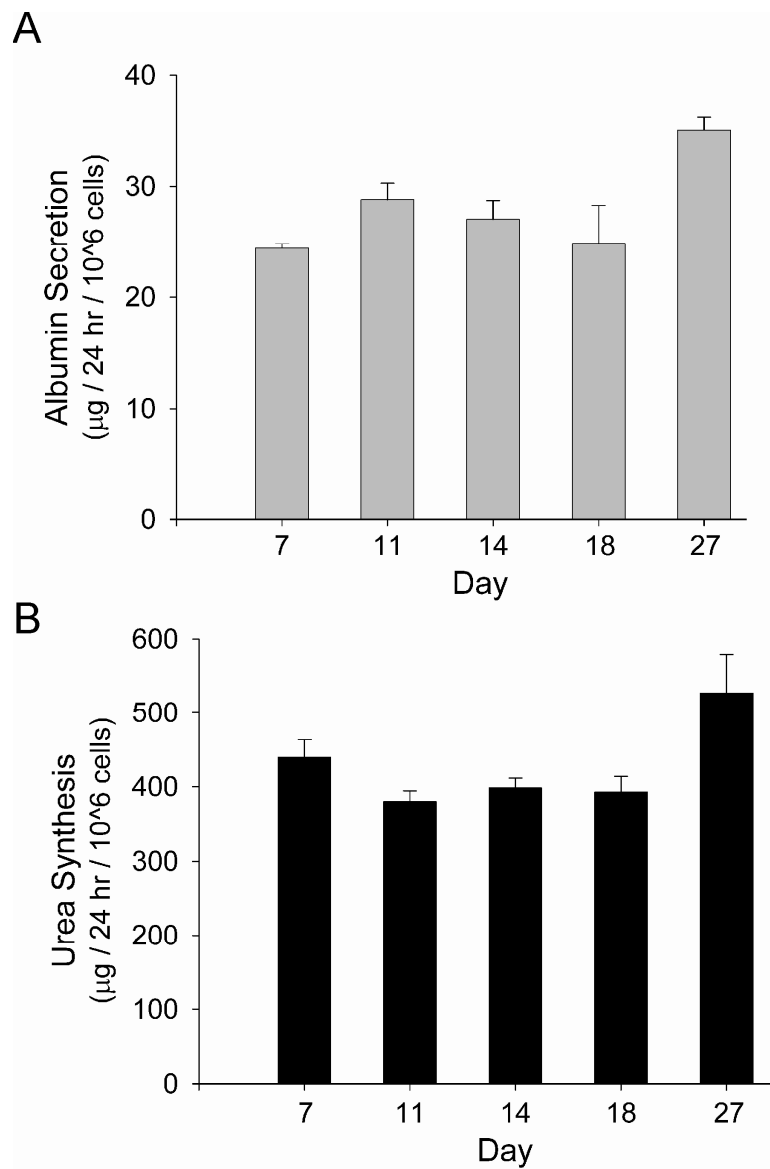


Figure 5.8: Liver-specific functions in microscale human liver tissues. Microscale tissues in a 24-well format were generated using the soft-lithographic process outlined in Figure 5.6 and represent micropatterned co-cultures of primary human hepatocytes and 3T3-J2 fibroblasts (500 µm islands, 1200 µm center-to-center spacing). **A)** Rate of albumin secretion over several weeks in microscale tissues is shown. **B)** Rate of urea synthesis in microscale tissues. Error bars represent SEM (n = 3).

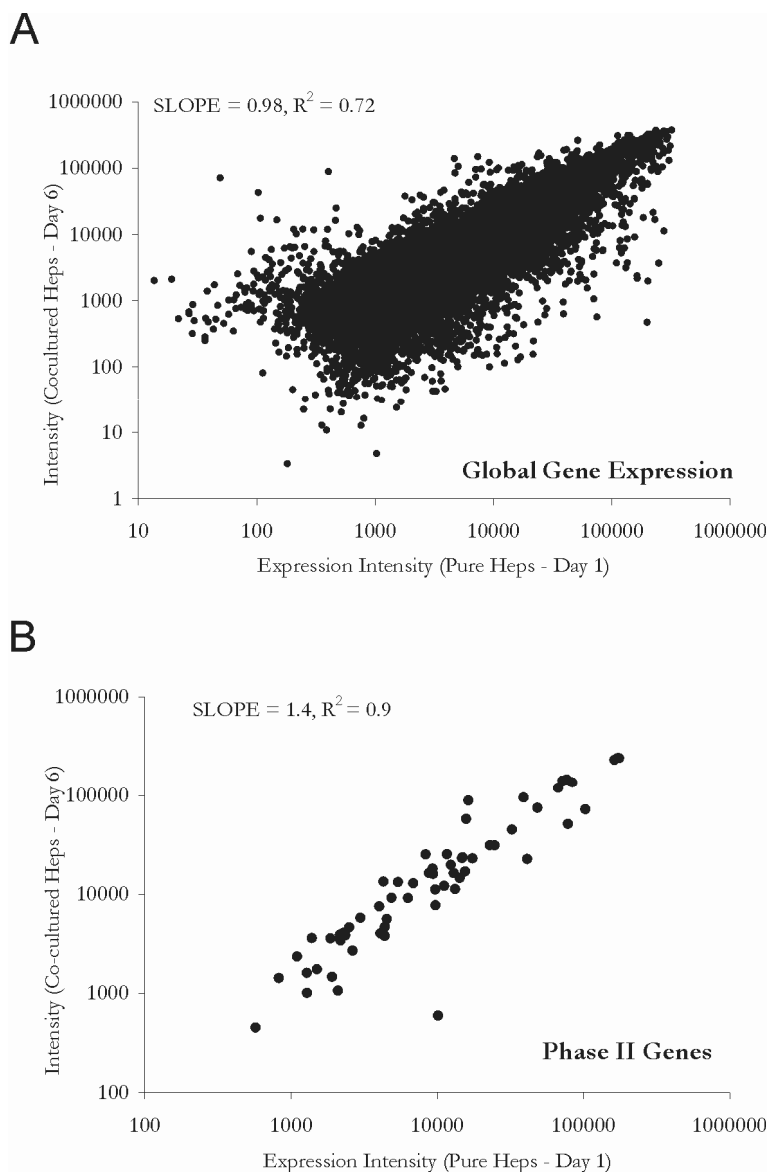


Figure 5.9: Transcriptional profiling of microscale human liver tissues. A) Global scatter plot comparing gene expression intensities (acquired via Affymetrix GeneChips) in primary human hepatocytes purified from microscale human liver tissues (day 6, see Methods for details) to gene expression intensities in fresh hepatocytes (12 hours of adherent culture, day 1). The values of the slope and the correlation coefficient (R^2) determined from a least-square linear fit are shown. **B)** Scatter plot limited to phase II xenobiotic metabolism genes (i.e. UDP-glycosyltransferases, glutathione transferase).

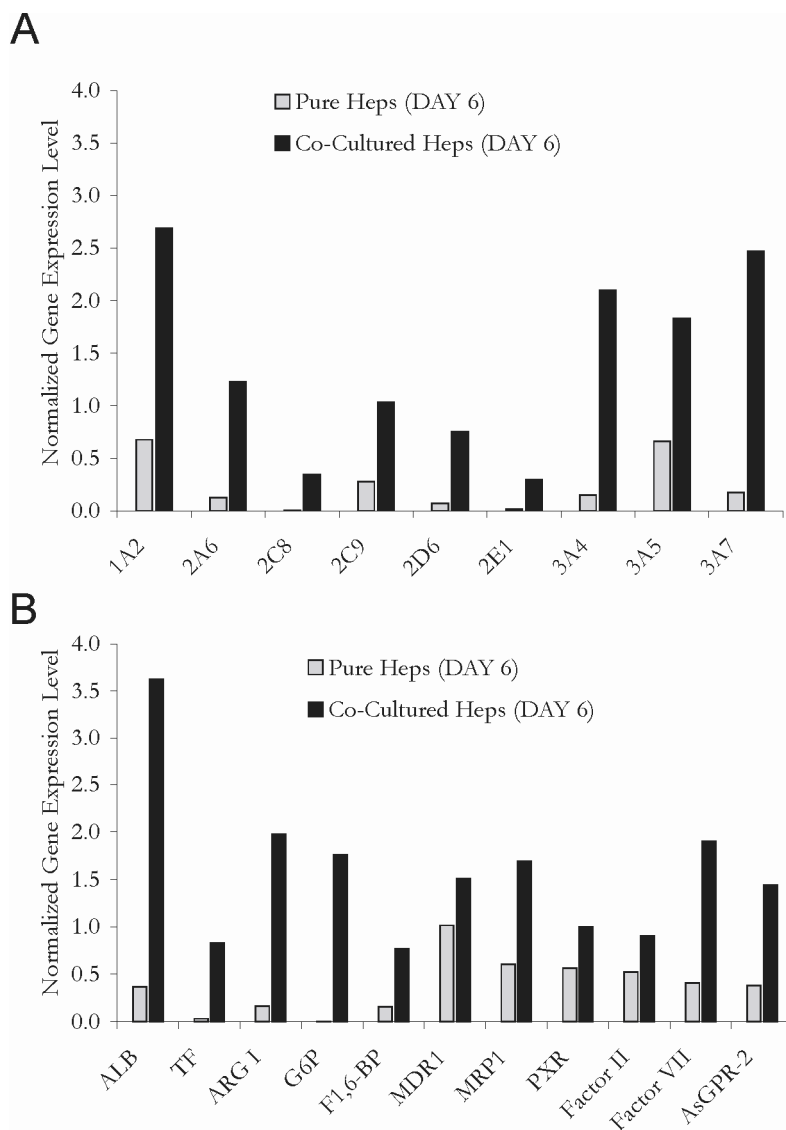


Figure 5.10: Gene expression level comparison between microscale human liver tissues and pure monolayers. A) Quantitative comparison of cytochrome-P450 (phase I) mRNA in hepatocytes from microscale human liver tissues to pure hepatocyte monolayers, both after one week of culture. All data was normalized to gene expression levels in pure hepatocyte monolayers on day 1. **B)** Quantitative comparison as in ‘e’ of a panel of key liver-specific genes: ALB, albumin; TF, transferrin (secreted protein); ARG I, arginase I (urea cycle enzyme); G6P, glucose-6-phosphatase (gluconeogenesis enzyme); F1,6-BP, fructose 1,6-bisphosphatase (gluconeogenesis enzyme); MDR1, multi-drug resistance gene (p-glycoprotein, drug transporter); MRP 1, multi-drug resistance protein (drug transporter); PXR, pregnane X receptor (nuclear receptor, regulator of xenobiotic metabolism); Factor II and VII are coagulation factors; AsGPR-2, Asialoglycoprotein receptor 2 (mediates binding, internalization and degradation of extracellular glycoproteins that have exposed terminal galactose residues).

5.4.4. Utility of Microscale Human Liver Tissues in Drug Development

In order to assess utility of the microscale human liver tissues for drug metabolism studies, we characterized CYP450 activity, drug-drug interactions, and phase-II metabolism. CYP450 activity was assessed using fluorescent substrates and found to be retained in untreated microscale tissues (Figure 5.11A). Such ‘baseline’ activity is critical for evaluation of metabolism-mediated mechanisms of toxicity. Competition for specific CYP450 enzymes was preserved in our platform as indicated by decreased substrate metabolism upon treatment with inhibitors. Phase-II activities (glucuronidation/sulfation) and their inhibition via prototypic compounds were also retained as determined by conjugation of 7-hydroxycoumarin (Figure 5.11B).

To assess utility of the microscale human liver tissues for cell-based toxicity assays, we quantified the acute and chronic toxic potential of model compounds, some with known clinical hepatotoxic potential. Compounds were characterized by their TC50 value, defined as the concentration which produced 50% reduction in mitochondrial activity after 24 hours of exposure (Figure 5.12A). Relative toxicity corresponded to relative hepatotoxicity of these compounds in humans. For example, the TC50 for troglitazone (oral hypoglycemic withdrawn from the market due to unforeseen hepatotoxicity) was two orders-of-magnitude lower than acetaminophen (over-the-counter analgesic). Importantly, relative toxicity of compounds in the same class such as troglitazone and its FDA-approved analogues, rosiglitazone and pioglitazone also corresponded to clinical reports (Figure 5.12B) [283]. Additionally, tolcapone (catechol-O-methyltransferase inhibitor used in Parkinson’s disease, withdrawn from the market due to hepatotoxicity) was found to be more toxic in our platform than its structural analogue entacapone, which is consistent with clinical cases of liver toxicity due to tolcapone (Figure 5.12C) [284, 285]. Established mechanisms of toxicity could also be

inferred from toxicity profiles in our platform (Figure 5.13). For instance, cadmium showed a relatively linear toxic profile while acetaminophen exhibited a toxicity ‘shoulder’ consistent with glutathione depletion as proposed elsewhere [170].

Establishment of liver tissue that is stable over several weeks is crucial for evaluating chronic toxicity due to repeated exposures. In Figure 5.14A, we demonstrate dose and time-dependent toxicity of acetaminophen. Concentrations that were not lethal after 24 hours of exposure caused extensive cell death (as measured by loss of mitochondrial activity) after prolonged exposure. Furthermore, morphologic changes were readily observed prior to cell death (Figure 5.14B), allowing the potential to detect sub-lethal toxicity at lower concentrations than those required for frank cell death [175].

Next, we demonstrated induction of CYP450 activity in our microscale human liver tissues using prototypic inducers and fluorescent substrates (Figure 5.15A). For example, we observed CYP2A6 induction upon treatment with Rifampin and Phenobarbital, while Omeprazole and β -Naphthoflavone had weaker effects. A reverse trend was seen for CYP1A2 induction. Such responses are consistent with the literature [189]. Modulation of CYP450 activities depends on both the dose and time of exposure to compounds. We demonstrate here that β -Naphthoflavone induces CYP1A2 activity in a dose and time-dependent manner in our platform (Figure 5.15B), while methoxsalen shows dose-dependent inhibition of CYP2A6 activity (Figure 5.15C). Furthermore, we demonstrated species-specific differences in induction by comparing the responses of microscale human and rat liver tissues (see chapter 6 for details on the development and characterization of a rat liver model). Omeprazole, reported to be a more effective inducer of human CYP1A2 than rat CYP1A [214, 286], was 8-fold more effective in human over rat models (Figure 5.16).

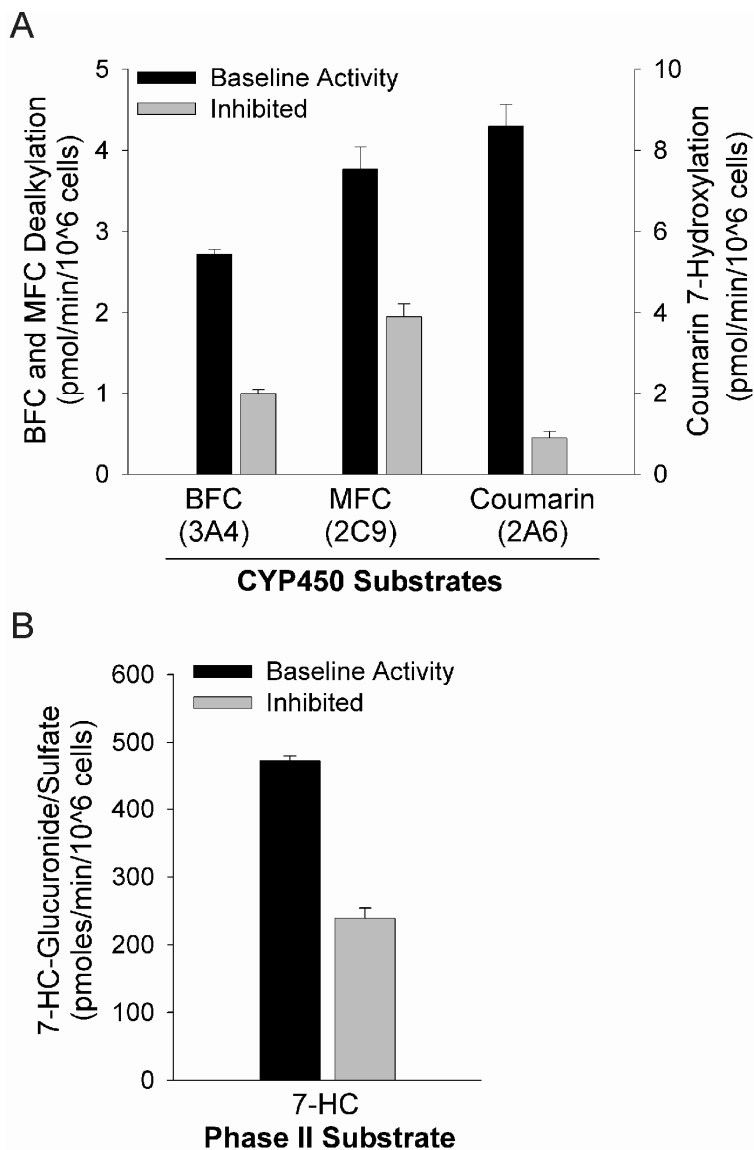


Figure 5.11: Phase I & II enzyme activity in microscale human liver tissues. A) Activity of phase I, cytochrome-P450 (CYP450) enzymes measured by coumarin analogs in microscale tissues at baseline (untreated, representative Day 10 shown) and upon treatment with competitive inhibitors. Specific activities of CYP3A4, 2C9 and 2A6 were demonstrated using substrate/inhibitor combinations, BFC/ketoconazole, MFC/sulfaphenazole and Coumarin/methoxsalen, respectively (MFC, 7-methoxy-4-trifluoromethylcoumarin; BFC, 7-benzyloxy-4-trifluoromethylcoumarin). **B)** Activity of phase II enzymes monitored by conjugation of glucuronic acid and sulfate groups to 7-Hydroxycoumarin (7-HC) in microscale tissues (day 10). Level of conjugation was determined by incubating supernatants from treated cells with β -glucuronidase/arylsulfatase and salicylamide was used as a competitive inhibitor. Error bars represent standard error of the mean ($n=3$).

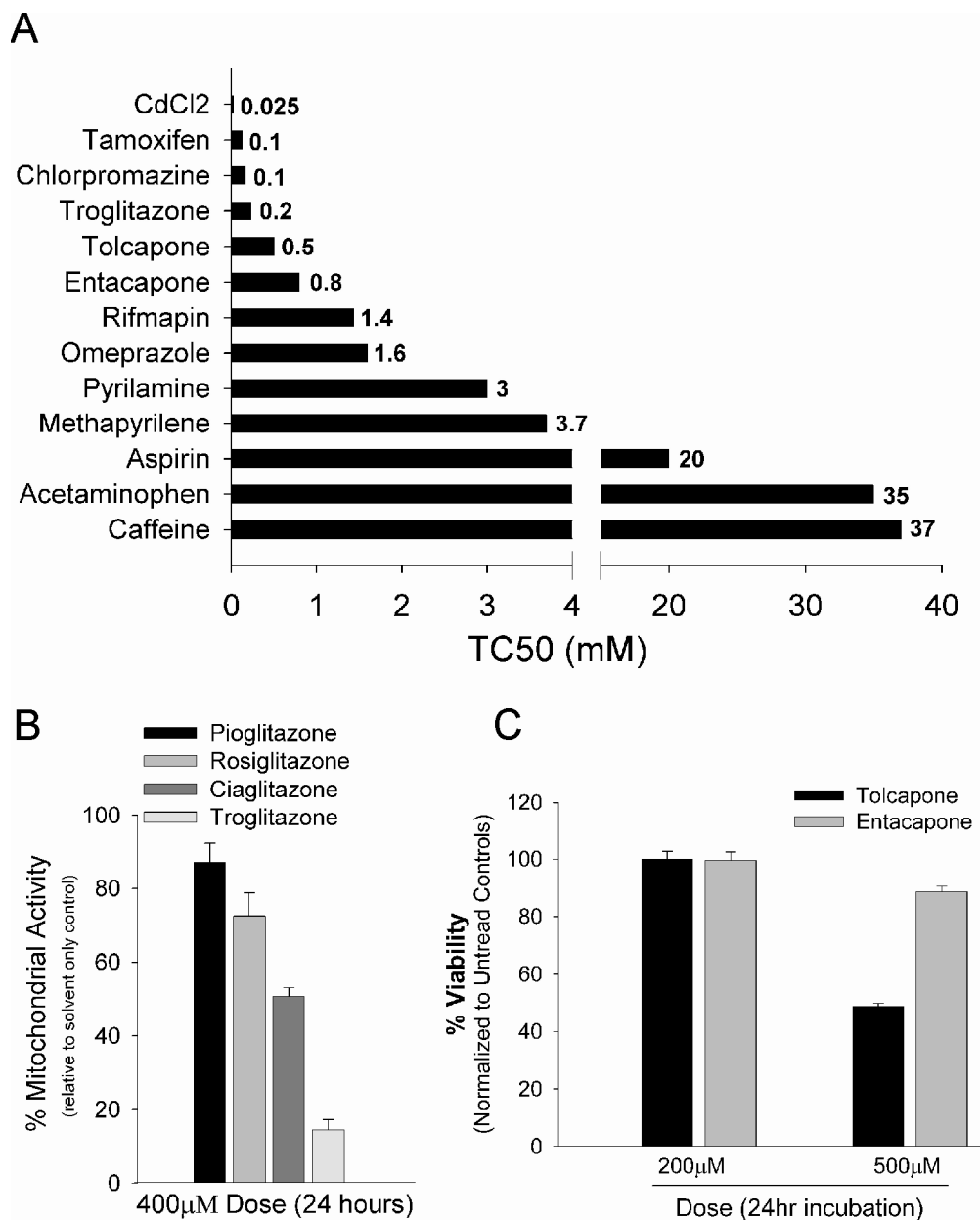


Figure 5.12: Relative toxicity of compounds in microscale human liver tissues. A) Rank ordering of compounds including several known hepatotoxins by TC₅₀ values—defined as the toxic concentration which produces 50% decrease in mitochondrial activity after 24 hours of exposure to 1-week old tissues (acute toxicity). TC₅₀ value for each compound was estimated from its dose-dependent toxicity profile. Mitochondrial toxicity was evaluated using the MTT assay (see Methods). **B)** Relative toxicity of structurally-related PPAR- γ agonists. Similar trends were seen for multiple doses. **C)** Relative toxicity of structurally-related COMT-inhibitors at multiple doses. All data were normalized to a solvent-only control (i.e. 100% viability). Error bars are SEM (n=3).

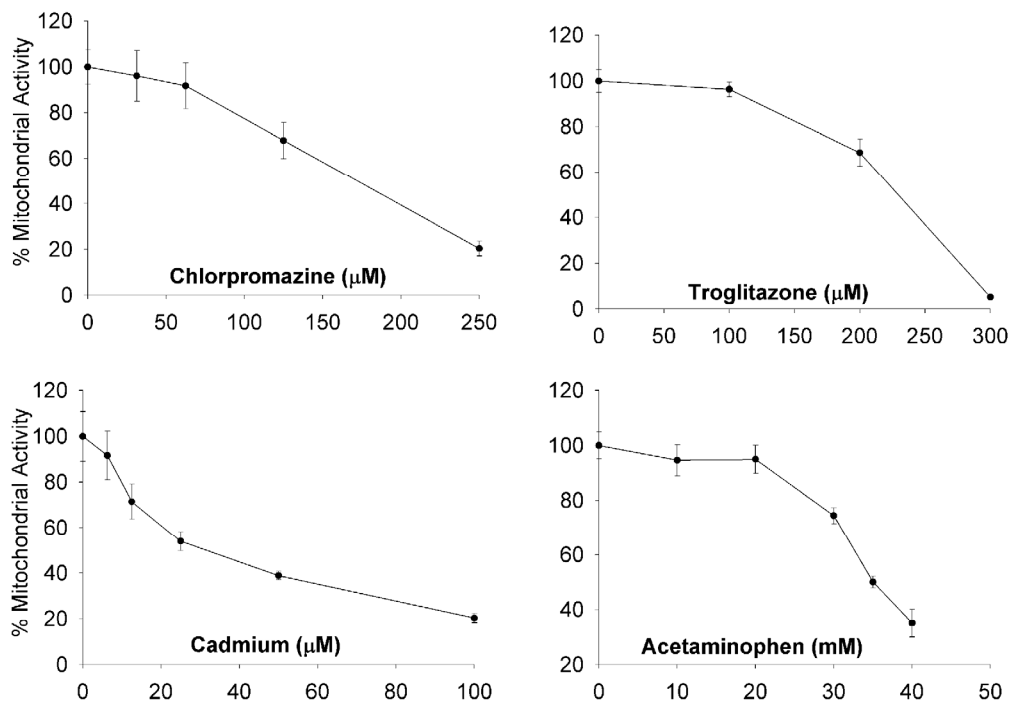


Figure 5.13: Toxicity profiles generated using microscale human liver tissues. Dose-dependent acute (24 hour incubations) toxicity of different types of hepatotoxins is shown. Chlorpromazine (Thorazine) is an anti-psychotic drug of low potency. Cadmium is an environmental toxin. Troglitazone (Rezulin) is an oral hypoglycemic withdrawn from the market due to unforeseen hepatotoxicity. Acetaminophen is an analgesic found in several over-the-counter drugs. Mitochondrial activity was evaluated using the MTT assay (see Methods). All data was normalized to mitochondrial activity in untreated or solvent-treated tissues (100% viability). Error bars represent standard error of the mean (n=3).

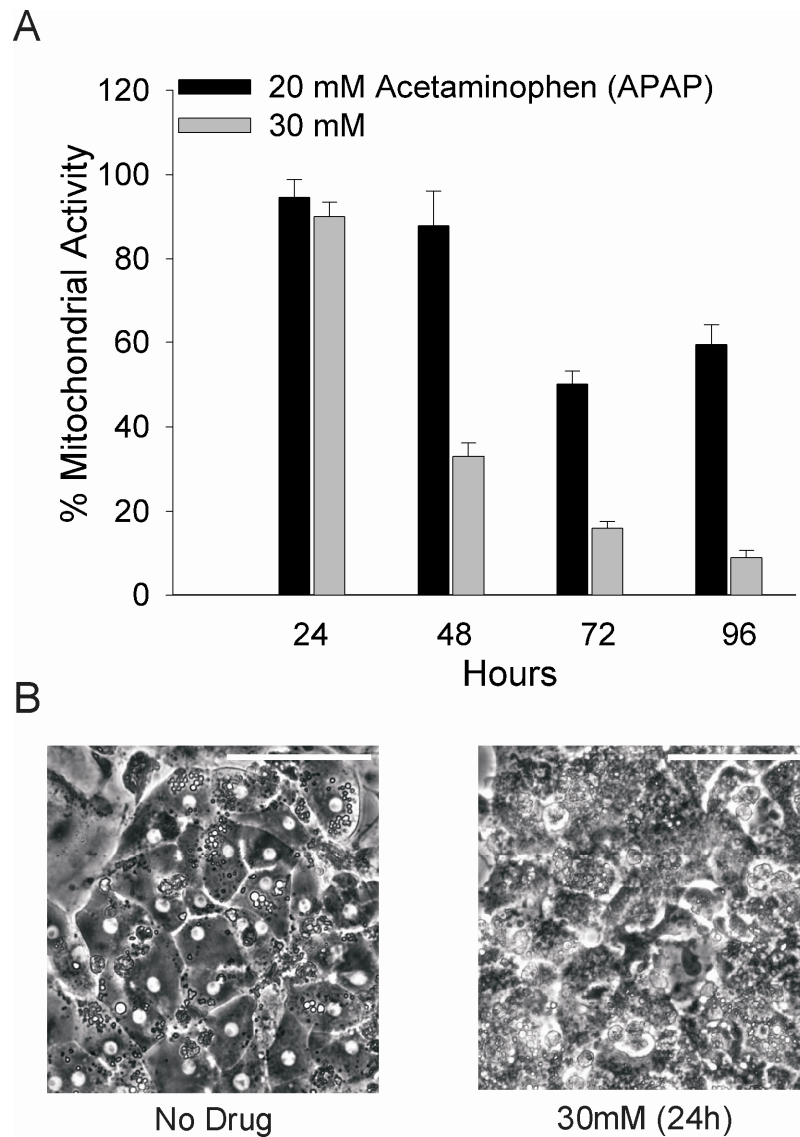


Figure 5.14: Chronic APAP toxicity in microscale human liver tissues. **A)** Shown here is time- and dose-dependent chronic toxicity of acetaminophen (APAP) in 1-week old microscale tissues. Tissues were dosed repeatedly every 48 hours. Mitochondrial activity was evaluated using the MTT assay (see Methods). All data was normalized to mitochondrial activity in untreated cultures (100% activity). **B)** Phase micrographs show human hepatocyte morphology under untreated conditions and after treatment with 30 mM of APAP for 24 hours (scale bars represent 100 μ m).

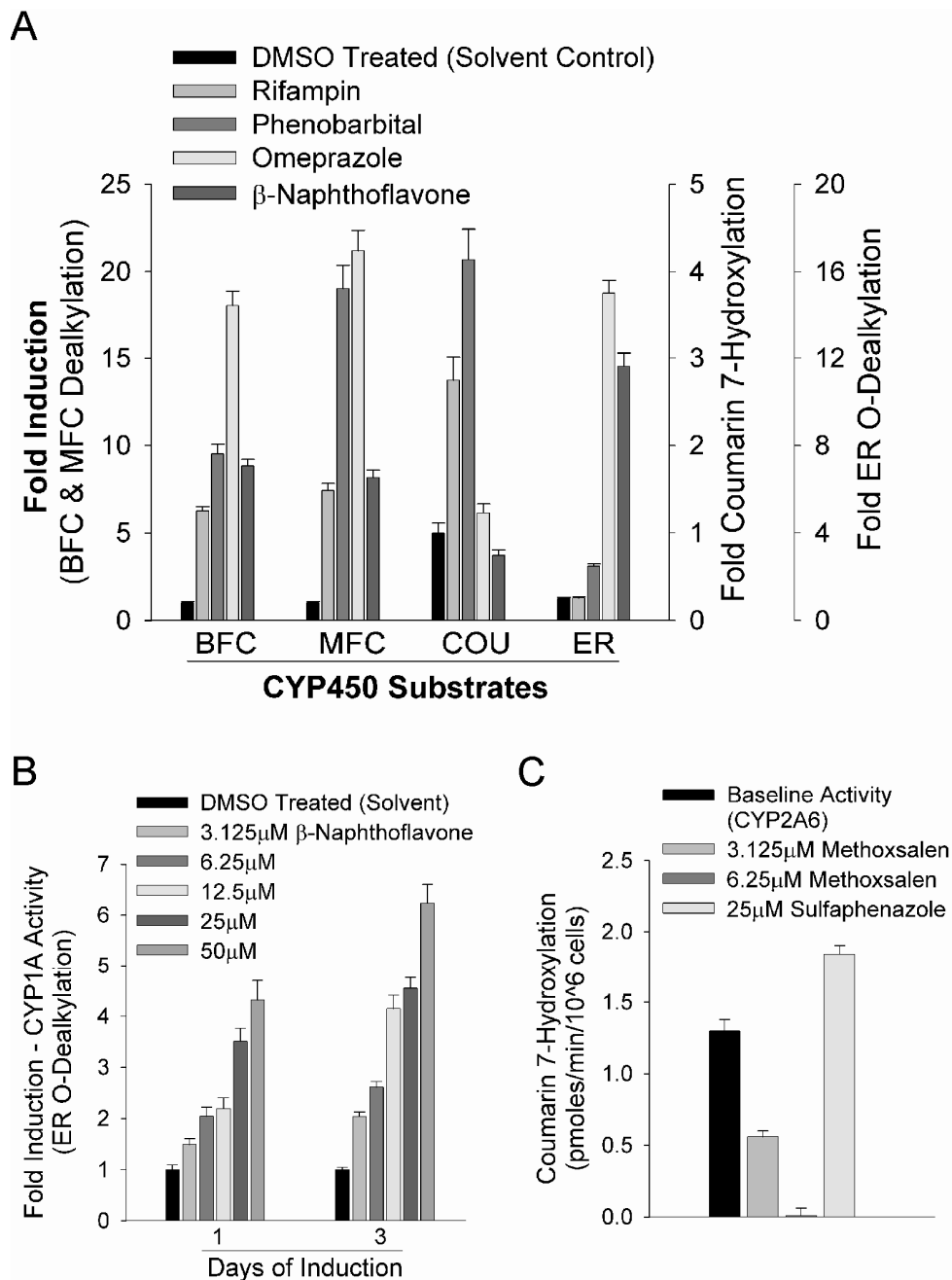


Figure 5.15: Drug-drug interactions in microscale human liver tissues. A) CYP450 induction via clinical inducers. Cultures were treated for 4 days with inducers before incubation with fluorimetric substrates. MFC, 7-methoxy-4-trifluoromethylcoumarin; BFC, 7-benzyloxy-4-trifluoromethylcoumarin; COU, Coumarin; ER, Ethoxy-resorufin. **B)** Dose and time-dependent CYP1A induction. Data was normalized to DMSO-only controls (fold change of 1). **C)** Dose-dependent CYP2A6 inhibition with Methoxsalen. Sulfaphenazole is an inhibitor of CYP2C9 (negative control). Error bars are SEM (n=3).

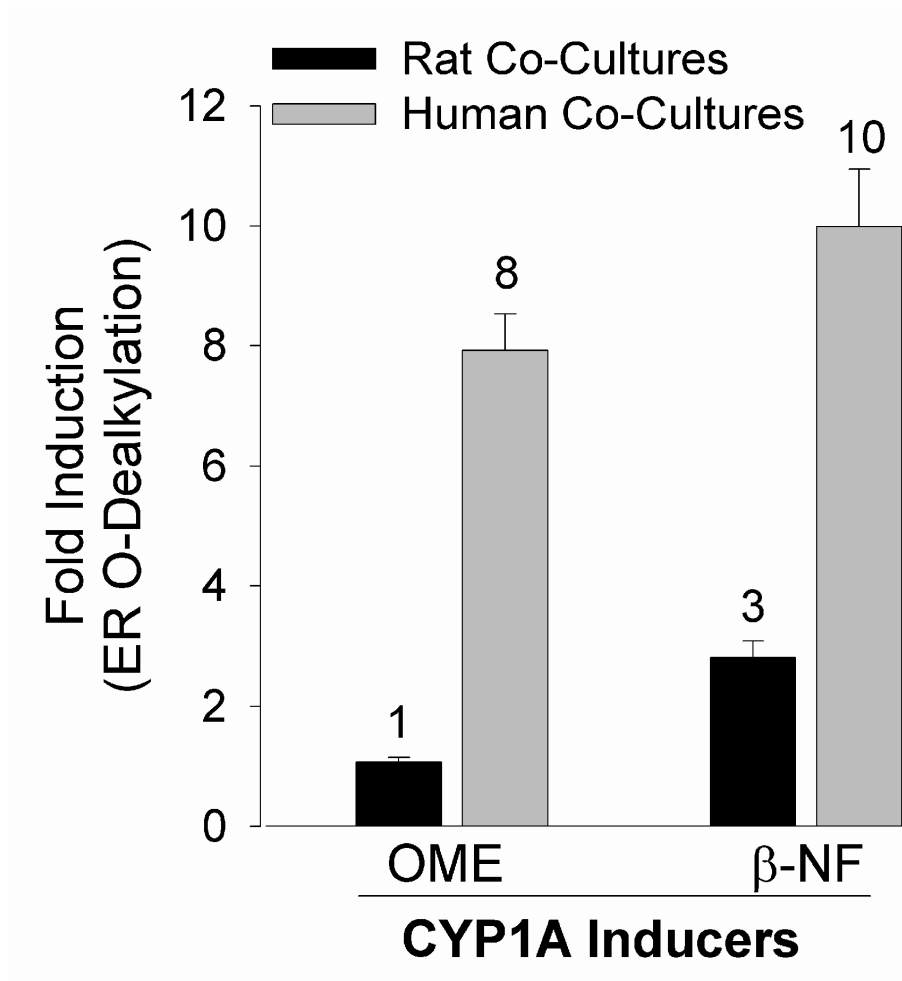


Figure 5.16: Species-specific induction of CYP1A isoforms in microscale liver tissues. Microscale tissues were generated using either primary rat or human hepatocytes, and subsequently treated for 4 days with prototypic CYP1A inducers, β -Naphthoflavone (β -NF) and Omeprazole (OME). For details on the development and characterization of the rat liver tissues, see Chapter 6. CYP1A activity was assessed via the dealkylation of ethoxyresorufin into fluorescent resorufin. Data were normalized to DMSO-only controls (fold change of 1). All error bars represent standard error of the mean ($n = 3$).

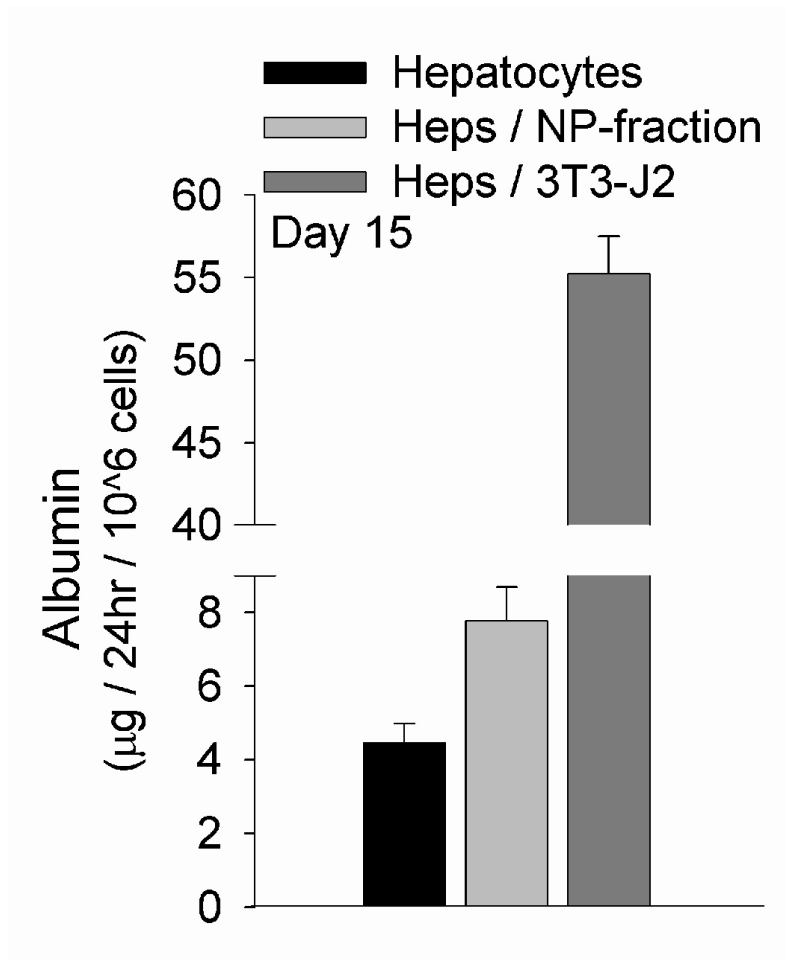


Figure 5.17: Albumin secretion in microscale tissues generated using non-parenchymal liver fraction. Primary human hepatocytes were micropatterned as per the process of Figure 5.6 and then co-cultivated with either the whole non-parenchymal fraction of the human liver (Kupffer cells, sinusoidal endothelia etc) or 3T3-J2 murine embryonic fibroblasts. Albumin secretion in such co-cultures was compared to pure micropatterned hepatocyte controls. Representative data from one day is shown, though trends were seen for multiple days. Error bars represent standard error of the mean (n=3).

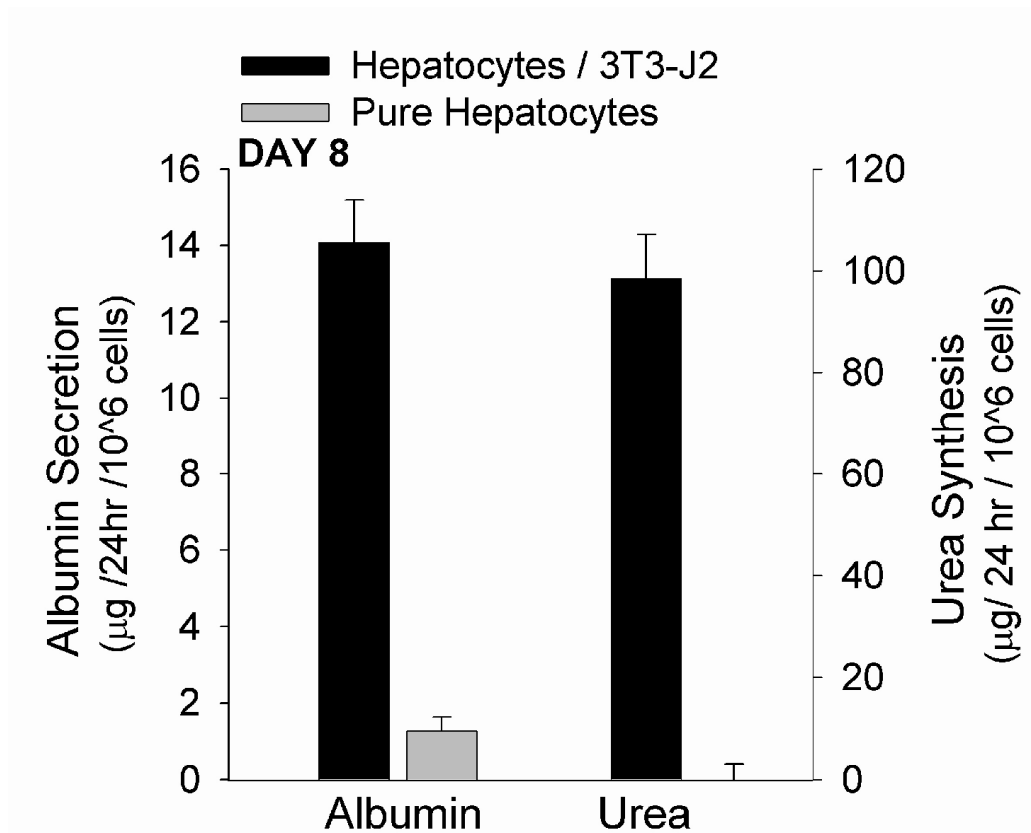


Figure 5.18: Liver-Specific functions in microscale tissues generated using cryopreserved human hepatocytes. ‘Plateable’ cryopreserved human hepatocytes were used to create microscale liver tissues via the process outlined in Figure 5.6. Shown here are liver-specific functions in pure hepatocyte cultures and hepatocyte-fibroblast co-cultures. Representative data from a single day is shown, though trends were seen for multiple days. Error bars represent standard error of the mean (n=3).

Table 5.1: Liver donor information. Reported here is specific information (age, sex, cause of death) on liver donors whose freshly isolated hepatocytes were purchased in suspension from multiple vendors for use in the experiments of this study.

Donor#	Age (years)	Sex	Cause of Death	Vendor
1	4	N/A	Anoxia	ADMET
2*	5	M	Anoxia	BD-Gentest
3	7	F	N/A	Cambrex
4	14	F	Gun shot wound	ADMET
5	19	M	Motor vehicle accident	In Vitro Technologies
6	20	M	Gun shot wound	In Vitro Technologies
7	52	M	Aortic dissection	In Vitro Technologies
8	53	M	Brain stem hemorrhage	Tissue Transformation Technologies
9	54	F	Cardiac arrest	In Vitro Technologies
10	55	M	Seizure	Tissue Transformation Technologies
11	60	M	N/A	CellzDirect
12	61	M	Motor vehicle accident	BD-Gentest
13*	69	M	Intracranial bleeding	In Vitro Technologies

* African-American Donors. All other donors were of Caucasian descent.
 'N/A' - not available at time of purchase.

5.5. Discussion

Microfabrication tools allow control over cell-cell and cell-surface interactions with micrometer-precision and have been used to investigate tissue functions in different model systems [274, 287]. Furthermore, such tools have spurred development of miniaturized cell-based assays in well-defined microenvironments towards reduction in culture-to-culture (and cell-to-cell) variability and less consumption of reagents [140]. In the context of drug development, where cell-based testing is well-established, minimal progress has been made towards using microtechnology to develop improved models of human tissues that are highly predictive of clinical outcomes [279]. Though primary human hepatocytes are ideally suited for evaluating drug metabolism and toxicity *in vitro*, they are notoriously difficult to maintain in culture as they rapidly lose viability and key liver-specific functions (i.e. cytochrome P450 activity) [176].

In this study, we have coupled microfabrication with tissue engineering to develop a robust model of the human liver that consists of primary human hepatocytes arranged in clusters of prescribed dimensions and surrounded by supportive fibroblasts (co-cultures). We first utilized photolithography to determine the pattern geometry which produced optimal liver-specific functions in such co-cultures. Next, we developed a novel stencil-based soft-lithographic process to create miniaturized micropatterned co-cultures in an industry-standard multi-well format amenable to the study of multiple drug candidates. We further characterized our microscale human liver tissues using biochemical assays for liver-specific protein secretion and nitrogen metabolism, transcriptional profiling, and assessments of phase I and II enzyme activities. Such characterization revealed that our platform retained liver-specific functions for several weeks in monolayer culture. Lastly, we demonstrated utility of our platform in drug

development by characterizing drug-drug interactions (CYP450 induction and inhibition) and susceptibility to a panel of hepatotoxins.

5.5.1. Comparison between Micropatterned Rat and Human Hepatocyte Co-Cultures

In order to enable comparisons across species, we utilized similar micropatterning process (i.e. photolithography) and microscale geometries for functional optimization of human hepatocyte co-cultures as utilized for rat hepatocytes in our previously published studies [123, 280]. In this study, our results indicated that primary human hepatocytes were more dependent on homotypic interactions than their rat counterparts (Figures 5.2, 5.5). In rat co-cultures, micropatterned configurations in which homotypic interactions were minimized and heterotypic interactions were maximized (i.e. single hepatocyte islands of 36 μm surrounded on all sides by fibroblasts) displayed highest liver-specific functions. On the other hand, co-cultures containing human hepatocytes displayed highest functions once the appropriate balance of homotypic and heterotypic interactions was achieved (i.e. 490 μm hepatocyte islands with 1230 μm center-to-center spacing).

5.5.2. Miniaturization of Micropatterned Co-Cultures Using Stencils

Though it yields robust cellular micropatterns, photolithography is an expensive, serial technique requiring specialized equipment for each experiment. Soft lithography, a set of techniques for fabricating microstructures for biological applications, overcomes many shortcomings of photolithography with its use of elastomeric polymeric devices that can be synthesized conveniently, rapidly and inexpensively [153]. Therefore, we utilized PDMS stencils to develop a process that yields miniaturized micropatterned co-cultures in a multi-well format (see Figure 5.6 and 5.7). These stencils can be used to create tens of thousands of repeating tissue units (i.e. island of hepatocytes surrounded by

nonparenchymal cells) in a matter of hours. Stencils can be reused many times (> 25) to create micropatterned co-cultures, which may justify the nominal cost of their initial fabrication. Furthermore, stencils can be used to micropattern extracellular matrix proteins (ECM) such as fibronectin and laminin, which unlike type-I collagen, are sensitive to the harsh processing procedures (i.e. sonication in acetone) used in photolithography. Micropatterning of different types of proteins (individual or combinations) may be necessary for future studies directed towards determining the optimal ECM microenvironment of co-cultures. Lastly, PDMS stencils seal under dry conditions to a culture substrate, which can vary from standard off-the-shelf tissue culture plastic or glass to customized self-assembled monolayers of functionalized thiols on gold-plated materials for exquisite control over surface biochemistry.

5.5.3. Modularity and Cost Benefits of Microscale Liver Tissues

An advantageous feature of our microscale liver tissue platform is its modular design in that various liver or non-liver derived nonparenchymal cells can be used to surround hepatocyte colonies to form micropatterned tissues. We chose 3T3 fibroblasts because of their ready availability, ease of propagation, and evidence showing that this immortalized cell line can induce high levels of liver-specific functions in hepatocytes from different species [65, 124, 288]. Nonetheless, in order to demonstrate versatility of our platform, we co-cultivated micropatterned human hepatocytes with the whole nonparenchymal fraction of the human liver (multiple cell types, including sinusoidal endothelial and kupffer cells) and observed stabilization of hepatocyte functions (though not to similar levels or duration as in 3T3 co-cultures, Figure 5.17). Furthermore, we used stencils to create a co-culture model of the rat liver that remains functional for over 2 months, allowing chronic studies to be conducted on hundreds of identical rodent liver

tissues, thereby reducing noise arising from animal-to-animal variability (see Chapter 6 for details on development and characterization of the rat model).

We have demonstrated that micropatterned clusters of human hepatocytes functionally outperformed their randomly distributed counterparts by several fold, consistent with reports that confluent hepatocyte cultures retain liver-specific functions better than sparse cultures, partly through cadherin interactions [87]. Subsequent introduction of non-parenchymal cells further enhanced hepatocellular functions and longevity of the liver tissues. Thus, our microscale platform uses an order-of-magnitude fewer hepatocytes (10K vs. 200K) and maintains phenotypic functions for a longer time than conventional pure monolayers (weeks vs. days) in similar multiwell formats [182]. With the high cost of human hepatocytes (~\$65-80 per million cells), such advantages represent a significant cost savings. Furthermore, we have utilized reusable stencils to develop a 24-well plate format that is amenable to the study of multiple drug candidates. Each well in our system uses ~150-200 μ L of culture media, allowing conservation of candidate drugs and other precious reagents during early phases of drug discovery.

We have explored many hepatocyte sources. In our microscale platform, we observed induction of liver-specific functions in freshly isolated hepatocytes across liver donors of multiple age groups, sexes and medical histories (Table 5.1). Nonetheless, due to limited availability of fresh cells, we also successfully incorporated cryopreserved human hepatocytes (see Figure 5.18) similar to those now widely utilized for short-term cultures [185, 186], thus providing potential to generate microscale tissue on demand.

5.5.4. Comparison of Microscale Liver Tissues with Other Platforms

Several other *in vitro* models of liver tissue have been proposed. In particular, multilayer or spheroid-based '3D' hepatocellular tissues, some with continuous perfusion,

have been reported [1, 30, 32, 127, 165, 188, 206, 210, 212, 289]. However, very limited progress has been made in the development of novel systems for culture of primary *human* hepatocytes. Most investigators have instead focused on *animal* hepatocytes; however, well-documented differences between animal and human hepatocellular functions [174, 175] makes translation of animal liver models to human ones difficult. Additionally, a few bioreactor designs have utilized tumor-derived human hepatic cell lines [1]. It is well accepted in the liver community that hepatic cell lines established to date contain abnormal levels and repertoire of liver-specific functions [1, 9, 176].

A handful of primary human hepatocyte-based spheroidal cultures (static conditions) [290, 291] and bioreactors (continuous perfusion) are described in the literature [188, 292]; however, they remain in experimental stages and have not been characterized to any great degree for drug development applications. Furthermore, these systems suffer from drawbacks which make their near term application in drug development probably unlikely. For instance, spheroidal cultures contain heterogeneous structures that have accumulation of toxic bile in the interiors. Additionally, large size spheroids display necrotic and hypoxic cells in the centers due to oxygen diffusion limitations [165]. The drawbacks of hepatocyte bioreactors include: 1) Limited phenotypic stability of hepatocytes (1-2 weeks at best); 2) Utilization of high culture media volumes (several liters in some cases) and high cell counts (several hundred million), making their use in drug discovery cost prohibitive; 3) Designs that are difficult to scale down for medium-to-high throughput screening applications; 4) Limited in situ imaging and visualization of hepatic morphology in heterogeneous aggregates of multiple liver cell types; and, 5) Nutrient and drug diffusion barriers in heterogeneous structures.

Due to a paucity of stable human liver models, the pharmaceutical industry, as well as academic laboratories investigating drug disposition typically rely on randomly

distributed confluent cultures of human hepatocytes which decline in function and viability over a few days. Though the microscale cellular architecture has been shown to be important in modulation of hepatic functions *in vitro*[65, 262], current models of the human liver have almost universally ignored this aspect.

By specifying the degree of homotypic and heterotypic interactions between hepatocytes and nonparenchymal cells via microfabrication technologies, we have shown here that our microscale human liver platform maintains phenotypic stability for 4-6 weeks, depending on the state of the procured human liver tissue (see Figure 5.8). Such prolonged stability is a significant improvement over monolayer models utilized in drug development, as well as the handful of human hepatocyte bioreactors. In our model, we have assessed phenotypic stability using a variety of different criteria (i.e. gene expression profiling, enzyme activity assays, albumin and urea secretion), which is an improvement over reported studies in which only a few functions are measured. Furthermore, we have characterized our microscale human liver tissues extensively for utility in drug development (see Figures 5.12 to 5.16), which remains to be done in most other models.

As the liver itself is composed of flat, anastomising ‘plates’ that are typically one cell thick, two dimensional (monolayer) platforms of the liver may suffice for many ADME/Tox applications. Furthermore, since monolayer systems (confluent monolayers, collagen sandwich or Matrigel overlay) are still the most commonly utilized platforms in industry [176, 182], the microscale tissue proposed here can be mapped easily to existing laboratory protocols including robotic fluid handling, *in situ* microscopy, and colorimetric and fluorescent plate-reader assays.

In chapter 6 of this dissertation, we demonstrate a micropatterned co-culture model of the *rat* liver that remains functional for over 2 months. To our knowledge, no other system has shown maintenance of liver-specific functions in *both* primary human

and rodent hepatocytes for such extended time periods. Therefore, our platform offers a modular design for constructing both animal and human liver models, making it quite suitable for integration into the drug development pipeline.

5.5.5. Evaluation of Hepatotoxicity in Microscale Liver Tissues

The most widely used model for toxicity screening is human hepatocytes in suspension [165]. However, being adherence-dependent cells, hepatocytes in suspension typically live for only a few hours. Thus, toxicity assays in such cultures involve the use of ‘high’ drug doses, which may not be similar to doses used in a clinical setting. With some improvement in culture of isolated hepatocytes, the pharmaceutical industry is moving towards using short-term adherent monolayer cultures for toxicity screening with clinically-relevant drug doses [176]. Primary human hepatocytes are increasingly utilized in such cultures since hepatic cell lines derived from hepato-carcinomas typically contain abnormal levels and repertoire of liver-specific functions [176]. Though toxicity due to repeated drug exposures is common in the clinic, current liver models are not suited for screening of such chronic toxicity primarily because they last for a few days at most. Furthermore, loss of liver-specific functions (i.e. drug metabolism enzymes) on the same time-scale as toxic responses (hours to days) may confound results even in short-term cultures, especially for those pharmaceutical compounds which undergo liver-specific metabolism (detoxification and/or activation into toxic metabolites).

The Scandinavian Society for Cell Toxicology conducted a multi-center evaluation of *in vitro* cytotoxicity (MEIC) study using 50 pre-selected test chemicals [293]. Ninety-six laboratories participated to assess *in vitro* methods for predicting acute toxic reactions in humans. Some of the findings indicate that liver-specific injury was difficult to predict. By comparing the response of primary hepatocytes to cell lines (quotient), only 2 of 8

known liver toxins were identified as having differential toxicity in hepatocytes (phenol, arsenic) whereas the others exhibited global cytotoxicity (acetaminophen, iron, 2,4-dichlorophenoxyacetic acid, paraquat, copper and thallium) [294]. Thus, there exists an urgent need for improved liver models for identification of acute and chronic toxicity.

In the last few years, some progress has been made in utilizing microfabrication to develop miniaturized platforms for screening of liver-specific toxicity [295-297]. However, these studies have focused on the technological platform exclusively, while ignoring the insufficient complexity or the phenotypic instability of the underlying liver models, typically isolated CYP450 enzymes or carcinoma-derived hepatic cell lines. For instance, Lee et al [297] recently developed a metabolizing enzyme toxicology assay chip (MetaChip) that combines high-throughput CYP450 catalysis with cell-based screening (breast cancer cell line) on a microscale platform. The MetaChip is a sol-gel microarray that contains one or more human P450 isoforms used to generate biologically active metabolites of a lead compound (e.g., a drug candidate). This microarray represents an advance in the use of microfabrication to create liver models; however, isolated enzymes lack the dynamic gene expression and protein machinery necessary to evaluate complex mechanisms underlying hepatotoxicity.

We have utilized microfabrication technologies to create a microscale liver platform that contains primary human hepatocytes (closest one can get to *in vivo* with isolated cells). In order to demonstrate utility of this microscale platform in drug development, we utilized assays (i.e. mitochondrial toxicity, fluorescent CYP450 assays) commonly employed by pharmaceutical scientists. Unlike existing systems, our microscale human liver tissue can be used for chronic toxicity studies due to its long-term phenotypic stability (see Figure 5.14). Additionally, our platform can be used with low drug doses which do not cause frank cell death but induce changes in hepatocyte

morphology and/or intracellular composition (i.e. steatosis, cholestasis) over many days to weeks, as has been shown in vivo [298-300]. Detection of such subtle toxic responses in a monolayer format improves the sensitivity of the screening assay [175].

With the rank ordering of model hepatotoxins, including structural analogs with varying clinical hepatotoxic potential, we have shown that our model can recapitulate known in vivo responses in vitro (see Figure 5.12). For instance, relative toxicity of compounds in the same class such as troglitazone (oral hypoglycemic withdrawn due to hepatotoxicity) and its FDA-approved analogues, rosiglitazone and pioglitazone corresponded to clinical reports [283]. A similar trend was observed for the hepatotoxic drug tolcapone (anti-Parkinson drug withdrawn from the market due to hepatotoxicity) and its less toxic structural analogue, entacapone [284]. Interestingly, no in vitro data exists for these structural analogues. Additionally, the TC50 values (concentration of drug at which 50% of cell viability is compromised) we report for some of the other classic hepatotoxins such as tamoxifen, chlorpromazine and acetaminophen are consistent with values reported in short-term hepatocyte cultures [186]. Furthermore, the number of compounds we have utilized to validate our platform is greater than what has been reported in the literature for other short-term human liver models [186, 295]. Lastly, besides rank ordering based on TC50 values, we also provide dose-response toxicity curves (see Figure 5.13). Such curves are utilized to gain insights into the potential mechanism underlying the toxic response.

5.5.6. Detection of Clinically Relevant Drug-Drug Interactions in Microscale Liver Tissues

Since drug-drug interactions can lead to serious pharmacological or toxicological consequences in the clinic, their detection in early phases of drug discovery is quite important. Such interactions typically occur at the level of cytochrome-P450 enzymes

(CYP450), which can be induced or inhibited by different pharmaceutical compounds [301]. In this study, we utilized fluorimetric assays using prototypic substrates to demonstrate the ability of our microscale human liver tissues to identify clinically-relevant drug-drug interactions. For instance, consistent with the literature [189], we demonstrated that Rifampin and Phenobarbital specifically induced CYP2A6 activity (hydroxylation of coumarin), while Omeprazole and β -Naphthoflavone specifically induced CYP1A2 activity (dealkylation of ethoxy-resorufin) – see Figure 5.15. On the other hand, we observed induction of BFC and MFC metabolism via all four inducers. BFC and MFC are both substrates for CYP1A2 [BD Gentest poster entitled “Human and Rat Cytochrome P450 Isoform Selectivity within a Panel of Fluorimetric Substrates”, www.gentest.com], which may be the underlying cause of induction via Omeprazole and β -Naphthoflavone. Furthermore, BFC and MFC are metabolized by CYP3A4 and CYP2B6, respectively. Both of these enzymes are known to be inducible by Rifampin and Phenobarbital [189].

For inhibition studies, we utilized BFC, MFC and Coumarin as CYP3A4, 2C9 and 2A6 substrates, respectively (see Figure 5.11). Tissues were incubated with substrates in the presence of known and specific competitive inhibitors for these CYP450s. Our results indicated baseline (i.e. untreated) substrate metabolism which was inhibited upon treatment with the respective inhibitors. Furthermore, we also demonstrated activity and inhibition of Phase II conjugation enzymes (glucuronidation and sulfation activities) using 7-HC as a prototypic substrate. The presence of active Phase I and II enzymes is important for screening of pharmaceutical compounds that rely on coupling of these two pathways for their complete metabolism.

In pre-clinical studies with live animals (required by the Food and Drug Administration), the selection of a species which closely resembles human-specific

metabolism of a candidate drug is very important. Availability of *in vitro* human and animal liver models can aid in this selection process. In chapter 6, we describe the development of a robust rodent liver model that utilizes micropatterned co-cultures of primary rat hepatocytes and 3T3 fibroblasts. In order to demonstrate that our human and rat microscale liver tissues maintain *in vivo*-relevant species-specific differences in hepatocellular functions, we incubated these tissues with Omeprazole and β -Naphthoflavone, and subsequently evaluated induction in CYP1A activity. As reported previously by others [189, 286], we saw no Omeprazole-mediated induction of CYP1A in rat liver tissues, whereas there was an 8-fold induction in the human model. On the other hand, β -Naphthoflavone caused an induction of CYP1A activity in both model systems. In Chapter 6, we demonstrate additional species-specific differences between our rat and human microscale liver models.

5.5.7. Conclusions

In conclusion, we have utilized microfabrication to fabricate and miniaturize human liver tissue that can be used for high-content cell-based assays in preclinical phases of drug development. We note future improvements to our microscale liver tissue platform in the 'Discussion' section of chapter 6 of this dissertation. Such a platform has the potential to reduce development costs, increase likelihood of clinical success, and reduce the risk for patient exposure to unsafe drugs. Beyond the liver, this study provides a generalizable framework for the development of other tissue models towards eventual integration into a multi-tissue, lab-on-a-chip platform [302]. In the future, improved *in vitro* tissue models with precisely defined microenvironments may be used to elucidate fundamental mechanisms underlying human physiology and disease.

Acknowledgements

We are grateful to Emanuele Ostuni and Surface Logix, Inc. for design and fabrication of the PDMS stencils, Howard Green for providing 3T3-J2 fibroblasts, Craig Sharp and Jennifer Koh for assistance with pilot studies, microfabrication, and biochemical assays. Funding was generously provided by NSF (awarded to S. Khetani), NSF CAREER, NIH NIDDK, Deshpande Center (MIT), and the David and Lucile Packard Foundation.

The text of this chapter, in part, has been submitted for publication (Khetani, S.R. and Bhatia, S.N., “Microscale Human Liver Tissue for Drug Development”). The dissertation author was the primary researcher and author and conducted the research that forms this chapter.

CHAPTER 6

A LONG-TERM MODEL OF THE RAT LIVER FOR EVALUATING DRUG DISPOSITION

6.1. Abstract

Whole animal models provide valuable *in vivo* data on the ADME/Tox (absorption, distribution, metabolism, elimination and toxicity) properties of new chemical entities and thus constitute a crucial and FDA-required component of drug development. However, significant animal-to-animal variability coupled with the need to screen large number of ‘lead’ compounds makes studies in live animals too slow for real-time feedback in a drug discovery campaign. As a result, high-throughput ADME/Tox screening and optimization with *in vitro* tissue models is increasingly becoming commonplace in the pharmaceutical industry. In the case of the liver, the major determinant of drug metabolism and toxicity, primary hepatocytes are generally considered to be the ‘gold standard’ for building *in vitro* tissues. However, hepatocyte cultures routinely utilized for evaluating drug disposition suffer from a precipitous decline in viability and liver-specific functions. In this study, we describe the development and characterization of an *in vitro* model of the rat liver that remains functional for several weeks in monolayer culture. The core of our model consists of primary rat hepatocytes that have been co-cultivated with nonparenchymal cells (co-cultures). Using microfabrication tools borrowed from the semiconductor industry, we discovered that arranging hepatocytes in clusters of empirically-derived dimensions consistently improved

the longevity of co-cultures from several weeks to over 2 months. Hepatocytes in co-cultures retained their characteristic morphology, secreted liver-specific products, metabolized compounds using active Phase I and II drug metabolism enzymes, and displayed functional bile canaliculi. We further show utility of our platform in drug development by characterizing drug-drug interactions, acute and chronic toxicity of model Hepatotoxins, and species-specific metabolism. In the future, continued development of improved tissue models and their integration into the so-called ‘animal-on-a-chip’ may revolutionize the current paradigm for high-throughput ADME/Tox screening. Beyond drug development, phenotypically stable cultures can be used to elucidate the fundamental mechanisms underlying physiology and disease.

6.2. Introduction

The process of drug discovery begins with the biochemical screening of vast libraries of compounds for activity against a chosen therapeutic target. The wealth of active compounds that emerge from these primary screens are further used to build a large class of ‘lead’ compounds. Lead compounds then undergo characterization and optimization of ADME/Tox properties to determine how they will interact with the body in terms of safety and efficacy. Preclinical ADME/Tox testing of new chemical entities typically includes a panel of screens with *in vitro* tissue models (human and animal), followed by *in vivo* studies in live animals [163]. For animal studies, the use of *in vitro* systems offers several advantages over *in vivo* whole animal testing: experimental conditions can be rigorously controlled; less compound is required for screening; confounding variables encountered *in vivo* (e.g. effect of multiple organs on compound metabolism) can be avoided; large number of experiments can be conducted with a single animal, thereby reducing animal-to-animal variability and enabling high-throughput

screening; and problematic compounds can be eliminated earlier from the drug development pipeline.

The liver is the central organ for the metabolism and toxicity of pharmaceutical compounds. Several different *in vitro* liver preparations have been used to study drug disposition *in vitro*, which include: perfused whole organs; liver slices; isolated primary hepatocytes in suspension or cultured upon extracellular matrix; immortalized liver cell lines; isolated organelles, membranes or enzymes; and recombinant systems (i.e. human B lymphoblastoid cell line expressing cDNAs for drug metabolism enzymes) [165, 176, 278]. Though perfused whole organs and liver slices maintain many aspects of liver's *in vivo* microenvironment and architecture, they suffer from limited drug availability to inner cell layers, and are not suitable for enzyme induction studies due to limited viability (<24 hours). Furthermore, whole organs do not reduce the number of animals required and are difficult to use in high throughput applications. Purified liver fractions (i.e. microsomes) and single enzyme systems, on the other hand, are used in high-throughput systems to identify enzymes involved in the metabolism of a particular drug; however, they lack the complete spectrum of gene expression and cellular machinery required for liver-specific metabolism and toxicity. Lastly, immortalized cell lines derived either from hepatoblastomas (i.e. HepG2) or from immortalization of primary hepatocytes (i.e. HepLiu, SV40 immortalized) are typically plagued by abnormal levels and repertoire of liver-specific functions.

Though each of the aforementioned liver models has been utilized for focused questions about metabolism and toxicity, isolated primary hepatocytes in adherent culture are widely considered to be the most suitable for evaluating drug disposition [176, 182]. Hepatocytes strike a balance between simplicity of use and maintenance of intact cellular architecture with complete, undisrupted enzymes and cofactors. In spite of their

recognized advantages, hepatocyte culture models typically used in the pharmaceutical industry have several key limitations, which include: diffusion barriers and limited scalability of collagen sandwich models; batch-to-batch variability and unknown molecular composition of basement membrane gels (i.e. tumor-derived Matrigel) [201]; and most importantly, rapid (hours) loss of viability and liver-specific functions [165, 176, 202]. Furthermore, such models rely on inconsistent, randomly distributed confluent monolayers while neglecting the impact of microscale cellular architecture on hepatocyte functions. Accordingly, there is a pressing need for better *in vitro* models of liver tissue that can eliminate compounds with undesirable ADME/Tox properties earlier in drug development, where chemical choices and modifications are made before commitment of significant development resources [279].

It has been known for over two decades now that a variety of nonparenchymal cells (i.e. fibroblasts, sinusoidal endothelia, biliary epithelia) from within and outside the liver can stabilize phenotypic functions of primary hepatocytes *in vitro* [65, 208]. Such co-cultures have been used for fundamental investigations in hepatology [111, 114, 116], and towards building engineered liver tissues for bio-artificial liver devices as temporary supports prior to organ transplantation [9, 32]. However, hepatic co-cultures have not been explored to any considerable extent for utility in drug development. In our previous studies, we showed that 3T3 murine embryonic fibroblasts can induce high levels of albumin and urea secretion in primary rat hepatocytes [123]. Further, we used microfabrication tools borrowed from the semiconductor industry to modulate liver-specific functions in co-cultures by defining the degree of homotypic (hepatocyte-hepatocyte) and heterotypic (hepatocyte-fibroblast) cellular interactions.

In this study, our objectives were to a) characterize the long-term morphological and functional stability of micropatterned and randomly distributed rat hepatocyte-

fibroblast co-cultures, b) evaluate the utility of co-cultures for assays commonly employed in drug development, and c) use a previously developed soft-lithographic process to miniaturize micropatterned co-cultures in a multi-well format amenable for higher-throughput experimentation. Our results indicate that co-cultures remain functional for several weeks as assessed by morphological analysis, biochemical assays of liver-specific protein secretion and nitrogen metabolism, and activity of major Phase I and II drug metabolism enzymes. Furthermore, we found that micropatterning consistently improved the longevity of such co-cultures from several weeks to over 2 months. Lastly, we show utility of co-cultures in drug development by characterizing the altered metabolism and hepatotoxicity of model compounds due to drug-drug interactions, and by quantifying the dose- and time-dependent hepatotoxicity of multiple liver toxins. In the future, we anticipate that our long-term rat liver model may enable high-throughput screening of lead candidates for liver-specific metabolism, drug-drug interactions, and chronic toxicity earlier in drug discovery, which may ultimately reduce development costs and help create safer drugs for patients.

6.3. Materials and Methods

6.3.1. Nonparenchymal Cell Culture

3T3-J2 murine embryonic fibroblasts were acquired and cultured as described in chapter 2 of this dissertation. In some cases, fibroblasts were growth-arrested by incubation with 10 $\mu\text{g}/\text{mL}$ Mitomycin C (Sigma, St. Louis, MO) in culture media for 2 hours at 37°C. The nonparenchymal fraction of the rat liver was recovered via centrifugation following digestion of the liver with collagenase. Briefly, a suspension with different types of liver cells (i.e. hepatocytes, sinusoidal endothelial cells, and kupffer

macrophages) was spun at 50 $\times g$ for 5 minutes to pellet the larger hepatocytes. The supernatant was re-spun 3 more times and each time the pellet of the hepatocytes was set aside for pure hepatocyte cultures. Lastly, the supernatant was spun at 1000 rpm for 10 minutes to pellet the nonparenchymal cells, which were re-suspended in hepatocyte culture medium. Hepatocytes, as judged by their size (~ 20 - $30 \mu\text{m}$ in diameter) and morphology (polygonal), were less than 1% in nonparenchymal fraction plated on uncoated tissue culture polystyrene.

6.3.2. Hepatocyte-Nonparenchymal Co-Cultures

Primary rat hepatocytes were isolated and purified as detailed in chapter 2 of this dissertation. For studies comparing species-specific responses, we purchased primary human hepatocytes in suspension from commercial vendors and cultured them as described in chapter 5. Randomly distributed hepatocyte-fibroblast co-cultures were generated as described in chapter 2. Briefly, collagen-coated polystyrene plates (24-well format) were seeded with hepatocytes (100,000 cells per well) in hepatocyte culture medium (500 μL per well). For co-culture experiments, 3T3 fibroblasts (1:1 ratio with hepatocytes) were seeded in their respective medium 12-24 hours after initiation of adherent hepatocyte cultures. The culture medium was replaced to hepatocyte culture medium the day after fibroblast cell seeding and subsequently replaced daily.

In order to generate micropatterned co-cultures, we utilized the soft-lithographic process described in chapter 5. Briefly, elastomeric polydimethylsiloxane (PDMS) stencil devices [157], consisting of thin membranes ($\sim 300 \mu\text{m}$) with through-holes (500 μm with 1200 μm center-to-center spacing) at the bottom of each well of a 24-well mold were used to create collagenous domains on tissue culture polystyrene. Hepatocytes were seeded in serum-free hepatocyte culture medium on collagen-patterned substrates,

resulting in a hepatocyte micropattern due to selective cell adhesion. The cells were washed with media 2 hours later to remove unattached cells and incubated with serum-supplemented hepatocyte media overnight. Growth-arrested 3T3 fibroblasts were seeded onto hepatocytes to create co-cultures as described above; however, a 3:1 fibroblast to hepatocyte ratio was used due to lack of fibroblast proliferation. In some cases, liver-derived nonparenchymal cells (10:1 nonparenchymal to hepatocyte ratio) were used instead of fibroblasts to create co-cultures.

6.3.3. Hepatocellular Function Assays

Spent media was stored at -20° C. Urea concentration was assayed using a colorimetric endpoint assay utilizing diacetylmonoxime with acid and heat (Stanbio Labs, Boerne, TX). Albumin content was measured using enzyme linked immunosorbent assays (MP Biomedicals, Irvine, CA) with horseradish peroxidase detection and 3,3',5,5'-tetramethylbenzidine (TMB, Fitzgerald Industries, Concord, MA) as substrate [197]. For some experiments, cultures were treated with $3\ \mu\text{M}$ 3-Methylcholanthrene (Sigma) dissolved in hepatocyte culture medium for 3 consecutive days to induce cytochrome-P450 1A (CYP1A) enzyme levels. Control cultures were treated with solvent alone (Dimethylsulfoxide, DMSO) to measure baseline enzyme activity. CYP1A1 activity was assessed via dealkylation of ethoxy-resorufin (ER, Sigma) into fluorescent resorufin, while methoxy-resorufin (MR, Sigma) was used as a substrate for CYP1A2. Briefly, cultures were incubated with $5\ \mu\text{M}$ substrate dissolved in DMEM without phenol red for 30-60 min. Resorufin fluorescence (excitation/emission: 530/590 nm) in collected supernatants was quantified by means of a fluorescence micro-plate reader (Molecular Devices, Sunnyvale, CA). Protocols in chapter 5 were followed to evaluate the Phase I-mediated hydroxylation of coumarin, dealkylation of 7-methoxy-4-trifluoromethylcoumarin (MFC)

and 7-benzyloxy-4-trifluoromethylcoumarin (BFC), and phase II-mediated conjugation of 7-Hydroxycoumarin (7-HC) in rat co-cultures.

6.3.4. Staining of Functional Bile Canaliculi

Co-cultures were washed three times with phenol-red free DMEM, incubated with 6 $\mu\text{g}/\text{mL}$ CFDA (5-and-6-carboxyfluorescein diacetate, mixed isomers – purchased from Invitrogen, Carlsbad, CA) for 10 minutes, and washed three times again prior to examination with fluorescence microscopy (excitation/emission: 495/520 nm). Specimens were observed and recorded using a Nikon Diaphot microscope equipped with a SPOT digital camera (SPOT Diagnostic Equipment, Sterling Heights, MI), and MetaMorph Image Analysis System (Universal Imaging, Westchester, PA) for digital image acquisition.

6.3.5. Acute and Chronic Toxicity Studies

All chemicals were purchased from Sigma. In order to evaluate the acute toxicity of compounds, cultures were incubated with various concentrations of compounds dissolved in culture medium for 24 hours. For chronic studies, culture media with fresh Hepatotoxins was added every 2 days. Cell viability at different time points was subsequently measured via the MTT assay as described in Chapter 5.

6.3.6. Drug-Drug Interaction Studies

All chemicals were purchased from Sigma. Co-cultures were first treated with dexamethasone (1-10 μM) or ethanol (2% vol/vol) dissolved in culture medium for 2 days to induce CYP3A levels. Next, co-cultures were incubated for 24 hours with either fresh media or fresh media supplemented with one or combinations of the following

compounds: Acetaminophen (5 mM in culture medium), Caffeine (5 mM), and Troleandomycin (TAO, 100 μ M). TAO was specifically used to inhibit CYP3A enzymes in co-cultures. Following the 24 hour incubation period, viability was assessed using the MTT assay as described in Chapter 5.

6.4. Results

6.4.1. Long-term Morphological and Functional Stability of Co-cultures

In chapter 5, we showed results from previously published studies in which a photolithographic cell micropatterning process was developed and subsequently used to functionally optimize co-cultures of primary rat hepatocytes and 3T3-J2 murine embryonic fibroblasts (see Figures 5.1 and 5.2). Briefly, rat hepatocytes were arranged in collagen-coated circular islands of prescribed dimensions and surrounded by 3T3-J2 fibroblasts to create micropatterned co-cultures. We found that co-cultures with a larger initial heterotypic interface (i.e. single hepatocyte islands surrounded by fibroblasts) had highest levels of liver-specific functions as compared to other configurations. Furthermore, hepatocytes in smaller patterns (<250 μ m) intermingled significantly to dissipate the pattern, whereas larger islands (> 450 μ m) assumed a relatively stable conformation for several weeks.

In this study, we wanted to characterize liver-specific functions in micropatterned and randomly distributed rat co-cultures over a period of several weeks. We chose to use the pattern geometry with \sim 500 μ m hepatocyte islands (\sim 1200 μ m center-to-center spacing) since it provided high functional capacity along with retention of pattern fidelity for the duration of the co-cultures. In order to create miniaturized micropatterned co-cultures in a multi-well format, we used the soft-lithographic process shown in chapter 5

(see Figure 5.6). The stability of the miniaturized rat liver tissues was assessed using both qualitative and quantitative criteria. We found that hepatocyte morphology in micropatterned co-cultures was stable for over 2 months (Figure 6.1A). That is, hepatocytes displayed a polygonal shape with distinct nuclei and nucleoli, and visible bile canaliculi as typically seen in freshly isolated cells and *in vivo*. On the other hand, hepatocytes in pure monolayers spread out to adopt a ‘fibroblastic’ appearance (Figure 6.1B). Furthermore, pattern fidelity was retained for the duration of the micropatterned co-cultures as assessed by phase contrast microscopy (Figure 6.1C).

Next, we characterized liver-specific functions in micropatterned pure hepatocyte cultures and co-cultures and compared them to their randomly distributed counterparts (random cultures and co-cultures). Consistent with our previous studies, we found that both albumin secretion (Figure 6.2A) and urea synthesis (Figure 6.2B) were upregulated in all co-cultures as compared to pure hepatocyte monolayers, which displayed a rapid decline in such functions. We further observed that after ~2 weeks, albumin secretion in random co-cultures showed a sharp decline to near undetectable levels, while urea synthesis remained at a low baseline. Micropatterned co-cultures, on the other hand, displayed relatively high levels of liver-specific functions for over 2 months. Albumin secretion in micropatterned co-cultures was induced by ~20 fold on average (relative to to day 1 pure hepatocyte function) for the first 4 weeks of culture and then stabilized down to ~10 fold for the next 6 weeks. Urea synthesis, however, was slightly upregulated to ~1.2 fold for the first 4 weeks in micropatterned co-cultures and then down-regulated slightly to ~0.7 fold for the next 6 weeks.

6.4.2. Activity of Phase I and Phase II Enzymes

In order to demonstrate activity of cytochrome-P450 (CYP450) phase-I enzymes in co-cultures of primary rat hepatocytes and 3T3-J2 murine embryonic fibroblasts, we utilized resorufin-derivatives, ethoxy-resorufin (ER) and methoxy-resorufin (MR). ER and MR dealkylation into fluorescent resorufin is mediated by CYP1A1 and CYP1A2 enzymes, respectively. We observed low levels of baseline (untreated) ER and MR metabolism in co-cultures. Therefore, in order to improve the signal-to-noise ratio, we ‘induced’ levels of CYP1A by pre-incubating co-cultures with 3 μ M 3-Methylcholanthrene (3-MC) for 3 days prior to assessment of substrate metabolism. 3-MC is a known inducer of CYP1A1 and CYP1A2 expression in hepatocytes via the ligand-activated nuclear receptor AHR (aryl hydrocarbon receptor) [303]. In Figure 6.3A, we show ER-dealkylation (post 3-MC induction for each data point) in co-cultures over a period of 10 weeks, while Figure 6.3B shows MR-dealkylation. We observed that, as with albumin secretion and urea synthesis, randomly distributed co-cultures displayed a dramatic decline in CYP1A1 and CYP1A2 enzyme activities to undetectable levels after \sim 2 weeks in culture. On the other hand, micropatterned co-cultures displayed CYP1A1 and CYP1A2 activities for 75 days. However, both CYP1A1 and CYP1A2 activities in micropatterned co-cultures declined over time, reaching to \sim 13% and \sim 20% on day 75 (relative to day 8 values), respectively.

ER and MR are fluorimetric substrates specific for CYP1A enzymes. 7-methoxy-4-trifluoromethylcoumarin (MFC) and 7-benzyloxy-4-trifluoromethylcoumarin (BFC), on the other hand, are dealkylated by a variety of different CYP450s (i.e. non-specific substrates) into the fluorescent product, 7-hydroxy-4-trifluoromethylcoumarin (7-HFC). Use of non-specific substrates provides for an ‘average’ value of CYP450 activity, and is useful to determine whether CYP450 enzymes are functional in a particular system. In Figure 6.4A, we show that co-cultures were able to successfully dealkylate BFC and MFC

into 7-HFC. The rate of BFC metabolism (picomoles per minute per 10^6 cells) was observed to be ~ 12 fold higher than the rate of MFC metabolism.

CYP450 enzymes are oxido-reductases that are part of the Phase I metabolic pathway in hepatocytes. The phase II family of enzymes, on the other hand, is typically involved in the conjugation of highly polar moieties (i.e. sulfate group, glucuronic acid) to xenobiotics to make them water-soluble for excretion out of the body via bile or through the kidneys. A useful substrate for evaluating conjugation reactions is the fluorescent substrate, 7-Hydroxycoumarin (7-HC), which gets modified to non-fluorescent compounds, 7-HC-Glucuronide and 7-HC-Sulfate. The level of conjugation can then be quantified by using bacterial-derived β -glucuronidase and aryl-sulfatase enzymes to ‘de-conjugate’ the Phase II products and recover 7-HC fluorescence. In our micropatterned rat co-cultures, we observed time-dependent conjugation of 7-HC by Phase-II enzymes (Figure 6.4B).

6.4.3. Functional Bile Canaliculi

Besides albumin secretion, urea synthesis and Phase I and II activities, another marker of liver-specific function is the formation of functional bile canaliculi between hepatocytes. In Figure 6.1, bile canaliculi are visible as distinct bright boundaries between hepatocytes. In order to demonstrate that these bile canaliculi are indeed functional, we utilized carboxyfluorescein diacetate (CFDA), which is known to be taken up by hepatocytes, cleaved by intracellular esterases into a fluorescent dye (fluorescein), and subsequently excreted across the apical membrane of the hepatocyte into bile canaliculi. We found that hepatocytes developed functional bile canaliculi (Figure 6.5) upon co-cultivation with 3T3-J2 fibroblasts, which did not take up CFDA to any considerable degree.

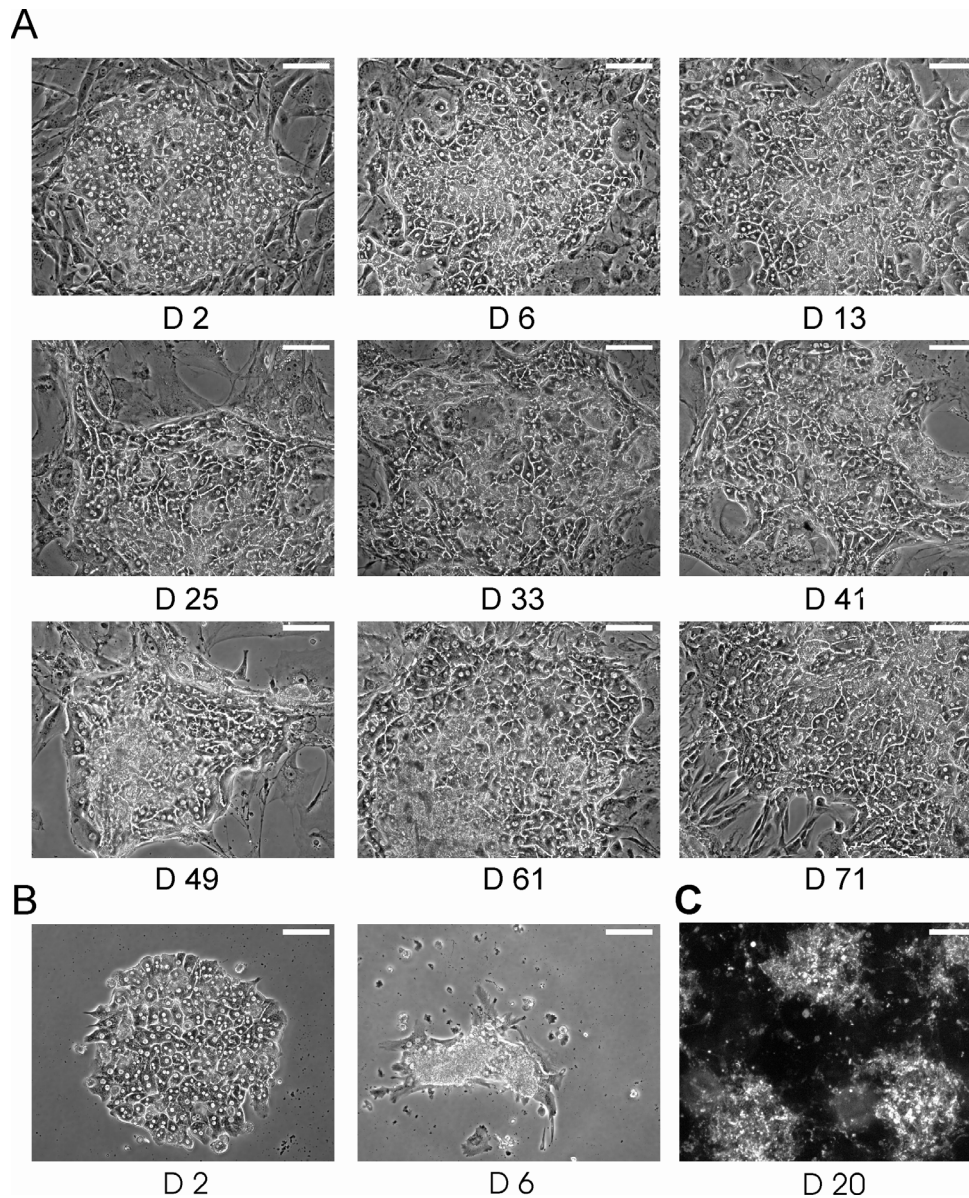


Figure 6.1: Maintenance of hepatocyte morphology in long-term micropatterned co-cultures. Elastomeric stencils (see Chapter 5 for details) were used to generate micropatterned co-cultures of primary rat hepatocytes and 3T3-J2 murine embryonic fibroblasts (500 μm islands, 1200 μm center-to-center spacing) in a multi-well format. **A)** Hepatocyte morphology remained relatively stable over time in co-cultures (phase contrast micrographs shown here up to Day 71). Hepatocytes maintained their polygonal shape, distinct nuclei and nucleoli, and visible bile canaliculi. **B)** Hepatocytes in pure cultures declined in viability and those surviving spread-out to adopt a ‘fibroblastic’ morphology (Days 2 & 6 shown to show the drastic differences). **C)** Pattern fidelity was well-maintained for the duration of the co-cultures (Day 20 ‘out-of-phase’ micrograph shown). Scale bars represent 100 μm .

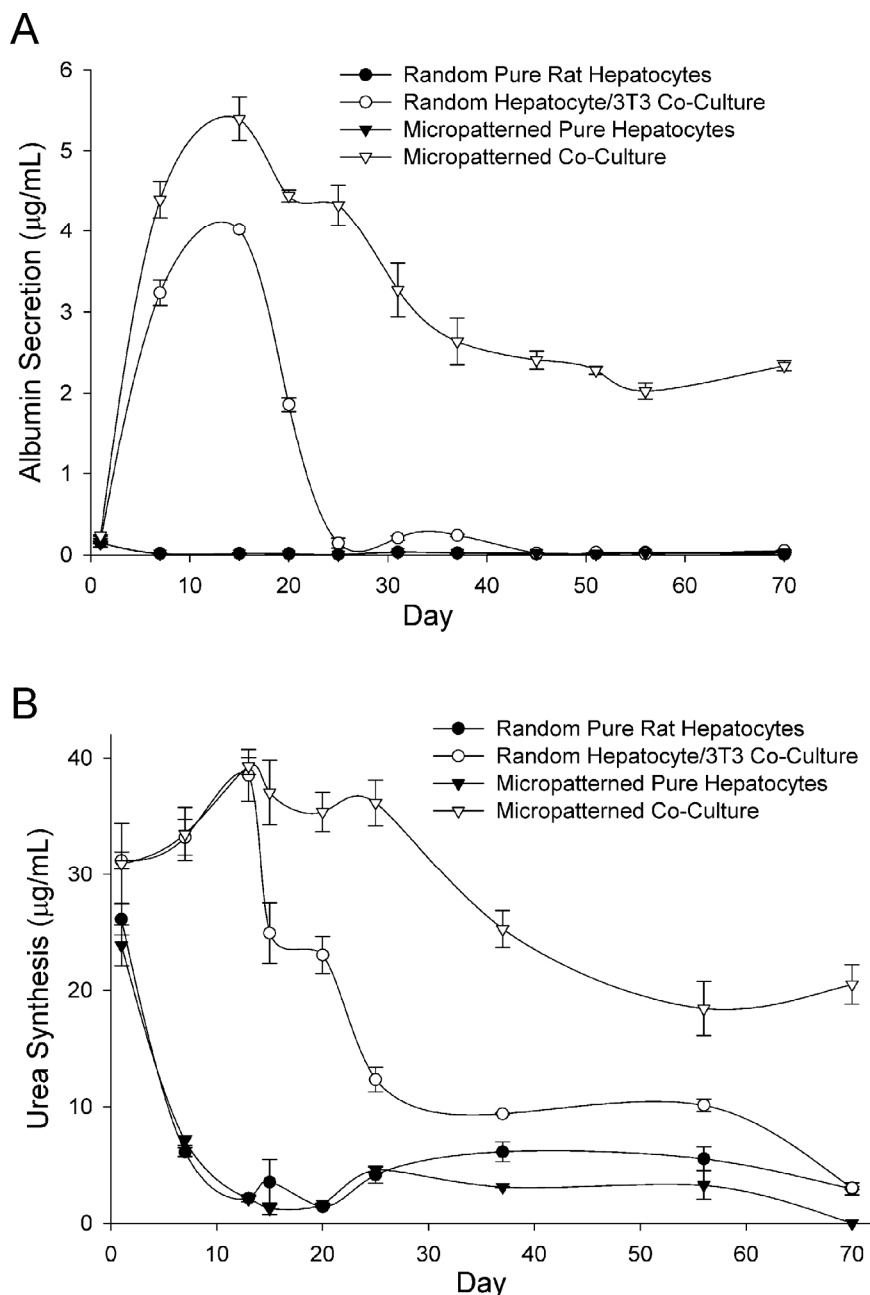


Figure 6.2: Long-term induction of hepatocellular functions in micropatterned co-cultures. Elastomeric stencils (see Chapter 5 for details) were used to generate micropatterned co-cultures of primary rat hepatocytes and 3T3-J2 murine embryonic fibroblasts (500 μm islands, 1200 μm center-to-center spacing) in a multi-well format. Randomly distributed cultures were created in wells with a uniform coating of type-I collagen. **A)** Time-course of albumin secretion in pure hepatocyte cultures and hepatocyte-fibroblast co-cultures (random and micropatterned). **B)** Time-course as in ‘A’ except urea synthesis is shown. Error bars represent standard error of the mean ($n=3$).

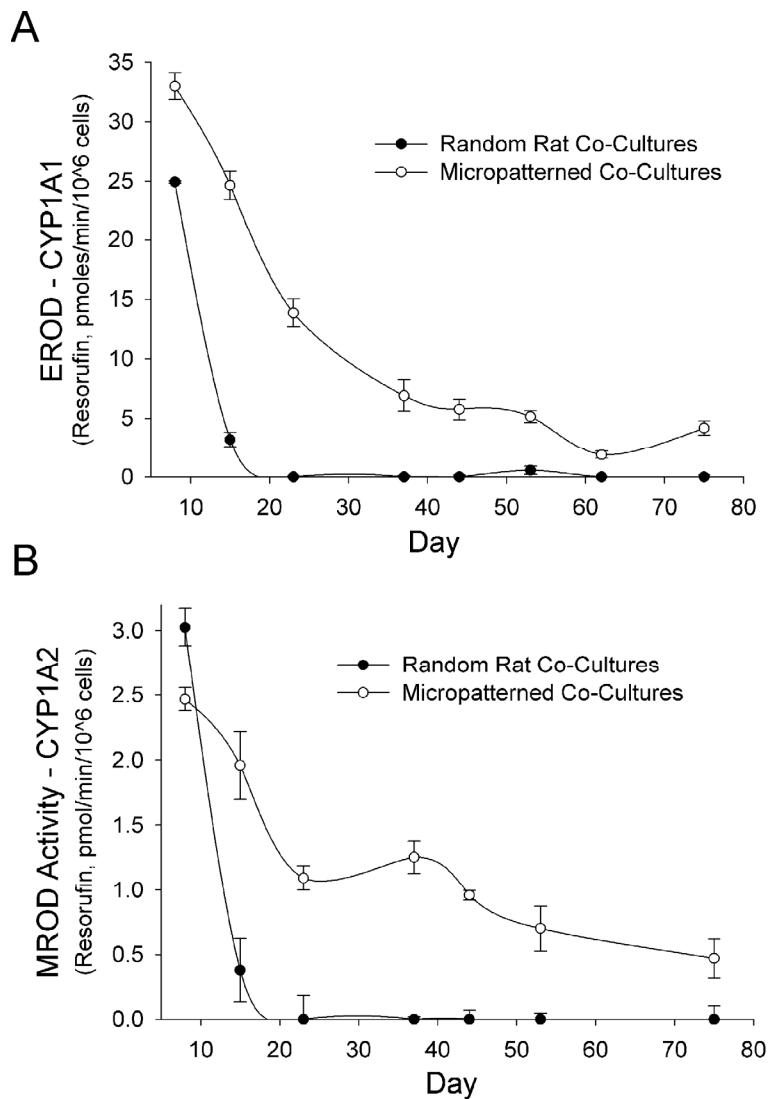


Figure 6.3: Long-term activity of CYP450 enzymes in micropatterned co-cultures. **A)** CYP1A1 activity over 75 days in micropatterned co-cultures is compared to activity in randomly distributed co-cultures. Dealkylation of ethoxy-resorufin (EROD Activity) into fluorescent resorufin was used to assess CYP1A1 activity. Co-cultures were treated with 3 μ M 3-Methylcholanthrene for 72 hours prior to assessment of CYP450 activity in order to induce enzyme levels to detectable levels. **B)** Time-course data as in 'A', except methoxy-resorufin (MR) was used as a substrate for CYP1A2. Error bars represent standard error of the mean (n=3).

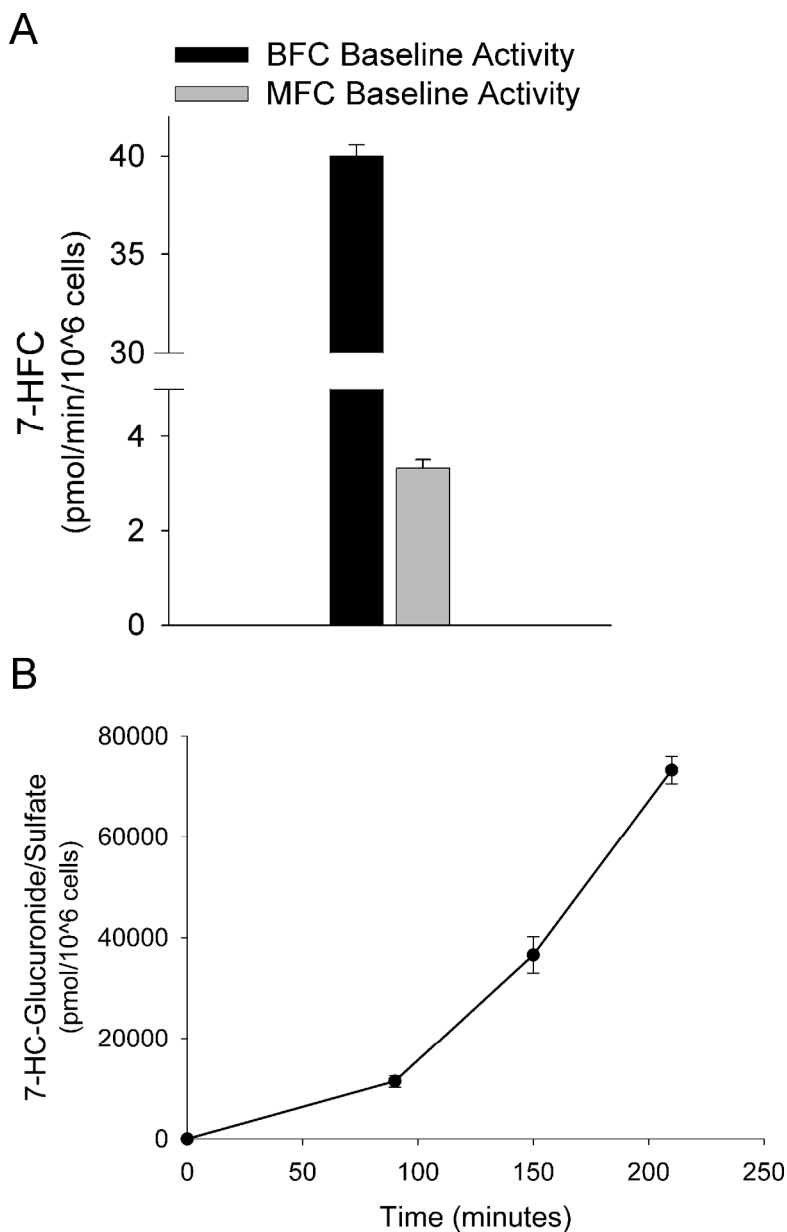


Figure 6.4: Metabolism of prototypic substrates via Phase I and Phase II pathways. **A)** Shown here is the rate at which CYP450 enzymes in micropatterned co-cultures dealkylate substrates, MFC and BFC, into fluorescent 7-HFC. MFC, 7-methoxy-4-trifluoromethylcoumarin; BFC, 7-benzyloxy-4-trifluoromethylcoumarin; 7-HFC, 7-hydroxy-4-trifluoromethylcoumarin. Data from a single representative day (14) is shown. **B)** Phase II-mediated conjugation of glucuronic acid and sulfate groups to 7-Hydroxycoumarin (7-HC) in micropatterned co-cultures. Error bars represent standard error of the mean (n=3). See ‘Methods’ for details of the assays.

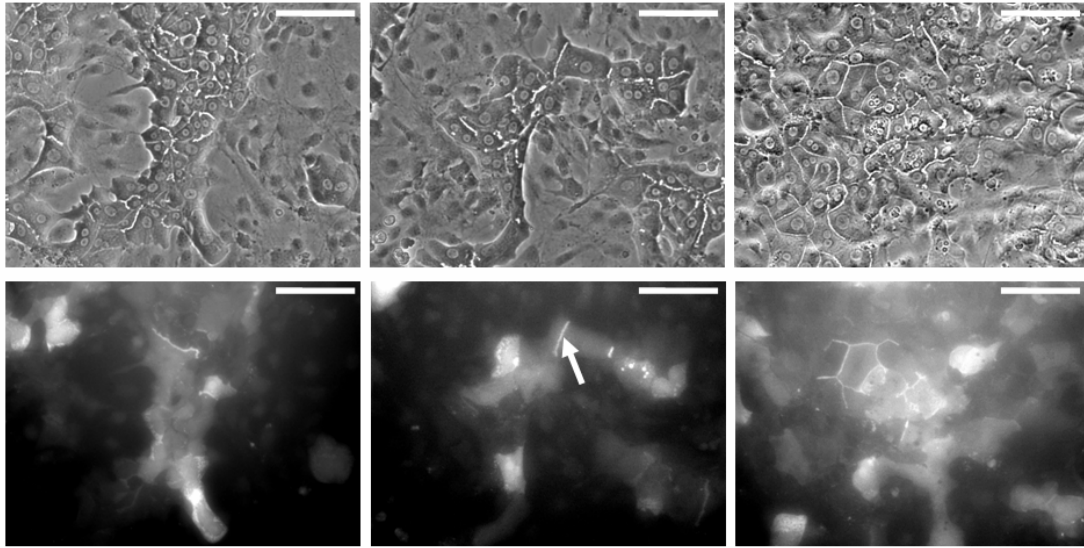


Figure 6.5: Staining of functional bile canaliculi in co-cultures. Randomly distributed co-cultures were incubated with carboxyfluorescein diacetate (CFDA), which gets internalized by hepatocytes, cleaved by esterases into a fluorescent dye and excreted into the bile canaliculi (see arrow in middle panel). Phase contrast micrographs of co-cultures are shown on the top while the corresponding fluorescent pictures are shown on the bottom. Scale bars represent 100 μm .

6.4.4. Drug-Drug Interactions

Modulation of CYP450 enzyme levels by pharmaceutical compounds is an important parameter in the occurrence of clinical drug-drug interactions [301]. Cultures of primary hepatocytes from different species (i.e. human, rodent) are widely utilized to evaluate CYP450 induction and inhibition by drugs. In order to demonstrate that CYP450 enzymes can be induced in co-cultures of rat hepatocytes and 3T3-J2 fibroblasts, we utilized the prototypic CYP1A inducer, 3-Methylcholanthrene (3-MC). Co-cultures were incubated with 3-MC for 72 hours before assessment of CYP1A1 and CYP1A2 activities via dealkylation of ethoxy-resorufin and methoxy-resorufin, respectively (Figure 6.6A). CYP1A1 was induced by ~5 fold over solvent-only controls, while CYP1A2 was induced by ~2 fold. Next, to show competitive inhibition of CYP450 activity, we utilized BFC as the substrate and ketoconazole as the inhibitor of CYP3A. Robust inhibition of BFC (~33%) dealkylation was seen when co-cultures were incubated with BFC in the presence ketoconazole (Figure 6.6B).

Drug-drug interactions due to the induction or inhibition of CYP450 enzymes can lead to serious toxicological consequences. In order to demonstrate such effects, we utilized a well-established *in vivo* model by which the toxicity of Acetaminophen (APAP, analgesic found in many over-the-counter medications including Tylenol) is enhanced upon induction of CYP3A [304]. We first pre-treated co-cultures with increasing doses of dexamethasone (DEX) for 2 days to induce CYP3A levels. Then, co-cultures were incubated with a 5 mM dose of APAP for 24 hours, followed by assessment of viability via the MTT assay (see Methods). Our data showed a substantial increase in APAP-mediated toxicity in DEX-treated co-cultures over untreated controls (Figure 6.7A). Specifically, inducing CYP3A levels with 1 μ M DEX caused ~25% decrease in viability, while 10 μ M DEX caused ~50%. To confirm that APAP-mediated cell death in DEX-

treated co-cultures was due to induced levels of CYP3A, we incubated DEX-treated co-cultures with APAP in the presence of a competitive CYP3A inhibitor, Troleandomycin (TAO). Co-cultures in which CYP3A was 'blocked' via TAO showed minimal toxicity as compared to controls. One of the advantages of a 2-dimensional monolayer co-culture system over 3-D spheroids is improved in situ observation of cell behavior via conventional microscopy techniques. In Figure 6.7B we show the interaction between APAP and DEX using morphological analysis. Severe changes in hepatocyte morphology were observed only in co-cultures that were treated with DEX prior to administration of APAP.

Ethanol (EtOH) has also been shown to induce CYP3A levels in rodents and humans [305, 306]. Furthermore, caffeine has previously been shown to activate CYP3A activity in vitro and to increase APAP hepatotoxicity in rodents pretreated with prototypic inducers of CYP3A (i.e. DEX and EtOH). In our rat model, we observed that pre-treating co-cultures with 2% EtOH for 2 days did *not* make them more susceptible to the toxic effects of APAP (Figure 6.8A). Furthermore, caffeine enhanced APAP-mediated hepato-toxicity in co-cultures only when CYP3A levels were pre-induced using EtOH or DEX (Figure 6.8A, B). Incubating ethanol-treated co-cultures with TAO protected them from caffeine-mediated enhancement of APAP toxicity; however, TAO protected DEX-treated co-cultures from such enhancement only to a limited degree (i.e. toxicity was still seen in co-cultures)

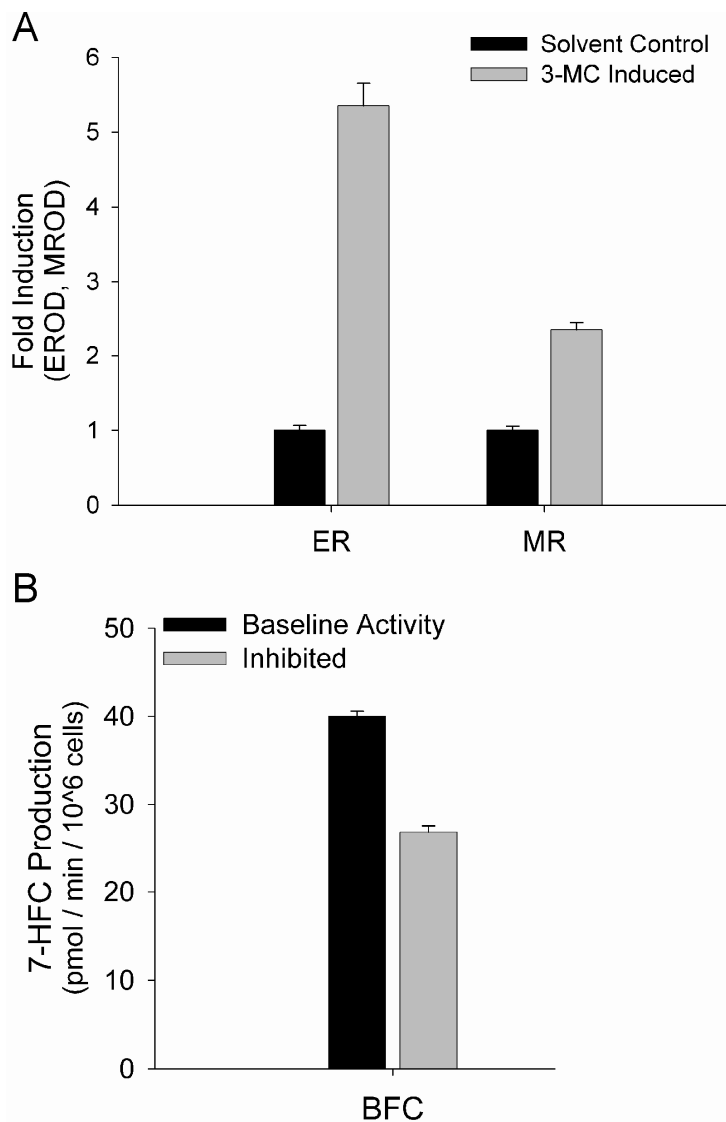


Figure 6.6: Modulation of CYP450 activity. **A)** Induction of CYP1A enzymes in co-cultures. Co-cultures were incubated with 3-Methylcholanthrene (3-MC) for 3 consecutive days to induce CYP1A enzyme levels. CYP1A1 and CYP1A2 activities were assessed by the dealkylation of ethoxy-resorufin (ER) and methoxy-resorufin (MR) into fluorescent resorufin, respectively. To calculate fold induction, levels of resorufin in 3-MC treated co-cultures were normalized to levels in solvent-only (dimethylsulfoxide) treated controls. **B)** Inhibition of CYP450-mediated substrate metabolism. Co-cultures were either incubated with CYP450 substrate, 7-benzyloxy-4-trifluoromethylcoumarin (BFC), or BFC in the presence of a CYP3A inhibitor, Ketoconazole. Dealkylation of BFC into fluorescent 7-hydroxy-4-trifluoromethylcoumarin (7-HFC) was quantified via a fluorimeter (see Methods for details). Error bars are standard error of the mean (n=3).

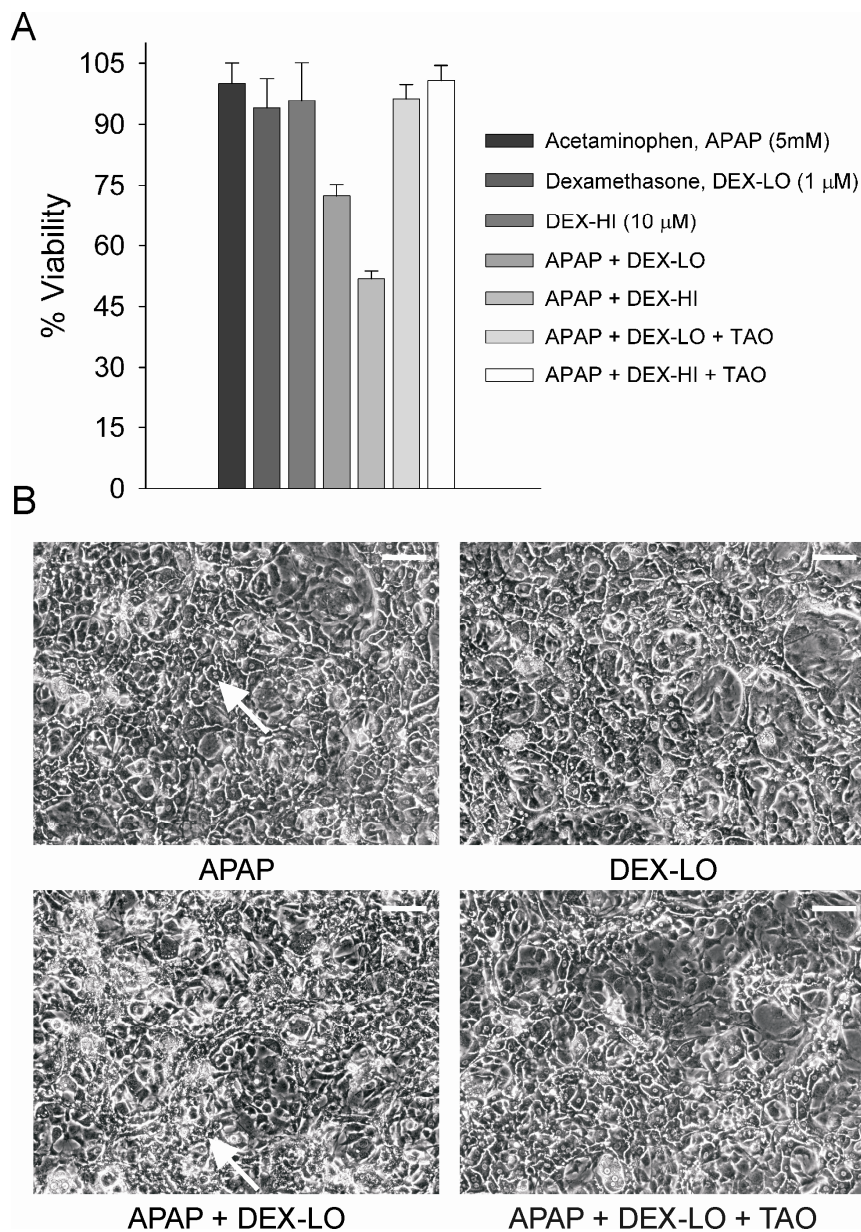


Figure 6.7: Dexamethasone-mediated enhancement of acetaminophen toxicity.

A) APAP was toxic only when co-cultures were pre-treated with DEX for 2 days. Dosing co-cultures with higher DEX concentrations further enhanced APAP-mediated toxicity. Inclusion of a CYP3A inhibitor, Troleandomycin (TAO, 100 μ M), reversed the toxic effects. **B)** Hepatocyte morphology remained relatively unchanged (see arrows in pictures) upon treatment with APAP or DEX. However, in co-cultures treated with DEX *and* APAP, severe changes in hepatocyte morphology were seen. These changes were reversed with TAO. Error bars are SEM (n=3). Scale bars represent 100 μ m.

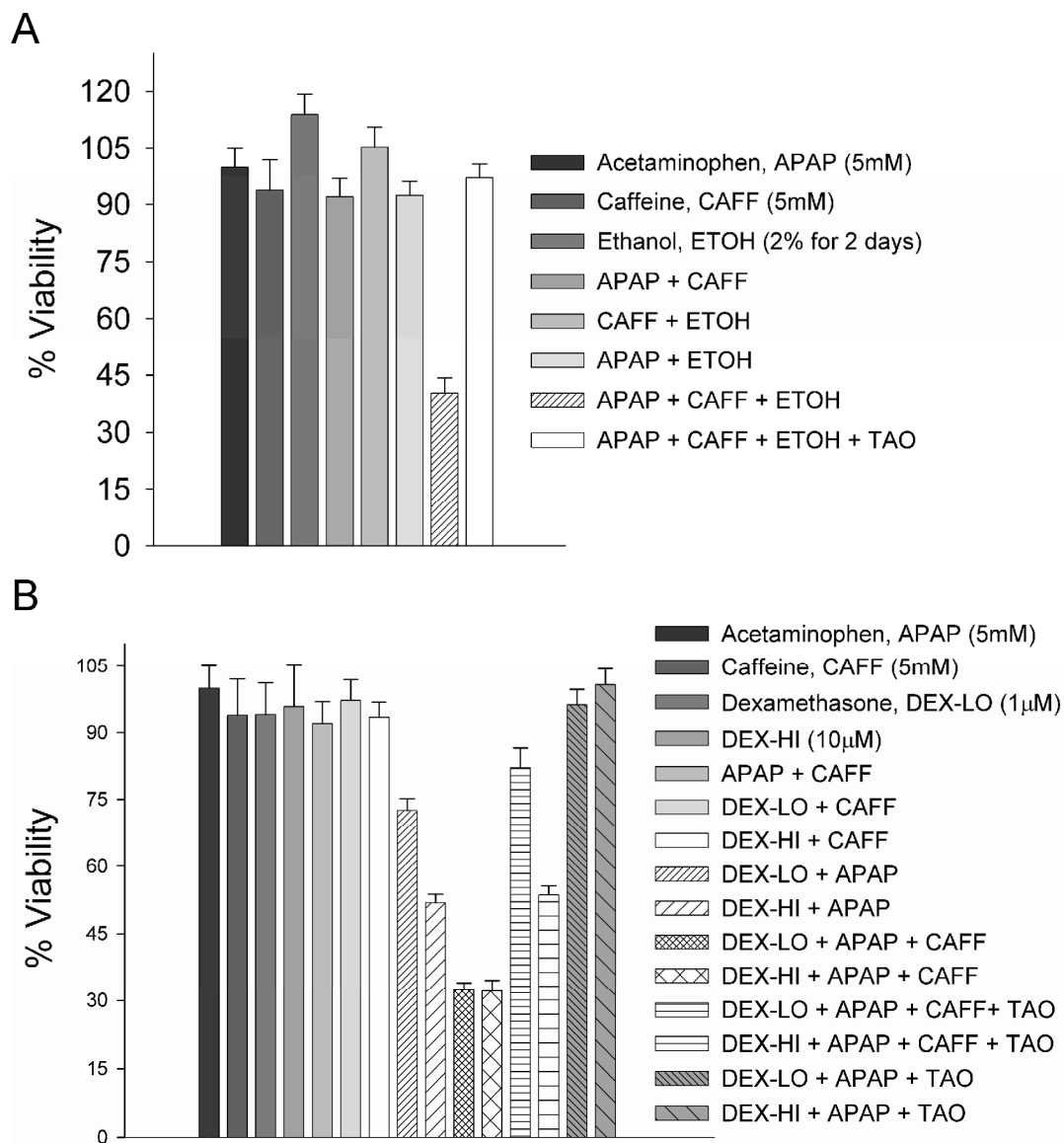


Figure 6.8: Caffeine-mediated enhancement of APAP toxicity in co-cultures treated with CYP3A inducers. Co-cultures were treated for 2 days with CYP3A inducers (EtOH, DEX) prior to administration of APAP. Following 24 hours of incubation with APAP, viability was assessed in co-cultures via the MTT assay (see Methods). **A)** Co-cultures pre-treated with EtOH were more susceptible to the toxic effects of APAP only in the presence of Caffeine. Inclusion of a CYP3A inhibitor, Troleandomycin (TAO, 100 μ M), in the incubation mixture reversed the observed toxicity. **B)** Caffeine enhanced APAP-mediated toxicity in co-cultures pre-treated with different doses of DEX. TAO protected co-cultures only to a limited degree from such enhancement. Error bars are standard error of the mean ($n=3$).

6.4.5. Chronic Toxicity of Model Hepatotoxins

Toxicity of pharmaceuticals due to chronic exposure is clinically relevant. Since hepatocyte culture models utilized in the pharmaceutical industry lose viability and phenotypic functions within a few days, toxicity due to repeated drug exposures over days or weeks cannot be evaluated. Since co-cultures remain functional for several weeks, we investigated dose- and time-dependent toxicity of four known Hepatotoxins, including: Acetaminophen, Methapyrilene, Pyrilamine and Troglitazone. Co-cultures were incubated with varying doses of toxins dissolved in culture medium over several days. Mitochondrial activity (MTT assay, see methods) was evaluated at different time points to assess viability in co-cultures.

Minimal toxicity (i.e. 90-100% viability relative to untreated controls) was seen in co-cultures that had been treated for 24 hours with Acetaminophen (APAP) doses ranging between 3 and 30 mM. However, following 6 days of repeated exposure, the viability in co-cultures ranged from 77% for 3 mM APAP to 19% for 30 mM (Figure 6.9A). The dose-dependent toxicity profile of APAP exhibited a 'shoulder', whereby significant loss of viability was seen once a dose threshold was reached (30 mM). Furthermore, consistent with MTT data, hepatocyte morphology was severely affected in co-cultures that had been treated for 6 days with APAP doses ranging between 12 and 30 mM (Figure 6.9B). However, no significant morphological changes were observed in co-cultures treated for 6 days with 3 or 6 mM APAP, even though mitochondrial activity was affected by ~20% as seen in Figure 6.9A.

In the case of Methapyrilene, we observed the shifting of TC50 values (dose of drug causing 50% loss in viability) to lower doses upon repeated exposures over 6 days (Figure 6.10A). Specifically, the TC50 value dropped from ~1.8 mM after 1 day of incubation with methapyrilene to ~1 mM after 6 days. As with APAP, we observed a

toxicity ‘shoulder’ when co-cultures were incubated with methapyrilene. However, methapyrilene was toxic to hepatocytes at doses that were an order-of-magnitude lower than APAP (i.e. 1.8 versus 30 mM). Lastly, morphological analysis of Methapyrilene-treated co-cultures correlated well with the MTT data (Figure 6.10B).

Next, we evaluated the chronic toxicity of pyrillamine in rat co-cultures. As with APAP and methapyrilene, we observed dose- and time-dependent toxicity in pyrillamine-treated co-cultures. Specifically, the TC50 value dropped from greater than 1 mM after 1 day of treatment to ~ 0.2 mM following 7 days of exposure (Figure 6.11A). Furthermore, observation of co-cultures over several days revealed minimal changes in fibroblast morphology at a 100 μ M dose of pyrillamine; however, hepatocyte morphology at that same dose was severely affected even after only 3 days of exposure (Figure 6.11B).

Lastly, we evaluated the effect of troglitazone (oral hypoglycemic withdrawn from the market due to liver toxicity) on co-cultures following repeated exposures. We observed drastic morphological changes in co-cultures that had been treated for 5 days with troglitazone doses ranging between 57 and 113 μ M (Figure 6.12A). However, no concomitant decline in viability was detected for such co-cultures (Figure 6.12B).

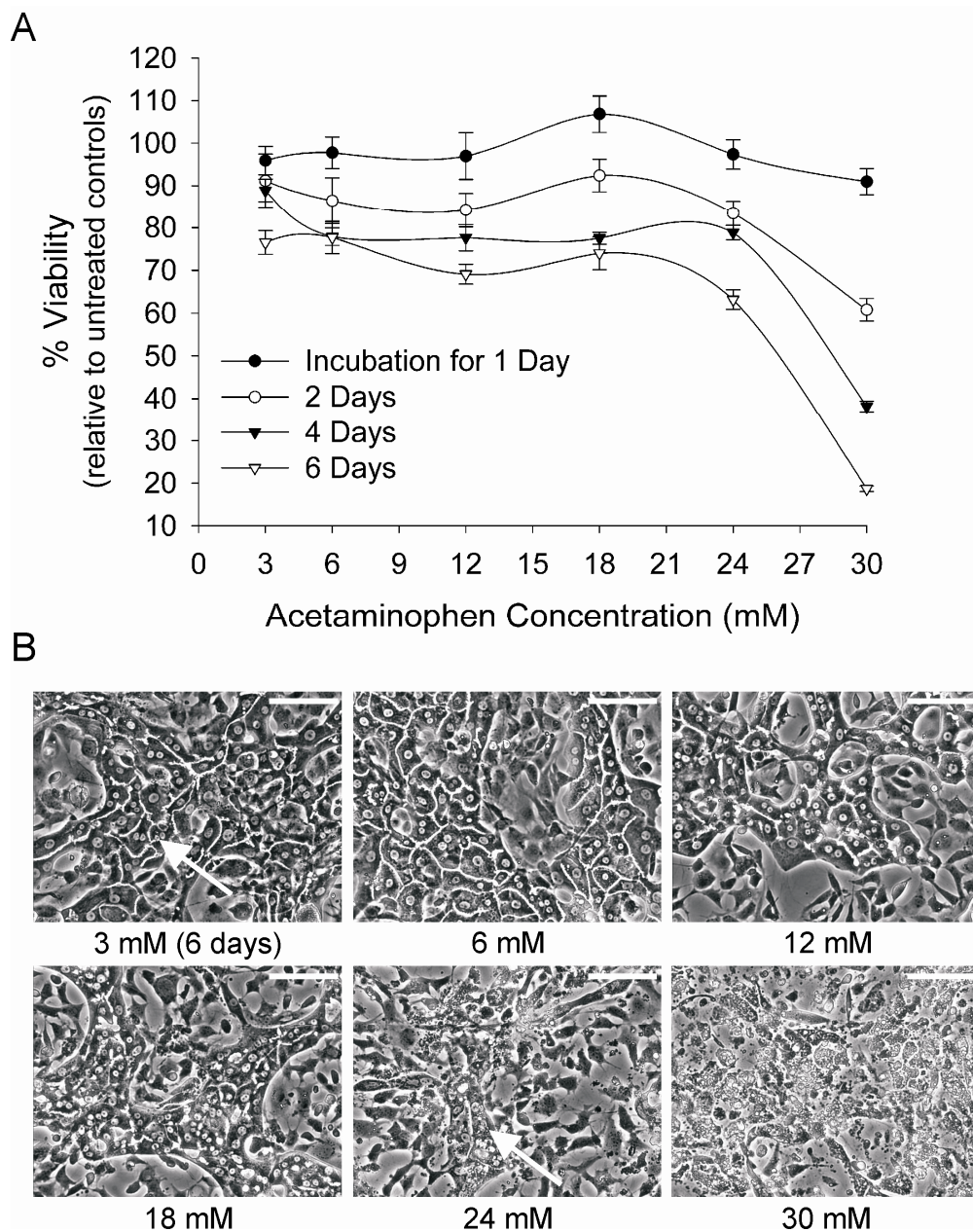


Figure 6.9: Dose- and time-dependent toxicity of acetaminophen. A) Viability in co-cultures following repeated exposures with increasing doses of acetaminophen (APAP). Co-cultures were treated with fresh toxin every 2 days. Viability was assessed via the MTT assay (see Methods). **B)** Phase contrast micrographs of co-cultures treated with varying doses of APAP for 6 days. Progressive changes in hepatocyte morphology (see arrows in select pictures) occurred with increasing APAP doses. Error bars are standard error of the mean (n=3). Scale bars represent 100 μ m.

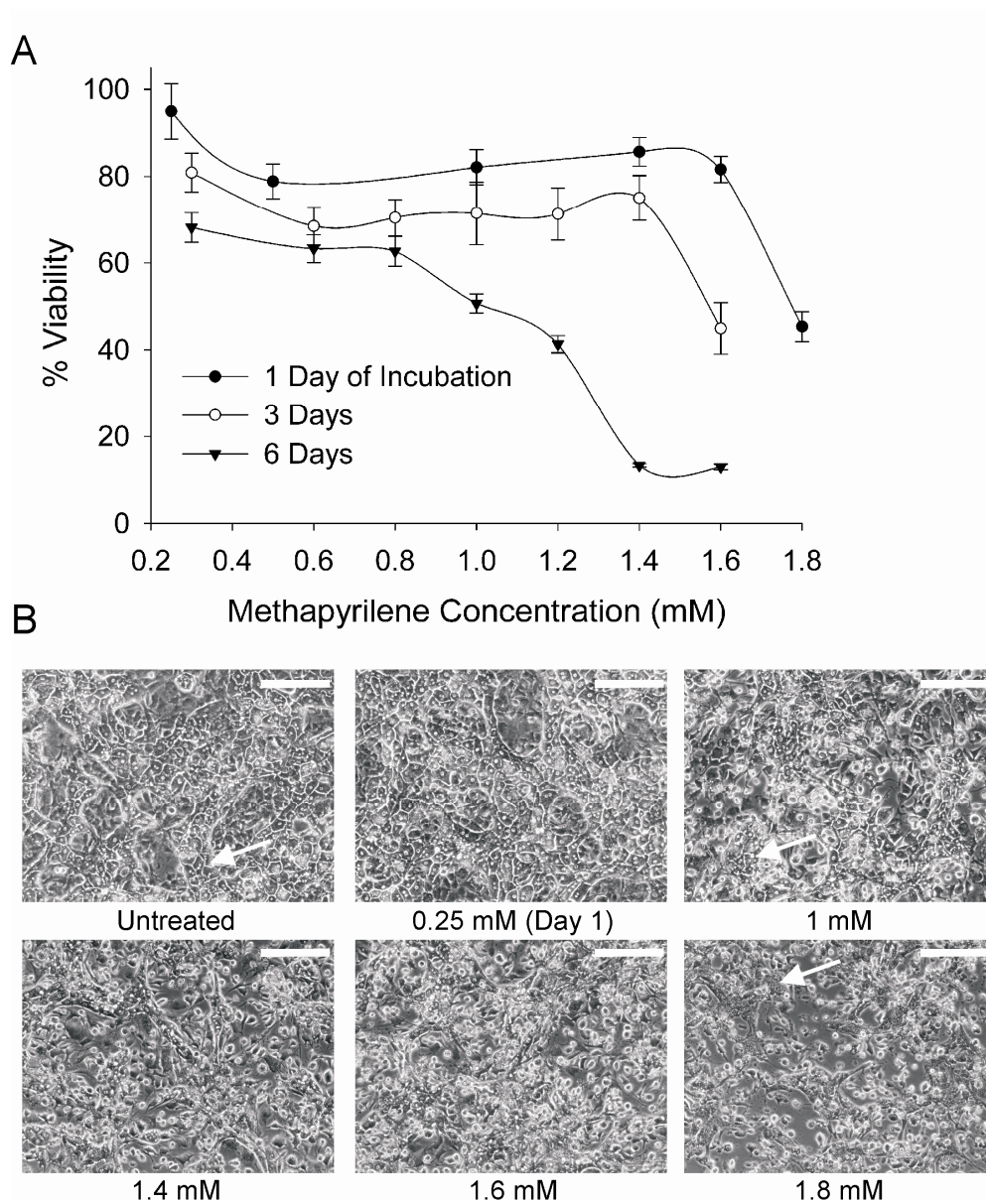


Figure 6.10: Dose- and time-dependent toxicity of methapyrilene. **A)** Viability in co-cultures following repeated exposures with increasing doses of methapyrilene. Co-cultures were treated with fresh toxin every 2 days. Viability was assessed via the MITT assay (see Methods). **B)** Phase contrast micrographs of co-cultures treated with varying doses of methapyrilene for 1 day. Progressive changes in hepatocyte morphology occurred with increasing toxin concentration (see arrows in select pictures). Error bars represent standard error of the mean ($n=3$). Scale bars represent $200\ \mu\text{m}$.

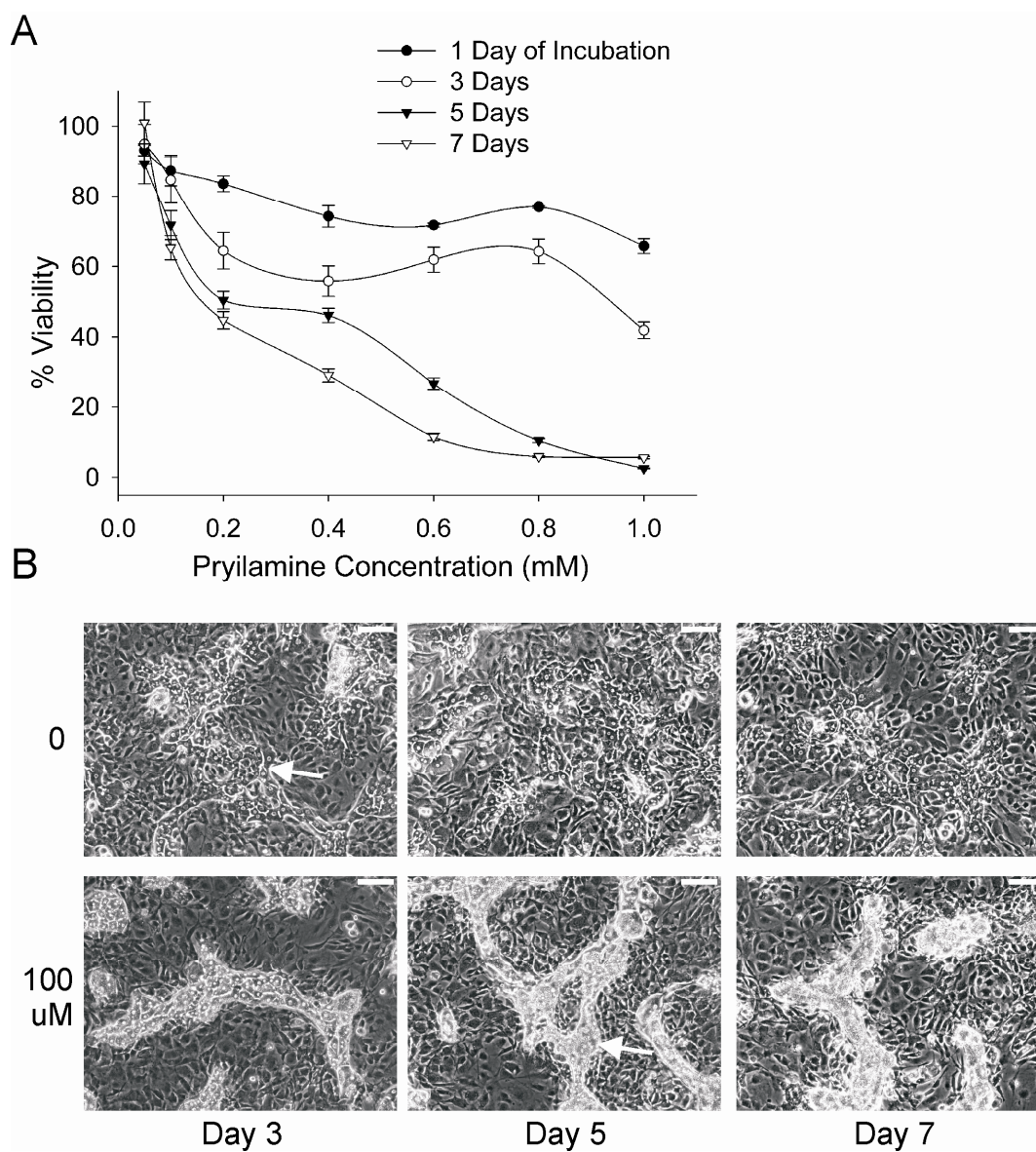


Figure 6.11: Dose- and time-dependent toxicity of pyrilamine. **A)** Viability in co-cultures following repeated exposures with increasing doses of pyrilamine. See text for additional details. **B)** Phase contrast micrographs of untreated co-cultures (first row) and those treated with a 100 μ M dose of pyrilamine for several days. Severe changes in hepatocyte morphology were seen in pyrilamine-treated co-cultures (see arrows in select pictures). Error bars are standard error of the mean ($n=3$). Scale bars are 100 μ m.

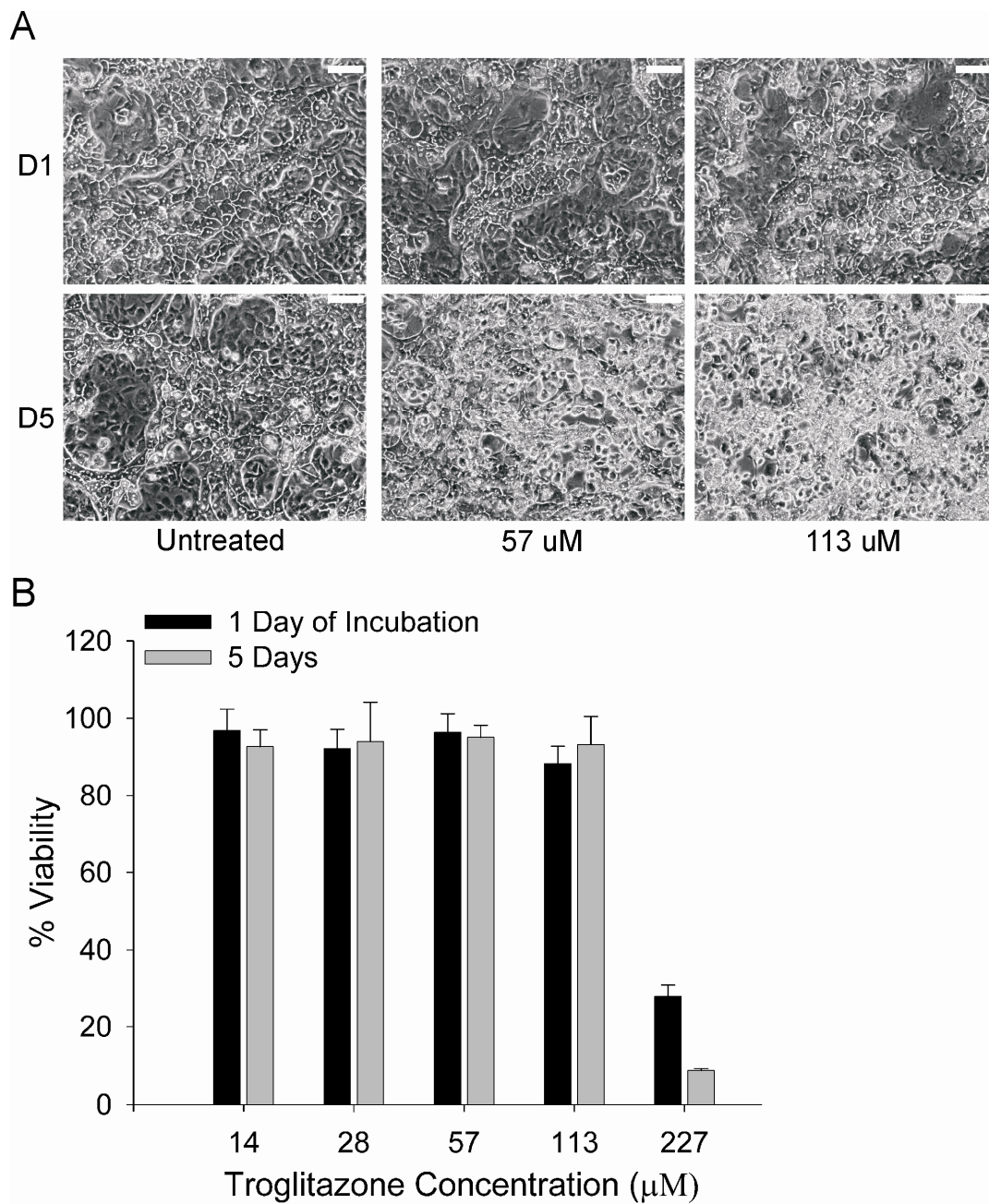


Figure 6.12: Changes in cellular morphology in co-cultures following repeated exposures with troglitazone. **A)** Phase contrast micrographs demonstrating cellular morphology in co-cultures treated with varying doses of troglitazone for 1 or 5 days. **B)** Bar graphs showing viability in troglitazone-treated co-cultures. For troglitazone doses less than or equal to 113 μM , viability was not affected even after 5 days of repeated exposure. Error bars are standard error of the mean ($n=3$). Scale bars are 100 μm .

6.4.6. Comparison of Drug Toxicity in Pure Hepatocyte Monolayers and Hepatocyte-Fibroblast Co-Cultures

Pure hepatocyte monolayers rapidly lose phenotypic functions and thus represent an ‘unstable’ model of the liver. On the other hand, as we have shown in Figures 6.1-6.5, 3T3-J2 fibroblasts can stabilize hepatic functions (i.e. albumin secretion, urea synthesis, Phase I and II enzyme activity) in co-culture for several weeks. Our objective here was to compare toxicity of model Hepatotoxins in pure hepatocyte monolayers and co-cultures. Pure hepatocyte monolayers (Day 2 of culture) or hepatocyte-fibroblast co-cultures (Day 13) prepared from the same rat liver were treated with Hepatotoxins for 24 hours, after which viability was assessed via the MTT assay.

In Figure 6.13, we show significant differences in toxic profiles of methapyrilene and pyriline across the two culture models. Specifically, we found that both compounds were more toxic to pure monolayers as compared to co-cultures. For instance, at a 1 mM compound dose, viability in pure monolayers had dropped to less than 6% (relative to untreated controls), while co-cultures showed greater than 80% viability. Furthermore, we observed quantitative differences in the TC50 values of methapyrilene (between 1.4 and 1.6 mM) and pyriline (between 1 and 1.2 mM) only in the stable co-culture model of the rat liver.

In contrast to methapyrilene and pyriline, acetaminophen (APAP) and troglitazone were found to be more toxic to co-cultures as compared to pure monolayers (Figure 6.14). For example, incubating pure monolayers with a 30 mM dose of APAP for 24 hours had no effect on their viability; however, co-cultures displayed a ~33% loss. Similarly, exposing co-cultures to a 170 μ M dose of troglitazone reduce their viability by ~44%; however, such a reduction was seen in pure monolayers only when the troglitazone concentration was raised to 227 μ M.

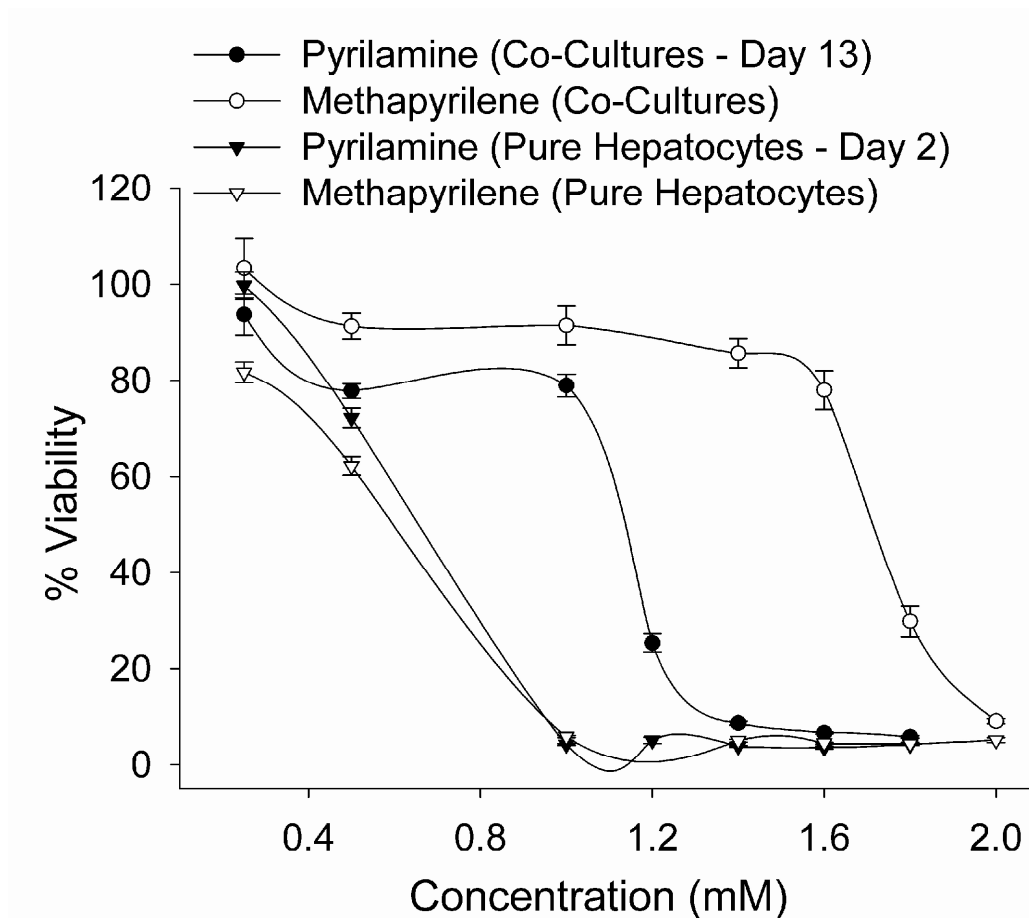


Figure 6.13: Methapyrilene and pyrilamine toxicity in pure hepatocyte monolayers and co-cultures. Pure hepatocyte monolayers (day 2 of culture) and hepatocyte-fibroblast co-cultures (day 13), prepared from the same rat liver, were incubated with varying doses of methapyrilene or pyrilamine dissolved in culture medium for 24 hours. Viability was subsequently assessed via the MTT assay (see Methods for details). Error bars represent standard error of the mean ($n=3$).

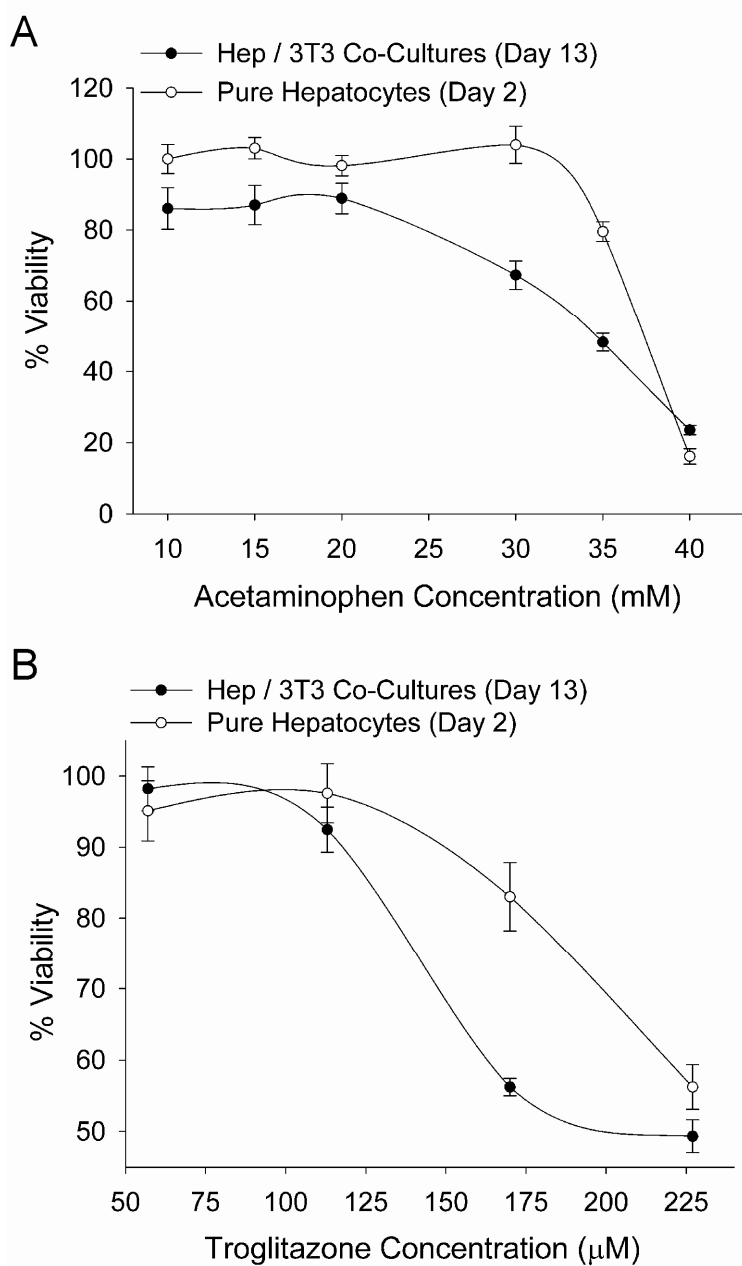


Figure 6.14: Acetaminophen and troglitazone toxicity in pure hepatocyte monolayers and co-cultures. Pure hepatocyte monolayers (day 2 of culture) and hepatocyte-fibroblast co-cultures (day 13), prepared from the same rat liver, were incubated with varying concentrations of acetaminophen or troglitazone dissolved in culture medium for 24 hours. Viability was subsequently assessed via the MTT assay (see Methods for details). Error bars represent standard error of the mean ($n=3$).

6.4.7 Species-Specific Phase I and Phase II Substrate Metabolism

Significant variations in hepatocellular functions (i.e. CYP450 enzymes) across different species have been implicated in the inability of animal models to adequately predict adverse outcomes in clinical trials involving humans [175]. Nonetheless, studies in live animals are required by the FDA since they provide valuable *in vivo* data in a preclinical setting. Therefore, the selection of an animal species (i.e. rat, mouse, monkey, guinea pig) in which the liver-specific metabolism and toxicity of a particular candidate drug are similar to that seen in humans is crucial for clinical success. *In vitro* human and animal models that closely resemble *in-vivo* functionality may find use in such a selection process.

Here, to demonstrate utility in drug development, we compared the metabolism of specific Phase I and II enzyme substrates in micropatterned co-cultures utilizing either primary human (see chapter 5) or rat hepatocytes (Figure 6.15). For instance, BFC was dealkylated in rat co-cultures at a rate (pmoles/min/ 10^6 cells) that was ~18 fold greater than the rate seen in human co-cultures. On the other hand, rat co-cultures were unable to hydroxylate coumarin, while human co-cultures did so at a rate greater than 6 pmol/min/ 10^6 cells. Lastly, we observed that both human and rat co-cultures displayed similar rates for a) CYP450-mediated dealkylation of MFC, and b) Phase II-mediated conjugation of 7-HC. Furthermore, in chapter 5 (Figure 5.16), we demonstrated species-specific differences in omeprazole-mediated CYP1A induction by comparing the responses of micropatterned human and rat co-cultures.

6.4.8 Co-Cultivation of Hepatocytes with Liver-derived Nonparenchymal Cells

In this study, we have utilized non-liver-derived 3T3 murine embryonic fibroblasts to stabilize phenotypic functions of rat hepatocytes *in vitro*. The 'co-culture

effect', however, has been reported for nonparenchymal cells from both within and outside the liver [65]. In this study, we wanted to functionally compare our 3T3 model with co-cultures that contained liver-derived primary nonparenchymal cells. Therefore, we co-cultivated primary rat hepatocytes with the whole non-parenchymal fraction of the rat liver (NP-fraction). In Figure 6.16A, we show albumin secretion in micropatterned co-cultures containing either the NP-fraction or 3T3 fibroblasts. Cumulative albumin secretion over a period of 11 days was ~ 1.7 fold higher in NP-fraction co-cultures and ~ 5.5 fold higher in 3T3 co-cultures as compared to unstable pure hepatocyte controls. Furthermore, liver-derived non-parenchymal cells proliferated over time in co-cultures, which induced changes in hepatocyte morphology (Figure 6.16B). Hepatocyte morphology in 3T3 co-cultures remained relatively stable for the duration of the experiment. Pure hepatocyte monolayers, on the other hand, adopted a spread-out, 'fibroblastic' morphology.

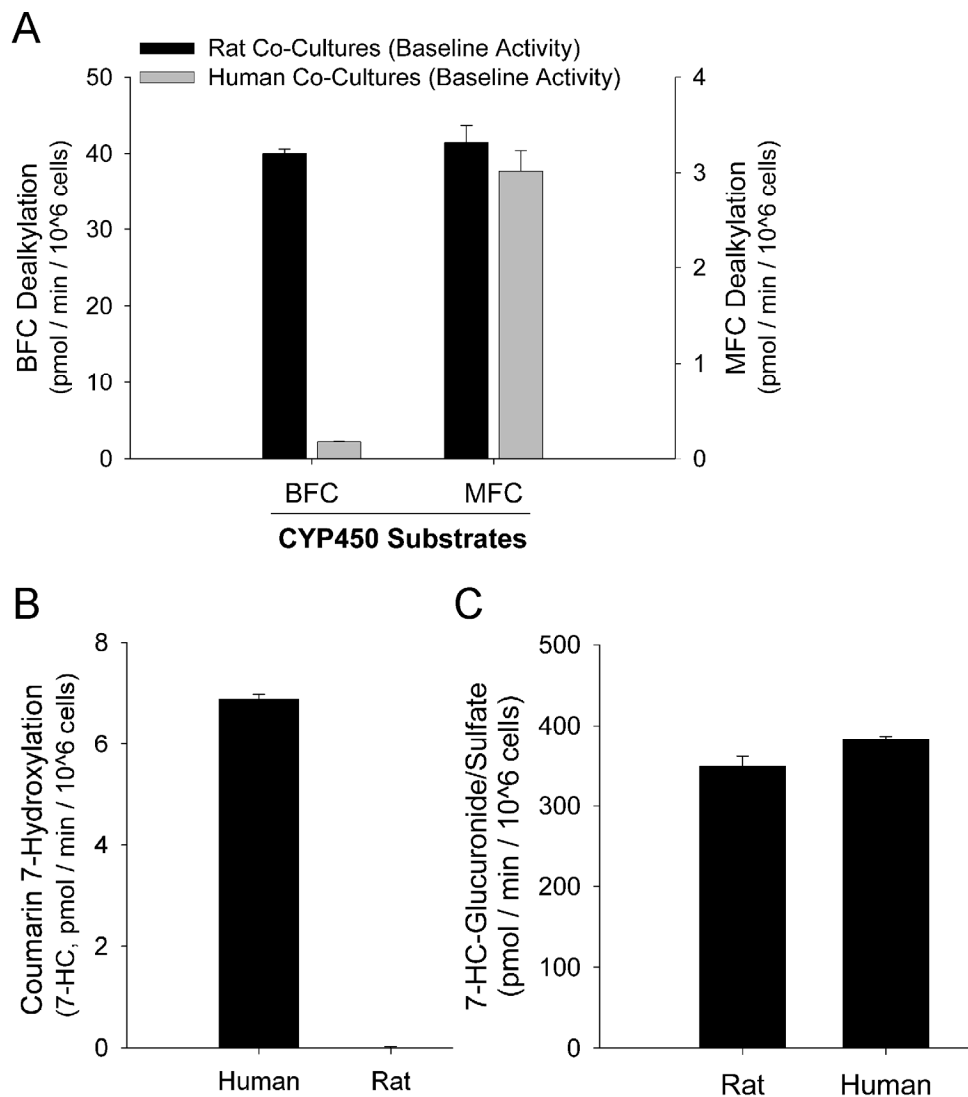


Figure 6.15: Comparison of Phase I- and Phase II-mediated substrate metabolism in human and rat co-cultures. Micropatterned cultures with either primary human or primary rat hepatocytes were created using the stencil-based process shown in chapter 5. Subsequent addition of 3T3-J2 fibroblasts created co-cultures. **A)** Rate of BFC and MFC dealkylation in untreated (baseline) micropatterned rat and human co-cultures. **B)** Rate of coumarin 7-hydroxylation (CYP2A specific) in micropatterned rat and human co-cultures. **C)** Rate at which 7-HC is conjugated with glucuronic acid and sulfate groups by Phase II enzymes in micropatterned rat and human co-cultures. Data from a single representative day is shown. MFC, 7-methoxy-4-trifluoromethylcoumarin; BFC, 7-benzyloxy-4-trifluoromethylcoumarin; 7-HC, 7-Hydroxycoumarin. Error bars represent standard error of the mean (n=3).

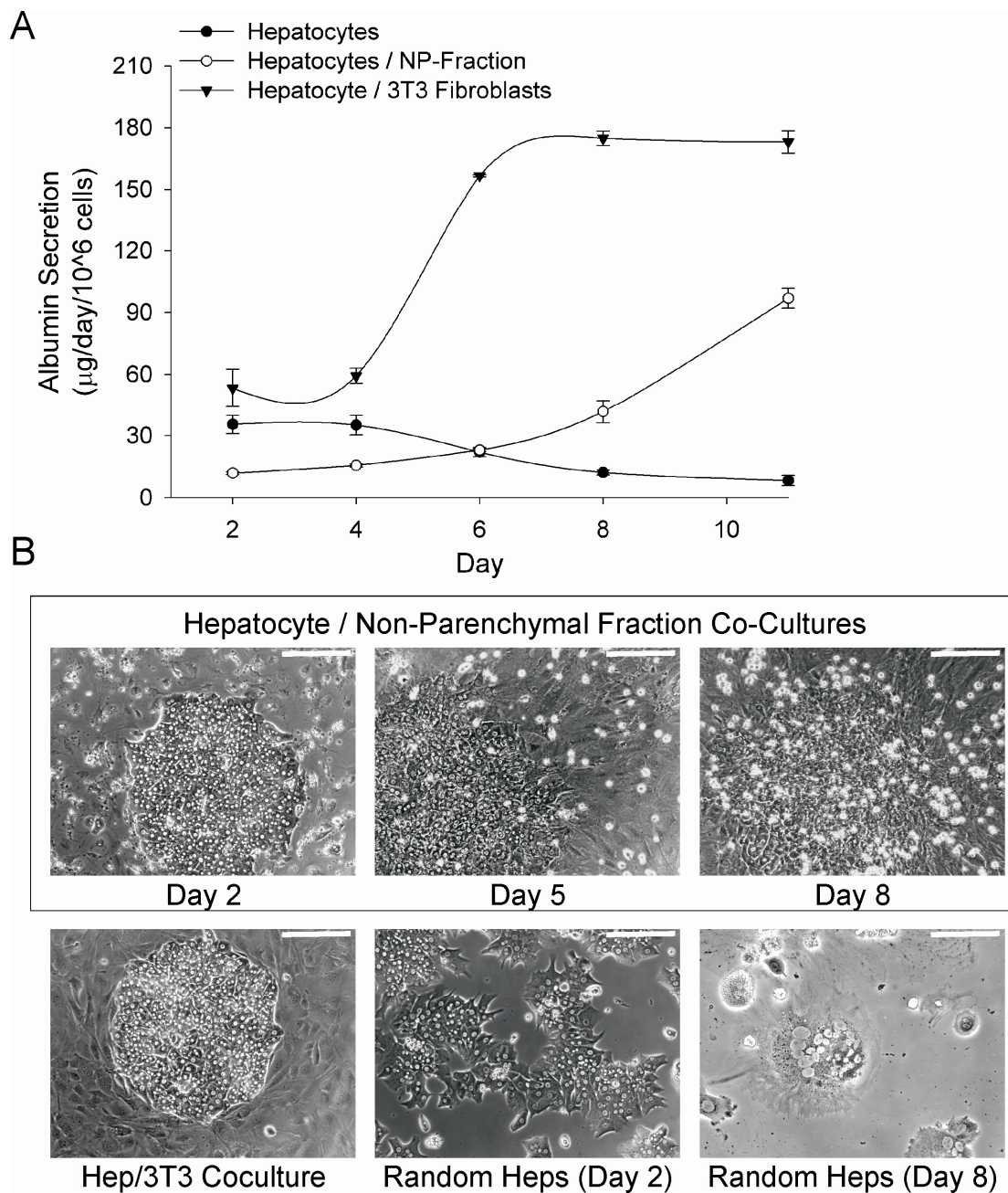


Figure 6.16: Co-cultivation of rat hepatocytes with nonparenchymal fraction of the liver. Micropatterned co-cultures with either 3T3 fibroblasts or the whole non-parenchymal fraction of the liver (NP-fraction) were created using the stencil-based process shown in chapter 5. **A)** Time-course of albumin secretion in the different cultures models. **B)** Phase contrast micrographs showing morphology of cells in the different culture models. Error bars represent SEM ($n=3$). Scale bars are 200 μm .

6.5. Discussion

Progress in molecular biology techniques and the ready availability of genomic data due to the advent of functional genomics has spurred remarkable advances in the identification of novel therapeutic targets for drug development. The pharmaceutical industry has responded by automating combinatorial synthesis and high-throughput screening (HTS) of new chemical entities (NCE) for activity against chosen targets. With such advances, the wealth of active compounds that emerge from primary screens has created a bottleneck downstream in drug development. Since first-round hits typically do not meet the safety and efficacy criteria to be effective in humans, sequential rounds of ADME/Tox optimization are typically required prior to clinical studies in humans. The goal of high-throughput ADME/Tox screening with *in vitro* tissue models is to identify problematic compounds early in the drug discovery process, which represents the single largest cost-savings opportunity in the pharmaceutical industry [169].

Though some progress has been made in incorporating hepatocyte culture models in ADME/Tox screening, current systems suffer from a precipitous decline in viability and key liver-specific functions [165, 176]. Co-cultivation of hepatocytes with a plethora of nonparenchymal cells from within and outside the liver has been shown to stabilize the hepatic phenotype *in vitro* [65]. A handful of studies have demonstrated activity of few drug metabolism enzymes in specific co-culture models [209]; however, the integration of hepatic co-cultures into an optimized and miniaturized platform, designed and validated specifically for drug development, remains an unexplored research interface.

In this study, we present the development of a co-culture model of the rat liver that maintains phenotypic stability for several weeks (i.e. long-term) as assessed by morphological analysis, albumin secretion, urea synthesis and activity of phase I and II drug metabolism enzymes. Specifically, primary rat hepatocytes were co-cultivated with

3T3 murine embryonic fibroblasts to stabilize a variety of liver-specific functions. Our results indicated that clustering hepatocytes onto collagen-coated islands of prescribed dimensions prior to seeding of fibroblasts (i.e. micropatterning) consistently improved the longevity of the co-cultures from several weeks to over 2 months when compared to a randomly distributed format. We show utility of our co-cultures in drug development by characterizing drug-drug interactions, acute and chronic toxicity of model hepatotoxins, and species-specific metabolism of prototypic Phase I and II substrates.

6.5.1. Functional Comparison Between Random and Micropatterned Co-Cultures

In our previously published studies, we demonstrated using a novel photolithographic cell patterning technique that liver-specific functions in co-cultures could be modulated upon engineering the balance between homotypic (hepatocyte-hepatocyte) and heterotypic (hepatocyte-fibroblast) cell-cell interactions [123]. In particular, we discovered that co-cultures with a maximal initial heterotypic interface (i.e. single hepatocyte islands surrounded by fibroblasts) had highest levels of liver-specific functions as compared to other micropatterned configurations with similar cell numbers and hepatocyte-to-fibroblast ratios. Furthermore, hepatocytes in smaller patterns (<250 μm) intermingled significantly to dissipate the pattern, whereas larger islands (> 450 μm) assumed a relatively stable conformation for several weeks in monolayer culture.

In this study, we chose the 500 μm hepatocyte island micropatterned configuration (with 1200 μm center-to-center spacing between islands) for further characterization since co-cultures displayed high levels of hepatic functions while maintaining micropattern fidelity for the duration of the experiment. Next, in order to avoid the well-known limitations of photolithography [153], we utilized a previously developed stencil-based process (see chapter 5 for details) to create miniaturized

micropatterned co-cultures in a multiwell format amenable for higher throughput experimentation. Thus, the rat liver model developed and characterized herein represent 24-well plates with each well containing ~12,000 hepatocytes organized in 37 colonies of 500 μm diameter, for a total of 888 repeating hepatic microstructures per plate.

We functionally compared micropatterned co-cultures with their randomly distributed counterparts seeded on substrates uniformly coated with collagen (i.e. random co-cultures). Our results indicated that for the first ~2 weeks of co-culture, a variety of liver-specific functions (albumin secretion, urea synthesis, and cytochrome-P450-1A activity) were similar in value in the two models (Figures 6.2 and 6.3). However, after that time period, functions in random co-cultures declined to near undetectable levels within a week, whereas micropatterned co-cultures remained functional for ~10 weeks. Morphological observation revealed that the functional decline in random co-cultures was accompanied by a loss of hepatocyte viability (data not shown). The timing of the functional decline in random co-cultures was not consistent between multiple repeat trials, as a range of 3-8 weeks was observed. Micropatterned co-cultures, on the other hand, reproducibly remained functional for up to 10 weeks.

The mechanism underlying dramatic functional differences between micropatterned and random co-cultures remains undetermined. It is plausible that in the chosen micropatterned configuration, rat hepatocytes experience the proper balance of homotypic and heterotypic interactions which allows them to survive and function for a longer time than in random co-cultures, where cell-cell interactions can vary significantly even in the same culture well. High variability in cell-cell interactions may also explain why random co-cultures survive for variable time periods across multiple experiments. Additionally, fibroblasts in micropatterned co-cultures were seeded on 'bare', un-coated culture substrate; however, in random co-cultures, fibroblasts experienced a collagen-

coated surface, which may affect their long-term induction capability. In the future, we plan to address this possibility by coating the bare areas in micropatterned hepatocyte cultures with collagen prior to seeding of fibroblasts. Gene expression profiling of fibroblasts isolated from micropatterned and random co-culture configurations may shed some insight on the genes/molecules underlying the differences in hepatic functions.

Regardless of any functional improvements, micropatterned co-cultures offer several advantages over randomly distributed ones, which include: precise control over homotypic and heterotypic interactions towards consistent modulation of phenotypic functions; and, imaging and tracking of individual hepatocyte islands over time to monitor cellular responses to specific stimuli. It should be noted though that in this work, a few studies demonstrating utility of co-cultures in drug development were carried out with 1-2 week old randomly distributed co-cultures (high functioning) partly due to the ease with which such co-cultures can be created as compared to micropatterned ones. Though we plan to repeat such studies with our micropatterned platform, we do not anticipate considerable differences in biological outcomes since liver-specific functions were similar in random and micropatterned co-cultures for at least the first few weeks.

6.5.2. Considerations in Development of the Long-term Liver Model

An advantageous feature of our co-culture model is that various liver and non-liver derived NPCs can be used to induce phenotypic functions in hepatocytes. We chose immortalized 3T3 murine embryonic fibroblasts because they have several advantages over using primary liver-derived nonparenchymal cells. Such advantages include: ready availability through ATCC (American Type Culture Collection) or academic laboratories; ease of propagation and cryopreservation; and, robust induction of a variety of hepatocyte functions [58]. Furthermore, murine 3T3 fibroblasts are known to induce the

highest levels of albumin secretion in rat hepatocytes as compared to other nonparenchymal cell types that have been used for co-culture in previously published studies [65]. Of the different 3T3 sub-clones readily available (i.e. swiss-3T3, NIH-3T3, L1-3T3, 3T3-J2), we specifically chose J2 cells since they induce the highest level of hepatic functions and improve the longevity of the co-cultures [58].

Nonetheless, in order to demonstrate versatility of our platform, we co-cultivated micropatterned rat hepatocytes with the whole non-parenchymal fraction of the rat liver (multiple cell types, including sinusoidal endothelial and kupffer cells) and observed upregulation of hepatocyte functions, though not to similar levels or duration as in 3T3 co-cultures (Figure 6.16). Use of co-cultures with liver-derived nonparenchyma may be important for studies that aim at evaluating the effects of liver-specific heterotypic cell-cell interactions on the metabolism and/or toxicity of specific compounds [106, 107, 220]. In chapter 5, we demonstrated co-cultivation of primary *human* hepatocytes with 3T3 fibroblasts towards development of a robust model of the human liver for drug development. Therefore, the type and species of cells in hepatocyte-nonparenchymal co-cultures can be ‘customized’ for the particular application at hand, making our system modular by design.

The use of nonparenchymal cells in co-cultures may be problematic if the proliferating NPCs overgrow, deplete nutrients in culture medium faster than the media change schedule, and ultimately cause loss of viability in the hepatocyte population. For example, in co-cultures of hepatocytes and the whole nonparenchymal fraction of the liver, we noted that the nonparenchymal cells grew uncontrollably and eventually caused the monolayer to ‘peel’ off the tissue culture substrate ~1.5 weeks into the experiment (data not shown). On the other hand, we noticed that the growth of 3T3 fibroblasts did not cause such peeling. Additionally, liver-specific functions were not down-regulated for

at least the first 2-3 weeks of hepatocyte-fibroblast co-cultures. However, following that time period, there was excessive intracellular accumulation of large particles (possibly lipids due to shutdown in lipid metabolism) in co-cultures and accompanying decline in hepatocyte functions. The mechanism underlying such responses has not yet been elucidated. Nonetheless, in order to improve the longevity of the co-cultures, we growth-arrested fibroblasts via mitomycin-C prior to seeding onto hepatocyte cultures and discovered that such co-cultures lasted for over 2 months as compared to 2-3 weeks for co-cultures with proliferating fibroblasts.

Though mitomycin-C is effective at preventing cell replication via its alkylation of DNA, cell viability is compromised over time, the length of which can vary with the cell type being used (unpublished observations). For growth-arrested 3T3 fibroblasts, we noticed loss of viability over several weeks in co-cultures, with only a handful of cells (estimated at 10%) surviving after 10 weeks. This decline in fibroblast viability may very well underlie the eventual demise of the hepatocytes, which need continuous nonparenchymal signaling to survive and function (as per our data in chapter 4). One possible strategy to further improve the longevity of co-cultures may be to ‘supplement’ with fresh growth-arrested fibroblasts every few weeks in order to provide continuous nonparenchymal stimulation. In spite of the eventual decline of co-cultures, maintenance of various liver-specific functions in hepatocytes for over 70 days represents a considerable improvement over models currently used in drug development, in which hepatic viability and functions are retained for a few days at most.

6.5.3. Functional Stability of Co-Cultures

The functional stability of hepatocyte-fibroblast co-cultures over several weeks was characterized using qualitative and quantitative criteria. Morphological observation

revealed that primary rat hepatocytes in co-cultures retained the stereotypical features (i.e. polygonal shape, distinct nuclei and nucleoli, visible bile canaliculi) seen in freshly isolated cells and in the liver *in vivo* (Figure 6.1). Pure hepatocytes, on the other hand, rapidly (few days) lost viability and surviving cells adopted a ‘fibroblastic’, spread-out morphology. Furthermore, albumin and urea secretion were maintained in co-cultures for as long as 2 months (micropatterned configuration), whereas in pure hepatocyte monolayers, these markers declined to undetectable levels within a few days. Albumin and urea are typically used to assess hepatic differentiation and represent liver-specific protein synthesis and nitrogen metabolism, respectively.

Fluorimetric substrates were used to assess the baseline (i.e. untreated) activity of Phase I (cytochrome-P450 or CYP450) and Phase II (conjugation) enzymes in co-cultures. The activity of drug metabolism enzymes is especially important in a drug development setting since such enzymes can detoxify drugs and/or generate toxic metabolites which can cause injury to the liver and other organs via circulation in the blood. Results of this study indicated that BFC and MFC were dealkylated to different extents in co-cultures, which may reflect differential expression of various CYP450 isoforms (Figure 6.4). BFC is known to be highly metabolized by rat CYP2B1 (reported value of 3.7 pmol product/min/pmol of enzyme), followed by 2C6 and CYP3A1/2 [BD Gentest poster entitled “Human and Rat Cytochrome P450 Isoform Selectivity within a Panel of Fluorimetric Substrates”, www.gentest.com]. On the other hand, MFC is highly metabolized by CYP2C6 (reported value of 11.5 pmol product/min/pmol enzyme), followed by 2C11, 2B1, 2E1 and 1A1/2. Thus, except for CYP3A1/2, several different CYP450 enzymes metabolize both BFC and MFC.

In addition to CYP450-mediated BFC and MFC metabolism, co-cultures were probed for phase II activity using fluorescent 7-HC as a prototypic substrate. Co-cultures

displayed time-dependent phase II-mediated conjugation of 7-HC with glucuronic acid and sulfate groups. Furthermore, we noted that the Phase I dealkylation product of BFC and MFC, namely 7-HFC, was also highly conjugated by Phase II enzymes, as determined by re-gain of fluorescence following incubation with β -glucuronidase/aryl-sulfatase enzymes ('de-conjugate' 7-HFC-glucuronide/sulfate back to fluorescent 7-HFC). Therefore, in our platform, there was effective coupling of Phase I and II pathways, which can be critical for complete metabolism (detoxification and/or generation of toxic metabolites) of certain xenobiotics.

Many compounds (endogenous and exogenous) undergo hepatic uptake and biliary excretion through a host of different carrier-mediated transporters [307]. Since drug-drug interactions have been reported for certain transporters, the pharmaceutical industry is increasingly evaluating the effect of xenobiotics on phase III pathways (i.e. sinusoidal and biliary excretion) [308, 309]. Hepatocytes in pure monolayers typically lose polarity and show a rapid decline in transport properties [310]. Likewise, hepatic cell lines also often lack liver-specific transport functions [311]. Pure hepatocyte monolayers overlaid with gelled collagen (sandwich configuration) and cultured up to 5 days have been shown to establish intact canalicular networks, maintain expression of transport protein Mrp2 (multi-drug resistance-associated protein), and re-establish polarized excretion of organic anions and bile acids [310]. However, sandwich cultures have not been evaluated beyond 5 days for functionality or retention of canalicular networks.

In co-cultures of hepatocytes and 3T3 fibroblasts, we routinely observe visible bile canaliculi between hepatocytes for the duration of the cultures. Our objective here was to determine whether these bile canaliculi are indeed functional. Co-cultures (2 week old) were incubated with CFDA, which is known to be taken up by hepatocytes, cleaved by intracellular esterases into a fluorescent dye (fluorescein) and excreted across the apical

membrane into bile canaliculi via specific transporters. The presence of fluorescent domains has been further correlated to biliary structures observed via electron microscopy [312]. We observed fluorescent staining of bile canaliculi in our co-cultures, which suggests functional transporter activity and intact tight junctions that seal the biliary structures (Figure 6.5). However, not all the bile canaliculi visible under phase contrast microscopy stained positive, and in some hepatocytes the dye was retained in the cytoplasm. Such observations may be attributed to either low excretion rate across the apical domain or loss of function of apical tight junctions; however, further studies are needed to determine the precise underlying mechanism.

In the future, we plan to assess presence of specific transporters (i.e. Mrp2, p-glycoprotein) in co-cultures using immunofluorescent staining, and determine the evolution of the functional canalicular network over time (i.e. amount of biliary secretion as the co-cultures age). Nonetheless, staining of functional bile canaliculi here indicates that at least some proportion of hepatocytes in co-cultures maintain functional polarity. Therefore, long-term co-cultures may allow for differentiation between sinusoidal and canalicular transport processes, and thus may represent a useful *in vitro* model system to evaluate the hepato-biliary disposition of pharmaceutical compounds.

6.5.4. Altered Substrate Metabolism and Toxicity Due to Drug-Drug Interactions

Modulation of CYP450 activities (induction and inhibition) has been known to cause drug-drug interactions, which can lead to serious pharmacological and/or toxicological consequences in the clinic [219, 313]. Primary hepatocytes are routinely utilized to assess CYP450 induction by xenobiotics [41, 176]. Typically, confluent monolayers cultured on collagen and overlaid with a gel of collagen or Matrigel are allowed to first ‘stabilize’ for 48 hours since during this time period, these cultures are

unresponsive to inducers [182]. Next, cultures are incubated for 2-4 days with inducer compounds and then CYP450 activity is assessed using prototypic substrates via fluorescence or conventional HPLC-based methods. Here, we utilized fluorimetric, resorufin-derived substrates, ethoxy-resorufin (ER) and methoxy-resorufin (MR) to demonstrate induction of CYP1A1 and CYP1A2 enzymes, respectively (Figure 6.6). Co-cultures were incubated with 3-Methylcholanthrene (3-MC) to induce CYP1A activities for 3 days followed by assessment of ER and MR dealkylation into fluorescent resorufin. Subsequently, CYP1A activities in co-cultures were allowed to return to baseline levels for 4-5 days and then the induction procedure was re-initiated. Our data showed that CYP1A remained inducible for several weeks in random co-cultures and for over 2 months in micropatterned co-cultures. In the future, we plan on evaluating the induction of other CYP450 isoforms such as CYP3A and CYP2B.

CYP450 inhibition is routinely evaluated using a-cellular microsomes that contain primarily Phase I enzymes. However, addition of cofactors is needed for such evaluations. Primary hepatocytes contain enzymes and cofactors required to assess CYP450 inhibition. Furthermore, modulation of CYP450 activities can be simultaneously studied with liver-specific toxicity, which requires use of dynamic cellular gene expression and other important protein machinery. In our co-cultures, we showed inhibition of BFC metabolism upon incubation with a CYP3A inhibitor, ketoconazole. Complete loss of BFC metabolism upon treatment with ketoconazole did not occur since BFC is also a substrate for other CYP450 enzymes as discussed previously.

Drug-drug interactions have been known to lead to serious clinical toxicity in multiple organ systems. One established model of such interactions is increase in acetaminophen (APAP) toxicity due to increase in CYP3A levels. APAP is a commonly used over-the-counter analgesic/antipyretic medication with clinical hepatotoxic potential

[314]. Such hepatotoxicity has been attributed to the generation of a highly toxic electrophilic metabolite, N-acetyl-p-benzoquinoneimine (NAPQI), which is produced by oxidation of APAP by various CYP450 enzymes, including CYP1A2, CYP2A5, CYP2E and CYP3A [315-317]. NAPQI can cause toxicity by binding to cellular proteins and/or producing oxidative damage [318]. Cultured hepatocytes treated with prototypic CYP3A inducers have been shown to be more susceptible to APAP-mediated toxicity [319]. We recapitulated this effect in our co-cultures by incubating them with increasing concentrations of a known CYP3A inducer, dexamethasone (DEX), for 2 days prior to incubation with APAP. Our data revealed that a 5 mM dose of APAP, which is not toxic under un-treated conditions, showed significant toxicity in DEX-treated co-cultures - up to ~50% reduction in viability (Figure 6.7). Toxicity as assessed via mitochondrial activity (MTT assay, see methods) correlated well with morphological observations. That is, hepatocytes in co-cultures pre-treated with DEX and then subjected to APAP displayed severe changes in morphology (probably necrosis) as compared to controls. Furthermore, a dose-dependent increase in APAP toxicity was seen with increasing doses of DEX, presumably due to higher induction of CYP3A levels, as reported elsewhere [319]. Co-incubation with a CYP3A inhibitor, Troleandomycin (TAO), protected co-cultures from DEX-mediated enhancement of APAP toxicity, and thus confirmed the role of CYP3A in such responses.

Besides DEX, ethanol has also been shown to increase hepatic CYP3A levels in addition to CYP2E levels in several experimental systems and in humans [304, 320, 321]. This model is relevant clinically since consumption of alcoholic beverages has been identified as a risk factor for the development of liver damage from APAP [305]. Numerous studies in rodents have also shown increased APAP hepatotoxicity in animals pretreated with ethanol alone [304, 306, 322]. Towards replicating the *in vivo* outcomes

in our *in vitro* liver model, we incubated co-cultures with 2% ethanol for 2 days prior to administration of 5 mM APAP. However, our data indicated that ethanol-treated co-cultures did not display increased susceptibility to APAP-mediated toxicity. Such a result is consistent with other *in vitro* studies which suggest that perhaps there are threshold levels of CYP activities required for APAP toxicity to develop [184]. In the future, we plan to assess the ethanol-mediated increase in CYP3A in co-cultures using western blotting. These increases will then be compared to the increases caused by DEX towards determining whether a threshold hypothesis underlies the differences between these two CYP3A inducers in their effect on APAP-mediated toxicity.

Caffeine has been shown to enhance APAP hepatotoxicity in rats pretreated with inducers of CYP3A [323]. In addition, caffeine has been shown to enhance the metabolism of APAP to NAPQI in rat liver microsomes [324]. Since several medications used to treat ethanol overindulgence contain caffeine and APAP, it is possible that intoxicated individuals taking such medications may be at a greater risk for APAP-mediated liver damage. Here, we demonstrated that caffeine enhanced APAP toxicity only when CYP3A levels in co-cultures were induced via DEX or ethanol (Figure 6.8), which is consistent with the *in vitro* literature [184]. Treatment with TAO inhibited CYP3A activity and increased viability in such co-cultures. In conclusion, the results from the aforementioned studies demonstrate that co-cultures are a robust model system for evaluating clinically relevant drug-drug interactions in a drug development pipeline.

6.5.5. Toxicity in Co-Cultures Due to Repeated Exposures with Model Hepatotoxins

Toxicity of pharmaceuticals due to repeated exposures over days to weeks (chronic toxicity) is a clinically relevant phenomenon. Hepatocyte culture models used in the pharmaceutical industry lose viability and liver-specific functions within a matter of

days; therefore, chronic toxicity studies cannot be carried out on such platforms. Since hepatocyte-fibroblast co-cultures utilized in this study remain functional for several weeks to months, we investigated dose and time-dependent toxicity of four known Hepatotoxins, which included: acetaminophen, methapyrilene, pyriline and troglitazone.

Overall, we found that all toxins displayed dose- and time-dependent toxicity to co-cultures, which points to the importance of conducting chronic toxicity studies. However, several qualitative and quantitative differences in toxic responses were observed across the various hepatotoxins. For instance, troglitazone was found to be most toxic to rat co-cultures following 24 hours of incubation, followed by pyriline, methapyrilene and acetaminophen. Except for methapyrilene and pyriline, for which mitochondrial toxicity data is lacking, such a rank ordering of compounds is consistent with published literature [325, 326]. Furthermore, data acquired on micropatterned *human* co-cultures (see chapter 5) supports the rank ordering of hepatotoxins seen here in rat co-cultures. Acetaminophen and methapyrilene exhibited a ‘shoulder’ in their toxic profiles (Figures 6.9-6.10) such that toxicity was seen when a dose threshold was reached. Since toxic metabolites of APAP and methapyrilene are known to be detoxified via glutathione [314, 327], depletion of this protective tri-peptide may underlie the shoulder response.

Observation of cells via microscopy may allow the potential to detect sub-lethal toxicity at lower concentrations than those required for frank cell death [175]. In our rat co-cultures, we observed that cells accumulated large particles (possibly lipids) upon incubation with non-lethal doses of troglitazone ($<115 \mu\text{M}$) over 5 days as compared to un-treated controls (Figure 6.12). Troglitazone is an oral hypoglycemic which was withdrawn from the market in the year 2000 following severe cases of hepatotoxicity. Like other thiazolidinediones, troglitazone works by activating the nuclear receptor

PPAR γ (peroxisome proliferators-activated receptor- γ). Several studies have demonstrated enhanced expression of lipogenic genes and increased expression of PPAR γ in animal models of steatotic (i.e. fatty) liver [328, 329]. Moreover, a role for PPAR γ has been established in maintenance of a steatotic phenotype in liver [329]. In vitro, a recent study has implicated PPAR γ as an inducer of steatosis (fat accumulation) in hepatocytes via de novo lipid synthesis [330]. This study also showed that treatment of hepatocytes with troglitazone further enhanced lipid accumulation. In our rat co-cultures, we have noted increased messenger-RNA expression of PPAR γ as compared to freshly isolated hepatocytes (gene expression profiling, data not shown). Therefore, it is plausible that troglitazone binds to PPAR γ in co-cultured hepatocytes and induces in them steatosis. Further studies with a lipid-binding dye (i.e. Oil Red-O) are needed to confirm the identity of the particles accumulating in co-cultures after treatment with troglitazone. Nonetheless, the detection of these particles was only possible via morphological observation since the 'bulk' MTT assay did not show any significant differences in viability between the troglitazone-treated and un-treated conditions.

6.5.6. Comparison of Drug Toxicity in Pure Hepatocyte Monolayers and Co-Cultures

The loss of liver-specific gene expression and functions in conventional hepatocyte cultures on collagen may alter the dose-dependent toxicity profile of those xenobiotics which are bioactivated and/or detoxified by phase I and II drug metabolism enzymes. Here, we compared the toxicity of four classic hepatotoxins (methapyrilene, pyrillamine, acetaminophen and troglitazone) in pure hepatocyte monolayers (48 hours post initiation of adherent culture) and hepatocyte-fibroblast co-cultures (day 13) prepared from the same rat liver. We observed that methapyrilene and pyrillamine were severely toxic to pure hepatocytes as compared to co-cultures (Figure 6.13).

Furthermore, co-cultures displayed quantitative differences in the TC50 (concentration at which 50% loss of viability is seen) values of the two compounds. Methapyrilene, in particular, is known to be metabolized into reactive metabolites by CYP2C11, and methapyrilene toxicity in vitro results in a decrease, but not depletion of the protective tripeptide, glutathione [327]. Though such mechanistic information on pyriline is lacking in the literature, we anticipate that being a structural analog of methapyrilene, some of the underlying bio-activation and detoxification schemes may be similar. Therefore, differences in the toxicity of methapyrilene and pyriline observed in pure monolayers and co-cultures could be due to higher levels of glutathione in co-cultures. It may be that CYP2C11 causes the production of reactive metabolites in both pure monolayers and co-cultures. However, with higher levels of glutathione, co-cultures are protected, while viability in pure monolayers is severely compromised. Further studies are needed to confirm this hypothesis. Although methapyrilene is shown to be more hepatocarcinogenic than pyriline [331], no study, to the best of our knowledge, has compared the effect of these drugs on mitochondrial toxicity. In this study, we observed that pyriline displayed higher mitochondrial toxicity in co-cultures than its analogue, methapyrilene.

In contrast to methapyrilene and pyriline, acetaminophen and troglitazone were found to be more toxic to co-cultures as compared to pure monolayers (Figure 6.14). APAP, in particular, is metabolized by a variety of CYP450 enzymes into toxic NAPQI. Reduced levels of CYP450 enzymes in pure monolayers may produce reduced levels of NAPQI and thus prevent toxicity. However, the reverse may be the case in co-cultures. Similar to APAP, troglitazone is metabolized by CYP3A and 2C into a quinone-type metabolite, which is considered to be an active intermediate in drug-induced hepatotoxicity [332, 333]. Additionally, troglitazone can induce levels of CYP3A and 2C

[334, 335]. From our drug-drug interaction studies, we determined that CYP3A is functional and inducible in co-cultures. Pure hepatocyte monolayers at day 2 are known to be unresponsive to inducers. Therefore, one hypothesis is that troglitazone induces CYP3A in 2-week old co-cultures, which then leads to generation of reactive metabolite and subsequent toxicity. Pure monolayers, on the other hand, are protected from troglitazone-mediated toxicity possibly due to reduced CYP3A levels and lack of induction capacity. Differences in the hepatotoxicity of model compounds between pure hepatocyte monolayers and co-cultures demonstrate that the use of phenotypically stable liver cultures is critical for assessments of xenobiotic hepatotoxicity.

6.5.7. Differences in Phase I and II Substrate Metabolism between Rat and Human Micropatterned Co-Cultures

Studies in live animals provide FDA-required *in vivo* data on the ADME/Tox properties of a drug candidate, and such data is required to initiate clinical trials in humans. However, differences between animals and humans in drug metabolism pathways have been noted in the literature and may underlie the failure of animal models to adequately predict human-specific responses [174, 175]. Thus, selection of an animal species which closely resembles human-relevant metabolism of a particular drug candidate is important for clinical predictability.

In chapter 5, we utilized stencil-based soft-lithography to create a robust micropatterned co-culture model of the human liver. Here, we have adapted such techniques to create a model of the rat liver. Our objectives were thus to demonstrate that *in vivo* differences in phase I and II-mediated metabolism of prototypic compounds between rat and human livers can be recapitulated *in vitro*. Towards that end, we incubated rat and human co-cultures with phase I and II substrates and noted several similarities and differences (Figure 6.15). In particular, coumarin was hydroxylated into

7-hydroxycoumarin by human co-cultures, whereas the metabolite was undetectable in the supernatants from rat co-cultures. Such a difference is consistent with previously published studies in live rats [336, 337].

Next, we compared human and rat co-cultures for their capacity to dealkylate BFC and MFC. MFC was metabolized by the two models at a similar rate, while BFC metabolism was ~10 fold higher in rat co-cultures as compared to human ones. Such responses are consistent with reported values for human and rat-specific metabolism of these two coumarin-derived substrates [BD Gentest poster entitled “Human and Rat Cytochrome P450 Isoform Selectivity within a Panel of Fluorimetric Substrates”, www.gentest.com]. MFC, in particular, has been reported to be metabolized by a variety of human and rat-specific CYP450 enzymes, and cumulative metabolism rates in the two models have been reported to be similar in magnitude (~25 pmol of product/min/pmol enzyme). Similar to MFC, BFC has been shown to be metabolized by a variety of human and rat-specific CYP450 enzymes. However, a greater variety of rat CYP450s metabolize BFC (1A1, 2A2, 2B1, 2C6, 2C11, 2C13, 2D1, 2D2, 3A1, 3A2) as compared to human CYP450s (1A1, 1B1, 2C19, 3A4, 3A7). Additionally, the cumulative dealkylation rate of BFC by rat CYP450 is higher than in the human model.

We observed that the rate of Phase II-mediated conjugation of 7-HC with glucuronic acid and sulfate groups was similar in the rat and human micropatterned co-cultures. Sulfation of 7-HC has been reported to be higher in pure monolayers of rat hepatocytes, while glucuronidation is higher in human hepatocytes [BD Gentest poster entitled “Comparison of Major Phase I and Phase II Metabolism Reactions in Cryopreserved Dog and Human Hepatocytes”, www.gentest.com]. Since in our assay, we utilized a mixture of glucuronidase/sulfatase enzymes, determination of which of the two pathways (i.e. sulfation, glucuronidation) is differentially regulated in the human and rat

models is difficult. In the future, we plan to use HPLC-based separation of metabolites to quantitatively assess any species-specific differences in 7-HC conjugation pathways.

6.5.8. Future Studies

In order to further improve our micropatterned co-culture model, we plan to explore several variables. First, the ratio of hepatocytes to fibroblasts which produces optimal functions in the long-term will be determined by varying the seeding density of growth-arrested fibroblasts. In our previously published work, we demonstrated that homotypic fibroblast interactions can indeed influence functions in hepatocytes [280]. Second, we will modulate the center-to-center spacing of hepatocyte islands in micropatterned co-cultures. In our micropatterned co-cultures utilizing *human* hepatocytes (chapter 5), we found that ‘high density’ cultures tended to outlast their ‘low density’ counterparts (data not shown). We anticipate that reducing the center-to-center spacing will increase hepatocyte density in rat co-cultures and may improve the longevity of the platform. Third, we will explore the use of different extracellular matrix molecules (ECM) and their combinations in micropatterned co-cultures. In our previously published work, we have demonstrated that combinations of a variety of ECM can modulate hepatocyte functions [338]; however, application to co-cultures has not yet been fully explored. Additionally, incorporation of hepatocyte-stabilizing molecules such as decorin (Chapter 2) and/or T-cadherin (Chapter 3) into the extracellular matrix scaffold may further enhance liver-specific functions and the longevity of the liver tissues. Fourth, we plan to supplement our functional stability data with gene expression profiling (similar to chapter 5) to characterize global mRNA levels in rat co-cultures.

Lastly, we plan to investigate alternative strategies to create miniaturized micropatterned co-cultures. Though stencils are reusable and can be used to create

thousands of repeating tissue structures in a matter of hours, the process of aligning a 'blank' 24-well PDMS device onto micropatterned collagenous islands (see Chapter 5 for details) can be cumbersome. Furthermore, stencils are made of PDMS (polydimethylsiloxane), which is permeable to specific hydrophobic compounds [339] and may cause depletion of drugs from culture medium. In our laboratory, we are investigating a strategy (work of David Eddington, post-doctoral fellow) in which standard 24- or 96-well tissue culture plastic plates are first coated with a monolayer of collagen and then a PDMS stamp with microposts (same dimensions as holes in stencils) is sealed to the collagen-coated plastic. Lastly, the entire assembly is exposed to oxygen plasma, which etches away collagen (i.e. exposes underlying plastic) selectively in areas that have not been protected by the PDMS micro-posts. We have used this strategy to successfully create micropatterned cultures of pure hepatocytes; however, adaptation to co-cultures remains a task for the near future.

6.5.9. Conclusions

In summary, we have shown in this chapter that co-cultivation of primary rat hepatocytes with 3T3 fibroblasts can stabilize hepatic morphology and a variety of liver-specific functions for several weeks in monolayer format. Hepatic functions that were assessed included albumin secretion, urea synthesis, CYP450 activity and inducibility, Phase II activity and functional bile canaliculi. Organizing hepatocytes onto collagen-coated domains of prescribed dimensions (500 μm islands with 1200 μm center-to-center spacing - micropatterning) further improved the longevity of co-cultures from a few weeks to over 2 months. We showed utility of co-cultures in drug development by 1) characterizing altered CYP450 substrate metabolism and toxicity due to drug-drug interactions, 2) quantifying the acute and chronic toxic potential of multiple model

hepatotoxins, and 3) demonstrating in vivo-relevant differences in Phase I and II substrate metabolism between rat and human micropatterned co-cultures. Combined with the human co-culture platform of chapter 5, we anticipate that the rat liver model presented here may find use in eliminating compounds with problematic ADME/Tox profiles earlier in drug discovery, which may ultimately reduce development costs, increase the likelihood of clinical success and reduce patient exposure to unsafe drugs. Integration of our microscale liver models into a lab-on-a-chip platform with multiple tissues may, in the future, constitute an important paradigm shift in preclinical testing of new drug candidates.

Acknowledgements

We are grateful to Emanuele Ostuni and Surface Logix, Inc. for design and fabrication of the PDMS stencils, Jennifer Felix and Kathryn Hudson for rat hepatocyte isolation, Howard Green for providing 3T3-J2 fibroblasts, Ihui Wu for assistance with toxicity studies, and Taylor Sittler for helpful discussions regarding experiment design and selection of Hepatotoxins.

CHAPTER 7

SUMMARY AND FUTURE DIRECTIONS

7.1. Overall Objectives

Highly functional *in vitro* models of the liver are useful for several different applications ranging from cell-based therapies for liver disease to drug development. Of the various cell sources available for such models (i.e. stem cells, cell lines), primary liver parenchymal cells or hepatocytes are generally considered to be the most suitable since they strike an appropriate balance between simplicity of use (as compared to liver slices or perfused whole organs) and maintenance of intact cellular architecture with complete, undisturbed enzymes and cofactors [165, 182, 301]. However, hepatocytes are notoriously difficult to maintain in culture as they undergo a precipitous decline in viability and liver-specific functions [176]. Over the last few decades, investigators have employed several strategies to stabilize hepatocytes. These strategies generally fall into the category of extracellular matrix manipulation (topography and/or composition), soluble factor supplementation (i.e. hormonally defined culture medium) and cell-cell interactions (homotypic and heterotypic). Of these, co-cultivation of hepatocytes with nonparenchymal cells derived from within and outside the liver has been shown to stabilize a variety of liver-specific functions *in vitro* [65]. Co-cultures have been shown to be robust models of the liver with potential applications in bioartificial liver devices, pharmaceutical drug screening and fundamental studies of liver physiology and pathophysiology.

In spite of significant investigation over the last two decades, several aspects of hepatic co-cultures are still unclear. In particular, the nonparenchymal-derived molecular mediators that induce functions in hepatocytes remain largely undiscovered. Furthermore, it is not clear whether continuous nonparenchymal signaling is required to maintain hepatic functions (i.e. dynamics of cell-cell interaction) *in vitro*. Lastly, the integration of co-cultures into an optimized and miniaturized platform, designed and validated specifically for drug development, is an unexplored research interface. Therefore, the objectives of this dissertation were to explore the aforementioned questions using novel methodologies and technological platforms. In particular, we wanted to a) Develop and experimentally validate a functional genomics approach to identify nonparenchymal-derived molecular mediators of the ‘co-culture effect’, b) Develop a method utilizing novel electroactive substrates to release nonparenchymal cells from co-cultures at various time points, and subsequently characterize morphology and phenotypic functions of hepatocytes, and c) Develop miniaturized, multiwell co-culture models of human and rat liver tissue with optimized microscale architecture for pharmaceutical drug discovery and development.

7.2. Microenvironmental Cues for a Engineering a Functional Hepatic Tissue

With the recent advent of functional genomics, the opportunity now exists to correlate global patterns of gene expression with functional responses resulting from cell-cell interactions. In this dissertation, we developed a gene expression profiling approach to rapidly identify potential molecular mediators of the co-culture effect (see chapter 2) [58]. A list of 17 candidate genes in the cell communication category (extracellular matrix, soluble factors and cell-cell contact molecules) was obtained, and two of these candidates were functionally validated in a specific co-culture model, one in which hepatocytes

interact with murine embryonic 3T3 fibroblasts. Cadherins (cell adhesion molecules) were implicated in co-cultures via immunofluorescent staining, while purified decorin (a small proteoglycan that binds collagen) was shown to induce liver-specific functions in primary rat hepatocytes in both pure cultures and co-cultures lacking endogenous decorin production. Our study produced the first global molecular definition of a hepatocyte-stabilizing microenvironment. Furthermore, the role of decorin in modulating hepatocyte functions and the presence of N-cadherin at heterotypic boundaries (i.e. between hepatocytes and fibroblasts) has not been reported previously in the literature. Decorin, in particular, may find use as a ‘coating’ for biomaterials (synthetic or natural) designed for inducing functions in pure hepatocytes or hepatocyte-nonparenchymal co-cultures.

We extensively characterized the role of one of our candidates, T-cadherin, in modulation of hepatocyte functions *in vitro* (see chapter 3). T-cad is atypical since it lacks transmembrane and cytoplasmic domains and is instead linked to the cell membrane via a GPI anchor [92]. Though the role of T-cad in various organ systems and in cancerous tissues has been studied over the past decade, its role in the liver remains unknown [93]. In this dissertation, we showed that both cellular and a-cellular (i.e. purified) presentation of T-cad upregulated a variety of liver-specific functions in primary hepatocytes. Our results demonstrate a novel role of T-cad in liver biology. Future studies in our laboratory are aimed at a) determining the molecular binding partner of nonparenchymal-derived T-cad on the hepatocyte surface, b) elucidating the role of T-cad in the liver *in vivo*, and c) incorporating T-cad into natural and synthetic biomaterials for 3-dimensional culture of hepatocytes and co-cultures.

The functional genomic approach and its validation constitute merely the first step in obtaining a complete picture of the molecular cues that stabilize hepatocyte functions in co-culture. Our laboratory is currently evaluating some of the other

candidate molecules for their inductive effects. In the future, a combinatorial screening process using high-throughput platforms (i.e. extracellular matrix microarray [338]) may provide molecular design criteria for engineering an optimal microenvironment for hepatocytes and other cell types of the liver.

Though we have applied our functional genomic approach to a co-culture model of the rat liver, we anticipate that it can be applied to other *in vitro* systems where cell-cell interactions modulate cell fate processes (i.e. differentiation, migration, apoptosis, and proliferation). For instance, different stromal cell lines used as feeder layers have variable capacities to maintain renewal of stem cells (i.e. replication into a daughter cell with equivalent developmental potential). Application of our methodology to such stromal cell lines may yield candidate molecules underlying the observed renewal responses. Indeed, a similar approach was utilized a few years ago by Hackney et al in a hematopoietic stem cell model [340].

7.3. Dynamic Substrates for Studies of Heterotypic Cell-Cell Signaling

Conventional cell culture approaches rely on an essentially irreversible adsorption of proteins onto a surface such as glass or polystyrene. These proteins undergo various conformational changes and can exchange with proteins in solution. As a result, dynamic control over the structure and density of adsorbed proteins on conventional surfaces is not possible. The advent of self-assembled monolayers (SAMs) of alkanethiolates on gold has recently enabled rigorous control over the structure, density and pattern of immobilized ligands (i.e. cell adhesion peptides) presented to cells [161]. These SAMs have been utilized to explore novel mechanisms underlying cellular behavior [148, 341]. A recent modification by the Mrksich group has linked ligands to the underlying SAMs via redox active groups that can be cleaved or conjugated to the surface in real-time [158].

Such chemistries have been used to dynamically control cell attachment to a surface [147, 162]. In this dissertation, we have developed and optimized novel soft-lithographic processes to employ electroactive substrates in the study of heterotypic signaling in hepatocyte-nonparenchymal co-cultures (see chapter 4). We showed that selective release of nonparenchymal cells from co-culture caused necrosis (cell death) in primary hepatocytes, suggesting that insoluble molecules (extracellular matrix and cell-cell contact molecules) may be required to maintain liver-specific functions *in vitro*.

Future studies with electroactive SAMs will involve obtaining global gene expression profiles of hepatocytes and fibroblasts after they have interacted with each other in co-culture. Furthermore, using recently developed electroactive chemistries that allow detachment and reattachment of secondary cell types [264], we plan to investigate how hepatocyte functions are affected once they are allowed to interact with multiple nonparenchymal cell types over a particular time course. Such dynamic heterotypic signaling is reminiscent of developmental pathways, and electroactive substrates may present the opportunity to recapitulate these *in vivo* responses *in vitro*.

Heterotypic cell-cell interactions are important in a variety of different *in vivo* and *in vitro* processes. Therefore, we anticipate that our methods utilizing electroactive substrates can be generalized to other model systems fairly seamlessly. Since the density and type of adhesion peptides can be engineered onto the electroactive SAMs with relative ease, other cell types can be used to study the dynamics of heterotypic cell-cell interactions. For instance, Song et al [271] recently discovered in an *in vitro* co-culture model that adult astrocytes from hippocampus are capable of regulating neurogenesis by instructing stem cells to adopt a neuronal fate. Electroactive substrates could be used to assess the dynamics of neurogenesis resulting from such cellular interactions.

7.4. Improved Tissue Models for Drug Development

The leading cause of pre-launch and post-market attrition of pharmaceuticals is drug-induced liver disease, which poses a significant challenge for clinicians, the pharmaceutical industry and regulatory agencies worldwide [172]. Animal models are useful for *in vivo* and *in vitro* evaluation of ADME/Tox (absorption, distribution, metabolism, excretion and toxicity) properties of drug candidates; however, significant and well-documented differences in hepatocellular functions across species necessitate the development and utilization of *in vitro* models of the human liver [174, 175]. Elimination of problematic compounds earlier in the drug development pipeline (i.e. before they reach clinical trials or the market) represents the single largest cost-savings opportunity for the pharmaceutical industry [169]. Recent progress has been made in incorporating human liver models in drug development; however, it is widely known that current systems need much improvement in terms of their functional stability [176]. In such models, primary human hepatocytes suffer from a rapid (few days) decline in viability and liver-specific functions, and thus cannot be used for studies in which cultures are exposed repeatedly to a compound over several weeks (i.e. chronic toxicity) in order to mimic clinical scenarios.

In this dissertation, we combined tissue engineering and microtechnology techniques to create a long-term (several weeks) model of human liver tissue with optimal microscale architecture (see chapter 5). Our previous data had indicated the utility of microfabrication tools (photolithography) in modulating liver-specific functions in co-cultures of primary *rat* hepatocytes and 3T3 fibroblasts [123]. In particular, we found that functions of primary rat hepatocytes were highest when heterotypic interactions were maximized and homotypic interactions between hepatocytes were minimized (i.e. single hepatocyte island surrounded on all sides by fibroblasts). Here, we extended this work to primary *human* hepatocytes and discovered that these cells were more dependent on

homotypic interactions than their rat counterparts. Furthermore, an appropriate balance of homotypic and heterotypic interactions produced optimal liver-specific functions in human hepatocytes. We subsequently developed a stencil-based soft-lithographic process to miniaturize these optimal micropatterned co-cultures in a multi-well platform for higher throughput experimentation. Next, we characterized long-term stability of the liver platform using a variety of different criteria which included: global gene expression profiling, secretion of liver-specific proteins, nitrogen metabolism and activity of drug metabolism enzymes (Phase I and II). Lastly, the platform was validated using clinically-relevant compounds and assays commonly employed in the pharmaceutical industry. Validation studies included modulation of drug metabolism enzyme activity due to drug-drug interactions, and ranking of hepatotoxins by their potential to cause acute mitochondrial toxicity. For example, Troglitazone (oral hypoglycemic withdrawn from the market due to severe hepatotoxicity) was found to be more toxic in our model as compared to its FDA-approved analogues, Rosiglitazone and Ciaglitazone.

Whole animal models provide valuable *in vivo* data and constitute a FDA-required component of drug development. However, they are too slow for real-time feedback in a drug discovery campaign. An *in vitro* model of the rat liver can be used to screen for ADME/Tox properties in high-throughput platforms. We have adapted some of the techniques utilized for developing our human liver model to create a co-culture model of the rat liver that remains functional for over 2 months (see chapter 6). We showed utility of the platform in drug development via studies of drug-drug interactions, hepatotoxicity (acute and chronic), and detection of *in vivo*-relevant species-specific differences in Phase I and II metabolism (i.e. rat versus human liver tissues).

Combined with our micropatterned human hepatocyte co-cultures, we anticipate that the rat liver model may find use in eliminating compounds with problematic

ADME/Tox profiles earlier in drug discovery, which may ultimately reduce development costs, increase the likelihood of clinical success and reduce patient exposure to unsafe drugs. Integration of our microscale liver models into a lab-on-a-chip platform with multiple tissues may, in the future, constitute an important paradigm shift in preclinical testing of new drug candidates.

Future studies in our laboratory will focus on a) further optimizing the microenvironment of human hepatocyte co-cultures to enable liver-specific stability for several months, and b) creating a soft-lithographic process that yields miniaturized micropatterned co-cultures in off-the-shelf multiwell polystyrene plates. In this dissertation, we have relied on collagen as the underlying extracellular matrix (ECM) for hepatocyte attachment and spreading. However, recently published work from our laboratory has shown that combinations of various ECM molecules (i.e. fibronectin, laminin) can be used to modulate hepatocyte functions [338]. In the future, we plan on using high-throughput spotting platforms to screen for matrix molecules and their combinations which provide for optimal liver-specific functions in human hepatocyte-fibroblast co-cultures. Besides the extracellular matrix scaffold, the culture medium used in this dissertation can also be optimized by supplementing it with various additives (those known in the literature to induce hepatic functions) in order to improve function and longevity of the liver tissues. Furthermore, the ratio of the two cell types and the center-to-center spacing of the micropatterned hepatocyte islands can be varied to determine the impact on hepatocyte functions. We have preliminary data which indicates that these parameters may indeed be useful in functional optimization of co-cultures.

Stencils are reusable, can yield thousands of repeating tissue structures in a matter of hours, and are a robust alternative to photolithographic micropatterning, which is a serial technique requiring specialized equipment for each experiment. However, there are

several limitations associated with stencil use, which include: use of non-standard multiwell plates, permeability of PDMS to hydrophobic compounds, and cumbersome alignment steps (see chapter 6 ‘Discussion’ section for additional details). To overcome these limitations, we are developing an alternative strategy (work of David Eddington, post-doctoral fellow) that can yield micropatterns rapidly in 24- to 96-well plates available from commercial vendors. Furthermore, this strategy is amenable to robotic manipulation for easier and faster manufacturability.

Microtechnology has been used by several investigators to a) probe and optimize cellular functions in different tissue models, and b) miniaturize platforms towards consumption of fewer reagents (i.e. microfluidics). In this dissertation, we have developed a framework that combines microtechnology with tissue engineering to create optimized and miniaturized tissues for *in vitro* studies (i.e. drug screening, cell-based therapies for liver disease). Though we applied this framework towards developing an urgently needed human liver tissue for drug development, we anticipate that our methods can be adapted seamlessly to build other tissues for eventual integration into a multi-tissue platform. Lastly, the development of better *in vitro* models for drug screening and fundamental studies of physiology and pathophysiology may represent a new direction for the field of tissue engineering, which until recently has been focused on clinical applications.

7.5. Conclusions

The microenvironment or ‘niche’ is an important regulator of cellular fates. Local microenvironmental stimuli surrounding a single cell typically include: neighboring cells, an extracellular matrix scaffold, soluble factors, and physical forces. In this dissertation, we have developed novel strategies to explore the underlying molecular mechanisms and

dynamics of cell-cell interactions. Furthermore, we have combined microtechnology with tissue engineering to build improved in vitro tissue models. Application of these strategies to a robust in vitro model of the liver, namely hepatocyte-nonparenchymal cocultures, yielded: a) discovery of molecules that induce liver-specific functions in hepatocytes, b) insights into the dynamics of heterotypic cell signaling, and c) optimized and miniaturized in vitro liver tissues that were subsequently validated for drug development. In the future, we anticipate that the techniques and data presented here will be useful for fundamental investigations of cell-cell interactions in a multitude of tissue models, and towards building highly functional tissues for different applications.

REFERENCES

1. Allen, J.W., T. Hassanein, and S.N. Bhatia, *Advances in bioartificial liver devices*. Hepatology, 2001. **34**(3): p. 447-55.
2. Strom, S.C., et al., *Hepatocyte transplantation as a bridge to orthotopic liver transplantation in terminal liver failure*. Transplantation, 1997. **63**(4): p. 559-69.
3. Rakela, J., et al., *Fulminant hepatitis: Mayo Clinic experience with 34 cases*. Mayo Clin Proc, 1985. **60**(5): p. 289-92.
4. Ostapowicz, G., et al., *Results of a prospective study of acute liver failure at 17 tertiary care centers in the United States*. Ann Intern Med, 2002. **137**(12): p. 947-54.
5. Lin, H.M., et al., *Center-specific graft and patient survival rates: 1997 United Network for Organ Sharing (UNOS) report [see comments]*. Jama, 1998. **280**(13): p. 1153-60.
6. Starzl, T.E., *Medawar Prize Lecture. Liver allo- and xenotransplantation*. Transplant Proc, 1993. **25**(1 Pt 1): p. 15-7.
7. Schmoeckel, M., et al., *Xenotransplantation of pig organs transgenic for human DAF: an update*. Transplant Proc, 1997. **29**(7): p. 3157-8.
8. Patience, C., Y. Takeuchi, and R.A. Weiss, *Infection of human cells by an endogenous retrovirus of pigs*. Nat Med, 1997. **3**(3): p. 282-6.
9. Allen, J.W. and S.N. Bhatia, *Engineering liver therapies for the future*. Tissue Eng, 2002. **8**(5): p. 725-37.
10. Mito, M. and M. Sawa, *Hepatocyte transplantation: past, present and future*. Wiad Lek, 1997. **50**(Su 1 Pt 1): p. 416-9.
11. Chowdhury, J.R., et al., *Human hepatocyte transplantation: gene therapy and more?* Pediatrics, 1998. **102**(3 Pt 1): p. 647-8.
12. Gupta, S., G.R. Gorla, and A.N. Irani, *Hepatocyte transplantation: emerging insights into mechanisms of liver repopulation and their relevance to potential therapies*. J Hepatol, 1999. **30**(1): p. 162-70.
13. Demetriou, A.A., et al., *Replacement of liver function in rats by transplantation of microcarrier-attached hepatocytes*. Science, 1986. **233**(4769): p. 1190-2.
14. Jauregui, H.O., N.R. Chowdhury, and J.R. Chowdhury, *Use of mammalian liver cells for artificial liver support*. Cell Transplant, 1996. **5**(3): p. 353-67.

15. McGuire, B.M., et al., *Review of support systems used in the management of fulminant hepatic failure*. *Dig Dis*, 1995. **13**(6): p. 379-88.
16. Rozga, J. and A.A. Demetriou, *Artificial liver. Evolution and future perspectives*. *Asaio J*, 1995. **41**(4): p. 831-7.
17. Taguchi, K., et al., *Development of a bioartificial liver with sandwiched-cultured hepatocytes between two collagen gel layers*. *Artif Organs*, 1996. **20**(2): p. 178-85.
18. Strain, A.J., *Ex vivo liver cell morphogenesis: one step nearer to the bioartificial liver? [editorial; comment]*. *Hepatology*, 1999. **29**(1): p. 288-90.
19. Dunn, J.C., et al., *Hepatocyte function and extracellular matrix geometry: long-term culture in a sandwich configuration [published erratum appears in FASEB J 1989 May;3(7):1873]*. *Faseb J*, 1989. **3**(2): p. 174-7.
20. Fox, I.J., et al., *Treatment of the Crigler-Najjar syndrome type I with hepatocyte transplantation [see comments]*. *N Engl J Med*, 1998. **338**(20): p. 1422-6.
21. Kaihara, S. and J.P. Vacanti, *Tissue engineering: toward new solutions for transplantation and reconstructive surgery*. *Arch Surg*, 1999. **134**(11): p. 1184-8.
22. Elcin, Y.M., V. Dixit, and G. Gitnick, *Hepatocyte attachment on biodegradable modified chitosan membranes: in vitro evaluation for the development of liver organoids*. *Artif Organs*, 1998. **22**(10): p. 837-46.
23. Mooney, D.J., et al., *Long-term engraftment of hepatocytes transplanted on biodegradable polymer sponges*. *J Biomed Mater Res*, 1997. **37**(3): p. 413-20.
24. Demetriou, A.A., et al., *Survival, organization, and function of microcarrier-attached hepatocytes transplanted in rats*. *Proc Natl Acad Sci U S A*, 1986. **83**(19): p. 7475-9.
25. Chang, T.M., *Bioencapsulated hepatocytes for experimental liver support*. *J Hepatol*, 2001. **34**(1): p. 148-9.
26. Cai, Z.H., et al., *Microencapsulated hepatocytes for bioartificial liver support*. *Artif Organs*, 1988. **12**(5): p. 388-93.
27. Griffith, L.G. and G. Naughton, *Tissue engineering--current challenges and expanding opportunities*. *Science*, 2002. **295**(5557): p. 1009-14.
28. Strain, A.J. and J.M. Neuberger, *A bioartificial liver--state of the art*. *Science*, 2002. **295**(5557): p. 1005-9.
29. Yarmush, M.L., J.C. Dunn, and R.G. Tompkins, *Assessment of artificial liver support technology*. *Cell Transplant*, 1992. **1**(5): p. 323-41.
30. Wolfe, S.P., et al., *A novel multi-coaxial hollow fiber bioreactor for adherent cell types. Part 1: hydrodynamic studies*. *Biotechnol Bioeng*, 2002. **77**(1): p. 83-90.

31. Gerlach, J.C., et al., *Bioreactor for a larger scale hepatocyte in vitro perfusion*. *Transplantation*, 1994. **58**(9): p. 984-8.
32. Tilles, A.W., et al., *Effects of oxygenation and flow on the viability and function of rat hepatocytes cocultured in a microchannel flat-plate bioreactor*. *Biotechnol Bioeng*, 2001. **73**(5): p. 379-89.
33. Naruse, K., et al., *Development of a new bioartificial liver module filled with porcine hepatocytes immobilized on non-woven fabric*. *Int J Artif Organs*, 1996. **19**(6): p. 347-52.
34. Gion, T., et al., *Evaluation of a hybrid artificial liver using a polyurethane foam packed-Bed culture system in dogs*. *J Surg Res*, 1999. **82**(2): p. 131-6.
35. Dore, E. and C. Legallais, *A new concept of bioartificial liver based on a fluidized bed bioreactor*. *Ther Apher*, 1999. **3**(3): p. 264-7.
36. Joly, A., et al., *Survival, proliferation, and functions of porcine hepatocytes encapsulated in coated alginate beads: a step toward a reliable bioartificial liver*. *Transplantation*, 1997. **63**(6): p. 795-803.
37. Ting, P.P. and A.A. Demetriou, *Clinical experience with artificial liver support systems*. *Can J Gastroenterol*, 2000. **14 Suppl D**: p. 79D-84D.
38. Watanabe, F.D., et al., *Clinical experience with a bioartificial liver in the treatment of severe liver failure. A phase I clinical trial*. *Ann Surg*, 1997. **225**(5): p. 484-91; discussion 491-4.
39. Sussman, N.L., et al., *The Hepatix extracorporeal liver assist device: initial clinical experience*. *Artif Organs*, 1994. **18**(5): p. 390-6.
40. Ellis, A.J., et al., *Pilot-controlled trial of the extracorporeal liver assist device in acute liver failure*. *Hepatology*, 1996. **24**(6): p. 1446-51.
41. Li, A.P., *Human hepatocytes as an experimental system for the evaluation of xenobiotics*, in *The Hepatocyte Review*, M.N.E. Berry, A. M., Editor. 2000, Kluwer Academic Publishers. p. 391-410.
42. Cederbaum, A.I., et al., *CYP2E1-dependent toxicity and oxidative stress in HepG2 cells*. *Free Radic Biol Med*, 2001. **31**(12): p. 1539-43.
43. Fukaya, K., et al., *Establishment of a human hepatocyte line (OUMS-29) having CYP 1A1 and 1A2 activities from fetal liver tissue by transfection of SV40 LT*. *In Vitro Cell Dev Biol Anim*, 2001. **37**(5): p. 266-9.
44. Liu, J., et al., *Characterization and evaluation of detoxification functions of a nontumorigenic immortalized porcine hepatocyte cell line (HepLin)*. *Cell Transplantation*, 1999. **8**(3): p. 219-232.
45. Dabeva, M.D. and D.A. Shafritz, *Hepatic stem cells and liver repopulation*. *Semin Liver Dis*, 2003. **23**(4): p. 349-62.

46. Thorgeirsson, S.S. and J.W. Grisham, *Overview of recent experimental studies on liver stem cells*. Semin Liver Dis, 2003. **23**(4): p. 303-12.
47. Jiang, Y., et al., *Pluripotency of mesenchymal stem cells derived from adult marrow*. Nature, 2002. **418**(6893): p. 41-9.
48. Schwartz, R.E., et al., *Multipotent adult progenitor cells from bone marrow differentiate into functional hepatocyte-like cells*. J Clin Invest, 2002. **109**(10): p. 1291-302.
49. Thomson, J.A., et al., *Embryonic stem cell lines derived from human blastocysts*. Science, 1998. **282**(5391): p. 1145-7.
50. Grompe, M., *Therapeutic liver repopulation for the treatment of metabolic liver diseases*. Hum Cell, 1999. **12**(4): p. 171-80.
51. Grompe, M., *The origin of hepatocytes*. Gastroenterology, 2005. **128**(7): p. 2158-60.
52. Shambloott, M.J., et al., *Derivation of pluripotent stem cells from cultured human primordial germ cells*. Proc Natl Acad Sci U S A, 1998. **95**(23): p. 13726-31.
53. Petersen, B.E., V.F. Zajac, and G.K. Michalopoulos, *Hepatic oval cell activation in response to injury following chemically induced periportal or pericentral damage in rats*. Hepatology, 1998. **27**(4): p. 1030-8.
54. Overturf, K., et al., *The repopulation potential of hepatocyte populations differing in size and prior mitotic expansion*. Am J Pathol, 1999. **155**(6): p. 2135-43.
55. Jang, Y.Y., et al., *Hematopoietic stem cells convert into liver cells within days without fusion*. Nat Cell Biol, 2004. **6**(6): p. 532-9.
56. Ruhnke, M., et al., *Human monocyte-derived neobepatocytes: a promising alternative to primary human hepatocytes for autologous cell therapy*. Transplantation, 2005. **79**(9): p. 1097-103.
57. Guguen-Guillouzo, C. and A. Guillouzo, *Modulation of functional activities in cultured rat hepatocytes*. Mol Cell Biochem, 1983. **53-54**(1-2): p. 35-56.
58. Khetani, S.R., et al., *Exploring interactions between rat hepatocytes and nonparenchymal cells using gene expression profiling*. Hepatology, 2004. **40**(3): p. 545-54.
59. Tzanakakis, E.S., et al., *Extracorporeal tissue engineered liver-assist devices*. Annu Rev Biomed Eng, 2000. **2**: p. 607-32.
60. Fausto, N., *Liver regeneration*. J Hepatol, 2000. **32**(1 Suppl): p. 19-31.
61. Reid, L.M., et al., *Extracellular matrix gradients in the space of Disse: relevance to liver biology [editorial]*. Hepatology, 1992. **15**(6): p. 1198-203.
62. Rappaport, A.M., et al., *Subdivision of hexagonal liver lobules into a structural and functional unit; role in hepatic physiology and pathology*. Anat Rec, 1954. **119**(1): p. 11-33.

63. Gebhardt, R., *Metabolic zonation of the liver: regulation and implications for liver function.* Pharmacol Ther, 1992. **53**(3): p. 275-354.
64. Lindros, K.O., *Zonation of cytochrome P450 expression, drug metabolism and toxicity in liver.* Gen Pharmacol, 1997. **28**(2): p. 191-6.
65. Bhatia, S.N., et al., *Effect of cell-cell interactions in preservation of cellular phenotype: cocultivation of hepatocytes and nonparenchymal cells.* Faseb J, 1999. **13**(14): p. 1883-900.
66. Angst, B.D., C. Marcozzi, and A.I. Magee, *The cadherin superfamily: diversity in form and function.* J Cell Sci, 2001. **114**(Pt 4): p. 629-41.
67. Steinberg, M.S. and P.M. McNutt, *Cadherins and their connections: adhesion junctions have broader functions.* Curr Opin Cell Biol, 1999. **11**(5): p. 554-60.
68. Omelchenko, T., et al., *Contact interactions between epitheliocytes and fibroblasts: formation of heterotypic cadherin-containing adhesion sites is accompanied by local cytoskeletal reorganization.* Proc Natl Acad Sci U S A, 2001. **98**(15): p. 8632-7.
69. Schnadelbach, O., et al., *N-cadherin influences migration of oligodendrocytes on astrocyte monolayers.* Mol Cell Neurosci, 2000. **15**(3): p. 288-302.
70. Voura, E.B., M. Sandig, and C.H. Siu, *Cell-cell interactions during transendothelial migration of tumor cells.* Microsc Res Tech, 1998. **43**(3): p. 265-75.
71. Knudsen, K.A., et al., *A role for cadherins in cellular signaling and differentiation.* J Cell Biochem Suppl, 1998. **30-31**: p. 168-76.
72. George-Weinstein, M., et al., *N-cadherin promotes the commitment and differentiation of skeletal muscle precursor cells.* Dev Biol, 1997. **185**(1): p. 14-24.
73. Burdsal, C.A., C.H. Damsky, and R.A. Pedersen, *The role of E-cadherin and integrins in mesoderm differentiation and migration at the mammalian primitive streak.* Development, 1993. **118**(3): p. 829-44.
74. Vleminckx, K. and R. Kemler, *Cadherins and tissue formation: integrating adhesion and signaling.* Bioessays, 1999. **21**(3): p. 211-20.
75. Daniel, J.M. and A.B. Reynolds, *Tyrosine phosphorylation and cadherin/catenin function.* Bioessays, 1997. **19**(10): p. 883-91.
76. Xu, Y., et al., *Interaction of the adaptor protein Shc and the adhesion molecule cadherin.* J Biol Chem, 1997. **272**(21): p. 13463-6.
77. Muller, K.M., et al., *Involvement of E-cadherin in thymus organogenesis and thymocyte maturation.* Immunity, 1997. **6**(3): p. 257-64.
78. Armeanu, S., et al., *E-cadherin is functionally involved in the maturation of the erythroid lineage.* J Cell Biol, 1995. **131**(1): p. 243-9.

79. Linask, K.K., K.A. Knudsen, and Y.H. Gui, *N-cadherin-catenin interaction: necessary component of cardiac cell compartmentalization during early vertebrate heart development*. Dev Biol, 1997. **185**(2): p. 148-64.
80. Radice, G.L., et al., *Precocious mammary gland development in P-cadherin-deficient mice*. J Cell Biol, 1997. **139**(4): p. 1025-32.
81. Rosenberg, P., et al., *A potential role of R-cadherin in striated muscle formation*. Dev Biol, 1997. **187**(1): p. 55-70.
82. Larue, L., et al., *A role for cadherins in tissue formation*. Development, 1996. **122**(10): p. 3185-94.
83. Scoazec, J.Y., *Adhesion molecules in normal human liver*. Hepatogastroenterology, 1996. **43**(11): p. 1103-5.
84. Bode, H.P., et al., *Expression and regulation of gap junctions in rat cholangiocytes*. Hepatology, 2002. **36**(3): p. 631-40.
85. Ihara, A., et al., *Expression of epithelial cadherin and alpha- and beta-catenins in nontumoral livers and hepatocellular carcinomas*. Hepatology, 1996. **23**(6): p. 1441-7.
86. Monga, S.P., et al., *Changes in WNT/beta-catenin pathway during regulated growth in rat liver regeneration*. Hepatology, 2001. **33**(5): p. 1098-109.
87. Hamilton, G.A., et al., *Regulation of cell morphology and cytochrome P450 expression in human hepatocytes by extracellular matrix and cell-cell interactions*. Cell Tissue Res, 2001. **306**(1): p. 85-99.
88. Gallin, W.J., *Development and maintenance of bile canaliculi in vitro and in vivo*. Microsc Res Tech, 1997. **39**(5): p. 406-12.
89. Moghe, P.V., et al., *Culture matrix configuration and composition in the maintenance of hepatocyte polarity and function*. Biomaterials, 1996. **17**(3): p. 373-85.
90. Hou, D.X., et al., *Expression of cell adhesion molecule and albumin genes in primary culture of rat hepatocytes*. Cell Biol Int, 2001. **25**(3): p. 239-44.
91. Brieva, T.A. and P.V. Moghe, *Functional engineering of hepatocytes via heterocellular presentation of a homoadhesive molecule, E-cadherin*. Biotechnol Bioeng, 2001. **76**(4): p. 295-302.
92. Ranscht, B. and M.T. Dours-Zimmermann, *T-cadherin, a novel cadherin cell adhesion molecule in the nervous system lacks the conserved cytoplasmic region*. Neuron, 1991. **7**(3): p. 391-402.
93. Takeuchi, T. and Y. Ohtsuki, *Recent progress in T-cadherin (CDH13, H-cadherin) research*. Histol Histopathol, 2001. **16**(4): p. 1287-93.
94. Fredette, B.J., J. Miller, and B. Ranscht, *Inhibition of motor axon growth by T-cadherin substrata*. Development, 1996. **122**(10): p. 3163-71.

95. Lee, S.W., *H-cadherin, a novel cadherin with growth inhibitory functions and diminished expression in human breast cancer*. Nat Med, 1996. **2**(7): p. 776-82.
96. Sato, M., et al., *The H-cadherin (CDH13) gene is inactivated in human lung cancer*. Hum Genet, 1998. **103**(1): p. 96-101.
97. Kawakami, M., et al., *Involvement of H-cadherin (CDH13) on 16q in the region of frequent deletion in ovarian cancer*. Int J Oncol, 1999. **15**(4): p. 715-20.
98. Tkachuk, V.A., et al., *Identification of an atypical lipoprotein-binding protein from human aortic smooth muscle as T-cadherin*. FEBS Lett, 1998. **421**(3): p. 208-12.
99. Hug, C., et al., *T-cadherin is a receptor for hexameric and high-molecular-weight forms of Acrp30/adiponectin*. Proc Natl Acad Sci U S A, 2004. **101**(28): p. 10308-13.
100. Ivanov, D.B., M.P. Philippova, and V.A. Tkachuk, *Structure and functions of classical cadherins*. Biochemistry (Mosc), 2001. **66**(10): p. 1174-86.
101. Philippova, M.P., et al., *T-cadherin and signal-transducing molecules co-localize in caveolin-rich membrane domains of vascular smooth muscle cells*. FEBS Lett, 1998. **429**(2): p. 207-10.
102. Douarin, N.M., *An experimental analysis of liver development*. Med Biol, 1975. **53**(6): p. 427-55.
103. Houssaint, E., *Differentiation of the mouse hepatic primordium. I. An analysis of tissue interactions in hepatocyte differentiation*. Cell Differ, 1980. **9**(5): p. 269-79.
104. Michalopoulos, G.K. and M.C. DeFrances, *Liver regeneration*. Science, 1997. **276**(5309): p. 60-6.
105. Olson, M.J., et al., *Hepatocyte cytodifferentiation and cell-to-cell communication*, in *Cell Intercommunication*, W.C. De Mello, Editor. 1990, CRC Press: Boca Raton, Florida. p. 71-92.
106. West, M.A., R. Manthei, and M.P. Bubrick, *Autoregulation of hepatic macrophage activation in sepsis*. J Trauma, 1993. **34**(4): p. 473-9; discussion 479-80.
107. Monden, K., et al., *Enhancement of hepatic macrophages in septic rats and their inhibitory effect on hepatocyte function*. J Surg Res, 1991. **50**(1): p. 72-6.
108. Strom, S., A.D. Kligerman, and G. Michalopoulos, *Comparisons of the effects of chemical carcinogens in mixed cultures of rat hepatocytes and human fibroblasts*. Carcinogenesis, 1981. **2**(8): p. 709-15.
109. Langenbach, R., H.J. Freed, and E. Huberman, *Liver cell-mediated mutagenesis of mammalian cells by liver carcinogens*. Proc Natl Acad Sci U S A, 1978. **75**(6): p. 2864-7.
110. Guillouzo, A., et al., *Use of human hepatocyte cultures for drug metabolism studies*. Toxicology, 1993. **82**(1-3): p. 209-19.

111. Mendoza-Figueroa, T., A. Hernandez, and M.L. Lopez, *Triglyceride accumulation in long-term cultures of adult rat hepatocytes by chronic exposure to Aroclor 1254*. J Toxicol Environ Health, 1989. **26**(3): p. 293-308.
112. Mertens, K., V. Rogiers, and A. Vercruyssen, *Glutathione dependent detoxication in adult rat hepatocytes under various culture conditions*. Arch Toxicol, 1993. **67**(10): p. 680-5.
113. Rincon-Sanchez, A.R., et al., *Synthesis and secretion of lipids by long-term cultures of female rat hepatocytes*. Biol Cell, 1992. **76**(2): p. 131-8.
114. De La Vega, F.M. and T. Mendoza-Figueroa, *Dimethyl sulfoxide enhances lipid synthesis and secretion by long-term cultures of adult rat hepatocytes*. Biochimie, 1991. **73**(5): p. 621-4.
115. Lebreton, J.P., et al., *Long-term biosynthesis of complement component C3 and alpha-1 acid glycoprotein by adult rat hepatocytes in a co-culture system with an epithelial liver cell-type*. Biochem J, 1986. **235**(2): p. 421-7.
116. Guillouzo, A., et al., *Long term production of acute-phase proteins by adult rat hepatocytes co-cultured with another liver cell type in serum-free medium*. Biochem Biophys Res Commun, 1984. **120**(2): p. 311-7.
117. Donato, M.T., J.V. Castell, and M.J. Gomez-Lechon, *Co-cultures of hepatocytes with epithelial-like cell lines: expression of drug-biotransformation activities by hepatocytes*. Cell Biol Toxicol, 1991. **7**(1): p. 1-14.
118. Jongen, W.M., et al., *A co-cultivation system consisting of primary chick embryo hepatocytes and V79 Chinese hamster cells as a model for metabolic cooperation studies*. Carcinogenesis, 1987. **8**(6): p. 767-72.
119. Guguen-Guillouzo, C., et al., *Modulation of human fetal hepatocyte survival and differentiation by interactions with a rat liver epithelial cell line*. Dev Biol, 1984. **105**(1): p. 211-20.
120. Clement, B., et al., *Long-term co-cultures of adult human hepatocytes with rat liver epithelial cells: modulation of albumin secretion and accumulation of extracellular material*. Hepatology, 1984. **4**(3): p. 373-80.
121. Bhatia, S.N., M.L. Yarmush, and M. Toner, *Controlling cell interactions by micropatterning in co-cultures: hepatocytes and 3T3 fibroblasts*. J Biomed Mater Res, 1997. **34**(2): p. 189-99.
122. Talbot, N.C., et al., *Colony isolation and secondary culture of fetal porcine hepatocytes on STO feeder cells*. In Vitro Cell Dev Biol Anim, 1994. **30A**(12): p. 851-8.
123. Bhatia, S.N., et al., *Probing heterotypic cell interactions: hepatocyte function in microfabricated co-cultures*. J Biomater Sci Polym Ed, 1998. **9**(11): p. 1137-60.
124. Bhandari, R.N., et al., *Liver tissue engineering: a role for co-culture systems in modifying hepatocyte function and viability*. Tissue Eng, 2001. **7**(3): p. 345-57.

125. Guguen-Guillouzo, C., et al., *Maintenance and reversibility of active albumin secretion by adult rat hepatocytes co-cultured with another liver epithelial cell type*. *Exp Cell Res*, 1983. **143**(1): p. 47-54.
126. Loreal, O., et al., *Cooperation of Ito cells and hepatocytes in the deposition of an extracellular matrix in vitro*. *Am J Pathol*, 1993. **143**(2): p. 538-44.
127. Kaihara, S., et al., *Survival and function of rat hepatocytes cocultured with nonparenchymal cells or sinusoidal endothelial cells on biodegradable polymers under flow conditions*. *J Pediatr Surg*, 2000. **35**(9): p. 1287-90.
128. Donato, M.T., M.J. Gomez-Lechon, and J.V. Castell, *Drug metabolizing enzymes in rat hepatocytes co-cultured with cell lines*. *In Vitro Cell Dev Biol*, 1990. **26**(11): p. 1057-62.
129. Utesch, D. and F. Oesch, *Dependency of the in vitro stabilization of differentiated functions in liver parenchymal cells on the type of cell line used for co-culture*. *In Vitro Cell Dev Biol*, 1992. **28A**(3 Pt 1): p. 193-8.
130. Shimaoka, S., T. Nakamura, and A. Ichihara, *Stimulation of growth of primary cultured adult rat hepatocytes without growth factors by coculture with nonparenchymal liver cells*. *Exp Cell Res*, 1987. **172**(1): p. 228-42.
131. Kuri-Harcuch, W. and T. Mendoza-Figueroa, *Cultivation of adult rat hepatocytes on 3T3 cells: expression of various liver differentiated functions*. *Differentiation*, 1989. **41**(2): p. 148-57.
132. Clement, B., et al., *Effect of hydrocortisone on deposition of types I and IV collagen in primary culture of rat hepatocytes*. *Cell Mol Biol*, 1988. **34**(5): p. 449-60.
133. Goulet, F., C. Normand, and O. Morin, *Cellular interactions promote tissue-specific function, biomatrix deposition and junctional communication of primary cultured hepatocytes*. *Hepatology*, 1988. **8**(5): p. 1010-8.
134. Baffet, G., et al., *Distinct effects of cell-cell communication and corticosteroids on the synthesis and distribution of cytokeratins in cultured rat hepatocytes*. *J Cell Sci*, 1991. **99 (Pt 3)**: p. 609-15.
135. Mesnil, M., et al., *Cell contact but not junctional communication (dye coupling) with biliary epithelial cells is required for hepatocytes to maintain differentiated functions*. *Exp Cell Res*, 1987. **173**(2): p. 524-33.
136. Corlu, A., et al., *A plasma membrane protein is involved in cell contact-mediated regulation of tissue-specific genes in adult hepatocytes*. *J Cell Biol*, 1991. **115**(2): p. 505-15.
137. Corlu, A., et al., *Tissue distribution of liver regulating protein. Evidence for a cell recognition signal common to liver, pancreas, gonads, and hemopoietic tissues*. *Am J Pathol*, 1994. **145**(3): p. 715-27.
138. Rojkind, M., et al., *Characterization and functional studies on rat liver fat-storing cell line and freshly isolated hepatocyte coculture system*. *Am J Pathol*, 1995. **146**(6): p. 1508-20.

139. Clemens, M.G., et al., *Hepatic intercellular communication in shock and inflammation*. Shock, 1994. **2**(1): p. 1-9.
140. Atencia, J. and D.J. Beebe, *Controlled microfluidic interfaces*. Nature, 2005. **437**(7059): p. 648-55.
141. Heller, M.J., *An active microelectronics device for multiplex DNA analysis*. IEEE Engineering in Medicine and Biology Magazine, 1996. **15**(2): p. 100-4.
142. Pease, A.C., et al., *Light-generated oligonucleotide arrays for rapid DNA sequence analysis*. Proceedings of the National Academy of Sciences of the United States of America, 1994. **91**(11): p. 5022-5026.
143. Ziauddin, J. and D.M. Sabatini, *Microarrays of cells expressing defined cDNAs*. Nature (London), 2001. **411**(6833): p. 107-110.
144. Seetharaman, S., et al., *Immobilized RNA switches for the analysis of complex chemical and biological mixtures*. Nature Biotechnology, 2001. **19**(4): p. 336-341.
145. MacBeath, G. and S.L. Schreiber, *Printing proteins as microarrays for high-throughput function determination*. Science (Washington D C), 2000. **289**(5485): p. 1760-1763.
146. Lee, K.-B., et al., *Protein nanoarrays generated by dip-pen nanolithography*. Science (Washington D C), 2002. **295**(5560): p. 1702-1705.
147. Yousaf, M.N., B.T. Houseman, and M. Mrksich, *Using electroactive substrates to pattern the attachment of two different cell populations*. Proc Natl Acad Sci U S A, 2001. **98**(11): p. 5992-6.
148. Chen, C.S., et al., *Geometric control of cell life and death*. Science, 1997. **276**(5317): p. 1425-8.
149. Singhvi, R., G. Stephanopoulos, and D.I.C. Wang, *Effects of Substratum Morphology On Cell Physiology - Review*. Biotechnology and Bioengineering, 1994. **43**(8): p. 764-771.
150. Clark, P., S. Britland, and P. Connolly, *Growth cone guidance and neuron morphology on micropatterned laminin surfaces*. J Cell Sci, 1993. **105**(Pt 1): p. 203-12.
151. Hammarback, J.A., et al., *Growth cone guidance by substrate-bound laminin pathways is correlated with neuron-to-pathway adhesivity*. Dev Biol, 1988. **126**(1): p. 29-39.
152. Voldman, J., M.L. Gray, and M.A. Schmidt, *Microfabrication in biology and medicine*. Annu Rev Biomed Eng, 1999. **1**: p. 401-25.
153. Whitesides, G.M., et al., *Soft lithography in biology and biochemistry*. Annu Rev Biomed Eng, 2001. **3**: p. 335-73.
154. Kane, R.S., et al., *Patterning proteins and cells using soft lithography*. Biomaterials, 1999. **20**(23-24): p. 2363-76.

155. Vozzi, G., et al., *Fabrication of PLGA scaffolds using soft lithography and microsyringe deposition*. *Biomaterials*, 2003. **24**(14): p. 2533-40.
156. Unger, M.A., et al., *Monolithic microfabricated valves and pumps by multilayer soft lithography*. *Science*, 2000. **288**(5463): p. 113-6.
157. Folch, A., et al., *Microfabricated elastomeric stencils for micropatterning cell cultures*. *J Biomed Mater Res*, 2000. **52**(2): p. 346-53.
158. Mrksich, M., *Tailored substrates for studies of attached cell culture*. *Cell Mol Life Sci*, 1998. **54**(7): p. 653-62.
159. Mrksich, M., et al., *Controlling cell attachment on contoured surfaces with self-assembled monolayers of alkanethiolates on gold*. *Proc Natl Acad Sci U S A*, 1996. **93**(20): p. 10775-8.
160. Mrksich, M., et al., *Using microcontact printing to pattern the attachment of mammalian cells to self-assembled monolayers of alkanethiolates on transparent films of gold and silver*. *Exp Cell Res*, 1997. **235**(2): p. 305-13.
161. Mrksich, M. and G.M. Whitesides, *Using self-assembled monolayers to understand the interactions of man-made surfaces with proteins and cells*. *Annu Rev Biophys Biomol Struct*, 1996. **25**: p. 55-78.
162. Yeo, W.S., C.D. Hodneland, and M. Mrksich, *Electroactive monolayer substrates that selectively release adherent cells*. *Chembiochem*, 2001. **2**(7-8): p. 590-3.
163. Gunaratna, C., *Drug Metabolism & Pharmacokinetics in Drug Discovery: A Primer for Bioanalytical Chemists, Part I*. *Current Separations*, 2000. **19**(1): p. 17-23.
164. DiMasi, J.A., R.W. Hansen, and H.G. Grabowski, *The price of innovation: new estimates of drug development costs*. *J Health Econ*, 2003. **22**(2): p. 151-85.
165. Sivaraman, A., et al., *A microscale in vitro physiological model of the liver: predictive screens for drug metabolism and enzyme induction*. *Curr Drug Metab*, 2005. **6**(6): p. 569-91.
166. Anand, S.S., et al., *Extent and timeliness of tissue repair determines the dose-related hepatotoxicity of chloroform*. *Int J Toxicol*, 2003. **22**(1): p. 25-33.
167. Venkatesh, S. and R.A. Lipper, *Role of the development scientist in compound lead selection and optimization*. *J Pharm Sci*, 2000. **89**(2): p. 145-54.
168. Tornell, J. and M. Snaith, *Transgenic systems in drug discovery: from target identification to humanized mice*. *Drug Discov Today*, 2002. **7**(8): p. 461-70.
169. Sussman, N.L., et al., *The predictive nature of high-throughput toxicity screening using a human hepatocyte cell line*. *Cell Notes*, 2002(3): p. 7-10.
170. Kaplowitz, N., *Idiosyncratic drug hepatotoxicity*. *Nat Rev Drug Discov*, 2005. **4**(6): p. 489-99.

171. Kaplowitz, N. and L. DeLeve, *Drug-Induced Liver Disease*. 2003, New York: Marcel Dekker. 773.
172. Kaplowitz, N., *Drug-induced liver disorders: implications for drug development and regulation*. *Drug Saf*, 2001. **24**(7): p. 483-90.
173. Lasser, K.E., et al., *Timing of new black box warnings and withdrawals for prescription medications*. *Jama*, 2002. **287**(17): p. 2215-20.
174. Olson, H., et al., *Concordance of the toxicity of pharmaceuticals in humans and in animals*. *Regul Toxicol Pharmacol*, 2000. **32**(1): p. 56-67.
175. Xu, J.J., D. Diaz, and P.J. O'Brien, *Applications of cytotoxicity assays and pre-lethal mechanistic assays for assessment of human hepatotoxicity potential*. *Chem Biol Interact*, 2004. **150**(1): p. 115-28.
176. Guillouzo, A., *Liver cell models in in vitro toxicology*. *Environ Health Perspect*, 1998. **106 Suppl 2**: p. 511-32.
177. Thohan, S. and G.M. Rosen, *Liver slice technology as an in vitro model for metabolic and toxicity studies*. *Methods Mol Biol*, 2002. **196**: p. 291-303.
178. Burwen, S.J., et al., *The perfused human liver wedge biopsy: a new in vitro model for morphological and functional studies*. *Hepatology*, 1982. **2**(4): p. 426-32.
179. Grosse-Siestrup, C., et al., *The isolated perfused liver. a new model using autologous blood and porcine slaughterhouse organs*. *J Pharmacol Toxicol Methods*, 2001. **46**(3): p. 163.
180. Venkatakrishnan, K., L.L. Von Moltke, and D.J. Greenblatt, *Evaluation of SupermixTM as an in vitro model of human liver microsomal drug metabolism*. *Biopharm Drug Dispos*, 2002. **23**(5): p. 183-90.
181. Donato, M.T., et al., *Fluorescence-based assays for screening nine cytochrome P450 (P450) activities in intact cells expressing individual human P450 enzymes*. *Drug Metab Dispos*, 2004. **32**(7): p. 699-706.
182. LeCluyse, E.L., *Human hepatocyte culture systems for the in vitro evaluation of cytochrome P450 expression and regulation*. *Eur J Pharm Sci*, 2001. **13**(4): p. 343-68.
183. Monteith, D.K., et al., *Induction of cytochrome P(1)450 RNA and benzo[a]pyrene metabolism in primary human hepatocyte cultures with benzoanthracene*. *Toxicol Appl Pharmacol*, 1990. **105**(3): p. 460-71.
184. DiPetrillo, K., et al., *Effect of caffeine on acetaminophen hepatotoxicity in cultured hepatocytes treated with ethanol and isopentanol*. *Toxicol Appl Pharmacol*, 2002. **185**(2): p. 91-7.
185. Li, A.P., et al., *Present status of the application of cryopreserved hepatocytes in the evaluation of xenobiotics: consensus of an international expert panel*. *Chem Biol Interact*, 1999. **121**(1): p. 117-23.

186. Li, A.P., et al., *Cryopreserved human hepatocytes: characterization of drug-metabolizing enzyme activities and applications in higher throughput screening assays for hepatotoxicity, metabolic stability, and drug-drug interaction potential*. Chem Biol Interact, 1999. **121**(1): p. 17-35.
187. Cross, D.M. and M.K. Bayliss, *A commentary on the use of hepatocytes in drug metabolism studies during drug discovery and development*. Drug Metab Rev, 2000. **32**(2): p. 219-40.
188. Gebhardt, R., et al., *New hepatocyte in vitro systems for drug metabolism: metabolic capacity and recommendations for application in basic research and drug development, standard operation procedures*. Drug Metab Rev, 2003. **35**(2-3): p. 145-213.
189. Madan, A., et al., *Effects of prototypical microsomal enzyme inducers on cytochrome P450 expression in cultured human hepatocytes*. Drug Metab Dispos, 2003. **31**(4): p. 421-31.
190. Inoue, C., et al., *Nicotinamide prolongs survival of primary cultured hepatocytes without involving loss of hepatocyte-specific functions*. J Biol Chem, 1989. **264**(9): p. 4747-50.
191. Laishes, B.A. and G.M. Williams, *Conditions affecting primary cell cultures of functional adult rat hepatocytes. II. Dexamethasone enhanced longevity and maintenance of morphology*. In Vitro, 1976. **12**(12): p. 821-32.
192. Laishes, B.A. and G.M. Williams, *Conditions affecting primary cell cultures of functional adult rat hepatocytes. 1. The effect of insulin*. In Vitro, 1976. **12**(7): p. 521-32.
193. Enat, R., et al., *Hepatocyte proliferation in vitro: its dependence on the use of serum-free hormonally defined medium and substrata of extracellular matrix*. Proc Natl Acad Sci U S A, 1984. **81**(5): p. 1411-5.
194. Reid, L.M., et al., *Matrix and hormonal regulation of differentiation in liver cultures*, in *Isolated and Cultured Hepatocytes*, A. Guillouzo and C. Guguen-Guillouzo, Editors. 1986, Les Editions INSERM and John Libbey Eurotext: Paris. p. 226-258.
195. Waxman, D.J. and L. Azaroff, *Phenobarbital induction of cytochrome P-450 gene expression*. Biochem J, 1992. **281** (Pt 3): p. 577-92.
196. Rojkind, M., et al., *Connective tissue biomatrix: its isolation and utilization for long-term cultures of normal rat hepatocytes*. Journal of Cell Biology, 1980. **87**(1): p. 255-263.
197. Dunn, J.C., R.G. Tompkins, and M.L. Yarmush, *Long-term in vitro function of adult hepatocytes in a collagen sandwich configuration*. Biotechnol Prog, 1991. **7**(3): p. 237-45.
198. Bissell, D.M., et al., *Support of cultured hepatocytes by a laminin-rich gel. Evidence for a functionally significant subendothelial matrix in normal rat liver*. J Clin Invest, 1987. **79**(3): p. 801-12.
199. Koebe, H.G., et al., *Collagen gel immobilization: a useful cell culture technique for long-term metabolic studies on human hepatocytes*. Xenobiotica, 1994. **24**(2): p. 95-107.

200. Kocarek, T.A., E.G. Schuetz, and P.S. Guzelian, *Expression of multiple forms of cytochrome P450 mRNAs in primary cultures of rat hepatocytes maintained on matrigel*. Mol Pharmacol, 1993. **43**(3): p. 328-34.
201. Vukicevic, S., et al., *Identification of multiple active growth factors in basement membrane Matrigel suggests caution in interpretation of cellular activity related to extracellular matrix components*. Exp Cell Res, 1992. **202**(1): p. 1-8.
202. Richert, L., et al., *Evaluation of the effect of culture configuration on morphology, survival time, antioxidant status and metabolic capacities of cultured rat hepatocytes*. Toxicol In Vitro, 2002. **16**(1): p. 89-99.
203. Saito, S., et al., *Long-Term Survival and Proliferation of Spheroidal Aggregate Cultured Hepatocytes Transplanted into the Rat Spleen*. Transplantation Proceedings, 1992. **24**(N4): p. 1520-1521.
204. Chang, T.M.S., *Artificial Liver Support Based on Artificial Cells with Emphasis on Encapsulated Hepatocytes*. Artificial Organs, 1992. **16**(N1): p. 71-74.
205. Landry, J., et al., *Spheroidal aggregate culture of rat liver cells: histotypic reorganization, biomatrix deposition, and maintenance of functional activities*. Journal of Cell Biology, 1985. **101**(3): p. 914-923.
206. Tong, J.Z., et al., *Long-term culture of adult rat hepatocyte spheroids*. Exp Cell Res, 1992. **200**(2): p. 326-32.
207. Koide, N., et al., *Formation of multicellular spheroids composed of adult rat hepatocytes in dishes with positively charged surfaces and under other nonadherent environments*. Exp Cell Res, 1990. **186**(2): p. 227-35.
208. Corlu, A., et al., *The coculture: a system for studying the regulation of liver differentiation/proliferation activity and its control*. Cell Biol Toxicol, 1997. **13**(4-5): p. 235-42.
209. Rogiers, V. and A. Verduyck, *Rat hepatocyte cultures and co-cultures in biotransformation studies of xenobiotics*. Toxicology, 1993. **82**(1-3): p. 193-208.
210. Eschbach, E., et al., *Microstructured scaffolds for liver tissue cultures of high cell density: morphological and biochemical characterization of tissue aggregates*. J Cell Biochem, 2005. **95**(2): p. 243-55.
211. Powers, M.J., et al., *A microfabricated array bioreactor for perfused 3D liver culture*. Biotechnol Bioeng, 2002. **78**(3): p. 257-69.
212. Naughton, B.A., et al., *A stereotypic, transplantable liver tissue-culture system*. Appl Biochem Biotechnol, 1995. **54**(1-3): p. 65-91.
213. Ponsoda, X., et al., *Drug biotransformation by human hepatocytes. In vitro/in vivo metabolism by cells from the same donor*. J Hepatol, 2001. **34**(1): p. 19-25.

214. LeCluyse, E., et al., *Expression and regulation of cytochrome P450 enzymes in primary cultures of human hepatocytes*. J Biochem Mol Toxicol, 2000. **14**(4): p. 177-88.
215. Silva, J.M., S.H. Day, and D.A. Nicoll-Griffith, *Induction of cytochrome-P450 in cryopreserved rat and human hepatocytes*. Chem Biol Interact, 1999. **121**(1): p. 49-63.
216. D'Arcy, P.F., *Drug interactions with oral contraceptives*. Drug Intell Clin Pharm, 1986. **20**(5): p. 353-62.
217. Flodin, N.W., *Micronutrient supplements: toxicity and drug interactions*. Prog Food Nutr Sci, 1990. **14**(4): p. 277-331.
218. Flockhart, D.A., *Drug interactions, cardiac toxicity, and terfenadine: from bench to clinic?* J Clin Psychopharmacol, 1996. **16**(2): p. 101-3.
219. Juurlink, D.N., et al., *Drug-drug interactions among elderly patients hospitalized for drug toxicity*. Jama, 2003. **289**(13): p. 1652-8.
220. Kmiec, Z., *Cooperation of liver cells in health and disease*. Adv Anat Embryol Cell Biol, 2001. **161**: p. III-XIII, 1-151.
221. Cunha, G.R., et al., *Stromal-epithelial interactions in adult organs*. Cell Differ, 1985. **17**(3): p. 137-48.
222. Wessely, R., et al., *A central role of interferon regulatory factor-1 for the limitation of neointimal hyperplasia*. Hum Mol Genet, 2003. **12**(2): p. 177-87.
223. Hayward, S.W., M.A. Rosen, and G.R. Cunha, *Stromal-epithelial interactions in the normal and neoplastic prostate*. Br J Urol, 1997. **79 Suppl 2**: p. 18-26.
224. Cascio, S. and K.S. Zaret, *Hepatocyte differentiation initiates during endodermal-mesenchymal interactions prior to liver formation*. Development, 1991. **113**(1): p. 217-25.
225. Falke, G., J. Caffaratti, and A. Atala, *Tissue engineering of the bladder*. World J Urol, 2000. **18**(1): p. 36-43.
226. Chang, H.Y., et al., *Diversity, topographic differentiation, and positional memory in human fibroblasts*. Proc Natl Acad Sci U S A, 2002. **99**(20): p. 12877-82.
227. Zaret, K.S., *Regulatory phases of early liver development: paradigms of organogenesis*. Nat Rev Genet, 2002. **3**(7): p. 499-512.
228. Jung, J., et al., *Initiation of mammalian liver development from endoderm by fibroblast growth factors*. Science, 1999. **284**(5422): p. 1998-2003.
229. Lipshutz, R.J., et al., *High density synthetic oligonucleotide arrays*. Nat Genet, 1999. **21**(1 Suppl): p. 20-4.
230. Seglen, P.O., *Preparation of isolated rat liver cells*. Methods Cell Biol, 1976. **13**: p. 29-83.

231. Rheinwald, J.G. and H. Green, *Serial cultivation of strains of human epidermal keratinocytes: the formation of keratinizing colonies from single cells*. Cell, 1975. **6**(3): p. 331-43.
232. Wodicka, L., et al., *Genome-wide expression monitoring in Saccharomyces cerevisiae*. Nat Biotechnol, 1997. **15**(13): p. 1359-67.
233. Zapala, M.A., et al., *Software and methods for oligonucleotide and cDNA array data analysis*. Genome Biol, 2002. **3**(6).
234. Sandberg, R., et al., *Regional and strain-specific gene expression mapping in the adult mouse brain*. Proc Natl Acad Sci U S A, 2000. **97**(20): p. 11038-43.
235. Laborda, J., *The role of the epidermal growth factor-like protein dlk in cell differentiation*. Histol Histopathol, 2000. **15**(1): p. 119-29.
236. Tanimizu, N., et al., *Isolation of hepatoblasts based on the expression of Dlk/Pref-1*. J Cell Sci, 2003. **116**(Pt 9): p. 1775-86.
237. Sosa-Pineda, B., J.T. Wigle, and G. Oliver, *Hepatocyte migration during liver development requires Prox1*. Nat Genet, 2000. **25**(3): p. 254-5.
238. Kittelberger, R., et al., *Distribution of type VIII collagen in tissues: an immunohistochemical study*. Connect Tissue Res, 1990. **24**(3-4): p. 303-18.
239. Shuttleworth, C.A., *Type VIII collagen*. Int J Biochem Cell Biol, 1997. **29**(10): p. 1145-8.
240. Pogany, G. and K.G. Vogel, *The interaction of decorin core protein fragments with type I collagen*. Biochem Biophys Res Commun, 1992. **189**(1): p. 165-72.
241. Gallai, M., et al., *Proteoglycan gene expression in rat liver after partial hepatectomy*. Biochem Biophys Res Commun, 1996. **228**(3): p. 690-4.
242. Avantaggiato, V., et al., *Embryonic expression pattern of the murine figf gene, a growth factor belonging to platelet-derived growth factor/vascular endothelial growth factor family*. Mech Dev, 1998. **73**(2): p. 221-4.
243. LeCouter, J., et al., *Angiogenesis-independent endothelial protection of liver: role of VEGFR-1*. Science, 2003. **299**(5608): p. 890-3.
244. Monaghan, A.P., et al., *Dickkopf genes are co-ordinately expressed in mesodermal lineages*. Mech Dev, 1999. **87**(1-2): p. 45-56.
245. Ramaswamy, S. and T.R. Golub, *DNA microarrays in clinical oncology*. J Clin Oncol, 2002. **20**(7): p. 1932-41.
246. Thomson, J., et al., *Isolation of a Primate Embryonic Stem Cell Line*. PNAS, 1995. **92**(17): p. 7844-7848.

247. DeLise, A.M. and R.S. Tuan, *Alterations in the spatiotemporal expression pattern and function of N-cadherin inhibit cellular condensation and chondrogenesis of limb mesenchymal cells in vitro*. J Cell Biochem, 2002. **87**(3): p. 342-59.
248. Luo, Y., et al., *Rescuing the N-cadherin knockout by cardiac-specific expression of N- or E-cadherin*. Development, 2001. **128**(4): p. 459-69.
249. Niemann, C., et al., *Rat adult hepatocytes in primary pure and mixed monolayer culture. Comparison of the maintenance of mixed function oxidase and conjugation pathways of drug metabolism*. Biochem Pharmacol, 1991. **42**(2): p. 373-9.
250. Makrigiannakis, A., et al., *N-cadherin-mediated human granulosa cell adhesion prevents apoptosis: a role in follicular atresia and luteolysis?* Am J Pathol, 1999. **154**(5): p. 1391-406.
251. Takeuchi, T., et al., *Expression of T-cadherin (CDH13, H-Cadherin) in human brain and its characteristics as a negative growth regulator of epidermal growth factor in neuroblastoma cells*. J Neurochem, 2000. **74**(4): p. 1489-97.
252. Joshi, M.B., et al., *T-cadherin protects endothelial cells from oxidative stress-induced apoptosis*. Faseb J, 2005. **19**(12): p. 1737-9.
253. Vestal, D.J. and B. Ranscht, *Glycosyl phosphatidylinositol--anchored T-cadherin mediates calcium- dependent, homophilic cell adhesion*. J Cell Biol, 1992. **119**(2): p. 451-61.
254. Ballmer, P.E., et al., *Chronic metabolic acidosis decreases albumin synthesis and induces negative nitrogen balance in humans*. J Clin Invest, 1995. **95**(1): p. 39-45.
255. Ulrich, C., et al., *Effects of acidosis on acute phase protein metabolism in liver cells*. Miner Electrolyte Metab, 1999. **25**(4-6): p. 228-33.
256. Brieva, T.A. and P.V. Moghe, *Engineering the hepatocyte differentiation-proliferation balance by acellular cadherin micropresentation*. Tissue Eng, 2004. **10**(3-4): p. 553-64.
257. Chen, A.A., et al., *Quantum dots to monitor RNAi delivery and improve gene silencing*. Nucleic Acids Res, 2005. **33**(22): p. e190.
258. Adachi, Y., et al., *An adiponectin receptor, T-cadherin, was selectively expressed in intratumoral capillary endothelial cells in hepatocellular carcinoma: possible cross talk between T-cadherin and FGF-2 pathways*. Virchows Arch, 2005: p. 1-8.
259. van Breemen, C., et al., *Endothelium-smooth muscle interactions in blood vessels*. Clin Exp Pharmacol Physiol, 1997. **24**(12): p. 989-92.
260. Davies, P.F., *Vascular cell interactions with special reference to the pathogenesis of atherosclerosis*. Lab Invest, 1986. **55**(1): p. 5-24.
261. Arias, A.M., *Epithelial mesenchymal interactions in cancer and development*. Cell, 2001. **105**(4): p. 425-31.

262. Singhvi, R., et al., *Engineering cell shape and function*. Science, 1994. **264**(5159): p. 696-8.
263. Yousaf, M.N., B.T. Houseman, and M. Mrksich, *Turning on Cell Migration with Electroactive Substrates*. Angewandte Chemie International Edition, 2001. **40**(6): p. 1093-1096.
264. Yeo, W.-S., M.N. Yousaf, and M. Mrksich, *Dynamic Interfaces between Cells and Surfaces: Electroactive Substrates that Sequentially Release and Attach Cells*. J. Am. Chem. Soc., 2003. **125**(49): p. 14994-14995.
265. Lahann, J., et al., *A reversibly switching surface*. Science, 2003. **299**(5605): p. 371-4.
266. Nandkumar, M.A., et al., *Two-dimensional cell sheet manipulation of heterotypically co-cultured lung cells utilizing temperature-responsive culture dishes results in long-term maintenance of differentiated epithelial cell functions*. Biomaterials, 2002. **23**(4): p. 1121-30.
267. Cheng, X., et al., *Novel cell patterning using microheater-controlled thermoresponsive plasma films*. J Biomed Mater Res A, 2004. **70**(2): p. 159-68.
268. Lutolf, M.P. and J.A. Hubbell, *Synthetic biomaterials as instructive extracellular microenvironments for morphogenesis in tissue engineering*. 2005. **23**(1): p. 47-55.
269. Hubbell, J.A., *Materials as morphogenetic guides in tissue engineering*. Curr Opin Biotechnol, 2003. **14**(5): p. 551-8.
270. Ma, S.H., et al., *An endothelial and astrocyte co-culture model of the blood-brain barrier utilizing an ultra-thin, nanofabricated silicon nitride membrane*. Lab Chip, 2005. **5**(1): p. 74-85.
271. Song, H., C.F. Stevens, and F.H. Gage, *Astroglia induce neurogenesis from adult neural stem cells*. Nature, 2002. **417**(6884): p. 39-44.
272. Villafuerte, B.C., et al., *Coculture of primary rat hepatocytes and nonparenchymal cells permits expression of insulin-like growth factor binding protein-3 in vitro*. Endocrinology, 1994. **134**(5): p. 2044-50.
273. Bedossa, P., et al., *Stimulation of collagen alpha 1(I) gene expression is associated with lipid peroxidation in hepatocellular injury: a link to tissue fibrosis?* Hepatology, 1994. **19**(5): p. 1262-71.
274. Folch, A. and M. Toner, *Microengineering of cellular interactions*. Annu Rev Biomed Eng, 2000. **2**: p. 227-56.
275. Bhatia, S.N. and C.S. Chen, *Tissue Engineering at the Micro-Scale*. Biomedical Microdevices, 1999. **2**(2): p. 131-144.
276. Lockhart, D.J. and E.A. Winzeler, *Genomics, gene expression and DNA arrays*. Nature, 2000. **405**(6788): p. 827-36.

277. Pritchard, J.F., et al., *Making better drugs: Decision gates in non-clinical drug development*. Nat Rev Drug Discov, 2003. **2**(7): p. 542-53.
278. Brandon, E.F., et al., *An update on in vitro test methods in human hepatic drug biotransformation research: pros and cons*. Toxicol Appl Pharmacol, 2003. **189**(3): p. 233-46.
279. Bhadriraju, K. and C.S. Chen, *Engineering cellular microenvironments to improve cell-based drug testing*. Drug Discov Today, 2002. **7**(11): p. 612-20.
280. Bhatia, S.N., et al., *Microfabrication of hepatocyte/fibroblast co-cultures: role of homotypic cell interactions*. Biotechnol Prog, 1998. **14**(3): p. 378-87.
281. Bhatia, S.N., et al., *Selective adhesion of hepatocytes on patterned surfaces*. Ann N Y Acad Sci, 1994. **745**: p. 187-209.
282. Price, R.J., et al., *CYP isoform induction screening in 96-well plates: use of 7-benzyloxy-4-trifluoromethylcoumarin as a substrate for studies with rat hepatocytes*. Xenobiotica, 2000. **30**(8): p. 781-95.
283. Isley, W.L., *Hepatotoxicity of thiazolidinediones*. Expert Opin Drug Saf, 2003. **2**(6): p. 581-6.
284. Gordin, A., S. Kaakkola, and H. Teravainen, *Clinical advantages of COMT inhibition with entacapone - a review*. J Neural Transm, 2004. **111**(10-11): p. 1343-63.
285. Borges, N., *Tolcapone in Parkinson's disease: liver toxicity and clinical efficacy*. Expert Opin Drug Saf, 2005. **4**(1): p. 69-73.
286. Shih, H., et al., *Species differences in hepatocyte induction of CYP1A1 and CYP1A2 by omeprazole*. Hum Exp Toxicol, 1999. **18**(2): p. 95-105.
287. Li, N., A. Tourovskaya, and A. Folch, *Biology on a chip: microfabrication for studying the behavior of cultured cells*. Crit Rev Biomed Eng, 2003. **31**(5-6): p. 423-88.
288. Chia, S.M., P.C. Lin, and H. Yu, *TGF-beta1 regulation in hepatocyte-NIH3T3 co-culture is important for the enhanced hepatocyte function in 3D microenvironment*. Biotechnol Bioeng, 2005. **89**(5): p. 565-73.
289. Roy, P., et al., *Effect of flow on the detoxification function of rat hepatocytes in a bioartificial liver reactor*. Cell Transplant, 2001. **10**(7): p. 609-14.
290. Tong, J.Z., et al., *Application of spheroid culture to human hepatocytes and maintenance of their differentiation*. Biol Cell, 1994. **81**(1): p. 77-81.
291. Chong, T.W., et al., *Primary human hepatocytes in spheroid formation to study hepatitis C infection*. J Surg Res, 2006. **130**(1): p. 52-7.
292. Zeilinger, K., et al., *Three-dimensional co-culture of primary human liver cells in bioreactors for in vitro drug studies: effects of the initial cell quality on the long-term maintenance of hepatocyte-specific functions*. Altern Lab Anim, 2002. **30**(5): p. 525-38.

293. Clemedson, C. and B. Ekwall, *Overview of the Final MEIC Results: I. The In Vitro--In Vitro Evaluation*. Toxicology in Vitro, 1999. **13**(4-5): p. 657-663.
294. Ekwall, B., *Overview of the Final MEIC Results: II. The In Vitro--In Vivo Evaluation, Including the Selection of a Practical Battery of Cell Tests for Prediction of Acute Lethal Blood Concentrations in Humans*. Toxicology in Vitro, 1999. **13**(4-5): p. 665-673.
295. Viravaidya, K., A. Sin, and M.L. Shuler, *Development of a microscale cell culture analog to probe naphthalene toxicity*. Biotechnol Prog, 2004. **20**(1): p. 316-23.
296. Sin, A., et al., *The design and fabrication of three-chamber microscale cell culture analog devices with integrated dissolved oxygen sensors*. Biotechnol Prog, 2004. **20**(1): p. 338-45.
297. Lee, M.Y., et al., *Metabolizing enzyme toxicology assay chip (MetaChip) for high-throughput microscale toxicity analyses*. Proc Natl Acad Sci U S A, 2005. **102**(4): p. 983-7.
298. Hardisty, J.F. and A.E. Brix, *Comparative hepatic toxicity: prechronic/chronic liver toxicity in rodents*. Toxicol Pathol, 2005. **33**(1): p. 35-40.
299. Celle, G., M. Doderio, and I. Pannacciulli, *The liver damaging effect of L-asparaginase--an experimental study of chronic toxicity*. Eur J Cancer, 1973. **9**(1): p. 55-7.
300. Freeman-Narrood, M., S.A. Narrood, and R.P. Custer, *Chronic toxicity of methotrexate in rats: partial to complete projection of the liver by choline: Brief communication*. J Natl Cancer Inst, 1977. **59**(3): p. 1013-7.
301. Li, A.P. and G.L. Kedderis, *Primary hepatocyte culture as an experimental model for the evaluation of interactions between xenobiotics and drug-metabolizing enzymes*. Chem Biol Interact, 1997. **107**(1-2): p. 1-3.
302. Khamsi, R., *Labs on a chip: meet the stripped down rat*. Nature, 2005. **435**(7038): p. 12-3.
303. Burbach, K.M., A. Poland, and C.A. Bradfield, *Cloning of the Ab-receptor cDNA reveals a distinctive ligand-activated transcription factor*. Proc Natl Acad Sci U S A, 1992. **89**(17): p. 8185-9.
304. Kostrubsky, V.E., et al., *Role of CYP3A in ethanol-mediated increases in acetaminophen hepatotoxicity*. Toxicol Appl Pharmacol, 1997. **143**(2): p. 315-23.
305. Zimmerman, H.J. and W.C. Maddrey, *Acetaminophen (paracetamol) hepatotoxicity with regular intake of alcohol: analysis of instances of therapeutic misadventure*. Hepatology, 1995. **22**(3): p. 767-73.
306. Kostrubsky, V.E., et al., *Protection of ethanol-mediated acetaminophen hepatotoxicity by triacetyloleandomycin, a specific inhibitor of CYP3A*. Ann Clin Lab Sci, 1997. **27**(1): p. 57-62.
307. Lecureur, V., et al., *Expression and regulation of hepatic drug and bile acid transporters*. Toxicology, 2000. **153**(1-3): p. 203-19.

308. Shitara, Y., et al., *Inhibition of transporter-mediated hepatic uptake as a mechanism for drug-drug interaction between cerivastatin and cyclosporin A*. *J Pharmacol Exp Ther*, 2003. **304**(2): p. 610-6.
309. Ayrton, A. and P. Morgan, *Role of transport proteins in drug absorption, distribution and excretion*. *Xenobiotica*, 2001. **31**(8-9): p. 469-97.
310. Liu, X., et al., *Biliary excretion in primary rat hepatocytes cultured in a collagen-sandwich configuration*. *Am J Physiol*, 1999. **277**(1 Pt 1): p. G12-21.
311. Petzinger, E. and M. Frimmer, *Comparative investigations on the uptake of phallotoxins, bile acids, bovine lactoperoxidase and horseradish peroxidase into rat hepatocytes in suspension and in cell cultures*. *Biochim Biophys Acta*, 1988. **937**(1): p. 135-44.
312. LeCluyse, E.L., et al., *Regeneration and maintenance of bile canalicular networks in collagen-sandwiched hepatocytes*. *Toxicol In Vitro*, 2000. **14**(2): p. 117-32.
313. Li, A.P., et al., *Preclinical evaluation of drug-drug interaction potential: present status of the application of primary human hepatocytes in the evaluation of cytochrome P450 induction*. *Chem Biol Interact*, 1997. **107**(1-2): p. 5-16.
314. Kaplowitz, N., *Acetaminophen hepatotoxicity: what do we know, what don't we know, and what do we do next?* *Hepatology*, 2004. **40**(1): p. 23-6.
315. Patten, C.J., et al., *Cytochrome P450 enzymes involved in acetaminophen activation by rat and human liver microsomes and their kinetics*. *Chem Res Toxicol*, 1993. **6**(4): p. 511-8.
316. Genter, M.B., et al., *Role of CYP2A5 and 2G1 in acetaminophen metabolism and toxicity in the olfactory mucosa of the Cyp1a2(-/-) mouse*. *Biochem Pharmacol*, 1998. **55**(11): p. 1819-26.
317. Thummel, K.E., et al., *Oxidation of acetaminophen to N-acetyl-p-aminobenzoquinone imine by human CYP3A4*. *Biochem Pharmacol*, 1993. **45**(8): p. 1563-9.
318. Nelson, S.D., *Molecular mechanisms of the hepatotoxicity caused by acetaminophen*. *Semin Liver Dis*, 1990. **10**(4): p. 267-78.
319. Kostrubsky, V.E., et al., *Effect of Taxol on cytochrome P450 3A and acetaminophen toxicity in cultured rat hepatocytes: comparison to dexamethasone*. *Toxicol Appl Pharmacol*, 1997. **142**(1): p. 79-86.
320. Sinclair, J.F., et al., *Ethanol increases cytochromes P450IIE, IIB1/2, and IIIA in cultured rat hepatocytes*. *Arch Biochem Biophys*, 1991. **284**(2): p. 360-5.
321. Roberts, B.J., S.E. Shoaf, and B.J. Song, *Rapid changes in cytochrome P4502E1 (CYP2E1) activity and other P450 isozymes following ethanol withdrawal in rats*. *Biochem Pharmacol*, 1995. **49**(11): p. 1665-73.
322. Zhao, P., T.F. Kalthorn, and J.T. Slattery, *Selective mitochondrial glutathione depletion by ethanol enhances acetaminophen toxicity in rat liver*. *Hepatology*, 2002. **36**(2): p. 326-35.

323. Kalthorn, T.F., et al., *Effect of methylxanthines on acetaminophen hepatotoxicity in various induction states*. J Pharmacol Exp Ther, 1990. **252**(1): p. 112-6.
324. Lee, C.A., et al., *Inhibition and activation of acetaminophen reactive metabolite formation by caffeine. Roles of cytochromes P-450IA1 and IIIA2*. Drug Metab Dispos, 1991. **19**(2): p. 348-53.
325. Allen, J.W., S.R. Khetani, and S.N. Bhatia, *In vitro zonation and toxicity in a hepatocyte bioreactor*. Toxicol Sci, 2005. **84**(1): p. 110-9.
326. Lloyd, S., et al., *Differential in vitro hepatotoxicity of troglitazone and rosiglitazone among cryopreserved human hepatocytes from 37 donors*. Chem Biol Interact, 2002. **142**(1-2): p. 57-71.
327. Ratra, G.S., et al., *Methapyrilene hepatotoxicity is associated with oxidative stress, mitochondrial dysfunction and is prevented by the Ca²⁺ channel blocker verapamil*. Toxicology, 1998. **130**(2-3): p. 79-93.
328. Yu, S., et al., *Adipocyte-specific gene expression and adipogenic steatosis in the mouse liver due to peroxisome proliferator-activated receptor gamma1 (PPARgamma1) overexpression*. J Biol Chem, 2003. **278**(1): p. 498-505.
329. Gavrilova, O., et al., *Liver peroxisome proliferator-activated receptor gamma contributes to hepatic steatosis, triglyceride clearance, and regulation of body fat mass*. J Biol Chem, 2003. **278**(36): p. 34268-76.
330. Schadinger, S.E., et al., *PPARgamma2 regulates lipogenesis and lipid accumulation in steatotic hepatocytes*. Am J Physiol Endocrinol Metab, 2005. **288**(6): p. E1195-205.
331. Cunningham, M.L., et al., *The hepatocarcinogen methapyrilene but not the analog pyrillamine induces sustained hepatocellular replication and protein alterations in F344 rats in a 13-week feed study*. Toxicol Appl Pharmacol, 1995. **131**(2): p. 216-23.
332. Yamazaki, H., et al., *Oxidation of troglitazone to a quinone-type metabolite catalyzed by cytochrome P-450 2C8 and P-450 3A4 in human liver microsomes*. Drug Metab Dispos, 1999. **27**(11): p. 1260-6.
333. Toyoda, Y., et al., *Toxic effect of troglitazone on cultured rat hepatocytes*. Life Sci, 2001. **68**(16): p. 1867-76.
334. Sahi, J., et al., *Effect of troglitazone on cytochrome P450 enzymes in primary cultures of human and rat hepatocytes*. Xenobiotica, 2000. **30**(3): p. 273-84.
335. Ramachandran, V., et al., *Troglitazone increases cytochrome P-450 3A protein and activity in primary cultures of human hepatocytes*. Drug Metab Dispos, 1999. **27**(10): p. 1194-9.
336. Lake, B.G., *Coumarin metabolism, toxicity and carcinogenicity: relevance for human risk assessment*. Food Chem Toxicol, 1999. **37**(4): p. 423-53.

337. Pelkonen, O., E.A. Sotaniemi, and J.T. Ahokas, *Coumarin 7-hydroxylase activity in human liver microsomes. Properties of the enzyme and interspecies comparisons*. Br J Clin Pharmacol, 1985. **19**(1): p. 59-66.
338. Flaim, C.J., S. Chien, and S.N. Bhatia, *An extracellular matrix microarray for probing cellular differentiation*. Nat Methods, 2005. **2**(2): p. 119-25.
339. Roman, G.T., et al., *Sol-gel modified poly(dimethylsiloxane) microfluidic devices with high electroosmotic mobilities and hydrophilic channel wall characteristics*. Anal Chem, 2005. **77**(5): p. 1414-22.
340. Hackney, J.A., et al., *A molecular profile of a hematopoietic stem cell niche*. Proc Natl Acad Sci U S A, 2002. **99**(20): p. 13061-6.
341. Dike, L.E., et al., *Geometric control of switching between growth, apoptosis, and differentiation during angiogenesis using micropatterned substrates*. In Vitro Cell Dev Biol Anim, 1999. **35**(8): p. 441-8.